

TR 79-36

OBLIQUE INCIDENCE INVESTIGATIONS OF THE
IONOSPHERE OVER THE SOUTHERN OCEAN

A Dissertation
submitted in fulfilment of the
requirements for the degree of
Doctor of Philosophy
of Rhodes University

by

JONATHAN PAUL STUART RASH

December 1978

ACKNOWLEDGEMENTS

The running of a project of this kind depends on the co-operation and assistance of a number of people. I wish to thank firstly my supervisor and Director of the Rhodes Antarctic Research Programme, Professor J.A. Gledhill, for the supervision, help and encouragement he has given me. I am also very grateful to the Antarctic Research Officer, Allon Poole, who is in charge of the running of the programme, for all his helpful instruction, advice and assistance; to the Assistant Antarctic Research Officer (Ionosphere), Ray Haggard, for all his helpful co-operation and collaboration, particularly in obtaining R.S.A. vertical incidence data; and to my successors as Ionospheric Physicist at SANAE, John Fisher, Geoff Evans, Errol de Kock and Ian Dore, for operation of the equipment and helpful suggestions. I also thank Sheri Lambert and Errol de Kock for their collaboration, and Pete Mountfort for his programming assistance.

For their considerable co-operation in the large amounts of computing and graph plotting involved in this work, I thank the following past and present members of the staff of the Rhodes University Computer Centre : Mike Lawrie, Martin Urry, Sean Haffey, Jenny Walker, Ray Diederiks and Eugene de Jager, and operators Moosa Sha and Hiram Mager. I also thank Dr. Pat Terry for computing assistance and in particular for the use of his ray tracing program and numerous other routines.

Thanks for providing data are due to : the N.I.T.R. for Marion Island ionograms; Dr. Doug Torr for AE-C satellite data; Dr. Antonio Gagliardini for magnetic field model program and maps; and World Data Centre A, Boulder, for DMSP satellite data and magnetic field model programs.

I am of course indebted to the Department of Transport for the unique, exciting opportunity of spending a year in Antarctica. Their financial support of the Rhodes Antarctic Research Programme, of which this work is a part, is gratefully acknowledged. I also thank the Council for Scientific and Industrial Research and the trustees of the Willem Hiddingh Scholarship, University of Cape Town, for their financial assistance which enabled me to complete this work. Thanks too to Maureen Jackson for her fine typing.

Finally, thank you to my mother for her patient understanding and encouragement and to Louise Torr for the same and more.

CONTENTS

	<u>Page</u>
CHAPTER 1 : INTRODUCTION	1
CHAPTER 2 : THE OBLIQUE INCIDENCE EXPERIMENT	7
2.1 The Oblique Chirpsounder	7
2.1.1 Chirpsounding Principles	7
2.1.2 The Oblique Incidence Case	9
2.2 The SANAE - Grahamstown Sounding Program	9
2.2.1 Equipment Parameters	9
2.2.2 The Transmission Path	11
2.3 Absolute Group Path Measurements	15
2.3.1 Synchronization of the Clocks	15
2.3.2 Absolute Delay Calibration	16
2.3.3 Offsets, Drift Rates and Timing Shifts	18
CHAPTER 3 : FIRST ANALYSIS	20
3.1 Oblique Ionogram Scaling Techniques	20
3.1.1 Nomenclature	20
3.1.2 The Equivalent Vertical Ionogram	22
3.1.3 Validity of the Ionospheric Curvature Correction	25
3.1.4 Inverse Transmission Curves	27
3.1.5 Mode Identification	30
3.2 Catalogue of SANAE - Grahamstown Oblique Ionograms	36
3.3 Monthly Median Analysis	49
3.3.1 Winter Month (August 1975)	49
3.3.2 Summer Month (January 1976)	53
3.3.3 Discussion	57
CHAPTER 4 : COMPUTER-AIDED SCALING OF OBLIQUE IONOGRAMS	58
4.1 Introduction	58
4.2 The Scaling Program	58
4.2.1 Overview	58
4.2.2 Basic Operation of the Program	60
4.2.3 Scaled Parameters	65
4.2.4 Control Commands	66
4.3 Further Computer Handling of Ionogram Data	71
4.4 Discussion	72

	<u>Page</u>
CHAPTER 5 : CALCULATION OF ELECTRON DENSITY PROFILES FROM OBLIQUE IONOGRAMS	74
5.1 Introduction	74
5.2 The Indirect Method	76
5.2.1 N(h) Profiles from Vertical Ionograms	76
5.2.2 The Method Used	77
5.2.3 Evaluation	78
5.3 Direct Methods	78
5.3.1 Theoretical Background	80
5.3.2 Application of the Theory	85
5.3.3 Allowed Elevation Angles	89
5.3.4 The First Segment	90
5.3.5 The Profile Peak	93
5.4 Evaluation of the Methods	94
 CHAPTER 6 : RESULTS FROM THE R.S.A. 'GREAT CIRCLE CRUISE' FEBRUARY 1977	 99
6.1 Introduction	99
6.2 First Analysis : Nighttime Ionograms	101
6.2.1 Nighttime Equivalent Vertical Ionograms and N(h) Profiles	101
6.2.2 Discussion	103
6.2.3 Diurnal Variation in Vertical Critical Frequencies	106
6.2.4 Nighttime Profiles Directly from Oblique Ionograms	109
6.3 Analysis of Daytime Ionograms	116
6.3.1 Selection of Ionograms	116
6.3.2 Preliminary Analysis : Equivalent Vertical Ionograms	117
6.3.3 Further Analysis : Daytime N(h) Profiles	123
6.4 Conclusions	135
 CHAPTER 7 : RAY TRACING AND THE REAL IONOSPHERE	 137
7.1 The Ray Tracing Program	137
7.2 Ray Tracing through Nighttime Profiles	138
7.3 Ionization Below the F2 Region	142
7.4 Ray Tracing through Daytime Profiles	148
7.5 Ionospheric Tilts	151

	<u>Page</u>
CHAPTER 8 : CORRELATIONS OF OBLIQUE INCIDENCE PARAMETERS WITH ELECTRON PRECIPITATION MEASUREMENTS	154
8.1 The Satellite Data	154
8.2 The Correlation Analysis	158
8.3 Further Analysis	165
8.3.1 Energy Dependence	165
8.3.2 "Area" Dependence	165
8.3.3 "Height" Dependence	167
8.4 Discussion	171
CHAPTER 9 : FURTHER OBSERVATIONS OF PARTICLE PRECIPITATION EFFECTS	173
9.1 The Event of 26 March 1976	173
9.1.1 AE-C Satellite Observations	173
9.1.2 Oblique Incidence Data	176
9.1.3 Vertical Incidence Data	178
9.1.4 Discussion	182
9.2 The Events of 19 and 24 September 1977	184
9.2.1 19 September	184
9.2.2 24 September	189
CHAPTER 10 : CONCLUSIONS	192
10.1 Summary of Results	192
10.2 Equipmental Improvements	194
10.3 Future Work	195
APPENDIX A : The Manual "User's Guide to Ionogram Scaling Using the Graf/Pen Digitizer"	197
APPENDIX B : The Ionogram Scaling Program IONO	216
1. Flowcharts	217
2. List of variable names	221
3. Listing	224
APPENDIX C : Ionogram Data Handling Programs	236
1. The program MAXI	237
2. The program FILE	241
3. The program FIND	243
4. The program FIDO	244
5. The program MEDI	245

	<u>Page</u>
APPENDIX D : Monthly Median Oblique Incidence Data for Winter (August 1975) and Summer (January 1976)	248
APPENDIX E : Programs for Obtaining N(h) Profiles from Oblique Ionograms	255
1. Stepwise formulation of the Smith Method	256
2. Listing of the program NHSMITH	262
3. Stepwise formulation of the Rao Method	269
4. Listing of the program NHRAO	278
5. Listing of the program NHGEORGE	287
APPENDIX F : Additional Computer Programs	290
1. Listing of the program OVIP	291
2. Listing of the program PROFILES	298
3. Listing of subroutine NEDNE	300
4. Listing of subroutine NHPR	301
5. Listing of subroutine CORR	303
REFERENCES	305

CHAPTER 1

INTRODUCTION

The region of the South Atlantic and Southern Oceans shown in Figure 1.1 is of considerable interest in ionospheric and aeronomic research owing to the presence of several 'anomalies' (Gledhill, 1976). The most notable of these is the South Atlantic (or Brazilian) Anomaly associated with the global minimum of magnetic field intensity off the coast of Brazil. Ginzburg *et al.* (1962) reported measurements of large fluxes of high energy particles at ionospheric heights by Soviet satellites in this area as well as in the areas of the Southern Anomaly and Particle Anomaly shown in Figure 1.1. Greenspan and Stone (1964) observed enhanced airglow in the area west of Cape Town shown as the Airglow Anomaly.

Vertical incidence 'soundings' of the ionosphere are routinely made at land-based stations surrounding this region; a vertical incidence ionosonde has been operated at the South African Antarctic base SANAE ($70^{\circ}\text{S } 2^{\circ}\text{W}$) since 1962 by the Rhodes Antarctic Research group (Gledhill, 1971). Ionospheric observations in the remote ocean region are naturally few and far between (Haggard and Gledhill, 1976). It has, however, been suggested that oblique incidence soundings could be used to supplement vertical soundings in determining ionospheric parameters in areas such as this where vertical incidence ionosondes cannot be deployed (e.g. George, 1970).

As can be seen from Figure 1.1, the great circle path between SANAE and Grahamstown ($33^{\circ}\text{S } 27^{\circ}\text{E}$) passes through the centre of the Southern Anomaly. The oblique incidence experiment set up over this path, which is described below, offers exciting prospects for the investigation of the ionosphere over this unique, remote region.

In 1972-73, two Barry Research VOS-1 Chirpsounder ionosondes, described in Chapter 2, were acquired by the Rhodes Antarctic Research group. These are each capable of vertical sounding and, in conjunction, oblique sounding. One of them has been continuously operated at Grahamstown. I maintained the other at Alice, 64 km north-east of Grahamstown, during 1974, prior to spending a year at SANAE. During this trial period some of the difficulties involved in maintaining the two ionosondes synchronously were recognised and resolved. Some of the short distance oblique ionograms obtained have been analysed by ray tracing (Lambert, 1977).

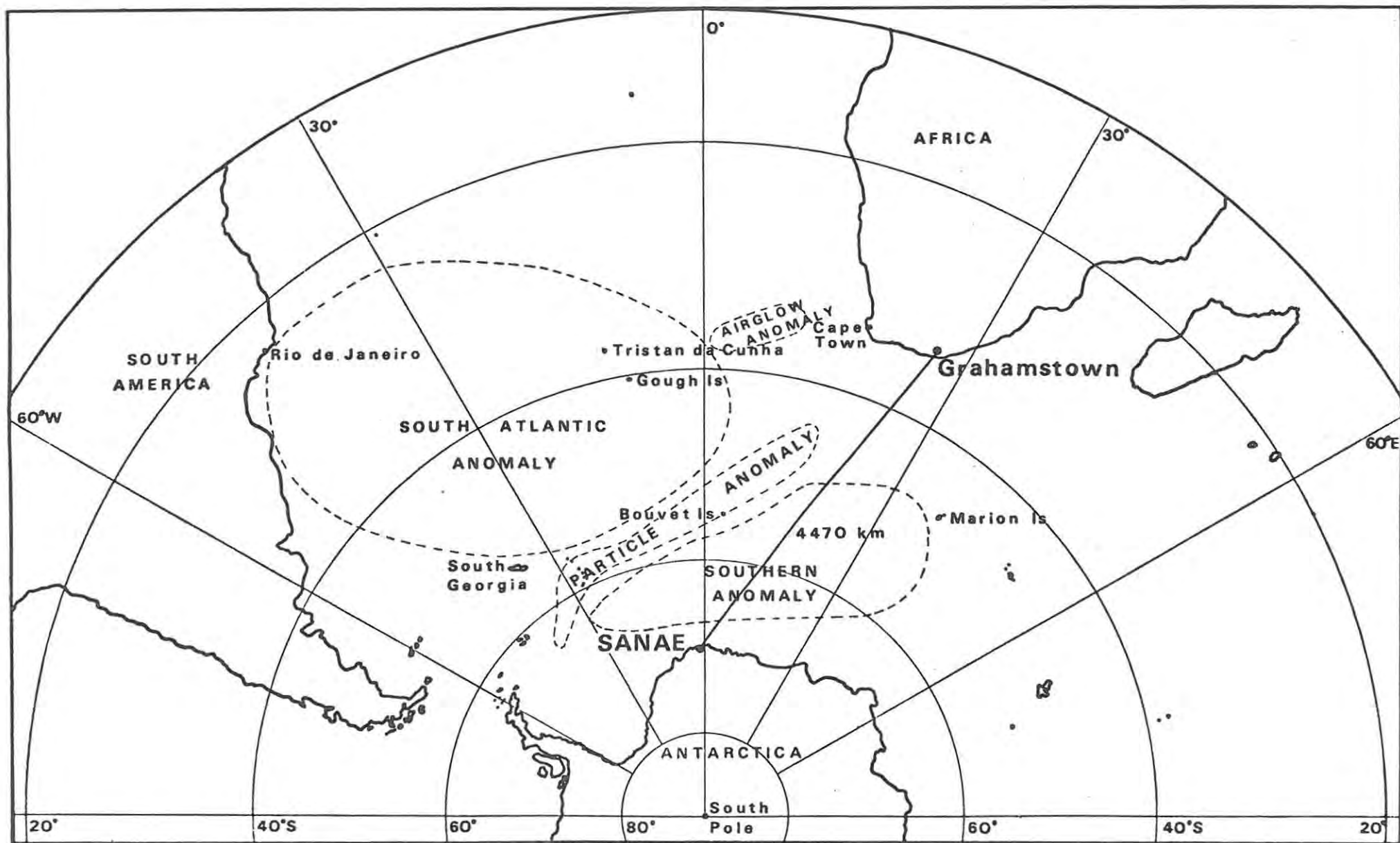


Figure 1.1 : The Southern Ocean area, showing the SANAE - Grahamstown transmission path and the various anomalous regions.

In February 1975 I installed the second instrument at SANAE, replacing the old Cossor pulse ionosonde (Gledhill, 1971). Transmissions were initiated shortly afterwards and the first oblique ionogram was received in Grahamstown on 7 March 1975. Synoptic quarter-hourly records have been obtained since that date, except during periods when synchronization between the two ionosondes has been lost, brief periods of other equipment failure, and times of special study. From 4 June 1975 absolute propagation times have been determined by means of a regular weekly calibration, described in Chapter 2.

During the course of the first year of operation of the oblique incidence experiment, several points were observed. There were often periods of complete absorption or 'blackout', as is the case with vertical observations at SANAE (Torr, 1966). In addition there was a large daily variability in the measurements; again this is also true for SANAE vertical incidence measurements and is considered to be associated with particle precipitation in the Southern Anomaly (Gledhill *et al.*, 1967). Both these factors contribute towards making synchronization of the two ionosondes, and interpretation of the results, more difficult.

In view of the large distance between SANAE and Grahamstown (4470 km) it was expected that "one-hop" propagation, involving only one ionospheric reflection between the two points, would not be possible. The early records appeared to show that the two-hop mode was the least-delayed observed; confirmation was given by considerations of self-consistency amongst the various multi-hop modes observed (Rash and Poole, 1975), and more conclusively by ray tracing simulations (Lambert, 1977). However, particularly more recently, the high-angle ray of the one-hop mode is observed during the day (Figure 1.2).

While there have been numerous oblique incidence experiments (e.g. Wieder, 1955; Sulzer, 1955; Möller, 1964) and oblique propagation is extensively used from an engineering viewpoint, there appear to have been few attempts to obtain synoptic oblique incidence data on a similar basis to vertical incidence data (Piggott and Rawer, 1972). On my return from Antarctica in 1976 the possibilities of such routine scaling were investigated to see if the supplementing of vertical data by this means was viable. A major problem with this approach is the identification of the modes of

propagation on the oblique ionograms (Davies, 1965). However, with the criteria given in Chapter 3, and some experience, it is believed that this has become a fairly reliable procedure. The first monthly median data thus obtained, for August 1975, are also presented in Chapter 3.

While this was shown to be a viable and worthwhile procedure, it was also found to be even more tedious and time-consuming than the scaling of vertical ionograms. With the availability of a digitizer and minicomputer and the development of a program for the scaling of vertical ionograms (de Kock, 1977), a computer-assisted scaling system for oblique ionograms was incorporated. This system is described in Chapter 4; a manual for its use was prepared and is included as Appendix A. Both as a thorough test of the system in comparison with manual scaling, and in order to obtain a summer month's median data, oblique ionograms for January 1976 were scaled. Further ionogram data handling systems were developed, with the help of Mr. P.I. Mountfort. Overall, the system has been shown to be a reliable and convenient means of obtaining oblique data.

Probably the best means of explaining observed oblique ionograms is by ray tracing (e.g. Radio Science 3, no. 1, 1968) through model electron density *vs.* real height, or $N(h)$, profiles. Such profiles may be routinely obtained from vertical ionograms by a number of different methods (Wright and Smith, 1967; Piggott and Rawer, 1972). An oblique ionogram may be easily converted to the 'equivalent vertical ionogram' (Chapter 3) and the same vertical reduction methods used on this; this is termed the 'indirect method' (Gething, 1969). Few 'direct methods' for the reduction of oblique ionograms to $N(h)$ profiles exist; the formulation of two such methods in the literature (Smith, 1970; Rao, 1973) is developed in Chapter 5. All three methods were used to obtain $N(h)$ profiles from a number of nighttime and daytime oblique ionograms, as described in Chapter 6. The encouraging results obtained from ray tracing through the profiles derived by the Rao method are given in Chapter 7.

The ray tracing studies of Lambert (1977) for the two-hop mode over the SANAE - Grahamstown path showed that the ground plans of the ray paths closely followed the great circle between the two places, and that, with varying ionospheric parameters, the two hops may be of different lengths. Conversely, in analysing a two-hop oblique ionogram, the relative values of these parameters are indeterminate and the relative importance of each of the two hops unknown. It was expected that, since SANAE generally has a smaller maximum electron density than Grahamstown, the range of

propagating frequencies would be limited by conditions on the first (southern) hop. An opportunity to help resolve this was provided by the voyage of the South African Antarctic supply ship R.S.A. on its return from Antarctica in February 1977. By arrangement with the Department of Transport the R.S.A. closely followed the SANAE - Grahamstown great circle while the vertical incidence ionosonde 'Minibal' was operated on board (Haggard, 1978). The results from this 'great circle cruise' are discussed in Chapter 6. These results enabled comparison of oblique and vertical data for different points along the path for the first time and aided considerably our understanding of ionospheric variations over the path.

Another topic of continuing interest in the Antarctic Research group is the effect of particle precipitation on the ionosphere. Torr (1966) and Gledhill *et al.* (1967) showed that there was a correlation between high precipitating electron fluxes in the conjugate area and ionospheric disturbances at SANAE. Such correlations rested, however, on indirect evidence since the observed electrons (with energies of 1 - 40 keV) would deposit most of their energy below the F2 region (Rees, 1963; Berger *et al.*, 1970), and it was simply assumed that they were accompanied by similarly high fluxes of lower energy electrons which could influence the F2 region. No direct evidence was available simply because there were no observations of such low energy electrons at ionospheric heights.

Recently, however, several satellites have begun making such observations; precipitating electron fluxes in the energy range 0.2 - 20 keV measured by the DMSP satellite over the Southern Ocean were made available to us in 1976 by World Data Centre A, Boulder. The investigation of possible direct correlations between these fluxes and oblique incidence parameters is the subject of Chapter 8. In Chapter 9, data from the satellite Atmosphere Explorer C during the intense ionospheric-magnetospheric event of 26 March 1976 are examined in conjunction with ionospheric data and some very interesting effects observed; the events of 19 and 24 September 1977 are also discussed.

This dissertation is largely an 'overview' of the oblique incidence experiment and together with the work of Lambert (1977) represents the first fruits of what promises to be a very worthwhile project. Suggestions for future work are made at various stages, and, in a way, if this work raises more questions than it answers, it will have largely succeeded in its aim.

GROUP
PATH
(km)

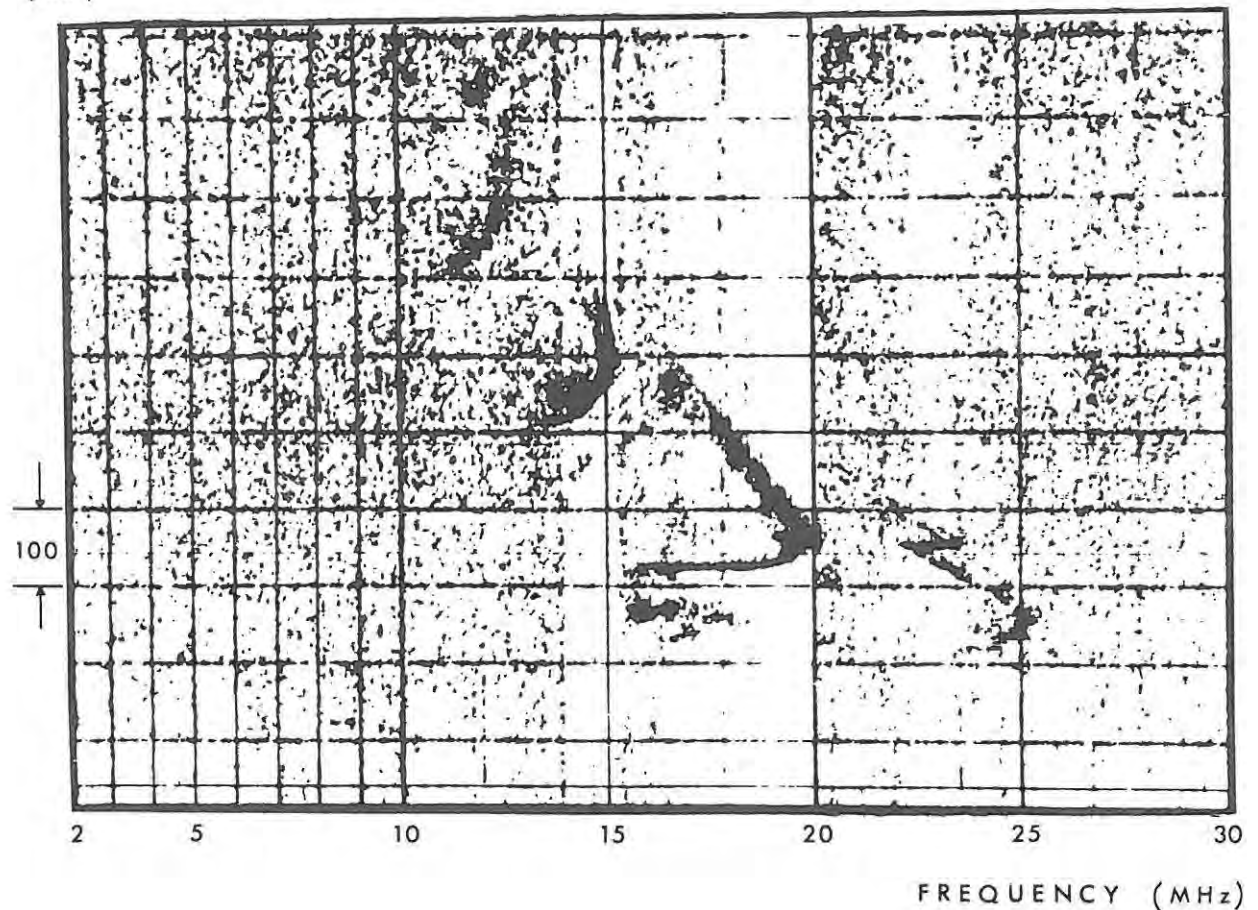


Figure 1.2 : An interesting example of an oblique ionogram obtained over the SANAE - Grahamstown path (20 September 1977, 1000 UT), showing a one-hop high-angle ray with a "ledge" and magnetoionic splitting, as well as two-hop, three-hop and four-hop traces.

CHAPTER 2

THE OBLIQUE INCIDENCE EXPERIMENT

2.1 The Oblique Chirpsounder

2.1.1 Chirpsounding Principles

In the *chirp* or FM CW ionosonde, as distinguished from the conventional pulse ionosonde, a continuous synthesised frequency *ramp*, in which frequency increases linearly with time, is transmitted. The upper part of Figure 2.1 (after Barry, 1971) shows a small section of this ramp (solid line) over a range of frequency equivalent to the receiver bandwidth. Provided that the total *sweep time* of the ramp from lowest to highest transmitted frequency is long compared to the signal travel time Δt between transmission and reception, the received signal (dashed line) may be regarded as being offset in frequency by an amount Δf (the *beat* frequency) from the transmitted frequency, where

$$\Delta f = \frac{df}{dt} \Delta t \quad (2.1)$$

and $\frac{df}{dt}$ is the linear *sweep rate*.

Subtraction of the received frequency from that simultaneously transmitted thus leads to an *echo* from the ionosphere at a particular time delay being observed as a beat tone, at a frequency proportional to that delay, which can be resolved by a spectrum analyser (lower part of Figure 2.1). The latter analyses a frequency range determined by the sweep rate and desired delay time range. For example, at a sweep rate of 100 kHz/sec, the range 0 - 500 Hz is used to give an echo delay time range or "time window" of 5 msec.

The effective bandwidth is thus very small, so that low transmitter power (8 W peak) can be used while still maintaining a good signal-to-noise ratio; narrow-band interference from, for example, broadcasting stations, is minimal. The difficulty of isolating the transmitter and receiver in the vertical incidence situation means that in this mode the transmitter and receiver must be gated on alternately using a T/R "gain weighting" technique. (An improved transmit/receive 'code' has recently been incorporated in our equipment (A.W.V. Poole, to be published)). The average transmitted power is then considerably reduced

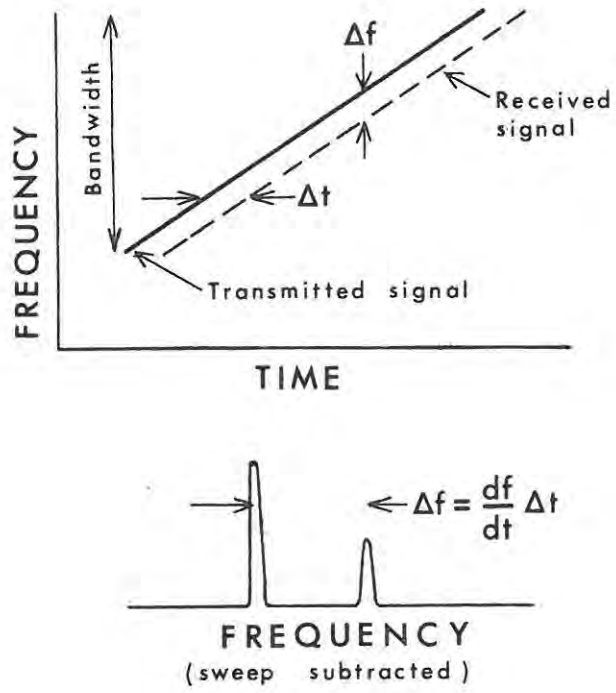


Figure 2.1 : The chirpsounder principle (after Barry, 1971).

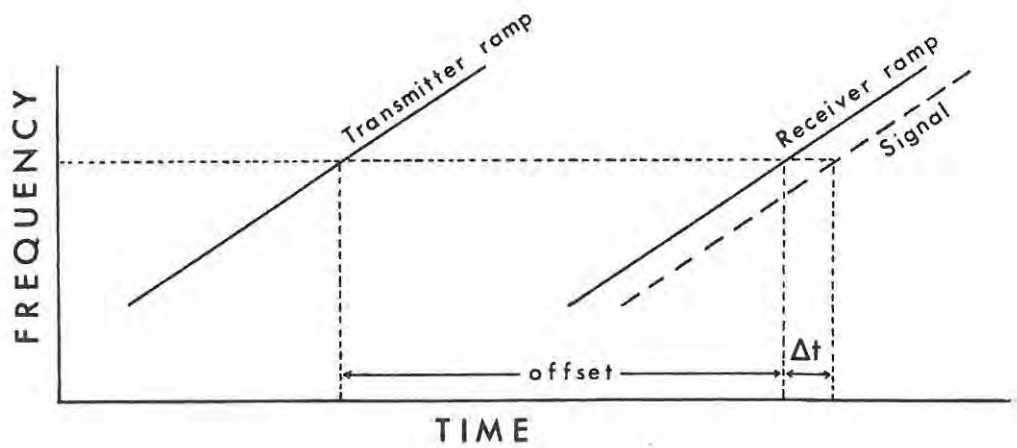


Figure 2.2 : The oblique incidence case with two chirpsounders.

(to 3W), whereas in the oblique transmit mode the transmitter is gated on continuously so that the average power is equal to the peak power. [It is interesting to note (Barry, 1971) that the FM CW technique was in fact in use in oblique incidence work for several years (Barry and Fenwick, 1965, 1969) before it could be adapted for use at vertical incidence.] The Barry Research VOS-1 Chirpsounder used here can be operated in any of the three modes vertical T/R, oblique transmit and oblique receive.

2.1.2 The Oblique Incidence Case

The oblique sounding case with the transmitting and receiving chirpsounders separated is represented in Figure 2.2. Both sounders generate identical frequency ramps (i.e. the same frequency range and sweep rate must be used for both), but the receiver ramp is delayed with respect to the transmitter; this delay or *offset* must be such that the signal falls within the receiver bandwidth. The relative time delay Δt of the signal with respect to the receiver clock may then be measured (at a given frequency on an oblique ionogram), and, if the offset t_0 is known, the total propagation time t is thereby determined. The determination of t_0 is described in section 2.3.

The group path P' of a signal (wave packet) is defined (Davies, 1965, p. 98) as

$$P' = ct = c (t_0 + \Delta t) \quad (2.2)$$

where c is the velocity of light *in vacuo*. An *oblique ionogram* is then simply a record of P' (on a scale whose zero and range are determined by t_0 and the receiver bandwidth respectively) *versus* frequency. Each distance *trace* on the ionogram is assumed to represent a particular *mode* of propagation (section 3.1).

2.2 The SANAE - Grahamstown Sounding Program

2.2.1 Equipment Parameters

The frequency limits and sweep rates for vertical and oblique sounding can be selected independently on the chirpsounder; for all the oblique ionograms discussed here the range 2-30 MHz and sweep rate 100 KHz/sec have been used. The total sweep time is thus 4 minutes 40 seconds. These and other equipment parameters of the SANAE - Grahamstown sounding

program, both vertical and oblique, are listed in Table 2-1. [In May 1975 the maximum transmitted frequency was in fact reduced to 28.56 MHz (by means of circuit modifications made by the author) to reduce interference on the 30 MHz riometer at SANAE. At that time (near solar minimum) this caused no loss of data. Currently however, frequencies up to this value are often observed, so the limit should be reset to 30 MHz, or more, when the SANAE base is resited in 1979.] Vertical or oblique sweeps may be programmed to start at each 5 minutes in the hour; the normal sounding schedule is also given in Table 2-1. This schedule has been changed during periods of special study, for instance the R.S.A. "great circle cruise" (Chapter 6), and during absolute delay calibrations (section 2.3.2).

Table 2-1 :

Equipment parameters for the sounding program.

	<u>Vertical</u>	<u>Oblique</u>
Frequency range	0.5-15 MHz	2-30 MHz
Linear sweep rate	50 kHz/sec	100 kHz/sec
Sweep duration	4 min 50 sec	4 min 40 sec
Peak transmitter power	8W	8W
Average transmitter power	3W	8W
Spectrum analyser frequency range	0-333 Hz	0-500 Hz
Echo delay time range	6.67 msec	3.33 msec
Virtual height/path range	0-1000 km	1000 km*
Equivalent 3dB pulse width	30 μ sec	30 μ sec
Virtual height/path resolution	4.5 km	9 km

* Actual range observed is dependent on the offset of the receiver.

Sweep commencement times for normal program (minutes in the hour) :

00, 15, 30, 45 mins : Vertical incidence at SANAE and Grahamstown

05, 20, 35, 50 mins : Oblique incidence (SANAE = transmitter, Grahamstown = receiver)

10, 25, 40, 55 mins : No sounding

The transmitting and receiving antennas are both identical rhombics with sides of 128 m and acute angles of 66° ; the transmitting antenna at SANAE is kept approximately 2 m above the snow surface, while the receiving antenna at Grahamstown is 24 m above the ground. The signal-loss effects of the ~500 m - thick ice-shelf on which SANAE is situated are considered to be small, although this is debatable (Yoshino, 1967; Evans, 1968).

Recently a sloping-V has been used at Grahamstown and found to be equal in performance to the rhombic; it has sides of 62.5 m, "V" angle 62° and angle of inclination 23° . The bearings of the antennas are the respective great circle bearings given in Table 2-2 (c).

2.2.2 The Transmission Path

The geographic and geomagnetic co-ordinates of SANAE and Grahamstown, as well as some of their magnetic field parameters, are given in Table 2-2 (a) and (b) respectively. The geomagnetic co-ordinates were derived assuming the dipole north pole co-ordinates, 70.35°N , 68.55°W , derived by Lambert (1977) for the dipole giving the 'best fit' for magnetic field parameters at SANAE and Grahamstown; this model was used in ray tracing through nighttime profiles, as described in section 7.2. The magnetic field parameters are for epoch 1975.0, and the L values (McIlwain, 1961) are from Barish and Roederer (1969). [The geographic position of SANAE changes slightly due to seaward flow of ice-shelf at the rate of approximately 8" northwards and 8" westwards annually for the period 1971-1978; the base is to be resited in 1979. The position given for Grahamstown is that of the Waainek field station where the chirpsounder is situated.] Details of the SANAE - Grahamstown great circle path are given in Table 2-2(c).

In the first analysis the propagation modes are assumed to be hops of equal length. The positions of the appropriate ionospheric *mirror points* or *reflection points* are given in Table 2-3 for 1 to 4 hops. Also given for each case are the ground range per hop over the curved earth (*hop length*), *chord length* S , defined by equation (3.2), and *arc height* b , defined by equation (3.3). The latter two parameters are used to correct for the curvature of the earth in calculations for long distance propagation (section 3.1.2; Möller, 1964). The appropriate value of the ionospheric curvature correction factor k (section 3.1.2; Davies, 1965) is also given.

Table 2-4 gives magnetic field parameters for points along the SANAE - Grahamstown great circle, in steps of 100 km, computed using the 8th order spherical harmonic model IGRF 75 (IAGA Commission 2, 1976) for epoch 1975.0, at an altitude of 100 km. The table lists ground distance D from SANAE in km; geographic latitude and longitude; electron gyrofrequency f_B in MHz; dip angle (practically constant over the path); horizontal and vertical intensities H and Z in units of 10^{-4} T ($= 10^5$ γ); declination; and the bearing of the great circle path with respect to the horizontal component of the earth's magnetic field.

Table 2-2 : Characteristics of the SANAE - Grahamstown transmission path (epoch 1975.0).

(a) SANAE (Transmitter)

Geographic latitude	70° 19' 12" S (-70.3200°)
Geographic longitude	2° 22' 20" W (-2.3722°)
Geomagnetic latitude	57.2° S
Geomagnetic longitude	34.7° E
Electron gyrofrequency	1.18 MHz
Magnetic dip angle	-62.50°
Magnetic declination	19.12° W
L value at 0 km	3.98

(b) Grahamstown (Receiver)

Geographic latitude	33° 18' 55" S (-33.3153°)
Geographic longitude	26° 30' 15" E (26.5042°)
Geomagnetic latitude	32.8° S
Geomagnetic longitude	82.1° E
Electron gyrofrequency	0.82 MHz
Magnetic dip angle	-65.21°
Magnetic declination	24.40° W
L value at 0 km	1.83

(c) SANAE - Grahamstown Great Circle Path

Ground distance	4469.0 km
True bearing (S to G)	38.682 °
Reverse bearing (G to S)	194.588 °
Spherical Earth radius	6371.2 km
Angle subtended by path at centre of earth	40.189 °
Theoretical "ground ray" propagation time	14.90 msec

Table 2-3 : Positions of idealized mirror ionospheric reflection points, hop lengths, chord lengths, arc heights and ionospheric curvature correction factors for equal hops over the SANAE - Grahamstown path.

	1 Hop	2 Hop	3 Hop	4 Hop
First hop	52° 33'S 18° 19'E	61° 47'S 10° 58'E	64° 45'S 7° 29'E	66° 12'S 5° 26'E
Second hop	-	43° 00'S 23° 03'E	52° 33'S 18° 19'E	61° 47'S 10° 58'E
Third hop	-	-	39° 47'S 24° 19'E	47° 48'S 20° 54'E
Fourth Hop	-	-	-	38° 10'S 24° 54'E
Hop length (km)	4469.0	2234.5	1489.7	1117.3
Chord length s (km)	4378.0	2223.1	1486.3	1115.8
Arc height b (km)	387.8	97.7	43.5	24.5
Ionospheric curvature correction factor k	1.230	1.077	1.042	1.024

Table 2-4 : Magnetic field parameters at points 100 km apart along the SANAE - Grahamstown great circle path at an altitude of 100 km, computed using the International Geomagnetic Reference Field IGRF75 (IAGA Commission 2, 1976).

GREAT CIRCLE FROM SANAE (LAT -70.32 LON -2.37) TO GRAHAMSTOWN (LAT -33.32 LON 26.50)
MAGNETIC FIELD PARAMETERS FOR EPOCH 1975.0 ALTITUDE 100.0 KM MODEL IGRF75

D (KM)	LAT	LOX	FB (MHZ)	DIP	H	Z	DEC	BEARING
0.0	-70.32	-2.37	1.1196	-62.93	0.182	-0.3556	-19.46	58.14
100.0	-69.61	-0.76	1.1064	-62.78	0.181	-0.3551	-20.39	57.56
200.0	-68.89	0.75	1.0933	-62.64	0.180	-0.3547	-21.23	56.99
300.0	-68.15	2.16	1.0802	-62.50	0.178	-0.3542	-22.00	56.44
400.0	-67.40	3.49	1.0672	-62.38	0.177	-0.3538	-22.69	55.90
500.0	-66.64	4.73	1.0543	-62.26	0.175	-0.3533	-23.32	55.38
600.0	-65.88	5.90	1.0415	-62.15	0.174	-0.3529	-23.89	54.88
700.0	-65.10	7.00	1.0288	-62.05	0.172	-0.3525	-24.40	54.40
800.0	-64.32	8.04	1.0163	-61.96	0.171	-0.3520	-24.87	53.93
900.0	-63.53	9.02	1.0040	-61.88	0.169	-0.3516	-25.30	53.48
1000.0	-62.73	9.95	0.9918	-61.81	0.167	-0.3512	-25.69	53.04
1100.0	-61.93	10.83	0.9799	-61.75	0.166	-0.3508	-26.04	52.61
1200.0	-61.12	11.66	0.9681	-61.70	0.164	-0.3505	-26.37	52.20
1300.0	-60.31	12.45	0.9566	-61.67	0.162	-0.3501	-26.66	51.81
1400.0	-59.49	13.21	0.9453	-61.64	0.160	-0.3497	-26.93	51.43
1500.0	-58.67	13.92	0.9343	-61.63	0.159	-0.3494	-27.18	51.06
1600.0	-57.85	14.61	0.9236	-61.64	0.157	-0.3490	-27.40	50.70
1700.0	-57.02	15.26	0.9132	-61.66	0.155	-0.3487	-27.61	50.35
1800.0	-56.19	15.89	0.9031	-61.69	0.153	-0.3484	-27.79	50.00
1900.0	-55.35	16.49	0.8933	-61.73	0.151	-0.3481	-27.96	49.66
2000.0	-54.52	17.06	0.8838	-61.79	0.149	-0.3478	-28.12	49.33
2100.0	-53.68	17.61	0.8745	-61.87	0.147	-0.3476	-28.25	49.00
2200.0	-52.83	18.14	0.8653	-61.95	0.146	-0.3473	-28.37	48.66
2300.0	-51.99	18.65	0.8561	-62.05	0.144	-0.3471	-28.48	48.33
2400.0	-51.14	19.14	0.8470	-62.17	0.142	-0.3469	-28.57	48.00
2500.0	-50.29	19.61	0.8380	-62.29	0.140	-0.3467	-28.64	47.67
2600.0	-49.44	20.07	0.8291	-62.43	0.138	-0.3465	-28.69	47.33
2700.0	-48.59	20.51	0.8203	-62.58	0.136	-0.3463	-28.72	47.00
2800.0	-47.74	20.93	0.8117	-62.73	0.134	-0.3462	-28.73	46.66
2900.0	-46.88	21.35	0.8033	-62.89	0.133	-0.3460	-28.72	46.33
3000.0	-46.02	21.75	0.7950	-63.07	0.132	-0.3459	-28.69	46.00
3100.0	-45.17	22.13	0.7868	-63.24	0.130	-0.3458	-28.62	45.66
3200.0	-44.31	22.51	0.7787	-63.42	0.129	-0.3457	-28.53	45.33
3300.0	-43.45	22.87	0.7707	-63.59	0.127	-0.3456	-28.41	45.00
3400.0	-42.58	23.23	0.7628	-63.77	0.126	-0.3456	-28.26	44.66
3500.0	-41.72	23.57	0.7550	-63.93	0.125	-0.3456	-28.07	44.33
3600.0	-40.86	23.91	0.7474	-64.09	0.124	-0.3455	-27.84	44.00
3700.0	-39.99	24.23	0.7400	-64.24	0.123	-0.3455	-27.57	43.66
3800.0	-39.13	24.55	0.7327	-64.37	0.123	-0.3455	-27.25	43.33
3900.0	-38.26	24.86	0.7257	-64.49	0.122	-0.3456	-26.90	43.00
4000.0	-37.39	25.17	0.7189	-64.59	0.122	-0.3456	-26.50	42.66
4100.0	-36.52	25.46	0.7123	-64.66	0.121	-0.3456	-26.05	42.33
4200.0	-35.66	25.75	0.7059	-64.70	0.121	-0.3457	-25.56	42.00
4300.0	-34.79	26.04	0.7000	-64.72	0.121	-0.3457	-25.03	41.66
4400.0	-33.92	26.32	0.6947	-64.70	0.121	-0.3458	-24.45	41.33
4469.0	-33.32	26.50	0.6903	-64.66	0.122	-0.3458	-24.02	58.61

2.3 Absolute Group Path Measurements

2.3.1 Synchronization of the Clocks

The chirpsounder clock is provided by a quartz oscillator with a measured stability of the order of 10^9 . Its rate is easily altered by means of front panel controls. The clock can also be advanced or retarded, by the addition or subtraction of clock pulses, at rates of 1, 10 or 100 msec/sec, so that *timing shifts* of the receiver with respect to the transmitter in order to synchronize the two are easily accomplished and can be measured by a pulse counter; each count represents a shift of 10 μ sec.

In practice, the process of synchronization is often difficult because of :

- (i) the narrow receiver bandwidth;
- (ii) the difficulty of obtaining a common time reference for approximate synchronization;
- (iii) the requirement of knowing the approximate frequency range over which signals should be received; if no signal is observed this can be due to absorption rather than lack of synchronization.

The first of these difficulties may be partly overcome by temporarily switching the spectrum analyser frequency range to a large value while 'searching' for the signal. The second may be partly overcome by regular measurement (e.g. every few days) of the delay and drift with respect to a known timing broadcast station (ZUO, WWV, etc.) of each of the two clocks. The different propagation times for signals from different timing stations may be approximately compensated for, using known great circle distances of the stations from the two end points. The third difficulty means a sometimes tedious search procedure; if a signal of any frequency is to be observed, the receiver clock should be left fixed throughout a sweep and shifted by an amount equal to the width of the "time window" of the spectrum analyser before the next sweep. Two oblique sweeps per quarter hour may be initiated to improve matters.

When the transmitter and receiver are synchronized the offset of the receiver with respect to the transmitter may be determined by the technique described in the next section. Another method has been described by Bates and Goddard (1964).

2.3.2 Absolute Delay Calibration

This is essentially a variation of the technique given by Möller (1964), p. 43, and was described by Rash and Poole (1975). Referring to the upper half of Figure 2.3, a signal at a particular frequency f from transmitter S is received at G, where its time delay Δt_G with respect to clock G is measured. The lower half of Figure 2.3 represents the situation exactly 5 minutes later; clock G is kept fixed, and G transmits to S. The latter clock is retarded by a measured amount T msec with respect to its previous (zero) position, where T is slightly less than twice the estimated propagation time from S to G (about 28 msec here), so that the signal falls within the bandwidth of S and its time delay Δt_S with respect to clock S at frequency f can be measured.

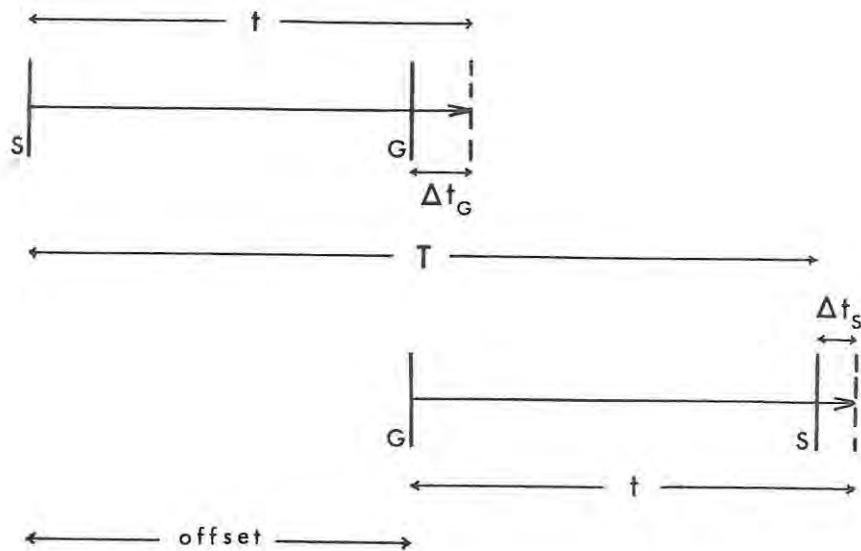


Figure 2.3 : Absolute delay calibration to determine the offset of receiver G (Grahamstown) with respect to transmitter S (SANAE).

We assume that

- (i) the ray paths are reciprocal, i.e. the ray with frequency f experiences the same total propagation delay t , and is propagated by the same mode, in either direction;
- (ii) conditions over the path remain essentially constant over the 5 minute interval involved;
- (iii) the "drift rate" of one clock with respect to the other is small.

Then, referring to Figure 2.3,

$$T = (t - \Delta t_G) + (t - \Delta t_S) \quad (2.3)$$

so that

$$t = \frac{T + \Delta t_G + \Delta t_S}{2} \quad (2.4)$$

and the required offset of clock G with respect to clock S is

$$t_o = t - \Delta t_G \quad (2.5)$$

At the end of the second 5 minute interval clock S is advanced back to its zero position and S transmits to G; the procedure may thus be repeated a number of times in order to check consistency and obtain a reliable average value. Such a "calibration" has normally been performed over the period 1205 - 1300 UT every Wednesday since June 1975, with S (SANAE) and G (Grahamstown) transmitting alternately for each 5 minute interval. The average offset in msec obtained is taken for convenience to be the offset at 1200 UT on that day.

The validity of assumption (i) above may be checked by comparing an oblique ionogram from one end point with the following one from the other end point. Assumption (ii) may be checked by comparing successive records from one end point. There are occasions when one or both of these assumptions are violated; detailed study of some of the records in the former case could provide information on ionospheric tilts. Assumption (iii) is justified since a typical observed drift rate of 1 msec/week is less than 2 km/hour in terms of P' measurement. The uncertainty involved in the measurement of Δt is approximately 10 μ sec (i.e. 3 km group path), the same as that involved in the measurement of T.

2.3.3 Offsets, Drift Rates and Timing Shifts

If no adjustments are made to the clocks in the intervening week, the difference between the offsets at 1200 UT on successive Wednesdays yields a linear *drift rate* of the receiver clock with respect to the transmitter clock in milliseconds per week. If, however, the drift rate is sufficiently rapid it will be necessary to make timing shift adjustments of the receiver clock in order to maintain synchronization; these must then of course be incorporated into the calculation of the drift rate. The following sign convention is used here for both drift rates and timing shifts : a positive value indicates a retardation (i.e. increase in offset), a negative value an advance (i.e. decrease in offset).

Observed drift rates have generally varied between 0 and ± 2 msec/week, although larger values have been observed on occasions. The two clocks may together drift more rapidly with respect to a common reference, but their relative drift may be kept within the above bounds by suitable adjustment of the receiver clock rate. In order to justify the assumption of a linear drift rate between two calibrations, these adjustments should be made at the time of calibration.

For the purposes of computing the group path P' on an oblique ionogram it is convenient to obtain the offset P_0 in km of that ionogram from the relation

$$P_0 = 300 t_0 = 300 (t_c - (T_c - T_i) \cdot \frac{d}{168} - t_a) \quad (2.6)$$

where t_c is the offset in msec at the next calibration,

T_c is the time of this calibration,

T_i is the time of the ionogram

($T_c - T_i$ is measured in hours),

d is the current drift rate in msec/week, and

t_a is the total timing shift in msec made between times

T_i and T_c .

Then the group path at a given frequency f is

$$P' = P_0 + \Delta P' \quad (2.7)$$

where $\Delta P'$ is the "relative group path" or "virtual height" measured on the ionogram at frequency f . The above formulation is used in both the "manual" (Chapter 3) and computer-assisted (Chapter 4) methods of scaling oblique ionograms.

If the drift rate does depart significantly from linearity, values of P' will obviously be innaccurate, especially at times furthest from a calibration. Measurement of P' is emphasised as it is important in mode identification (Chapter 3), in computing electron density profiles (Chapers 5 and 6), and in ray tracing (Chapter 7).

CHAPTER 3

FIRST ANALYSIS

3.1 Oblique Ionogram Scaling Techniques

3.1.1 Nomenclature

While the nomenclature for vertical ionogram scaling (Piggott and Rawer, 1972) has been standardised since the IGY, that for oblique ionogram scaling has not. The first recommendations were published in IQSY Notes (Dieminger, 1963) following an informal meeting at Lindau; these were subsequently summarised by Davies (1965), p. 175, and (1967). The nomenclature used in this work is given below; it is similar to that used by Möller (1964), which differs slightly from the recommendations.

- (i) Individual modes are designated by the total number of reflections in each "layer" regardless of order; thus, for example, $2F + E$ represents two reflections in the F2 region and one reflection in a sporadic-E layer (in any order) with intermediate ground reflections. (The "standard" specifies the order of reflection; the above example could be E_s-2F_2 , $F_2-E_s-F_2$ or $2F_2-E_s$ (where a dash indicates an intermediate ground reflection). Particularly in the absence of angle of arrival measurement and vertical incidence observations at points along the path, there is no means of distinguishing these three cases). "M-type" modes, where the ray is reflected at the top of a sporadic - E layer between two F region reflections instead of at the ground, are designated, for example, $2F-E$. All E region reflections are presumed to be from sporadic - E layers. Our nomenclature does not cater for "supermodes" which can occur in a tilted ionosphere; in these cases the ray undergoes two successive F region reflections (Davies, 1967). Mode identification is discussed in Section 3.1.5.

- (ii) Capital letters are used for all oblique parameters, as in the recommendations, to distinguish them from vertical parameters. The (standard) frequency parameters scaled directly for an individual mode are (Figure 3.1) :

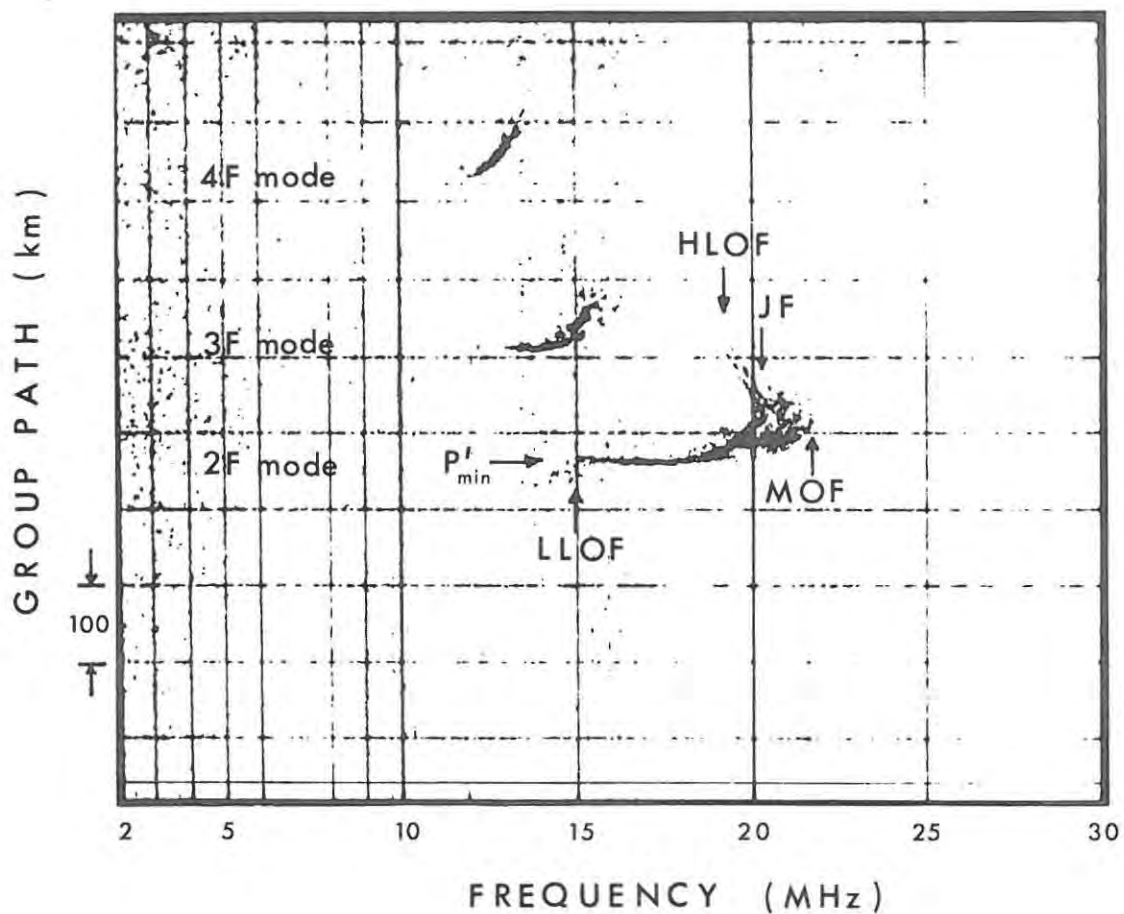


Figure 3.1 : An oblique ionogram showing the scaled parameter nomenclature; the difference between JF and MOF (the "nose extension") is clearly seen on the 2F mode.

LLOF : the lowest observed frequency on the low angle ray;

MOF : the maximum observed frequency;

JF : the junction frequency at which the low and high angle rays intersect;

HLOF : the lowest observed frequency on the high angle ray.

The ordinary and extraordinary rays are not normally distinguished; where they are separable, JF, LLOF and HLOF are measured on the ordinary and MOF on the extraordinary. The mode is placed in parentheses after the parameter name, for example MOF (2F).

(This differs from the recommendations.)

(iii) In addition the (non-standard) frequency parameter EVFO, the ordinary ray "equivalent vertical critical frequency", is scaled by using either an inverse transmission curve overlay in "manual" scaling (section 3.1.4), or a 3-point parabolic fit in computer-assisted scaling (section 4.2.3).

(iv) The minimum group path P' of the mode (irrespective of whether or not this is at the LLOF) is scaled by adding the "virtual height" reading to the offset (section 2.3.3). For multiple-F or multiple-E modes the (non-standard) parameter EVH'F or EVH'E : the "equivalent vertical virtual height" of the F or E layer is then calculated from P' assuming equal hops (section 3.1.2). This parameter is often useful in identifying modes (section 3.1.5).

3.1.2 The Equivalent Vertical Ionogram

This formulation, for a curved earth and ionosphere, follows that of Möller (1964); similar formulations are given by numerous authors, for example Davies (1965). Given a set of points (f, P') constituting a one-hop oblique ionogram, the *equivalent vertical ionogram* consists of the set of points (f_v, h') , where

(i) the virtual height of reflection h' corresponding to the group path P' is given by simple geometry (Figure 3.2) and Martyn's Equivalent Path Theorem (Martyn, 1935) as

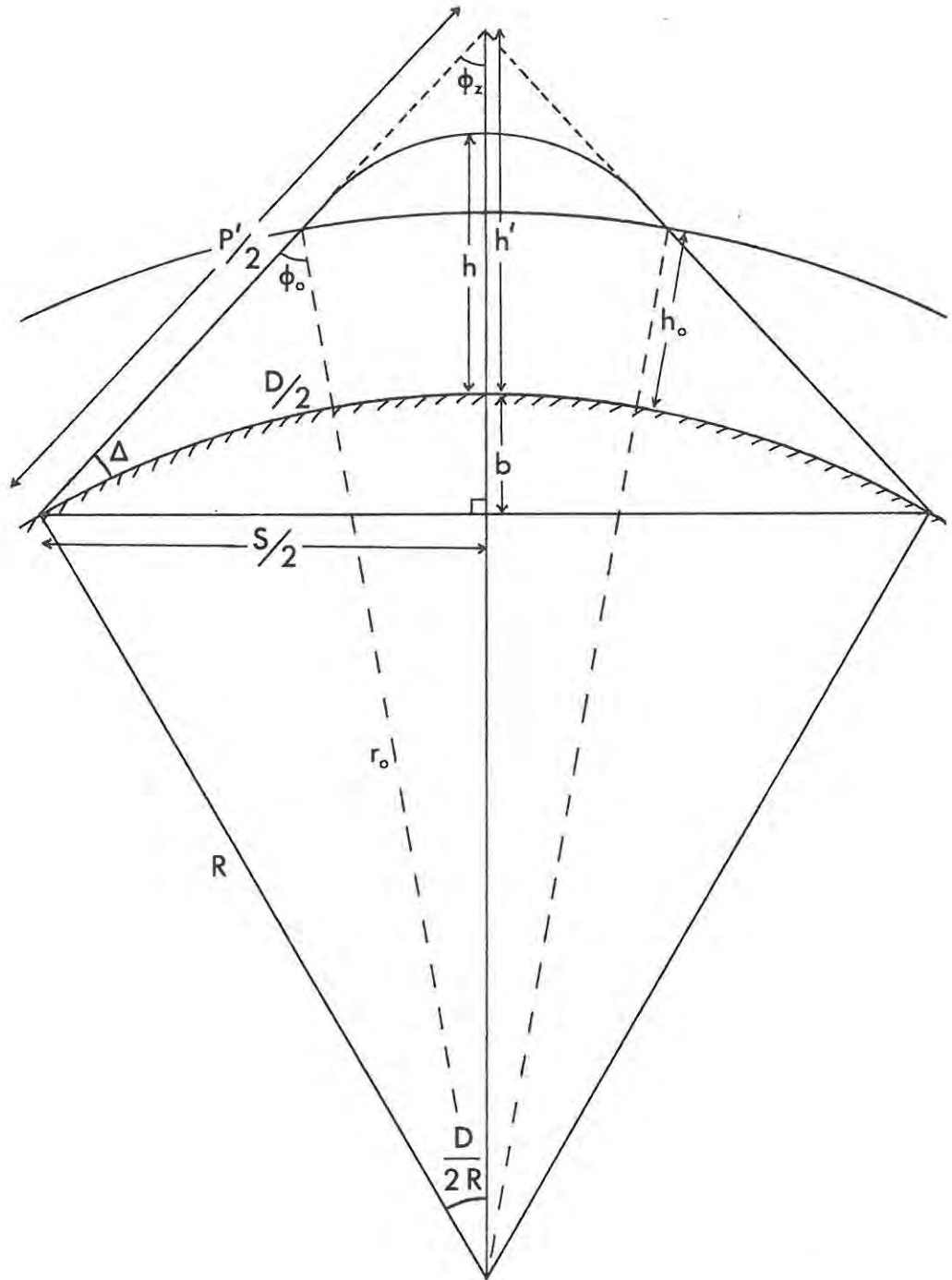


Figure 3.2 : Geometry of the ray path over one hop for a curved earth (radius R) and ionosphere (base height h_0).

$$h' = \frac{1}{2} \sqrt{P'^2 - S^2} - b \quad (3.1)$$

$$\text{where chord length } S = 2 R \sin \frac{D}{2R}, \quad (3.2)$$

$$\text{arc height } b = R \left(1 - \cos \frac{D}{2R} \right), \quad (3.3)$$

D is the ground range
and R is the radius of the earth.

Martyn's Theorem allows one to put h' equal to EVH' , the "height" calculated from the right hand side of equation (3.1); strictly, this only holds in a plane ionosphere.

- (ii) the *equivalent vertical incidence frequency* f_v is such that, if incident vertically on the ionosphere, it will be reflected at the same real height that the frequency f is reflected from at oblique incidence, and is given by the (corrected) Secant Law (Smith, 1939 ; Davies, 1965) :

$$f_v = \frac{f}{k \sec \phi_o} = \frac{f}{k \sqrt{1 + \frac{S^2}{4 (h' + b)^2}}} \quad (3.4)$$

where the correction factor k allows for ionospheric curvature (ϕ_o the angle of incidence on the base of the ionosphere is not equal to the angle ϕ_z at the virtual reflection point) and is distance dependent. For our 2F propagation mode distance of 2235 km, the value of k read from the graph of Wieder (1955) (also reproduced in Davies (1965), p. 170) is 1.077. More correctly, k varies with pathlength (Möller, 1964) . The latter gives the expression (corrected here from his equation (D3.10))

$$f_v = f \cos \phi_z \sqrt{1 - \frac{2 (h' - h) \tan^2 \phi_z}{R + h_o}}, \quad (3.5)$$

showing that k is dependent on the difference between the virtual and real heights of reflection h' and h , as well as on the ionospheric base height h_o .

3.1.3 Validity of the Ionospheric Curvature Correction

The values of the factor k given by Wieder (1955) and Davies (1965) are derived from the above formulation for "median mid-latitude quiet profile" values of $h'-h$ and are plotted as a function of ground range D .

In order to check how well these values applied to our case, the following analysis was performed :

(1) Firstly the 24 daytime vertical ionograms from SANAE, the R.S.A. and Grahamstown used in the $N(h)$ profile analysis (Chapter 6) were reduced to electron density - real height or $N(h)$ profiles using the method outlined in section 5.2.2. The values of h' from these ionograms were also used to compute corresponding values of group path P' for two equivalent hops at oblique incidence, using equation (3.1) given in terms of P' . $h'-h$ was then derived as a polynomial function of $P'-P'_{\min}$, P'_{\min} being here the value of P' derived from h'_{\min} , the minimum virtual height on the ionogram. This polynomial analysis gave surprisingly consistent results. In all cases a linear relation was found to be adequate, and the median values of the coefficients were :

SANAE	:	$a_0 = 19.2$	$a_1 = 0.468$
R.S.A.	:	$a_0 = 24.5$	$a_1 = 0.465$
Grahamstown	:	$a_0 = 23.5$	$a_1 = 0.441$

$$\text{where } h'-h = a_0 + a_1 (P' - P'_{\min}) \quad (3.6)$$

(2) The median values of a_0 and a_1 from the R.S.A. were then used to generate $h'-h$ from $P'-P'_{\min}$ (where P'_{\min} is now the minimum group path) on the corresponding oblique ionograms. The angle ϕ_z was derived from P' in each case by simple geometry (Figure 3.2); the base height h_0 was calculated from P'_{\min} assuming no underlying ionization (i.e. putting $h_0 = h'_{\min}$). The factor k , given from equation (3.5) by

$$k = 1 / \sqrt{1 - \frac{2(h'-h) \tan^2 \phi_z}{R+h_0}} \quad (3.7)$$

was then plotted against $P' - P'_{\min}$.

This, unfortunately, did not give such consistent results. However, median values of the coefficients of a degree 2 polynomial were

$$a_0 = 1.047 \quad a_1 = 3.4 \times 10^{-4} \quad a_2 = -1.6 \times 10^{-6}.$$

More important, perhaps, from the point of view of determining MUF's from vertical records, is the value of k at the MOF of the oblique record; for the 8 daytime oblique ionograms used in the analysis in Chapter 6, k_{MOF} had a median value of 1.053 with upper and lower quartiles of 1.057 and 1.043 respectively. Thus in the conversion from vertical to oblique, it would appear that use of the k value from Wieder (1955) will tend to overestimate the MUF (or JF) by about 2%; the difference between the JF and MOF (the "nose extension") is very often greater than this in practice.

On the other hand, in the conversion from an oblique ionogram to the equivalent vertical one, the value of k near the vertical critical frequency f_oF2 may be considered of prime importance. The oblique ionogram point which transforms to the point closest to f_oF2 on the equivalent vertical ionogram is that with the largest group path P'_{max} (the value of f_v calculated from this point is usually slightly less than f_oF2 , due to absorption). The median value of k at P'_{max} for the same group of oblique ionograms was 1.063; in this conversion, therefore, it would appear that using the Wieder values will lead to an underestimation of f_oF2 by about 1%. The extrapolation used to obtain f_oF2 from the equivalent vertical ionogram points, variability in the nose extension, and possible unequal hop lengths, will probably cause errors considerably greater than this.

For our purposes therefore, in view of the sources of error mentioned above, it was considered justifiable to use the values of k read from the graph of Wieder (1955). For ground ranges D between 1000 and 3000 km (appropriate to our 2, 3 and 4 hop modes), the graph is, to the accuracy to which it can be read, a straight line with equation

$$k = 0.970 + 4.8 \times 10^{-5} D \quad (3.8)$$

for D in km. This was used in the computer programs to allow flexibility for different modes of propagation.

3.1.4 Inverse Transmission Curves

The standard *transmission curve* introduced by Smith (1939) is routinely used to transform from the (f_v, h') co-ordinate system to the (f, P') co-ordinate system and thereby obtain the "equivalent oblique" MUF for a given distance from a vertical ionogram (Piggott and Rawer, 1972). The use of an inverse transmission curve to perform the reverse transformation and determine the equivalent vertical foF2 from an oblique ionogram appears to have been introduced by Möller (1964).

The equation of an inverse transmission curve is easily derived from the geometry of Figure 3.2, where

$$P' = \frac{S}{\sin \phi_z} = \frac{S}{\sqrt{1 - \cos^2 \phi_z}} \quad (3.9)$$

and substitution of $\cos \phi_z$ from equation (3.4), assuming $\phi_z = \phi_o$. This yields

$$P' = \frac{S}{\sqrt{1 - \left(\frac{k f_y}{f}\right)^2}} \quad (3.10)$$

where this P' is the group path for one complete "hop". Then for n equal hops over the total ground range D we can plot total group path nP' against f for a given equivalent vertical frequency f_v using equation (3.10), where S and k have the values S_n and k_n appropriate to a ground range of D/n . The family of curves obtained with $n = 2$, $D = 4470$ km and $f_v = 1, 2, \dots, 10$ MHz is shown in Figure 3.3. The dashed line in this figure is the 2F trace of an oblique ionogram, showing how the high angle ray is asymptotic in a particular value of f_v , in this case 7.3 MHz by interpolation. This is then the maximum frequency that would be reflected at vertical incidence and is the equivalent vertical critical frequency EVFO.

A convenient practical form in which to use these inverse transmission curves as a "slider" or overlay is a series of curves of "excess path" $\Delta P' = P' - D$ vs. f for different values of f_v . The "zero" of the P' scale is then $D = 4470$ km and this may then be made coincident with a height i km on the virtual height scale of the oblique ionogram given by

$$i = D - P_o \quad (3.11)$$

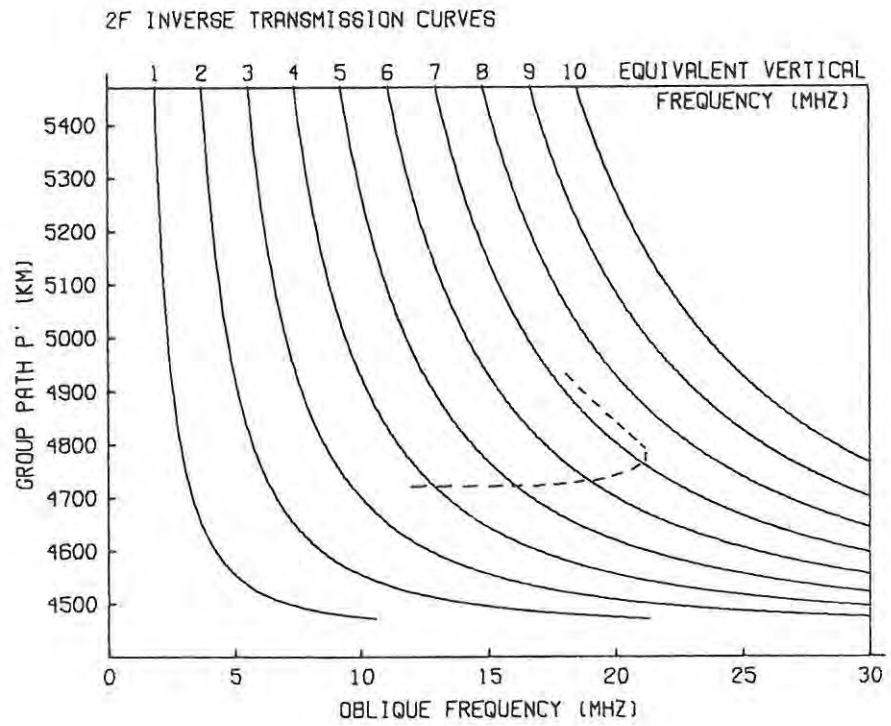


Figure 3.3 : Use of inverse transmission curves in determining the equivalent vertical critical frequency EVFO from the 2F trace of an oblique ionogram (dashed line).

where P_0 is the offset of the oblique ionogram in km.

If the horizontal oblique frequency scales of the oblique ionogram and overlay are also made to coincide, the value of EVFO can immediately be read off by interpolating for the asymptote of the high angle ray. This technique does not appear to have been emphasised previously.

The August 1975 oblique incidence data described in section 3.3.1 were scaled "manually", prior to the development of the computer-assisted scaling methods described in Chapter 4. In this manual method a frequency/group path grid and inverse transmission curve overlay were used, in a manner similar to the normal scaling procedure for vertical ionograms (Piggott and Rawer, 1972). A useful aid in the scaling was an HP-25 programmable pocket calculator; a program was written which :

- (a) computed the offset in km at a given ionogram time given its value in msec at 1200 UT on that day and the current drift rate in msec/week (equation (2.6)). The values of i (equation (3.11)), for positioning the zero of the inverse transmission curve, and P' for a given trace given the "virtual height" on the ionogram, could then be displayed in turn.
- (b) calculated EVH' from P' for a given number n of equal hops (equations (3.1) - (3.3)). This aided considerably in the identification of modes (next section).

In scaling "mode by mode" it is generally convenient to proceed in order of increasing minimum group path for the trace. Some of the qualifying and descriptive letters used in vertical incidence scaling (Piggott and Rawer, 1972) are also useful here in describing doubtful values, peculiar conditions, or why a value could not be scaled. They are used with the same meanings, except that R after a P' value means retardation at the low frequency end of a trace. Some examples are given in Table 4-3.

3.1.5 Mode Identification

The identification of traces on an oblique ionogram with individual modes of propagation is undoubtedly a major difficulty in the interpretation of the ionogram (Davies, 1965, p. 188). Kift (1960) presented a detailed mode analysis for the Ascension Island - Slough path (6750 km), showing, in particular, "mode plots" of excess time Δt and angle of elevation Δ against ground range D (an example is quoted by Davies (1965), p. 190), using the Appleton and Beynon (1940) parabolic layer method for F reflections and assuming mirror reflections at sporadic-E layers. Ray tracing procedures will generally provide unambiguous mode identification (e.g. Kuriki *et al.*, 1974; Lambert, 1977), but, because of the time required, cannot be used for routine scaling. Some criteria are therefore required upon which the designation of modes on an oblique ionogram can be based; those used in this work are outlined below.

The value of $EVH'F$ computed from the measured P'_{\min} for an assumed mode designation can be used to test the "reasonableness" of this designation. For multiple-F modes ($n_F F$, say), $EVH'F$ is simply calculated using equation (3.1) after dividing P'_{\min} by n_F . For modes involving E layer reflections as well, it is conveniently found by interpolation in a table of P' values for a number of different modes, a fixed value of $EVH'E$, and a range of $EVH'F$ values, such as is shown in Table 3-1, in which each entry for an $n_F F + n_E E$ mode is calculated according to the following formulation :

- (i) Suppose that all F hops are equal and each covers a ground range D_F , and that all E hops are equal and each covers a ground range D_E ; the respective half-angles at the centre of the earth are then (Figure 3.4)

$$\theta_F = \frac{D_F}{2R} \quad \text{and} \quad \theta_E = \frac{D_E}{2R} \quad (3.6)$$

$$\text{where} \quad n_F \theta_F + n_E \theta_E = \theta = \frac{D}{2R} \quad (3.7)$$

$$\text{so that} \quad \theta_F = \frac{\theta - n_E \theta_E}{n_F} \quad (3.8)$$

(The total ground range D is known.)

Table 3-1 : Group path P' for given modes (1F, 1F+E, etc.) and virtual heights h'_E (= 110 km) and h'_F (= 200, 205, ... km) of the E and F layers respectively. (Ground range D = 4470 km.)

H'E = 110 KM		EFFECTIVE PATHLENGTH (KM)																
H'F	1F	1F+E	1F+2E	2F-E	2F	2F+E	2F+2E	3F-2E	3F-E	3F	3F+E	3F+2E	4F-2E	4F-E	4F	4F+E	4F+2E	5F
200	4534	4563	4597	4575	4604	4643	4693	4614	4647	4693	4750	4818	4694	4748	4812	4886	4970	5134
205	4537	4566	4600	4580	4609	4649	4700	4621	4655	4702	4761	4829	4706	4761	4827	4903	4988	5164
210	4539	4568	4602	4585	4614	4655	4706	4629	4664	4712	4771	4841	4719	4775	4842	4920	5006	5195
215	4542	4571	4605	4590	4620	4661	4713	4636	4673	4722	4782	4853	4731	4789	4858	4937	5024	5225
220	4545	4573	4608	4595	4625	4667	4720	4644	4682	4732	4793	4865	4744	4804	4874	4954	5043	5257
225	4547	4576	4611	4600	4631	4673	4727	4652	4691	4742	4805	4877	4757	4818	4890	4972	5062	5289
230	4550	4579	4614	4605	4636	4679	4734	4660	4700	4752	4816	4890	4771	4833	4907	4989	5081	5321
235	4553	4581	4617	4610	4642	4686	4741	4668	4709	4763	4827	4902	4785	4849	4923	5008	5101	5354
240	4555	4584	4620	4616	4648	4692	4748	4677	4719	4773	4839	4915	4799	4864	4940	5026	5120	5387
245	4558	4587	4623	4621	4654	4699	4755	4685	4728	4784	4851	4928	4813	4880	4958	5045	5140	5421
250	4561	4590	4626	4627	4660	4705	4762	4694	4738	4795	4863	4941	4828	4896	4975	5063	5160	5455
255	4564	4592	4629	4632	4666	4712	4770	4703	4748	4806	4875	4954	4842	4913	4993	5083	5181	5490
260	4567	4595	4632	4638	4672	4719	4777	4712	4758	4817	4887	4968	4858	4929	5011	5102	5201	5525
265	4570	4598	4635	4643	4678	4726	4785	4721	4768	4829	4900	4981	4873	4946	5029	5122	5222	5560
270	4572	4601	4638	4649	4684	4732	4792	4730	4779	4840	4913	4995	4889	4963	5048	5141	5243	5596
275	4575	4604	4641	4655	4690	4739	4800	4740	4790	4852	4925	5009	4905	4981	5067	5161	5265	5633
280	4578	4607	4644	4660	4697	4747	4808	4749	4800	4864	4938	5023	4921	4998	5086	5182	5286	5669
285	4581	4610	4648	4666	4703	4754	4816	4759	4811	4876	4951	5037	4937	5016	5105	5202	5308	5707
290	4584	4613	4651	4672	4710	4761	4823	4769	4822	4888	4965	5051	4954	5034	5124	5223	5330	5744
295	4587	4616	4654	4678	4716	4768	4831	4779	4834	4901	4978	5065	4971	5053	5144	5244	5352	5782
300	4590	4619	4658	4684	4723	4776	4840	4789	4845	4913	4992	5080	4988	5072	5164	5265	5374	5820
305	4593	4622	4661	4690	4730	4783	4848	4800	4857	4926	5005	5094	5006	5090	5184	5287	5397	5859
310	4596	4625	4664	4696	4737	4791	4856	4810	4868	4939	5019	5109	5024	5110	5205	5308	5420	5898
315	4599	4628	4668	4703	4744	4798	4864	4821	4880	4951	5033	5124	5042	5129	5226	5330	5443	5937
320	4602	4631	4671	4709	4751	4806	4873	4832	4892	4965	5047	5139	5060	5149	5246	5352	5466	5977
325	4605	4635	4674	4715	4758	4814	4881	4843	4904	4978	5062	5155	5079	5169	5268	5375	5489	6017
330	4608	4638	4678	4722	4765	4822	4890	4854	4917	4991	5076	5170	5097	5189	5289	5397	5513	6057
335	4611	4641	4681	4728	4772	4829	4898	4865	4929	5005	5090	5185	5116	5209	5310	5420	5537	6098
340	4615	4644	4685	4735	4779	4837	4907	4877	4942	5018	5105	5201	5136	5230	5332	5443	5561	6139
345	4618	4648	4688	4742	4787	4845	4916	4888	4955	5032	5120	5217	5155	5250	5354	5466	5585	6180
350	4621	4651	4692	4748	4794	4854	4926	4900	4968	5046	5135	5233	5175	5271	5376	5489	5609	6222

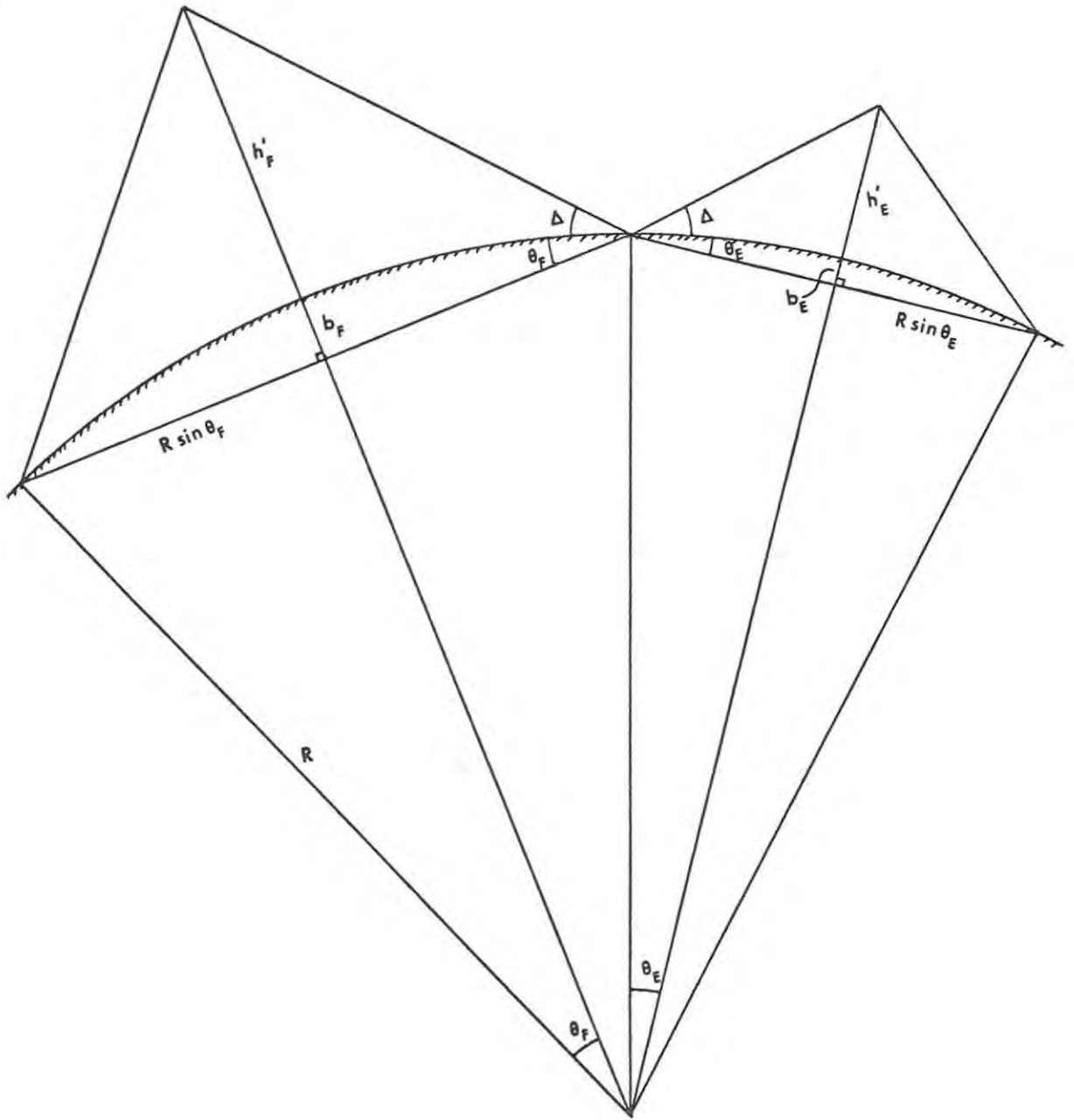


Figure 3.4 : The geometry of an F + E mode with virtual heights of refl h'_F and h'_E respectively.

- (ii) Suppose that the ray undergoes specular reflections at the ground; then its elevation angle is (Figure 3.4, with b_E given by equation (3.3))

$$\Delta = \tan^{-1} \left[\frac{h'_E + R(1 - \cos \theta_E)}{R \sin \theta_E} \right] - \theta_E \quad (3.9)$$

and from similar geometrical considerations

$$h'_F + R(1 - \cos \theta_F) = R \sin \theta_F \tan (\Delta + \theta_F) . \quad (3.10)$$

- (iii) Substitution for θ_F from (3.8) and Δ from (3.9) then yields an equation implicit in θ_E ,

$$f(\theta_E) = R \sin \theta_F \tan (\Delta + \theta_F) - R(1 - \cos \theta_F) - h'_F = 0 \quad (3.11)$$

which is used to generate a value of θ_E from the Newton-Raphson algorithm. Initial values of P' and θ_E are obtained from consideration of the plane earth case, where

$$P' = \sqrt{4 (n'_E h'_E + n'_F h'_F)^2 + D^2} \quad (3.12)$$

and
$$D_E = \frac{D h'_E}{n'_E h'_E + n'_F h'_F} . \quad (3.13)$$

- (iv) For each iteration θ_F and Δ are found from (3.8) and (3.9) respectively, and P' is then given by (Figure 3.4)

$$P' = 2n_F R \sin \theta_F \sec (\Delta + \theta_F) + 2n_E R \sin \theta_E \sec (\Delta + \theta_E) . \quad (3.14)$$

The procedure is continued until successive values of P' converge to within, say, 1 km of each other.

(For $n_{F'} - n_E$ modes a negative value of n_E is used in the above formulation).

The value of $EVH'F$ obtained can be used in three ways to test whether the mode designation is "reasonable" :

- (a) it should lie within a "reasonable" range, say 150 - 500 km;
- (b) it should not differ too greatly from the value for the same mode (if present) on the previous ionogram;
- (c) if tilts are small, it should be consistent with values for other modes on the same ionogram.

Other criteria which are sometimes helpful are :

- (d) traces involving reflections at the bottom of an E-layer should be relatively weaker than ones involving reflections at the top of the layer as the latter spend considerably less time in the D region where most absorption occurs;
- (e) modes involving sporadic E layers would be expected to be less stable and continuous than multiple-F modes.

Multiple-E modes (generally 3E, 4E and 5E here) are easily recognized as "flat" traces with low P' in which P' does not appreciably increase with frequency and which lack a high-angle ray. $EVH'E$ can of course be calculated from P' in the same manner as $EVH'F$ for multiple-F modes.

Daytime oblique ionograms are generally simple, showing only multiple-F modes, and the least delayed trace can usually be identified as the 2F mode (sunspot minimum) or 1F mode (sunspot maximum). Around sunset in winter, however, the ionograms often contain a number of intermediate traces (often spread), interpretation of which may be difficult. The regularity with which they occur suggests that they may be due to large tilts and/or gradients caused by the different times of sunset along the path, rather than to the presence of sporadic-E layers. Shortly after this there is generally a period of heavy absorption, so that continuity is lost, making nighttime mode designations probably less reliable than daytime ones.

When analysing oblique ionograms from a "communications" viewpoint it would probably be more satisfactory to simply number the modes consecutively

1, 2, 3, in order of ascending minimum group path, rather than attempt to define individual modes (The "equivalent vertical" parameters EVFO and EVH' will then of course be meaningless). However, as long as LLOF, JF, MOF, HLOF and P' for every trace on the ionogram are scaled, the data can be analysed in this manner equally well, so that such parameters as the overall LOF, MOF and MRF (Davies, 1965, p. 193) can be easily obtained for comparison with predictions. It is generally convenient to scale the modes in order of ascending P'_{\min} in any case.

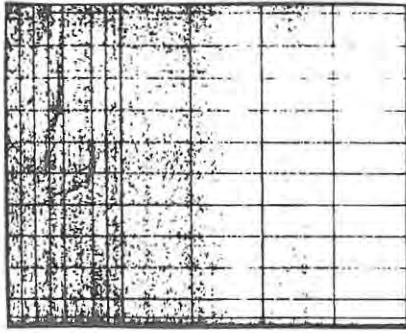
Angle of arrival measurements would be of considerable assistance in the designation of modes (Gething, 1978); it is planned to introduce these measurements shortly.

3.2 Catalogue of SANAE-Grahamstown Oblique Ionograms

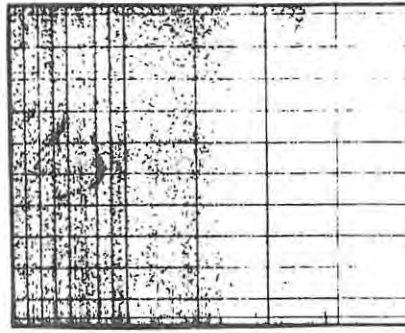
In this section some examples of oblique ionograms obtained on the SANAE - Grahamstown path are used to illustrate particular features. As in the work of Möller (1964), sequences of ionograms are shown in order to illustrate temporal variations as well. In some cases they may be compared with examples in Agy *et al.* (1959). The times of the ionograms are given, as recorded, in SAST = 30°E meridian time. The frequency and group path scales of all the ionograms are as given in Figure 3.1.

- (1) Day 085 (25 March) 1976, 0535-0820 SAST
(Figure 3.5)

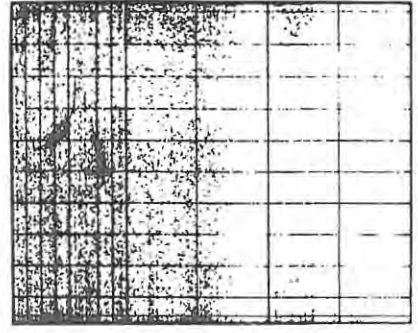
A morning sequence showing the transition from nighttime to daytime conditions, often accompanied by high absorption. The 2F and 3F modes are present in the first four ionograms; at 0635 SAST the 2F mode has disappeared, the 3F is very weak and the 4F is present. The 2F mode reappears between 0720 and 0735, and the 5F also appears.



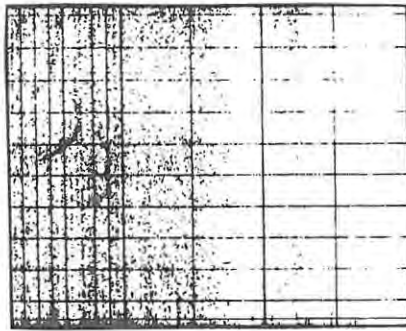
0535



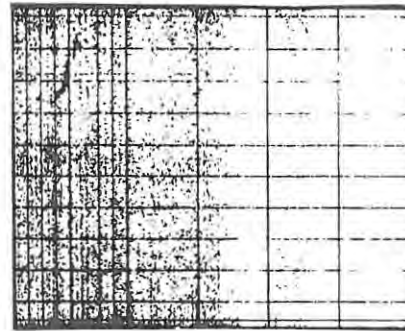
0550



0605



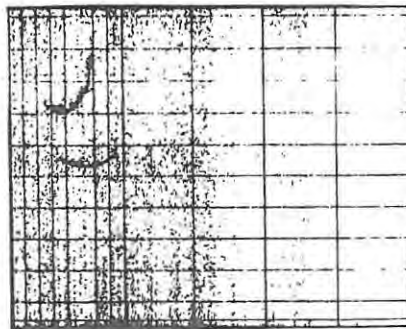
0620



0635



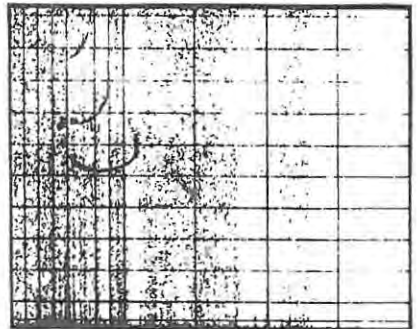
0650



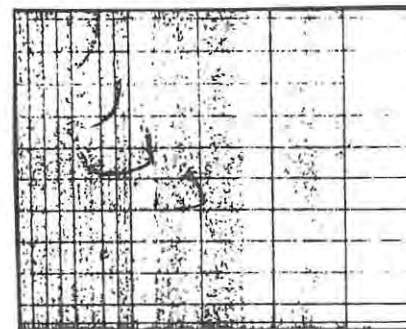
0705



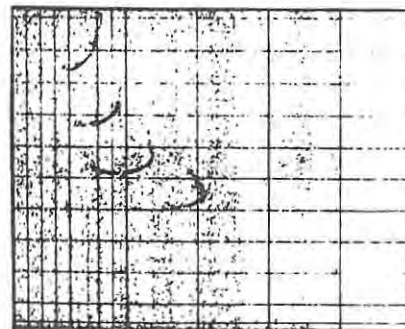
0720



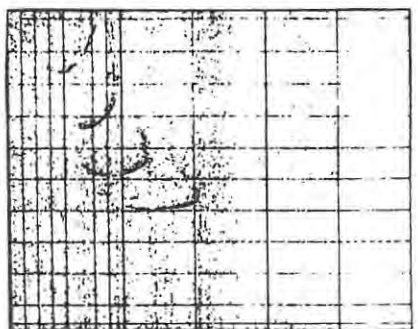
0735



0750



0805



0820

Figure 3.5 : 1976 Day 085 0535-0820 SAST.

(2) Day 085 (25 March) 1976, 1250-1450 SAST

(Figure 3.6)

A daytime sequence showing the development of a "nose extension" on the 2F mode due to scattering (Möller, 1964) with a well defined lower edge; the three modes present are the 2F, 3F and 4F.

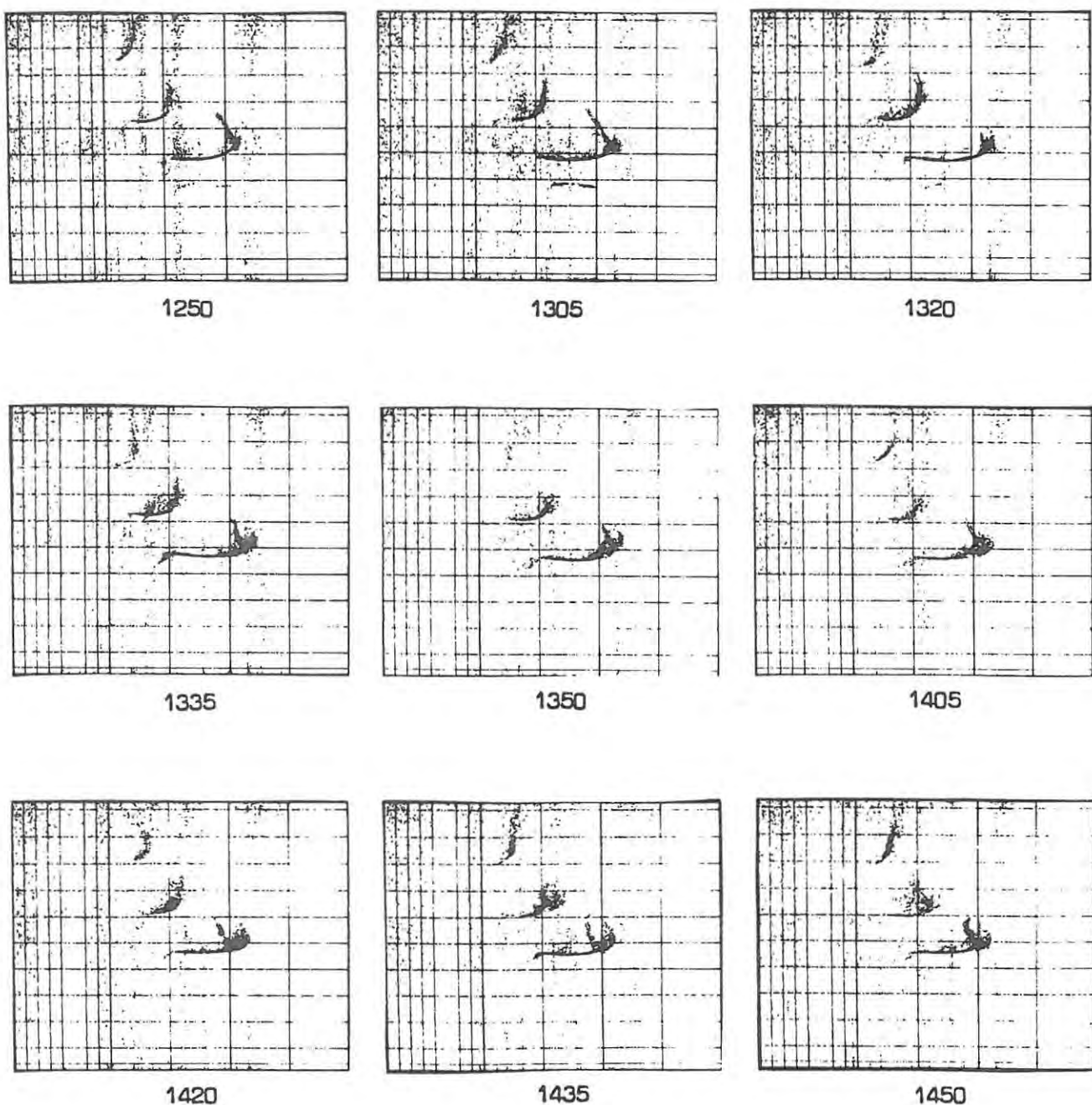


Figure 3.6 : 1976 Day 085 1250-1450 SAST.

(3) Day 085 (25 March) 1976, 1835-2120 SAST

(Figure 3.7)

An evening sequence showing the transition from daytime to nighttime behaviour. An intermediate mode (possibly $2F + E$) is present from the beginning of the sequence. Further traces appear at 1935 and 1950 (possibly $2F + 2E$, $3F + E$ and $3F + 2E$), but by 2035 the normal $2F$, $3F$ and $4F$ traces are restored. Absorption then begins to increase rapidly; by 2105 the $2F$ mode has disappeared and at 2120 the $3F$ mode is weak and spread.

(4) Day 272 (29 September) 1975, 0805-1120 SAST

(Figure 3.8)

An unusual daytime sequence showing the development of an F_1 trace below the F_2 on the $2F$, $3F$ and $4F$ modes. In addition the $1F$ Pedersen (high-angle) ray is present from 0950 SAST, showing splitting into o- and x- components. (The records between 0835 and 0935 SAST as well as the 1050 record are missing because of power failures at Grahamstown. A timing advance of approximately 0.5 msec was made between 1105 and 1120 SAST).

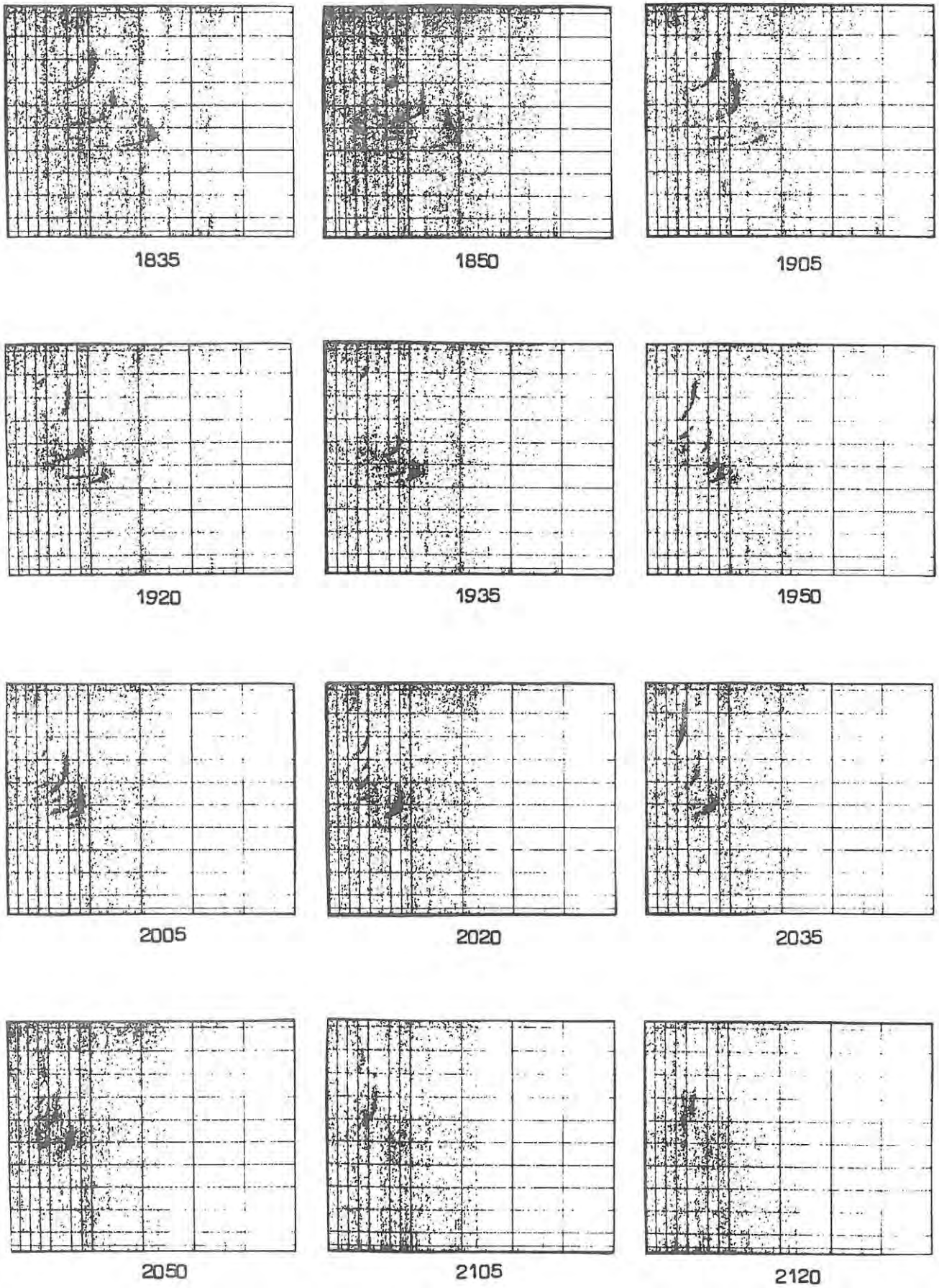
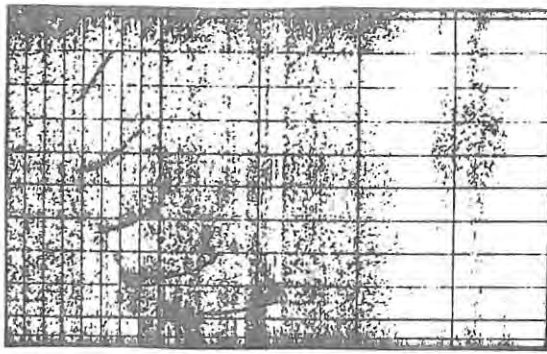
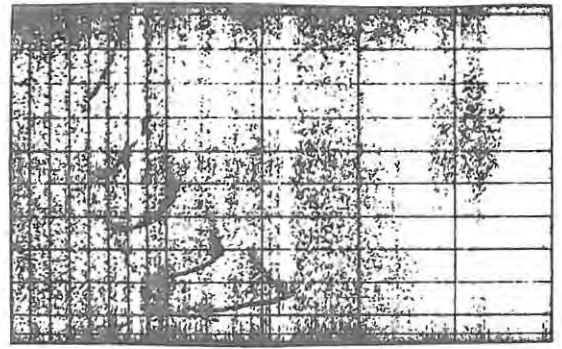


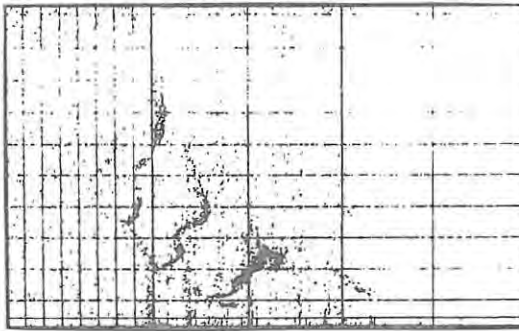
Figure 3.7 : 1976 Day 085 1835-2120 SAST.



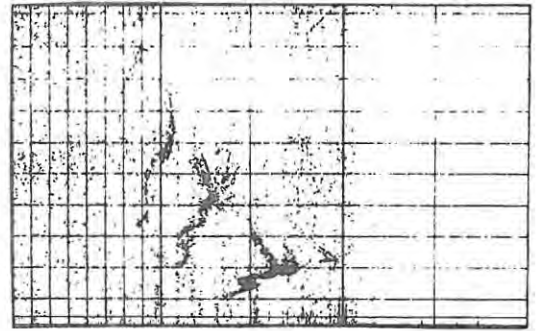
0805



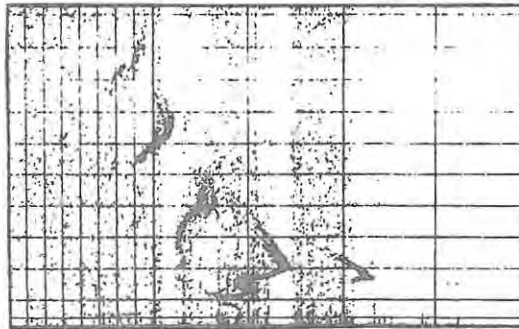
0820



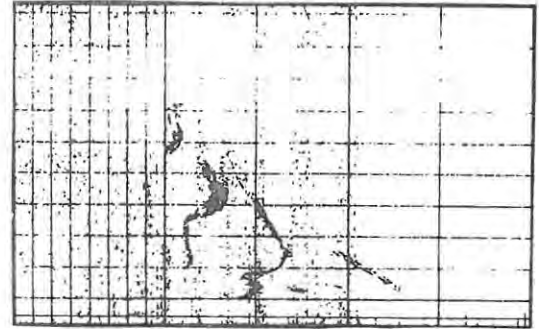
0950



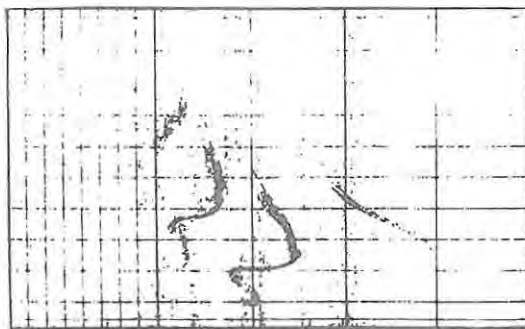
1005



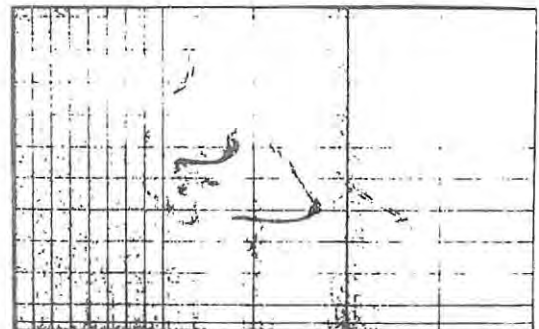
1020



1035



1105

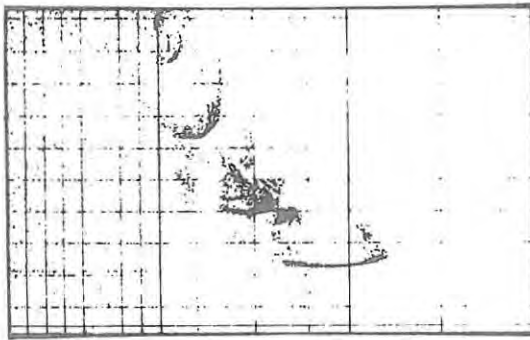


1120

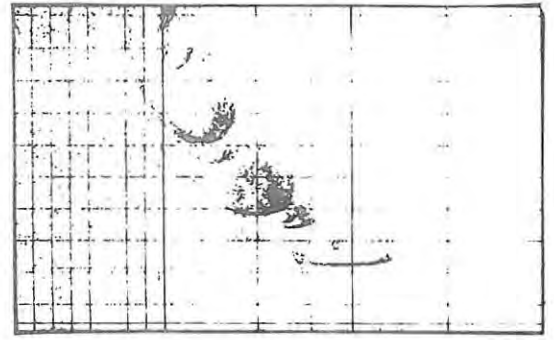
Figure 3.8 : 1975 Day 272 0805-1120 SAST.

- (5) Day 348 (14 December) 1975, 1005-1105 SAST
(Figure 3.9)

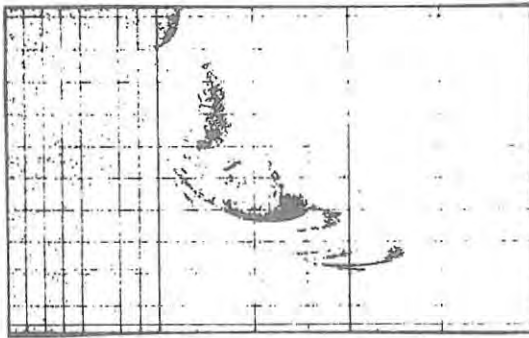
A daytime sequence showing strong retardation at the low frequency end of the 2F, 3F and 4F modes, presumably due to the presence of a thick underlying layer of ionization.



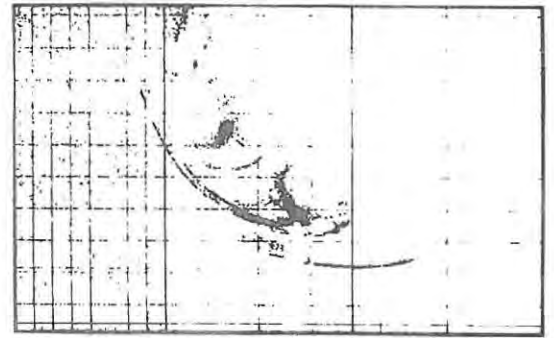
1005



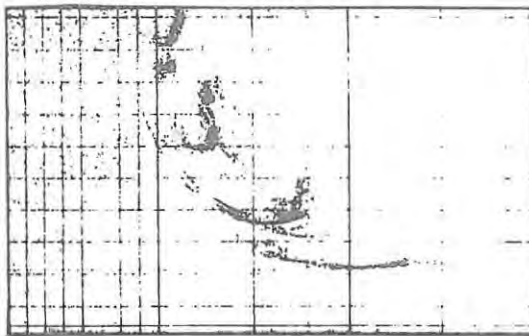
1020



1036



1050

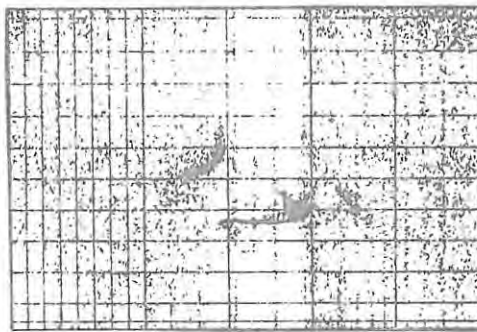


1105

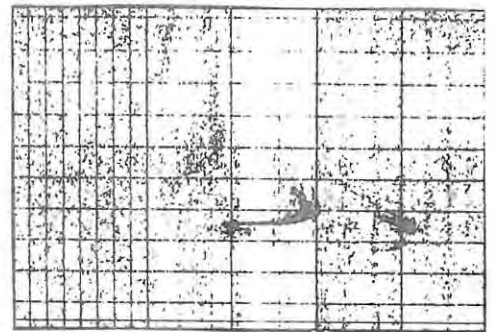
Figure 3.9 : 1975 Day 348 1005-1105 SAST.

- (6) Day 260 (17 September) 1977, 1135-1235 SAST
(Figure 3.10)

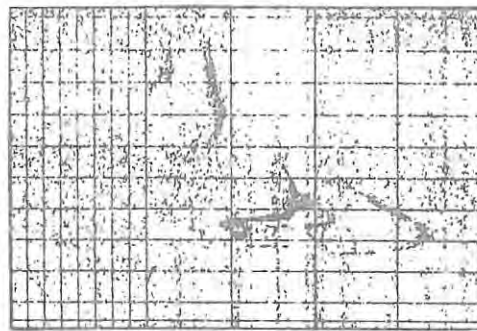
A daytime sequence showing the appearance and disappearance of the 4F mode and the 1F Pedersen ray, the latter attaining an MOF of nearly 28 MHz at 1220 SAST. A weak 1F low angle ray is present at 1205 SAST, an unusual occurrence.



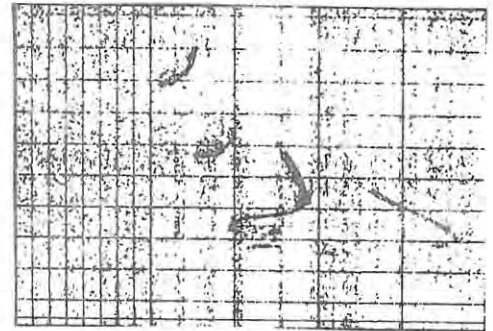
1135



1150



1205



1220



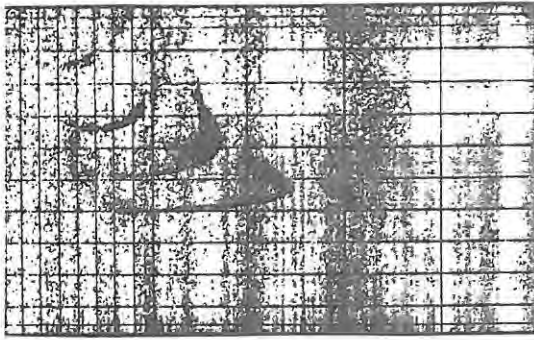
1235

Figure 3.10 : 1977 Day 260 1135-1235 SAST.

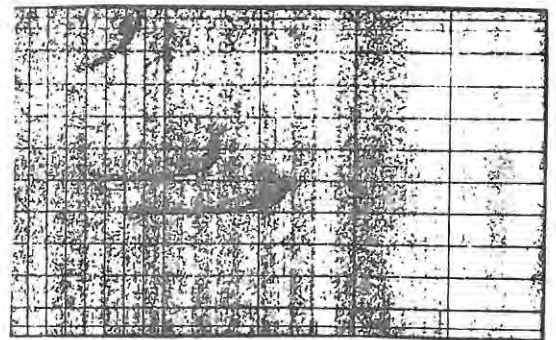
- (7) Day 232 (20 August) 1975, 1720-1850 SAST
(Figure 3.11)

A late afternoon sequence showing successive fading of modes. At 1720 the 1F (Pedersen ray), 2F, 3F, 4F and 5F modes are present. The 1F and 4F have disappeared by 1735; at 1750 the 5F disappears and the 4F reappears; at 1805 the 4F disappears again and a low-lying trace, possibly 2F-E, appears. At 1820 the high frequency end of the 2F trace apparently experiences strong deviative absorption and the 4F and 5F modes reappear; another mode, possibly 4F-E, is also present. By 1835 the 2F and 4F modes have almost disappeared, but at 1850 all four modes are present again.

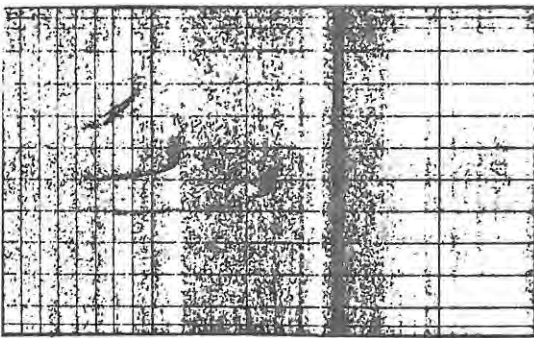
An alternative explanation for this behaviour can be given in terms of increased curvature at each of the reflection points in turn, caused by a northward-propagating travelling ionospheric disturbance (TID). If this is at the 4F first reflection point at 1735 and at the second (the same as the 2F first reflection point) an hour later, its velocity is $\sim 300 \text{ ms}^{-1}$, near the upper limit of velocities observed for medium-scale TID's (Francis, 1974, 1975).



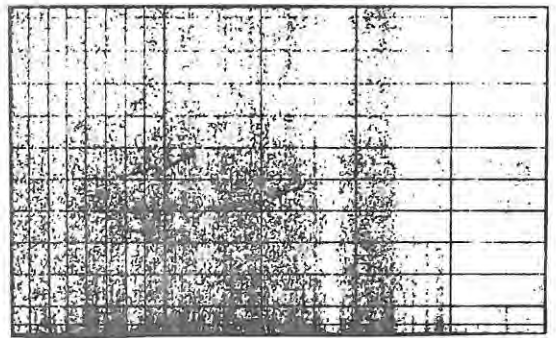
1720



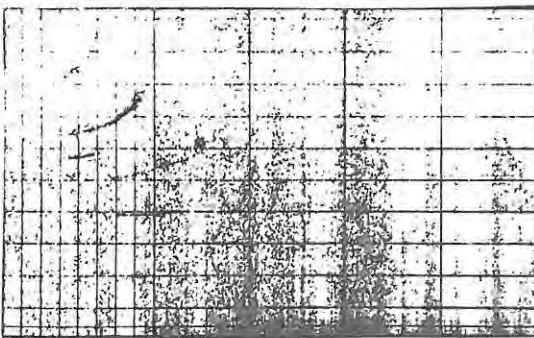
1735



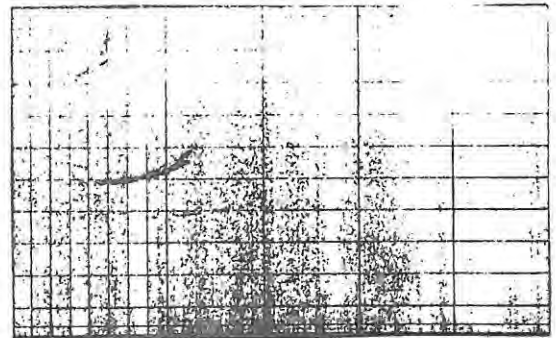
1750



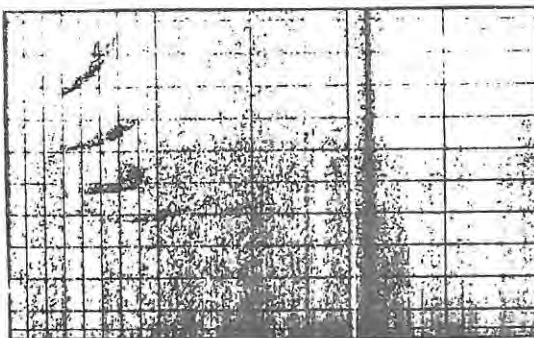
1805



1820



1835



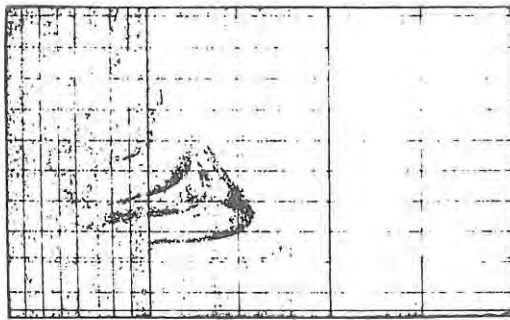
1850

Figure 3.11 : 1975 Day 232 1720-1850 SAST.

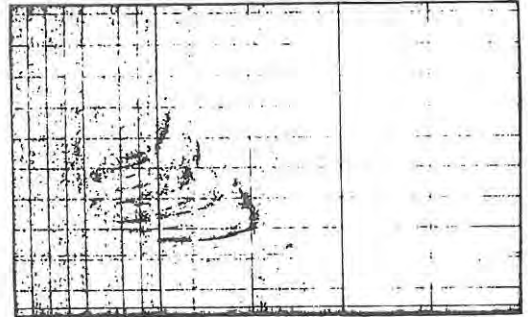
(8) Day 348 (14 December) 1975, 2120-2250 SAST

(Figure 3.12)

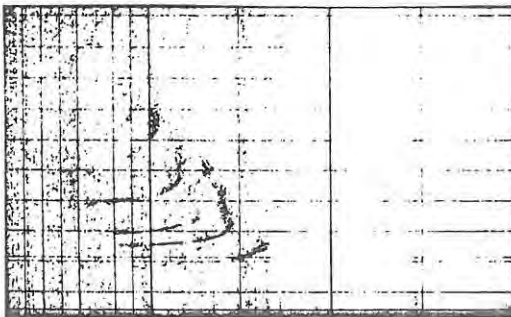
A summer evening sequence showing intermediate traces, possibly due to gradients, and the disappearance of the 2F mode from 2250 SAST.



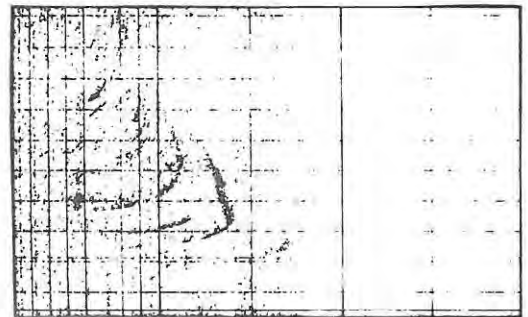
2120



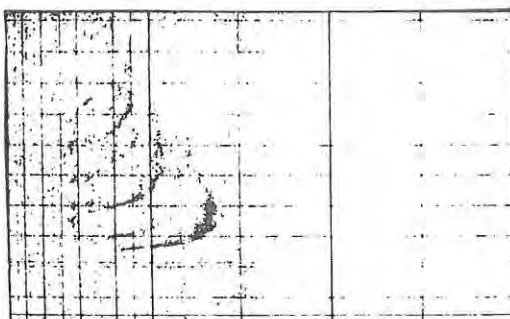
2135



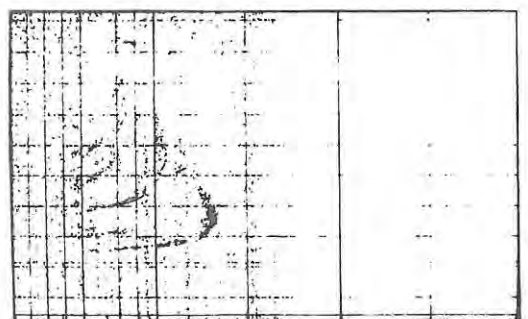
2150



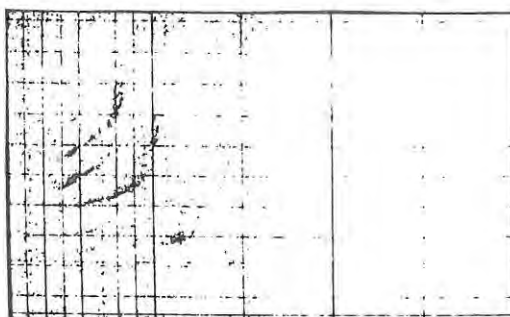
2205



2220



2235

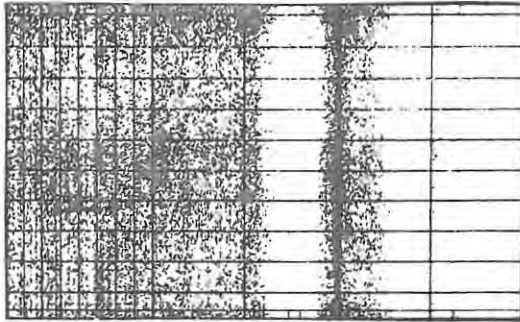


2250

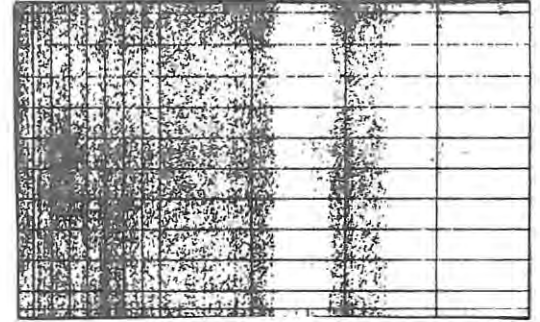
Figure 3.12 : 1975 Day 348
2120-2250 SAST

(9) Day 158 (8 June) 1975, 0120-0305 SAST
(Figure 3.13)

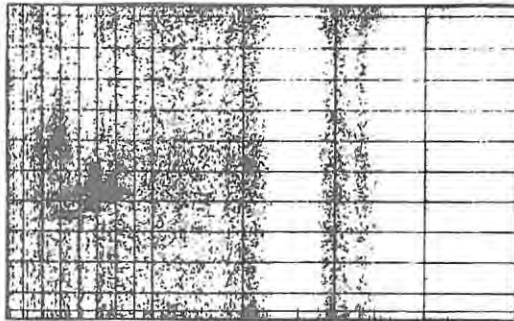
A winter nighttime sequence showing the appearance of the 2F and 3F modes, as well as other modes involving sporadic-E layer reflections, with spread traces. Ionograms such as this are often difficult to interpret.



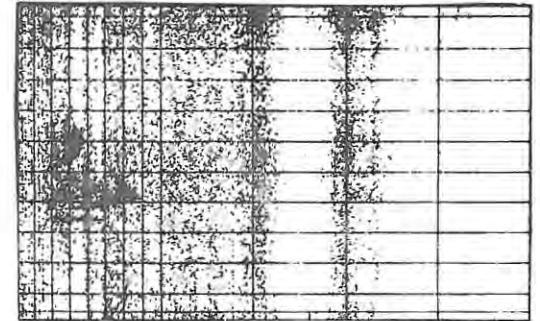
0120



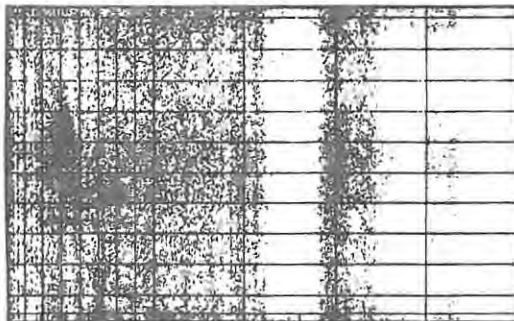
0135



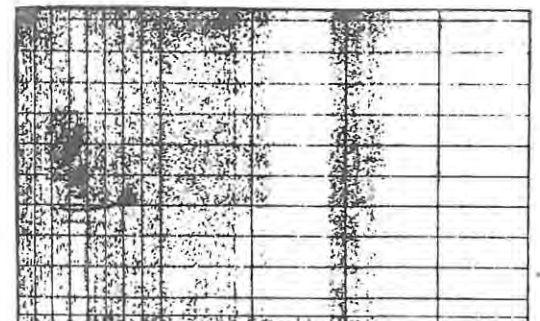
0150



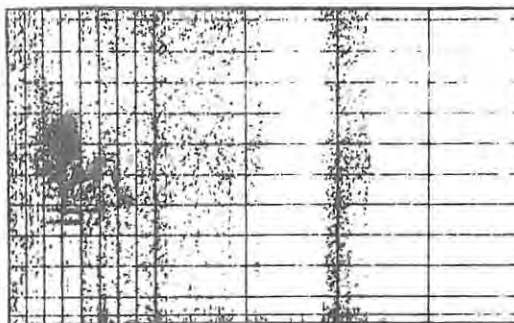
0205



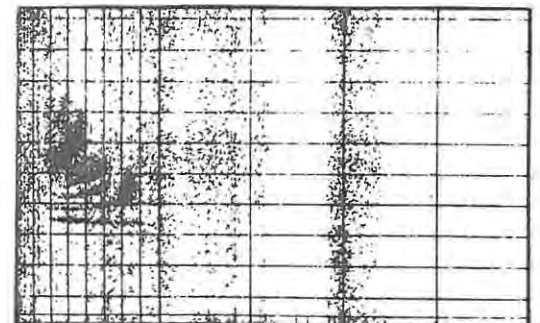
0220



0235



0250



0305

Figure 3.13 : 1975 Day 158 0120-0305 SAST.

(10) Day 262 (19 September) 1977 0905-0950 SAST
(Figure 3.14)

A morning sequence showing multiple-E (3E, 4E, 5E) traces
(over the frequency range 6 - 10 MHz).

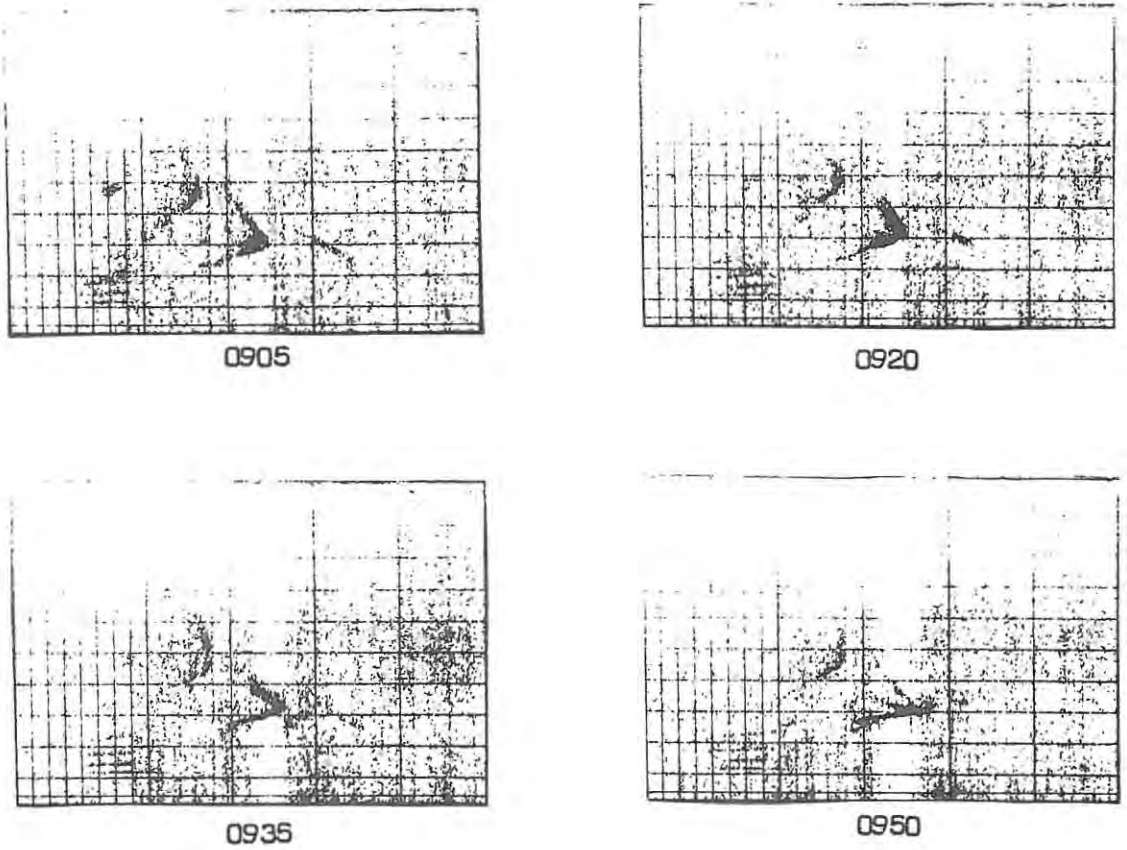


Figure 3.14 : 1977 Day 262 0905-0950 SAST.

3.3 Monthly Median Analysis

3.3.1 Winter Month (August 1975)

The month of August 1975 was chosen for the first analysis because

(i) the offset was known for almost the entire month,
and (ii) magnetic and ionospheric conditions were generally quiet so there was little loss of data due to blackout.

It was felt that a median analysis would serve as a first test of the "mode analysis" outlined in sections 3.1.4 and 3.1.5, and also provide some reliable data representative of quiet conditions. Hourly oblique ionograms (those with the sweep commencing at 05 minutes in the hour) were scaled "manually" (section 3.1.4). From the tabulated data median values of MOF, LLOF, EVFO and P'_{\min} , as well as EVH'F from the latter, for each of the modes 2F, 3F and 4F for each hour of the day were computed manually; these medians, together with the counts for each mode, are tabulated in Appendix D.

Median values with counts of 5 or greater are plotted against time (UT) in figures 3.15 - 3.20, where the symbols 2, 3 and 4 represent the 2F, 3F and 4F modes respectively. These show that :

- (i) The MOF's and LLOF's (Figures 3.15 and 3.16) of all three modes increase consistently during the day to peak in the early afternoon;
- (ii) The high-angle ray asymptotes for all three modes are normally identical, as evidenced by the consistency in EVFO shown in Figure 3.17; the latter may be compared with Figure 3.18, which shows the variation of foF2 at the end points on the same scale. (Data for Hermanus instead of for Grahamstown were used because the latter were not available; the two usually have almost identical characteristics). The EVFO's clearly follow the behaviour of foF2 at SANAE rather than at Hermanus, although they are slightly greater than the former after sunrise (0600-1100 UT) and sunset (2000-2200 UT). EVFO (2F) does appear to be significantly higher than EVFO (3F) and EVFO (4F) at night.

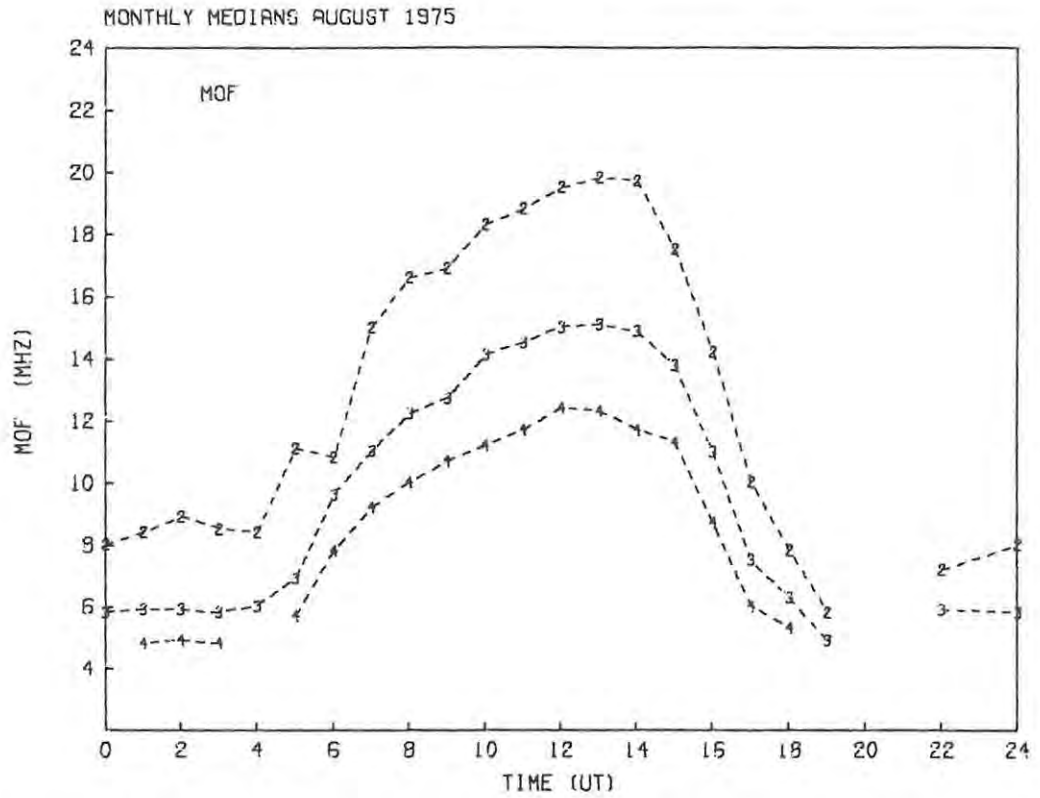


Figure 3.15 : Diurnal variation in monthly median MOF for August 1975 for the 2F, 3F and 4F modes (symbols 2, 3 and 4 respectively).

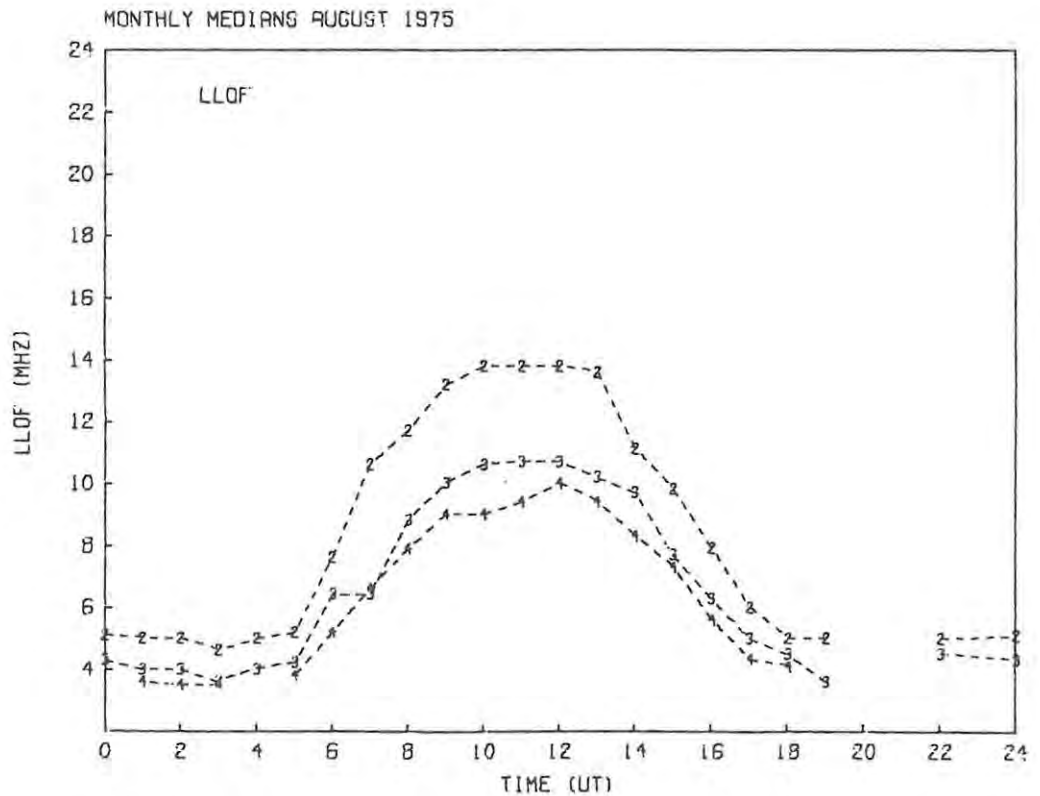


Figure 3.16 : Diurnal variation in monthly median LLOF for August 1975 for the 2F, 3F and 4F modes (symbols 2, 3 and 4 respectively).

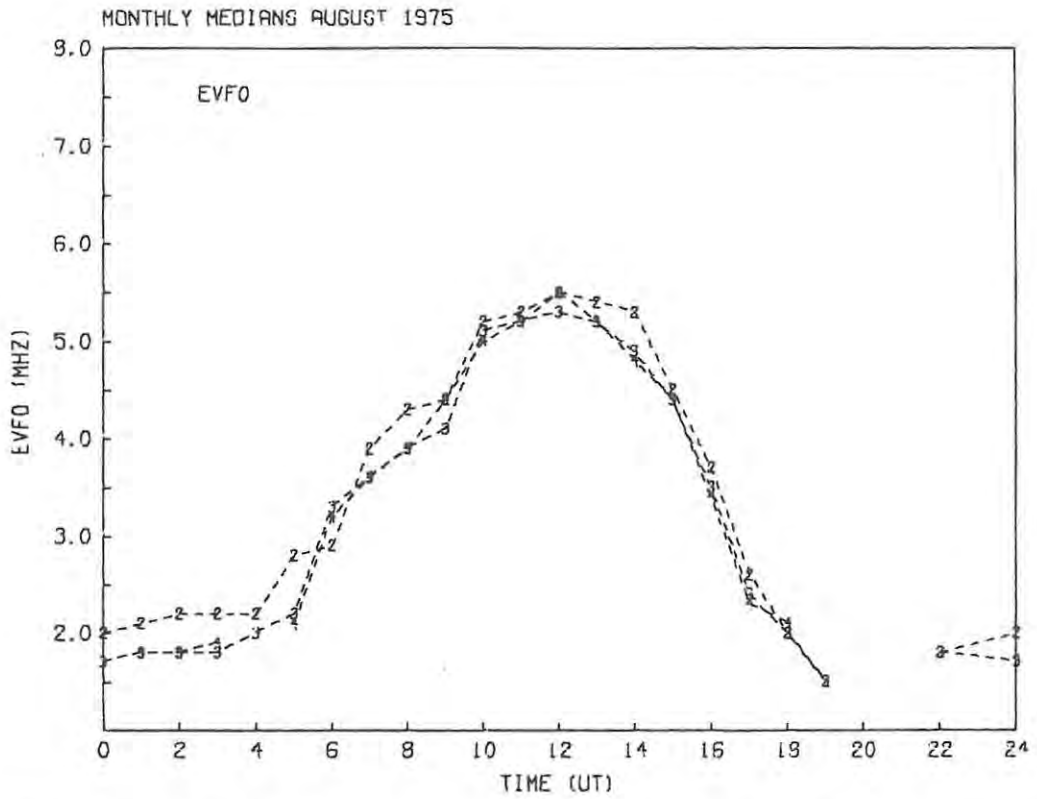


Figure 3.17 : Diurnal variation in monthly median EVFO for August 1975 for the 2F, 3F and 4F modes (symbols 2, 3 and 4 respectively).

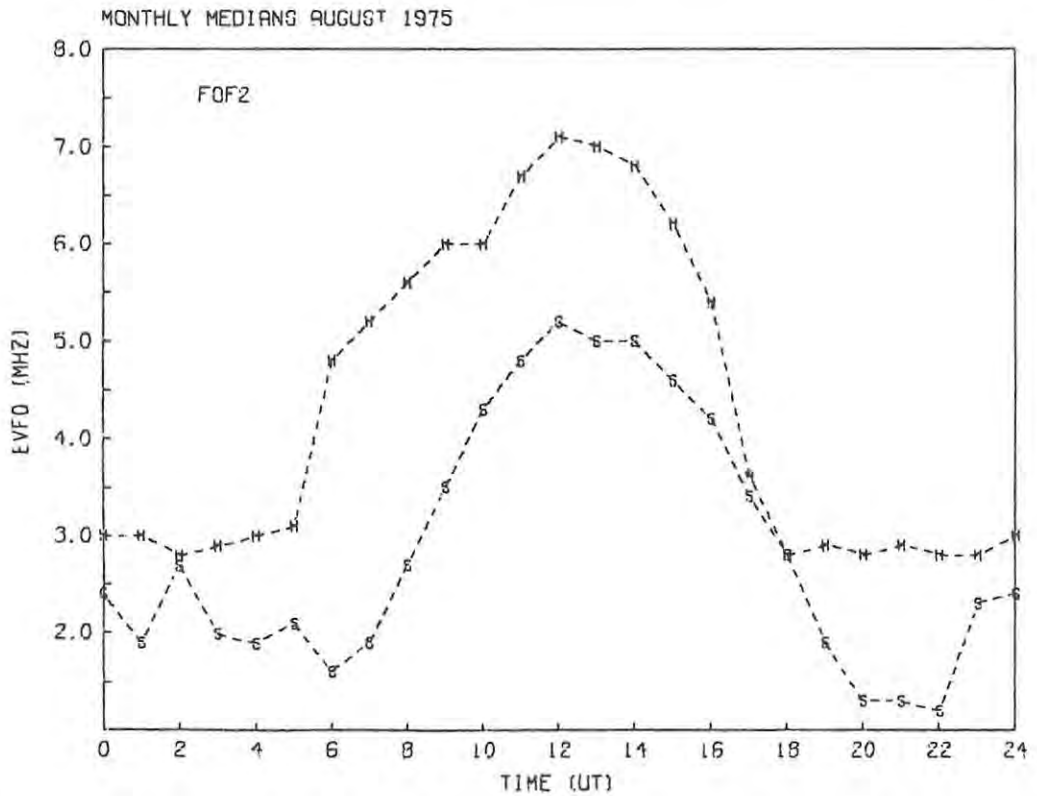


Figure 3.18 : Diurnal variation in monthly median foF2 for August 1975 at SANAE (S) and Hermanus (H).

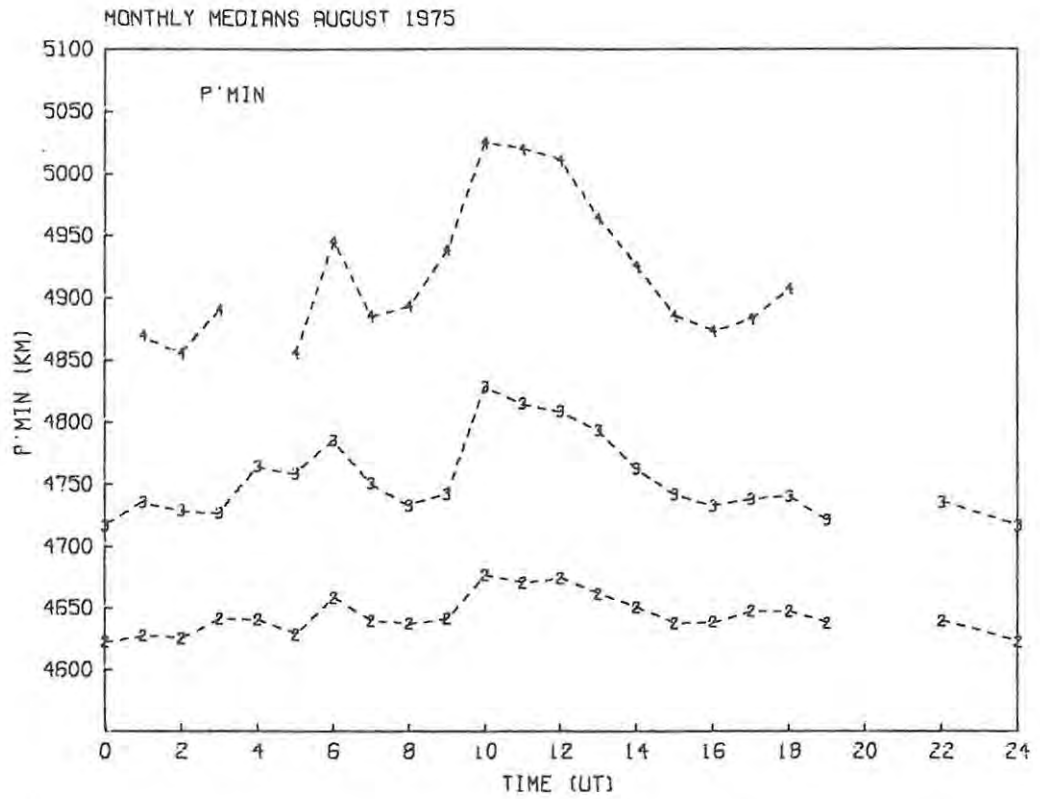


Figure 3.19 : Diurnal variation in monthly median P'_{min} for August 1975 for the 2F, 3F and 4F modes (symbols 2, 3 and 4 respectively).

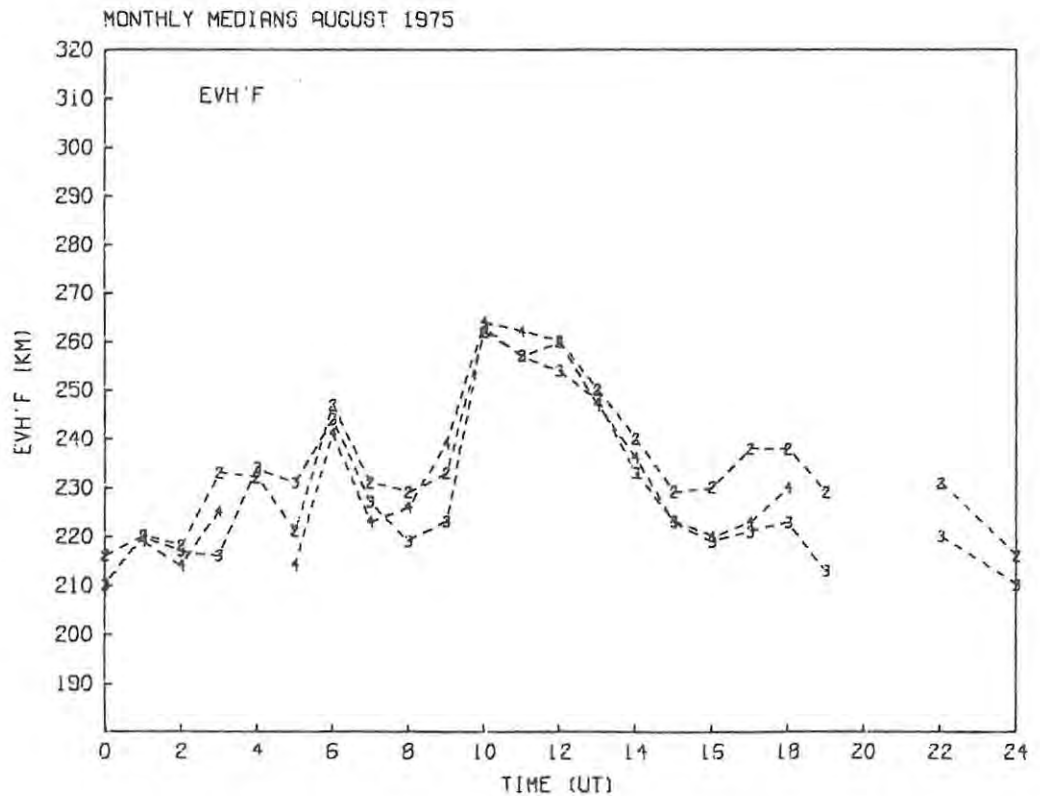


Figure 3.20 : Diurnal variation in monthly median EVH'F for August 1975 for the 2F, 3F and 4F modes (symbols 2, 3 and 4 respectively).

- (iii) P'_{\min} for each mode and the EVH'F derived from it in each case are plotted in Figures 3.19 and 3.20 respectively; the main feature is a consistent increase in P' for all three modes during the day. The apparently more erratic behaviour at night is probably due to incorrect mode designations and less significant (lower count) median values.

3.3.2 Summer Month (January 1976)

In this case the oblique ionograms were scaled by the computer-assisted method described in Chapter 4; the mutual consistency of the two sets of data is discussed in section 4.4.

The median data are again tabulated in Appendix D, and values with counts of 5 or greater plotted in Figures 3.21 - 3.26, which show that :

- (i) The MOF's and LLOF's (Figures 3.21 and 3.22) of the 2F and 3F modes are essentially constant between 0600 and 1800 UT, showing the effect of the longer daylight hours.
- (ii) The 4F and higher order modes are now rarely observed during the day, showing the effects of higher absorption in summer.
- (iii) The EVFO values from the different modes (Figure 3.23) are not as consistent as the winter values. There are significant differences between the three in the early morning hours, possibly indicating the presence of ionization gradients (foF2 increasing towards SANAE).
- (iv) The latter is consistent with the variation of foF2 at SANAE (S) and Hermanus (H) shown in Figure 3.24 for comparison. foF2 at SANAE is practically constant, with some evidence of a UT-controlled maximum at 0600 UT (Gledhill and Williams, 1971).
- (v) The increase in P'_{\min} during the day is less clearly defined and is less consistent in terms of EVH'F (Figure 3.26). The values are also somewhat more erratic, although again the low counts of the 4F values reduce their significance.

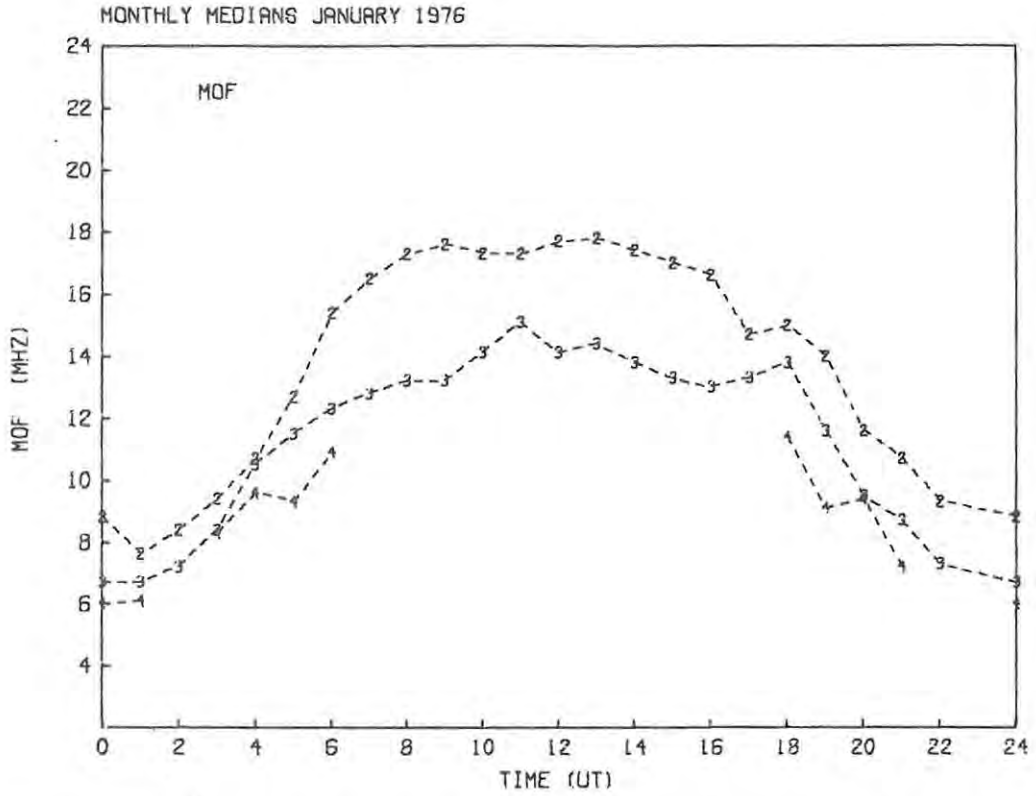


Figure 3.21 : Diurnal variation in monthly median MOF for January 1976 for the 2F, 3F and 4F modes (symbols 2, 3 and 4 respectively).

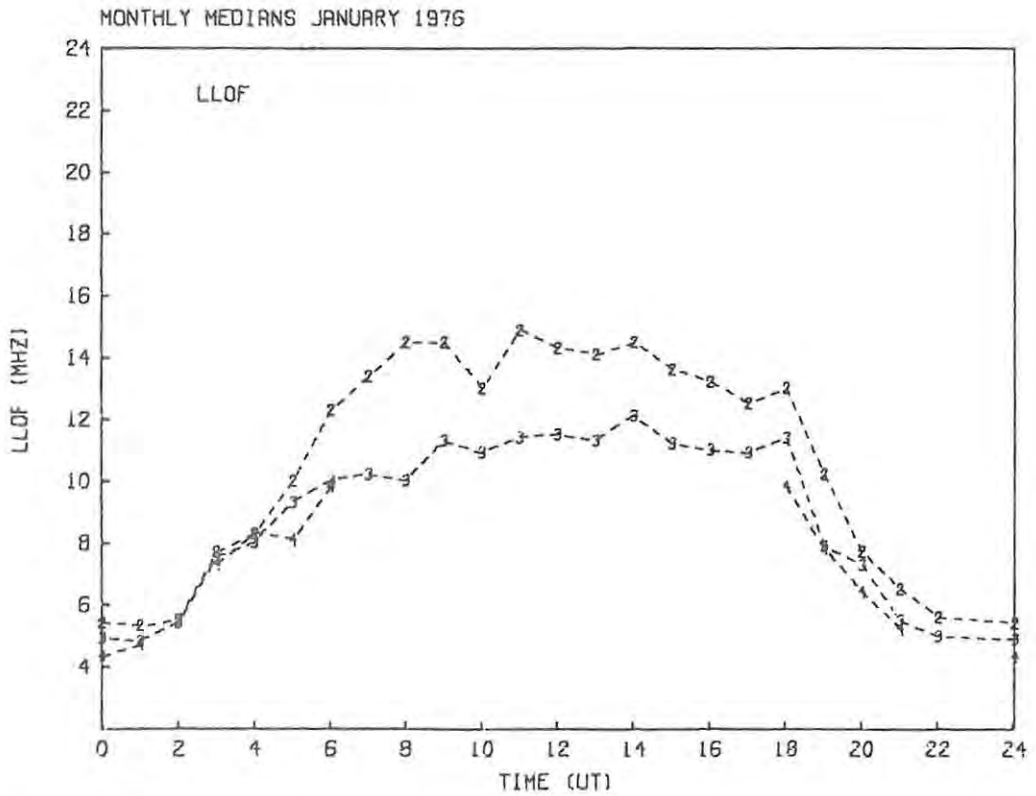


Figure 3.22 : Diurnal variation in monthly median LLOF for January 1976 for the 2F, 3F and 4F modes (symbols 2, 3 and 4 respectively).

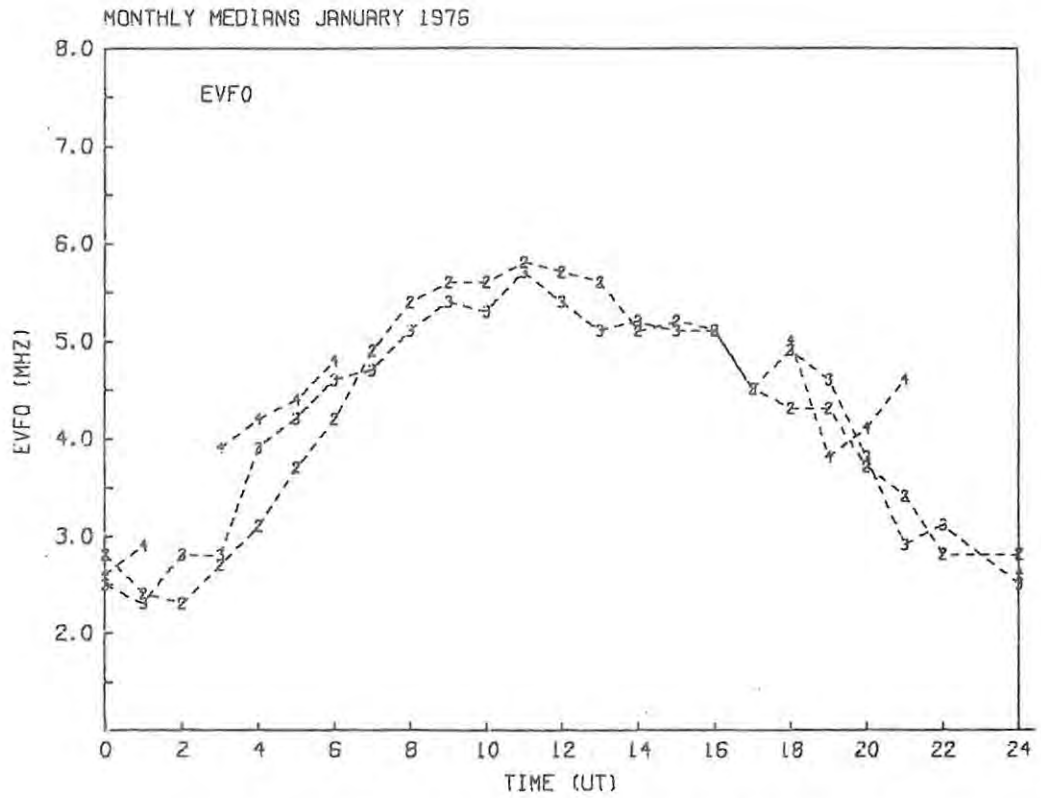


Figure 3.23 : Diurnal variation in monthly median EVFO for January 1976 for the 2F, 3F and 4F modes (symbols 2, 3 and 4 respectively).

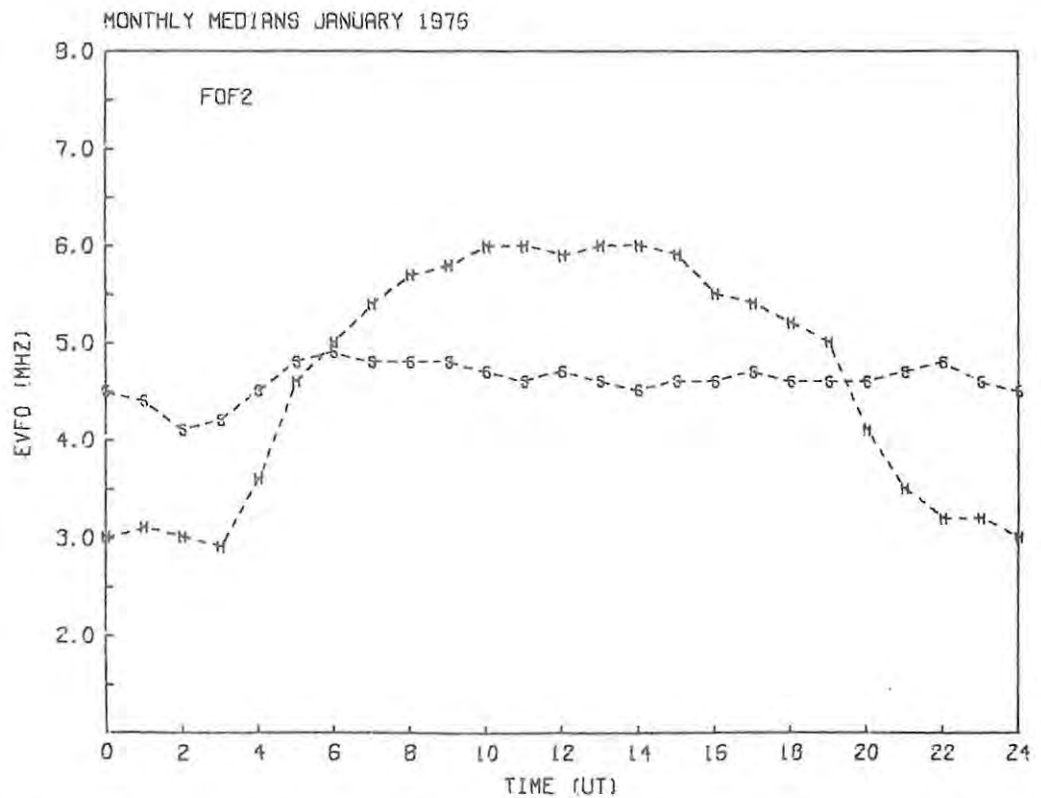


Figure 3.24 : Diurnal variation in monthly median foF2 for January 1976 at SANAE (S) and Hermanus (H).

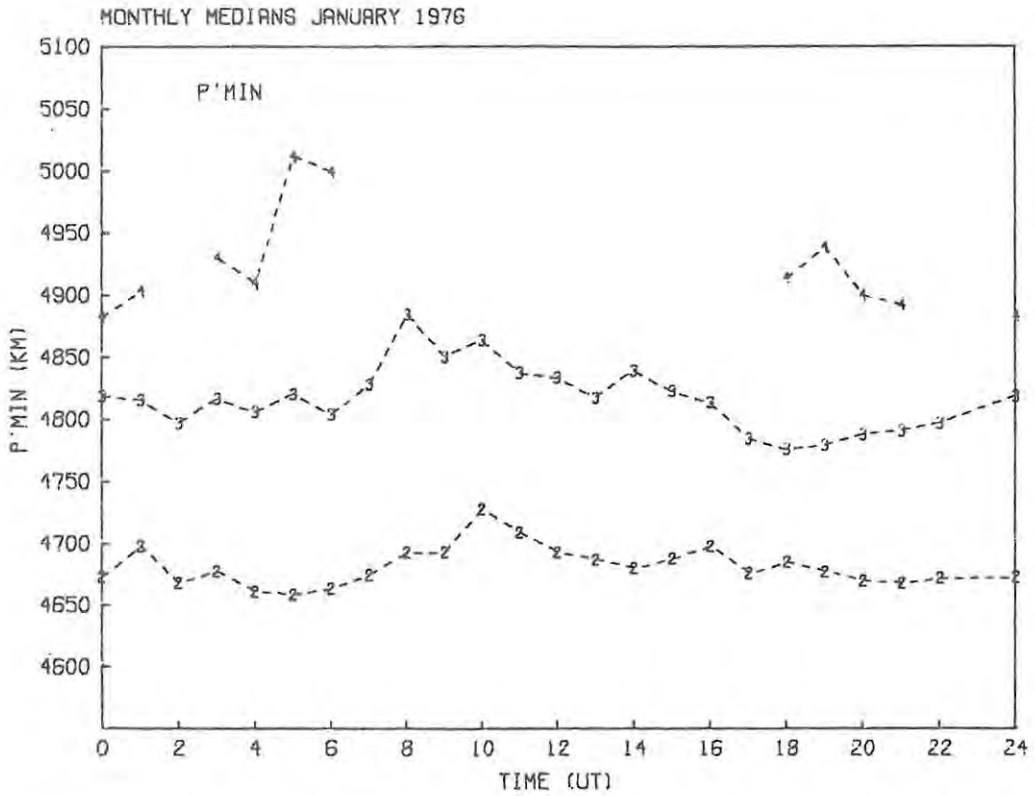


Figure 3.25 : Diurnal variation in monthly median P'_{min} for January 1976 for the 2F, 3F and 4F modes (symbols 2, 3, and 4 respectively).

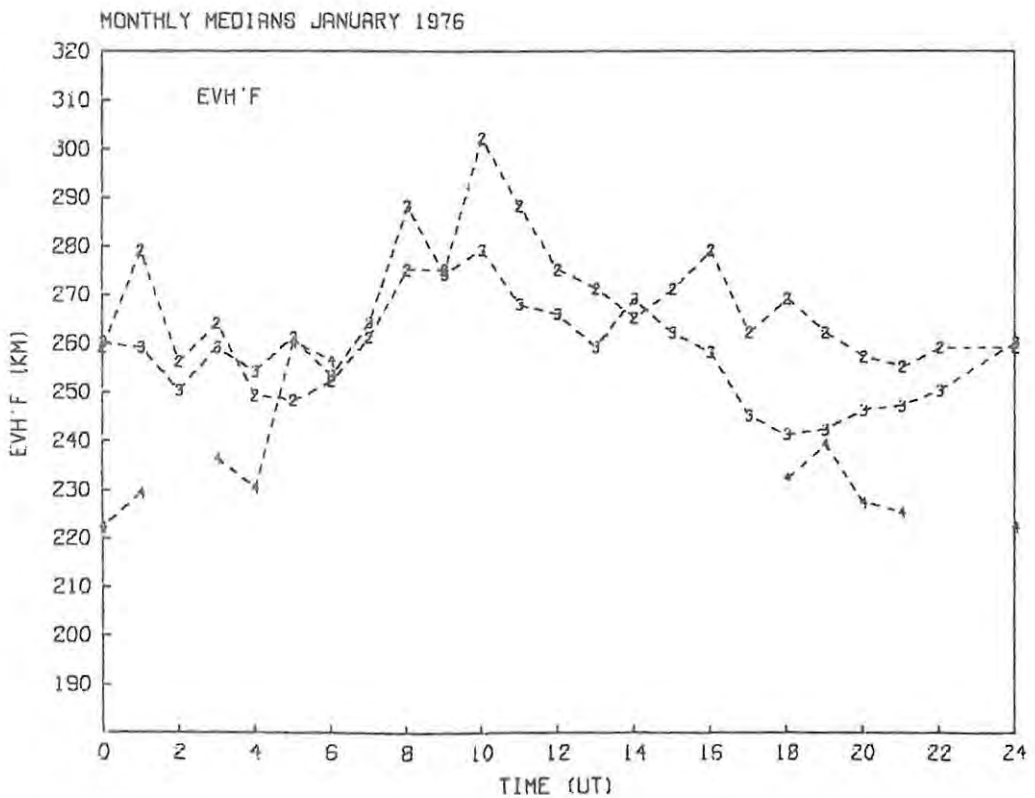


Figure 3.26 : Diurnal variation in monthly median EVH'F for January 1976 for the 2F, 3F and 4F modes (symbols 2, 3 and 4 respectively).

3.3.3 Discussion

The median is used as a measure of "average conditions", for the same reasons as in vertical incidence analysis (Piggott and Rawer, 1972), in order to obtain data representative of quiet conditions. Overall, the mode analysis approach used appears to have been successful; although some individual mode designations may be incorrect, the compilation of monthly median values (with reasonable counts) should smother these errors. Several further observations can be made regarding these (solar minimum) data :

- (i) During winter daytime the consistency of the EVFO's of the different modes and their similarity to foF2 at SANAE indicate that over the relatively small region covering the first ionospheric "reflection points" of these modes (an extent of 560 km along the great circle), foF2 is essentially constant and similar to the lower SANAE value, and that this is the "control area" limiting the MOF's. This idea is examined further in Chapter 6.
- (ii) During summer daytime the MOF's are again apparently limited by the lower foF2 towards the SANAE end of the path; their values are considerably less than the winter daytime maximum value.
- (iii) The 3F and 4F mode counts and the values of LLOF (Appendix D and Figures 3.16 and 3.22) show the effects of the expected increase in absorption around midday in summer, and greater daytime absorption in summer than in winter (Davies, 1965). The 4F mode is often observed in winter but rarely in summer.
- (iv) The behaviour of EVH'F (Figures 3.20 and 3.26) during the day is opposite to that of h'F at SANAE and Hermanus. At both end points h'F is greatest at night and falls to its minimum value in the early afternoon. This probably means that EVH'F is not a reliable measure of h'F and there are other causes of retardation leading to the higher values of P' during the day. It is unlikely that EVH'F represents h'F2 in winter as F1-F2 separation is rarely observed on SANAE ionograms then. The consistency of the EVH'F values for the different modes (they are generally within about 20 km of each other) is, however, encouraging in terms of our mode designations and assumption of small tilts and therefore approximately equal hops.

CHAPTER 4

COMPUTER-AIDED SCALING OF OBLIQUE IONOGRAMS

4.1 Introduction

The results obtained in the first median analysis described in section 3.3.1 suggested that the routine scaling of hourly oblique ionograms and compilation of monthly medians was a worthwhile procedure. In order to reduce the large amount of time spent in scaling, and to benefit from improved data handling facilities, a computer-aided scaling system was developed and thoroughly tested on the January 1976 data (section 3.3.2). The system utilized a NOVA 2 minicomputer, with VDU and dual floppy-disk drive for program and data storage, to which was interfaced a GRAF PEN sonic digitizer (manufactured by Science Accessories Corporation). The hardware and software interfaces were developed by de Kock (1977), who also wrote a BASIC program for the scaling of vertical ionograms on this system. I then extensively revised and expanded this program to allow the scaling of oblique ionograms in addition to vertical ones.

The operation of the final version of the scaling program "IONO" is described in section 4.2. Its use in the routine scaling of both vertical and oblique ionograms is described in the manual "User's Guide to Ionogram Scaling using the Graf/Pen Digitizer", which is included as Appendix A. The variable names used in the scaling program, flowcharts of its overall operation, and a listing of the program itself are given in Appendix B. Further computer handling of the ionogram data obtained is described in section 4.3; the programs used are given in Appendix C. Finally a discussion of the advantages and reliability of the system is given in section 4.4.

4.2 The Scaling Program

4.2.1 Overview

The program utilizes two areas of the digitizer table (Figure 4.1) :

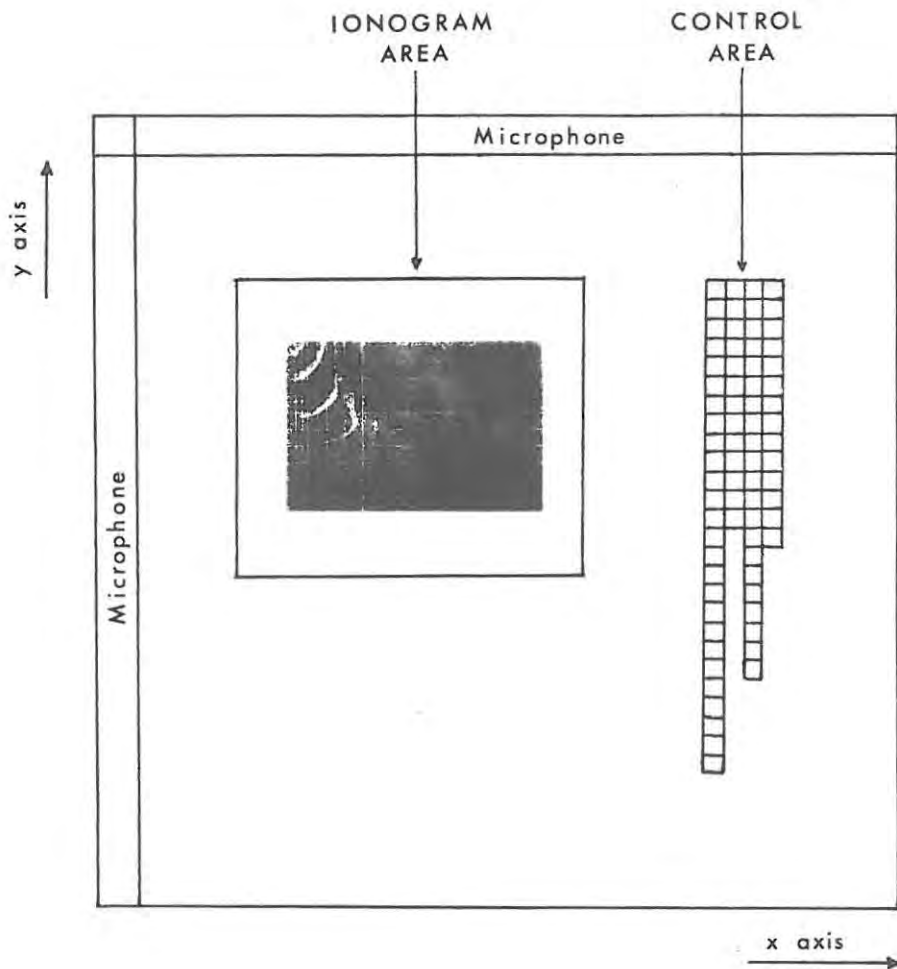


Figure 4.1 : Layout of the digitizer table.

- (i) the "ionogram area" onto which ionograms on 35 mm film are projected, and
- (ii) The "control area", which provides facilities for the inclusion of qualifying and descriptive letters and the allocation of values to specific parameters, as well as various program control commands. The program operates in a "Reverse Polish" manner : any ionogram points and/or letter blocks corresponding to a particular parameter are first digitized with the digitizer "pen", when data are stored in an initial storage buffer. These data are then interpreted and operated on when the appropriate parameter or control command "block" is digitized.

A specific command is used to indicate the end of scaling of a particular ionogram and the data from this ionogram are then automatically filed on the NOVA floppy disk in a file whose name is characterized by the place code letter, year and day number of the ionogram in order to make later access to the data simple. (A file contains all the data for one day, one line per ionogram, each line containing the scaled ionogram data in a fixed format which is independent of the order in which the parameters are scaled). The time is automatically incremented at the end of an ionogram to assist in routine scaling, but other facilities are provided, for instance to allow the "scaling" of points on an ionogram trace for the purpose of determining an electron density profile, so that the system is versatile.

With minor exceptions, once initialized the entire program is controlled from the digitizer table. Prompts, parameter names and values, and error messages are output on the VDU, and scaled points displayed on a Hewlett-Packard "X-Y Display" oscilloscope, to provide feedback to the user.

The program is examined in some detail in the following three sections as it is both difficult and pointless to consider the oblique scaling operations only, and in addition there is a need for reasonable documentation of a program of this size and complexity.

4.2.2 Basic Operation of the Program

On initialization of the program, arrays of X and Y values, which define the ionogram area and individual control blocks in digitizer co-ordinates

are set up, as are strings containing the qualifying and descriptive letters (Piggott and Rawer, 1972) and the parameter names, etc. for later reference. The program then issues a prompt to provide the day number, time, year and place code of the first ionogram to be scaled (these normally only need be provided on initialization), and enables the digitizer.

When a point is digitized the call driver POINT (de Kock, 1977) returns to the program the values of

$$\sum_{i=1}^n x_i, \quad \sum_{i=1}^n y_i, \quad \sum_{i=1}^n x_i^2, \quad \sum_{i=1}^n y_i^2$$

for a given number n (set to 5 in practice) of samples i of the point (x, y) in digitizer co-ordinates. The program then : rejects margin points and samples with wrong digits; checks that at least one valid sample point remains; determines the mean x and y of these valid samples; and checks that the standard deviations of the x and y values are each not greater than 7 (corresponding to an uncertainty of approximately 2 km in virtual height or 0.03 MHz in oblique frequency; these values are dependent on the magnification of the ionograms).

If any of these checks are violated an appropriate error message and the prompt "REDIGITIZE" are output on the VDU. By comparing the co-ordinates (x, y) with the arrays X and Y the program then determines in what area of the digitizer table the point lies, and therefore what action should be taken. (See the flowcharts in Appendix B).

- (i) If the point is in the ionogram area and the axes of the ionogram have been previously defined, a co-ordinate transformation (de Kock, 1977, p. 20) is performed to give the point in ionogram co-ordinates, say (f, h') ; these co-ordinates are then stored in the next two elements of the initial storage buffer. (If the axes have not been defined, x and y are stored instead for use in defining the transformation matrices in the AXES command).
- (ii) If the point lies in the control area a column number I and row number J are defined (see Table 4-1). For column 1 (qualifying and descriptive letters) the number $-J$, and for column 2 (numbers,

signs and point) the number $-J -26$ is entered into the next element in the storage buffer. (Negative numbers are used so as to distinguish easily between ionogram and control points later).

- (iii) If the point is in column 3 of the control area, control passes to the appropriate "scaled parameter" subroutine depending on the value of J (Table 4-1 and section 4.2.3), after checking that :
at least one point has been scaled; the axes have been defined; the parameter is a vertical or oblique one as the case may be; and, if oblique, the mode has been defined. If any of these checks are violated an appropriate error message is output and control returned.
- (iv) If the point is in column 4, control passes to the control command subroutine specified by the value of J (Table 4-1 and section 4.2.4).
- (v) If the point is in none of the above areas the error message "POINT IN UNDEFINED REGION" is issued and control returned.

In all cases the steps in the appropriate subroutine(s) are performed (during which time the digitizer is disabled), messages output on the VDU, etc., and control returned to the NPT call driver in the main program to await digitization of the next point.

Table 4-1 : Rows and columns of the control area

J	I =	1 (Letters)	2 (Numbers, etc.)	3 (Parameters)	4 (Control Commands)
=					
1		A	0	foF2	RUBOUT
2		B	1	h'F2	DELETE
3		C	2	foF1	RESTART
4		D	3	h'F	DOMAIN
5		E	4	foE	DISPLAY
6		F	5	h'E	h' and f
7		G	6	foEs	DAY
8		H	7	h'Es	TIME
9		I	8	fbEs	YEAR/PLACE
10		J	9	fmin	AXES
11		K	-	MUF	END
12		L	+	fxI	OBLIQUE
13		M	.	Es type	HOP
14		N		All values	MODE
15		O		LLOF	
16		P		MOF	
17		Q		JF	
18		R		HLOF	
19		S		EVFO	
20		T		P'	
21		U		S	
22		V			
23		W			
24		X			
25		Y			
26		Z			

Table 4-2 : Sample vertical incidence data (the file S78:025 for SANAE 1978 day 025).

YR	DAY	TIME	FOF2	H'F2	FOF1	H'F	FOE	H'E	FOES	H'ES	FBS	FMIN	MUF	M3000	FXI	ESTYPE
S78	02	0000	066-F			271	136	108				114	193-F	292	071	
S78	02	0100	072UF	275	233UL	265	138UR	102				114	213UF	296	081	
S78	02	0200	072UF	279	254-L	278EA	129EB		020	121	020	113	F		083	H
S78	02	0300	069-F		301UL	255-A	148-B		026JA	128	023	144	185-F	268	077	H
S78	02	0400	069-F	331L	326	246	184UR					120	185	268		
S78	02	0500	077	333	353	236	189					141	215	279		
S78	02	0600	078	308	380	228	249		029	126	029	118	227	291		H,L
S78	02	0700	071	318	392	219	277		031	128	030	278	195	275		H
S78	02	0800	065	346			284		045JA	114	045	230	186	286		H
S78	02	0900	061	353	427A	219A	294		032	115	032	252	171	273		H
S78	02	1000	062	376	438	216			037	101	035	268	169	273		L
S78	02	1100	064	370	440	343EA			050JA	098	040	306	175	273		L
S78	02	1200	066	331	437	343AB	298	103	046	110	043	252	198	300		C
S78	02	1300	061	331	447UB							449	186	305		L
S78	02	1400	056	307	448	211			036	101	036	304	181	305		L
S78	02	1500	055	321	436-R	202	305	106				247	171	311		L
S78	02	1600	054	368	419-R	234	262UR	108				237	154	355		L
S78	02	1700	053	374	432-R	215UH	243	101	027	123	027UY	156	153	289		H
S78	02	1800	055	377	395	221	214DR	101	029	124	029	163	163	296		H
S78	02	1900	053	322	391-L	238	201UR	107				152	146UF	275	059	
S78	02	2000	055UF	317	339-L	246	205	104	027	121	026	121	157UF	285	062	H
S78	02	2100	054UF	320	317-L	278	199	122				125	154UF	285	061	
S78	02	2200	049-F	317	281-L	292	187	144				131	135-F	276	058	
S78	02	2300	B	B	B	B	B	B	B	B	B	B	B	B	B	

Table 4-3 : Sample oblique incidence data (the file O76:009 for Oblique 1976 day 009).

YEAR	DAY	TIME	MODE	LLOF	NOF	JF	HLOF	EVFO	P'	EVH'	S	OFFSET
076	009	0005	2F	075	094	089UF	078	026UF	4671	259	2	4228
076	009	0005	F+E	056	080				4681		1	4228
076	009	0005	F+E	053	071				4733		1	4228
076	009	0005	F+E	049	081	077	074	031	4771	239	1	4228
076	009	0005	F+E	049	069				4838		1	4228
076	009	0105	F+E	071	096	F	088	F	4698	280	2	4227
076	009	0105	F+E	053	087				4729		1	4227
076	009	0105	F+E	051	078	F	072	F	4786	245	1	4227
076	009	0105	F+E	043	059				4816		1	4227
076	009	0205	F+E	054	115				4621		1	4225
076	009	0205	F+E	062	103	090UF	084UF	029UF	4664	253	1	4225
076	009	0205	F+E	064	089				4721		1	4225
076	009	0205	F+E	064	079				4803		0	4225
076	009	0205	F+E	046	071	R	R	R	4830	265	0	4225
076	009	0205	F+E	042	057				4873		0	4225
076	009	0305	F+E	052	115				4607		1	4223
076	009	0305	F+E	054	111	105UF	100	F	4636	229	1	4223
076	009	0305	F+E	070	092				4687		1	4223
076	009	0305	F+E	064	089	085	083	029UR	4732	220	1	4223
076	009	0405	F+E	063	092	F	083	F	4695	278	1	4221
076	009	0405	F+E	053	084				4738		1	4221
076	009	0405	F+E	053	069				4793		0	4221
076	009	0405	F+E	048	059	057	056	024UR	4887	289	0	4221
076	009	0505	F+E	087	096	090	089	F	4739	311	0	4219
076	009	0605	F+E	082	137				4618		0	4217
076	009	0705	F+E	122	142	140R	099	031UR	4690	274	0	4217
076	009	0705	F+E	084	107	F	137	042	4684	269	1	4215
076	009	0805	F+E	105	155	F	138	046	4886	289	1	4215
076	009	0805	F+E	078	131	128R	099	046	4708	288	0	4213
076	009	0905	F+E	106	165	F	161	046	4847	272	2	4213
076	009	0905	F+E	097	127	124F	120	F	4690	274	0	4211
076	009	1005	F+E	084	116	F	120	050	4881	287	0	4211
076	009	1105	F+E	086	115	F	105	048	4916	301	0	4210
076	009	1205	F+E	137	144	F	105	048	4930	306	1	4208
076	009	1305	F+E			F	140	R	4748	317	0	4206
076	009	1405	F+E			F		R			1	4204
076	009	1405	F+E	125	164	B	B	B	4732	306	0	4202
076	009	1405	F+E	098	114	163	156	056	4963	319	0	4202
076	009	1505	F+E	158	177	110	103	046	4691	275	0	4200
076	009	1605	F+E			R	R	R			0	4200
076	009	1705	F+E	156	206	B	B	B	4569		0	4198
076	009	1705	F+E	163	173				4657		0	4196
076	009	1805	F+E	137	167	170R	164	050UR	4631	224	0	4194
076	009	1805	F+E	109	132	R	112	R	4735	221	0	4194
076	009	1905	F+E	124	151	126R	143	F	4656	246	1	4193
076	009	1905	F+E	123	144	148UF			4734		1	4193
076	009	2005	F+E	145	170	F	156	F	4613	208	0	4191
076	009	2005	F+E	130	151				4649		0	4191
076	009	2005	F+E	113	143	141UF	133	049UF	4709	208	2	4191
076	009	2105	F+E	098	115	F	111	F	4808	198	0	4191
076	009	2105	F+E	141	178	F		R	4595	190	1	4189
076	009	2105	F+E	083	135	117F	112	038	4705	206	1	4189
076	009	2105	F+E	088	108	F	100	F	4815	201	0	4189
076	009	2205	F+E	111	151	141	138	033	4593	198	1	4187
076	009	2205	F+E	079	118	107	099	036	4691	188	1	4187
076	009	2205	F+E	066	091	F	086	F	4771	186	1	4187
076	009	2305	F+E	083	128	F		R	4622	216	1	4185
076	009	2305	F+E	078	097				4663		0	4185
076	009	2305	F+E	052	096	F	087	F	4699	203	0	4185
076	009	2305	F+E	050	076				4737		1	4185
076	009	2305	F+E	053	084	R	074	R	4798	195	0	4185
076	009	2305	F+E	046	065				4849		0	4185

4.2.3 Scaled Parameters

- (i) If the parameter is a normal frequency parameter (foF2, foF1, foE, foEs, fbEs, fmin, fxI for vertical or LLOF, MOF, JF, HLOF for oblique) the contents of the storage buffer are examined and the frequency (in the first element) is converted to an integer in units of 0.1 MHz (except foF1, foE and fmin, which are converted to integers in units of 0.01 MHz), the standard format for the vertical parameters (Piggott and Rawer, 1972) and used for convenience for the oblique parameters as well. Any negative numbers in the storage buffer are decoded to the appropriate qualifying and descriptive letters. The parameter value and letters are then copied into the output buffer at the appropriate position, according to the format of Table 4-2 (vertical) or 4-3 (oblique), and together with the parameter name are displayed on the VDU.
- (ii) For a virtual height (h'F2, h'F, h'E or h'Es) or group path P', the second element of the storage buffer contains its value in km; as in (i), letters may follow this. To obtain P' the offset in km of the oblique ionogram (computed automatically for each ionogram by a control command subroutine) is added to the h' value, and if the defined mode is a multiple-F or multiple-E mode, EVH' is calculated (equations (3.1) - (3.3)). The numbers and letters are again copied into the output buffer at the appropriate position, and displayed on the VDU.
- (iii) The MUF (in vertical scaling) or EVFO (in oblique) subroutines each require 3 ionogram points as input data in the storage buffer. For the MUF these three points are digitized around the curve of the F2 ordinary ray trace, and for EVFO they are from the high-angle ray of the oblique trace. In each case a frequency transformation from vertical to oblique or vice-versa, according to the equivalent vertical ionogram formulation of section 3.1.2, is performed. For the MUF the three vertical (f_v , h') points are converted to oblique (f_{ob} , h') where, from equation (3.4),

$$f_{ob} = f_v \cdot k \sec \phi_o = f_v \cdot k \sqrt{1 + \left(\frac{s}{2(h'+b)}\right)^2} \quad (4.1)$$

and S and b are given by (3.2) and (3.3) for ground range D = 3000 km. For EVFO the oblique (f_{ob} , P') points are converted to (f_v , h') where f_v is given by (3.4) and h' by (3.1), where P' is first divided by the number of F-reflection "hops", and S, b and k have the values appropriate to the hop distance (Table 2-3). In both cases the maximum frequency in the converted co-ordinates is required; this is achieved by fitting a parabola

$$f = a h'^2 + b h' + c \quad (4.2)$$

to the three transformed points (f_i , h'_i) using Cramer's Rule (e.g. Dahlquist and Björck (1974); see also section 5.3.5), and determining the required maximum frequency from the condition

$$\frac{df}{dh'} = 2 ah' + b = 0 \quad (4.3)$$

and equation (4.2). In the case of the MUF, if foF2 has already been scaled, the factor M3000 is also calculated. The remainder of the processing of the data (conversion to an integer in units of 0.1 MHz, copying and displaying) is as in (i).

- (iv) The remaining three parameters are all similar in that they require only letters or numbers, and not ionogram points, as input data. "Es type" requires one or more letters (and possibly numbers), "All values" (which may be used for both vertical and oblique scaling) requires one replacement letter which it allocates to all parameters, and signal strength S requires one number (between 0 and 5 - an estimate of the strength of the oblique trace). In all cases the letters or numbers will be decoded from the negative numbers in the storage buffer and copied and displayed in the usual way.

4.2.4 Control Commands

These subroutines will be dealt with in row order.

1. RUBOUT : This erases an incorrect ionogram data point by decrementing the pointer in the storage buffer.

2. DELETE : This is used to erase an incorrect parameter value. The DELETE control block is digitized (when the number -99 is entered into the storage buffer) followed by the block corresponding to the parameter whose value is to be deleted. When this number is detected in the parameter subroutine, control is transferred to the DELETE subroutine, which writes blanks over the appropriate positions in the output buffer. The command may also be used to delete all the data for the particular mode being scaled in the oblique case.
3. RESTART : This resets the output buffer to blanks and is equivalent to parts (viii) and (ix) of the END command (see below), except that the time is not incremented.
4. DOMAIN : Three ionogram points are digitized before this command to define a small domain of the ionogram around the next ionogram point to be digitized when this would be inaccurate because of non-linearity in the ionogram. The three points are any three of the four surrounding intersections of virtual height and frequency markers.
5. DISPLAY : This command does not require any data, and changes the mode of operation; the axes of the ionogram must, however, have been defined. On first call the subroutine enables all subsequent ionogram points (until DISPLAY is digitized a second time) to simply be displayed on the X-Y Display so that an ionogram may be traced out.
6. h' and f : This allows the scaling and filing of a number of points (up to 50) from a trace (ordinary or extraordinary) of an ionogram (vertical or oblique) for use in computing an electron density profile. The axes of the ionogram must have been defined, and if oblique the mode must have been defined. The ionogram points are digitized in the required order; if the data are for the extraordinary ray the letter X is digitized (otherwise it is assumed to be the ordinary ray). On digitization of the "h' and f" control block, the subroutine : checks that not more than 50 points have been scaled; opens a separate file identifying the data by the place-code, year, day number and time of the ionogram; and writes to this file place headings and other preliminary data in accordance with the input data format of the N(h) profile programs (section 5.2 for the vertical case, section 5.3 for oblique). The h' and f values are then

written to this file and displayed on the VDU. In the vertical case the last frequency value is assumed to be foF2; in the oblique case the last three points on the high ray are used to determine EVFO by calling the EVFO subroutine. The terminating line 9999 with the appropriate critical frequency is then written, the file closed and normal scaling resumed.

7. DAY : Up to three numbers from column 2 are provided as data for this subroutine and are interpreted as the day number of the ionogram. The subroutine then checks that this is not greater than 366 and displays the value on the VDU. If digitized after initialization the previously opened file is closed and a new one for the given day opened.

8. TIME : This requires 4 or 6 numbers as data; the first 4 represent the time of the ionogram in HHMM format; the last two (optional) represent the time interval in minutes between successive ionograms to be scaled. If the latter is not given a default value of 60 minutes is assumed.

9. YEAR/PLACE : The input data for this subroutine are two numbers (the year) and a letter (the place code). After decoding this, if the given place code is not "O", the subroutine calls part of the END subroutine to open the appropriate file and display the year-day-time information of the first ionogram. (If requested after initialization the previous file is first closed). If the given place code is "O" the prompt "OBLIQUE SCALING ?" is displayed on the VDU.

10. AXES : This requires three specific ionogram points as data; for vertical ionograms these points are

(1 MHz, 1000 km), (1 MHz, 100 km), (10 MHz, 100 km);

and for oblique ionograms they are

(3 MHz, 1000 km), (3 MHz, 100 km), (20 MHz, 100 km).

From the three x and y values in the buffer corresponding to these points the subroutine computes the matrices A and B (de Kock, 1977, p. 20) which define the transformation $(x, y) \rightarrow (f, h')$ for subsequent ionogram points until the next END or RESTART command is given. The axes must be defined before any parameters on the ionogram can be scaled. For oblique scaling the prompt "HOP/MODE OF FIRST TRACE ?" is issued as the mode must also be defined before any oblique parameters can be scaled.

11. END : When all the parameters of an individual ionogram (the "old ionogram") have been scaled, this command is digitized and performs a number of functions :
- (i) In the vertical case the subroutine first checks if any of the essential parameters foF2, h'F, fmin and MUF have not been scaled; if so an appropriate warning is issued and control returned to the main program to allow the parameter(s) to be scaled. (These checks are not made if END is digitized a second time).
 - (ii) In the vertical case the ionogram place code-year-day-time information is copied into the start of the output buffer.
 - (iii) In the oblique case this information and the offset are copied into each "line" (for each mode) of the output buffer.
 - (iv) In either case the output buffer is then written to the disk file containing data for that day, in the vertical case as one line of 96 characters, in the oblique case as one line of 72 characters² for each mode scaled; the filed data are also listed on the VDU.
 - (v) The time is then incremented by the amount specified in the TIME command to yield the time of the next ionogram.
 - (vi) If the new time is greater than 24 hours it is reset and the day number incremented; the file containing data for the "old" day is then closed and a file with a name containing the "new" day number opened. (Likewise, if the new day number is greater than 365 or 366 it is reset to 1 and the year incremented).
 - (vii) In the oblique case a check is made that the new time is not later than the time of the calibration given on oblique initialization (see 12. below); if it is, control is transferred to this subroutine to request new calibration data. If the check is satisfied the offset of the new ionogram is computed (equation (2.6)).
 - (viii) The output buffer is reset to a "line" of 96 blanks in order to receive the data from the new ionogram.

(ix) The place code, year, day and time (and offset if oblique) of the new ionogram are then displayed on the VDU and a prompt to define the axes of the new ionogram given.

12. OBLIQUE : This subroutine initializes (on first call) or terminates (on second call) the scaling of oblique ionograms. The frequencies of the axes points are redefined and the oblique scaling flag set. The subroutine then requests absolute delay calibration data (sections 2.3.2 and 2.3.3) to enable the offsets of the ionograms to be determined. The following data are typed in on the VDU in response to the appropriate prompts :

- (i) the day number of the next calibration day after the day of the ionograms to be scaled; (If the ionogram day - time is later than the calibration day - time the prompt "NEXT CALIBRATION DAY ?" is repeated.)
- (ii) the offset in milliseconds measured in this calibration;
- (iii) the drift rate in milliseconds/week for the week between the previous calibration and this one (i.e. the "current drift rate");
- (iv) the number of timing adjustments ("shifts") made between the time of the ionogram and the time of the calibration;
- (v) for each such shift (if the number is non-zero) the day number, time and value of the shift in milliseconds (see section 2.3.3 for sign convention).

When all this information has been provided the subroutine transfers control to the END subroutine to open the appropriate file and compute the offset of the first ionogram, etc.

13. HOP : This is used to define a multiple-F mode trace on an oblique ionogram; it requires one number n as datum which is interpreted as nF MODE. If this is not the first mode scaled on the ionogram the output buffer is extended to include a new blank line for the data from this mode. This "hop number" is also used in the computation of EVFO and EVH' (section 4.2.3).

14. MODE : This is similar to HOP but caters for non-multiple-F or "intermediate" modes involving E reflections, e.g. 2F + E. The "hop number" is set to zero; the calculation of EVFO and EVH' then cannot be attempted (unless the mode is multiple-E). The output buffer is extended as for HOP. In both cases if the number -99 is detected in the buffer (entered when the DELETE block is digitized), control is transferred to the DELETE subroutine which decrements the mode (or line) counter by one so that all the data for the current mode are deleted.

4.3 Further Computer Handling of Ionogram Data

The vertical or oblique data output by the scaling program in the form of Table 4-2 or 4-3 may be transferred from files on the NOVA disk to MAXIMOP subfiles on the ICL 1902T. This is achieved by a BASIC program written by P.I. Mountfort which was modified to allow, optionally, the transfer of a number of consecutive days' data files. The use of this program MAXI is described in Appendix A; it is listed in Appendix C.

Data in one or more such subfiles may then be transferred to a data file or magnetic tape using a FORTRAN program FILE also written by Mr. Mountfort incorporating the "Disc Handling Package" of Bulmer (1977). The data may then be conveniently accessed from the data file using the ICL "Direct Access" file interrogation and sorting packages (ICL, 1969, 1975), to find, for example, all 2F mode oblique data at 1205 SAST on days 001 to 031 of 1976, ordered with respect to decreasing MOF (see Appendix C).

The first three columns for each parameter (Tables 4-2 and 4-3) always contain numbers; if a replacement letter is given instead of a value this is placed in the fourth column (normally used for qualifying letters) and the first three left blank. This allows the latter to be defined as a number field instead of a character field if so required for subsequent computation. Although programs to compute monthly median vertical and oblique data have not yet been implemented it is envisaged that they will be shortly.

In the case of "h" and "f" data (points along an ionogram trace), these may be transferred from NOVA files to MAXIMOP subfiles, one file at a time, using the same program as above. They may then be used immediately as input data for the appropriate (vertical or oblique) electron density routines described in the next chapter, as the formats are compatible with the requirements of these latter routines.

4.4 Discussion

The computer-aided scaling system reduced drastically the time spent in scaling ionograms, particularly in the oblique case. During the course of fairly extensive testing by R. Haggard for vertical ionograms and myself for oblique, a number of improvements and extensions suggested themselves and were incorporated in the final version of the scaling program.

In particular the original filing system (de Kock, 1977, p. 24) was found to be very inefficient and time consuming. In this original system a separate file was allocated for each ionogram, in which the parameter names and values were stored in the order scaled. A second "sorting" program then had to be run to extract the values and rearrange them into a format essentially the same as that of Table 4-2. When an appreciable number of ionograms had been scaled with this system, however, because of the large number of files on the disk, it took longer to allocate a file and store the data from an ionogram than to scale the ionogram. This led to the idea of allocating one file per day rather than one file per ionogram. In addition the time spent running the sorting program was considerable, so the direct formatting method of the final version was developed.

There were occasions when the digitizer itself was unreliable (there appeared to be a temperature threshold, below which difficulties were almost invariably experienced), but the program checks successfully prevented any "bad" data from being used : no points could be digitized correctly. In addition rough visual checking of the parameter value displayed on the VDU with the appropriate ionogram point usually showed up any values that were seriously in error. In general, therefore, the system was felt to be reliable.

In order to check the accuracy and reliability a number of ionograms scaled using the system were rescaled manually and vice-versa. On only two occasions did normal frequency values scaled by the two methods differ by more than the accuracy to which the values are read (0.1 MHz). The virtual heights (y axis of the digitizer) appeared to be slightly less reliable; on several occasions the difference between the manually- and digitizer- scaled values was greater than 5 km. The MUF and EVFO

were not as reliable at first, although with experience in the use of the MUF curves the choice of points on the part of the F2 trace near the expected point of tangency for use in the program improved the reliability. There are occasions, however, when the digitized MUF may be suspect, particularly for cases where the F2 and F1 critical frequencies are close to one another, in which case the F1 MUF may be higher than the F2 (G condition (Piggott and Rawer, 1972)). This is easily discernable when using transmission curves but not when using the digitizer. EVFO also differed appreciably from the inverse transmission curve value on a number of occasions; in addition slight variations in the positions of the three points used to determine it can lead to large differences in its value, particularly when only a small portion of the high-angle ray is visible because of absorption.

Overall, the system has been shown to be a viable ionogram scaling and data acquisition system, and previously slow, tedious procedures such as the routine scaling of ionograms, data compilation, and the extraction of ionogram points for use in electron density profile analysis, are made considerably more rapid and convenient. The system is at present being transferred to a Midwest Scientific Instruments 6800 microcomputer and Summagraphics digitizer. The use of the latter should avoid the problems of unreliability with the sonic digitizer mentioned above.

CHAPTER 5

CALCULATION OF ELECTRON DENSITY PROFILES FROM OBLIQUE IONOGRAMS

5.1 Introduction

The reduction of vertical incidence ionograms to electron density - real height profiles has received considerable attention, and there are numerous methods routinely available for performing this reduction (section 5.2). The similar (though perhaps slightly more complex) problem of reducing an oblique ionogram to an electron density profile (or $N(h)$ profile) has, however, received relatively little attention.

One obvious approach, suggested by Gething and Maliphant (1967) amongst others, is the two-stage procedure ("indirect method") whereby

- (1) the oblique ionogram is reduced to the equivalent vertical one using the simple techniques of Martyn's Theorem and the modified Secant Law (section 3.1.2 and Davies (1965) p. 160)
- (2) this vertical ionogram is then reduced to an $N(h)$ profile by standard techniques (section 5.2). This simple procedure can give good results (e.g. Gething, 1969).

Techniques for solving the inverse problem of tracing rays of given frequencies through a given ionospheric profile are also readily available. Thus another method of deriving the profile which suggests itself is the adjustment of a trial profile until a "synthetic oblique ionogram", obtained by tracing rays of a number of different frequencies through it, is in satisfactory agreement with the observed oblique ionogram. Gething (1969) provided a simple algorithm for such a procedure, although still proceeding from oblique ionogram to $N(h)$ profile by the above two-stage process.

More recently Chuang and Yeh (1977) have suggested a more rigorous inversion technique using the Backus and Gilbert (1967) method developed for the inversion of seismic data. This technique presupposes, however, a "zeroth order guess about the profile", ray tracing through which will yield an initial trial oblique ionogram, and further requires that this does not differ too markedly from the actual profile in order that the problem may be linearised. The method has not yet been applied to real oblique data.

Few direct methods of reduction of oblique ionograms to $N(h)$ profiles have been reported. Unz (1966) presented a theoretical formulation for oblique incidence based on earlier work for vertical incidence (Unz, 1963) using Schlomilch's integral equation. Gething and Maliphant (1967), however, corrected errors in Unz's work and suggested that the two-stage reduction procedure be followed in view of the large number of numerical integrations required in the direct method.

George (1970) generalized to oblique incidence the method used by Jackson (1956) for vertical incidence. This simple rapid method involves the same order of approximation as the conversion to equivalent vertical ionograms.

Smith (1970) presented a new direct reduction method derived from first principles, but with several approximations to simplify the analysis. Rao (1973) gave a more rigorous formulation of this method, with fewer simplifying approximations.

All these methods, like the vertical ionogram reduction methods, are "lamination methods" which take a set of (f, P') data with arbitrary intervals from an oblique ionogram and use each pair of points to define a segment or lamina within which N is assumed to be a simple function of h . Very often, for convenience of manipulation, the functional relation is assumed between some simple monotonic function ϕ of N and radius r from the centre of the earth. In the methods studied in this chapter (including the vertical ionogram reduction method in section 5.2) the function ϕ used is the square of the plasma frequency f_N . Thus

$$\phi = f_N^2 = \frac{e^2}{4\pi\epsilon_0 m} N \tag{5.1}$$

$$= 8.06 \times 10^{-5} N \text{ for } f_N \text{ in MHz, } N \text{ in cm}^{-3},$$

$$\text{and } r = R + h \tag{5.2}$$

$$\begin{aligned} \text{where } R &= \text{earth radius} \\ &= 6371 \text{ km.} \end{aligned}$$

In the George (1970) method the segments are linear (i.e. f_N^2 is a linear function of r), while in the Smith (1970) and Rao (1973) methods "quasi-linear" segments with two segment constants are used.

We examine the indirect method in section 5.2, considering the reduction

of equivalent vertical ionograms (computed using the method outlined in section 3.1.2) to $N(h)$ profiles. Direct reduction methods are discussed in section 5.3; the theory and formulation of the three methods mentioned above are developed in 5.3.1 to 5.3.5. The methods are finally discussed and evaluated in terms of our requirements in section 5.4.

5.2 The Indirect Method

5.2.1 $N(h)$ Profiles from Vertical Ionograms

The "indirect method" is the two-stage process whereby an oblique ionogram is reduced to an equivalent vertical ionogram (section 3.1.2) and the latter then reduced to an $N(h)$ profile by standard techniques. The latter is a topic which has generated a vast amount of literature (e.g. a complete number of Radio Science, that introduced by Wright and Smith (1967)), and has now come to be regarded as standard practice. For the sake of completeness, however, we mention here the method used in our analysis for conversion from $h'(f)$ to $N(h)$, or more correctly $h(N)$, records. It is also useful to examine it in some detail because of its similarity to the methods of section 5.3 for obtaining $N(h)$ profiles from oblique ionograms. Using Wright and Smith's terminology the method would be classified as a "second order", "lamination", "machine" method. This formulation and an EMA program to perform it were developed by Poole (1974) from the methods in the literature (Paul, 1967; Howe and McKinnis, 1967). Lambert (1977) translated the program to FORTRAN for use in the ray-tracing program described in Chapter 7, and extended it to include calculation of the base height and peak parameters.

The problem is to solve (numerically, since no analytical solution is possible) the inverse of the integral equation

$$h'(f) = \int_0^{h(f)} \mu'(f, f_N, f_B, \Psi) dh \quad (5.3)$$

where the group refractive index μ' is a function of ray frequency f , plasma frequency f_N , electron gyrofrequency f_B and angle Ψ between ray and magnetic field (Howe and McKinnis, 1967). Thus we wish to find h as a function of N (or f_N , etc. - see equation (5.1)) given the corresponding h' .

5.2.2 The Method used

The input data required for the simple, rapid FORTRAN subroutine NHPR are the electron gyrofrequency f_B and magnetic dip angle I (which yields Ψ) for the station (f_B and I are assumed to be constant with respect to height) and a number of conveniently spaced (f_n, h'_n) points from the ordinary ray trace on the vertical ionogram. Up to 50 points may be used for an ionogram with E, F1 and F2 traces. The points must be such that $f_n \geq f_{n-1}$; valleys in the profile are not allowed for. The profile may be built up from the base in a step-by-step procedure since, to evaluate the real height of reflection h_n of a ray with frequency f_n , we only require information about the profile at heights below h_n . The two successive heights h_{n-1} and h_n define a segment n within which, in our second order method, $\frac{d^2h}{d\phi^2}$ is assumed to be a constant, i.e. we assume

h to be quadratic in ϕ (defined by equation (5.1)) :

$$h = A_n \phi^2 + B_n \phi + C_n \quad (5.4)$$

with segment constants A_n and B_n to be determined. Continuity at (ϕ_{n-1}, h_{n-1}) immediately gives C_n , so that at height h in segment n ($h_{n-1} \leq h \leq h_n$),

$$h(\phi) = A_n (\phi^2 - \phi_{n-1}^2) + B_n (\phi - \phi_{n-1}) + h_{n-1} \quad (5.5)$$

The other boundary condition which we apply is continuity of gradient

$$\frac{dh}{d\phi} = 2A\phi + B \quad (5.6)$$

Given the points (ϕ_i, h_i) for all i up to $n-1$, the routine reads in a point (f_n, h'_n) , puts $\phi_n = f_n^2$, evaluates (5.3) as a sum of numerical integrals over all the underlying segments, and determines B_n . A_n is then found from application of (5.6) at (ϕ_{n-1}, h_{n-1}) , and hence h_n from (5.5) with $\phi = \phi_n$.

To start this process h_1 is simply set equal to h'_1 , the height of the lowest observed frequency (f_{min}) on the ionogram, and the second segment, $h_1 \leq h \leq h_2$, is constrained to be linear, i.e. $A_2 = 0$. The base height h_0 is then found by simply extrapolating this linear section to $\phi = 0$ (Lambert, 1977). This procedure is obviously more satisfactory the lower the value of f_{min} .

The profile peak is assumed to be parabolic (Lambert, 1977); N_{\max} , the peak electron density, is found from the critical frequency foF2. By fitting a parabola such that it passes through the last two points (N_{N-1}, h_{N-1}) , (N_N, h_N) on the profile and has $\frac{dN}{dh} = 0$ at $N = N_{\max}$, the parabolic coefficients a, b, c where

$$N = ah^2 + bh + c, N_{N-1} \leq N \leq N_{\max} \quad (5.7)$$

may be determined. The real height of the peak is then

$$h_{\max} = -\frac{b}{2a} \quad (5.8)$$

5.2.3 Evaluation

Although the form of the profile described by the simple relation within the segments is satisfactory - particularly since, when a large number of points are used, the derived profile is not strongly dependent on the particular relation - there are obvious shortcomings in this method. These are :

- (i) no real correction is made for underlying D-region ionization and the base height is consequently overestimated; however the profiles computed from oblique ionograms (section 5.3) suffer from similar (or even greater) inadequacies, so that comparison of the two, as done in Chapter 6, is probably reasonable.
- (ii) the profile is monotonic, i.e. no allowance is made for 'valleys' between, for example, the E and F1 regions.
- (iii) although the value of N_{\max} may be fairly reliably found for ionograms showing low attenuation in the vicinity of the critical frequency, the determination of h_{\max} by parabolic extrapolation is probably not very reliable.

5.3 Direct Methods

There are a number of difficulties common to the three methods examined in detail below. The first of these difficulties is the assignment of an ionospheric base height h_o from the given set of data (this problem is of course common to vertical ionogram reduction techniques (section 5.2)).

An upper limit for h_o may be calculated from P'_{min} (assumed to be at the LLOF on the oblique ionogram, assuming that the ray with this frequency undergoes a "mirror" (thin - layer approximation) reflection at the base of the ionosphere. In the more rapid and approximate George (1970) method this is used as the true value of h_o , while in the Smith (1970) and Rao (1973) methods it is used as an upper limit in a double interpolation, using information from the first two points on the oblique ionogram (section 5.3.4).

The second difficulty arises from lack of information concerning the angle of elevation of a ray with a particular frequency; the angles of departure and arrival are assumed to be equal since we make the assumption of a spherically stratified ionosphere, i.e. layer tilts are neglected. In our case, as in most, these angles are unknown, and one then has to resort to either :

- (i) using an estimated value of elevation angle (Gething, 1962) (George method), or
- (ii) performing an interpolation amongst a number of trial values to determine the correct angle (Smith and Rao methods).

Fortunately this latter procedure is not too formidable as there are fairly close limits on the range of possible angles (Smith (1970) equations (13) and (14); and section 5.3.3).

In common with the vertical reduction methods we assume :

- (i) a monotonic profile, i.e. 'valleys' are again neglected;
- (ii) that the input data set (f, P') from the oblique ionogram is ordered, i.e. successive points refer to successively higher points on the profile;
- (iii) that the profile in the vicinity of the peak is parabolic.

5.3.1 Theoretical Background

As emphasised by Rao (1973), the only two fundamental assumptions required in this development are :

- (i) a spherically symmetrical ionosphere concentric with the earth,
and
- (ii) that the earth's magnetic field may be neglected.

We start with the curved earth and ionosphere version of Snell's Law (Bouger's Rule)

$$\mu r \sin \phi = \text{constant} \quad (5.9)$$

for a ray at radius r in a spherically stratified refracting medium where the phase refractive index is μ and angle of incidence ϕ . Writing

$$\Delta = \frac{\pi}{2} - \phi_E \quad , \quad (5.10)$$

where Δ is the elevation (take-off) angle and ϕ_E the angle of incidence at the earth's surface (radius R), Bouger's Rule becomes

$$R \cos \Delta = \mu r \sin \phi \quad . \quad (5.11)$$

Referring to Figure 5.1, the ground range D of the ray is given by

$$D = \int_{\text{path}} R \, d\theta = \int_{\text{path}} \frac{R \tan \phi \, dr}{r} \quad (5.12)$$

and the group path P' by (neglecting collisions)

$$P' = \int_{\text{path}} \mu' \, ds = \int_{\text{path}} \frac{ds}{\mu} = \int_{\text{path}} \frac{\sec \phi}{\mu} \, dr \quad (5.13)$$

(where μ' is the group refractive index).

Now from (5.11),

$$\tan \phi = \frac{\sin \phi}{\sqrt{1 - \sin^2 \phi}} = \frac{R \cos \Delta}{\sqrt{\mu^2 r^2 - R^2 \cos^2 \Delta}} \quad (5.14)$$

and

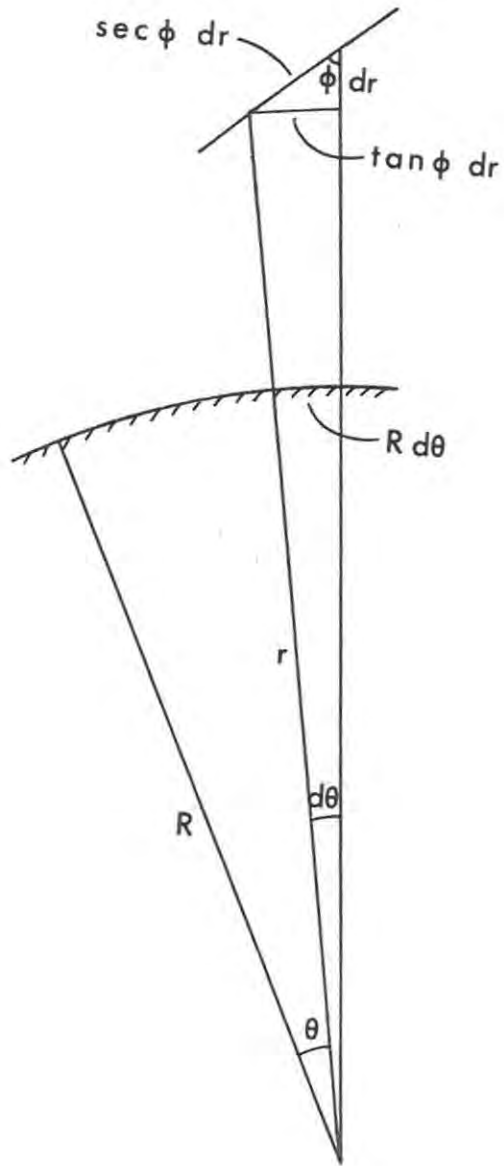


Figure 5.1 : A section of an arbitrary ray path over a curved earth, radius R .

$$\sec \phi = \frac{1}{\sqrt{1 - \sin^2 \phi}} = \frac{\mu r}{\sqrt{\mu^2 r^2 - R^2 \cos^2 \Delta}} \quad (5.15)$$

so that the expressions for ground range and group path become (Croft and Hoogasian, 1968)

$$D = R^2 \cos \Delta \int_{\text{path}} \frac{dr}{r \sqrt{\mu^2 r^2 - R^2 \cos^2 \Delta}} \quad (5.16)$$

and

$$p' = \int_{\text{path}} \frac{r dr}{\sqrt{\mu^2 r^2 - R^2 \cos^2 \Delta}} \quad (5.17)$$

To evaluate these integrals analytically requires that there be a simple relation between μ and r , i.e. that the electron density N be a simple function of r (De Voogt, 1953). [The equivalence of these two statements is seen from the Appleton-Hartree formula in the case of no magnetic field or collisions (Davies, 1965, p. 71)]

$$\mu^2 = 1 - \frac{f_N^2}{f^2} \quad (5.18)$$

where f_N is related to N by (5.1)]. Division of the ionospheric profile into concentric segments or laminae, within each of which there is such a simple relation, permits this evaluation. Although the models are simple, as in the vertical case, "as the number of laminae used is increased, the result becomes less and less dependent on the form of the assumed distribution within each segment" (Davies, 1965, p. 196). In the George (1970) method linear segments of the form

$$f_N^2 = A_i (r - r_{i-1}) + f_{N_{i-1}}^2, \quad r_{i-1} \leq r \leq r_i \quad (5.19)$$

are used, whereas in the Smith (1970) and Rao (1973) methods "quasi-linear" segments of the form

$$f_N^2 = A_i - \frac{B_i}{r}, \quad r_{i-1} \leq r \leq r_i \quad (5.20)$$

with two segment constants A_i and B_i in segment i are used.

Consider a ray with frequency f_n whose total group path (such as is measured on an oblique ionogram) is P'_n and total ground range D . The contributions to D and P'_n from the section of the ray path below the ionosphere are easily obtained either from simple geometry (see Figure 5.2) or by evaluating the integrals in (5.16) and (5.17) between R and r_o with $\mu = 1$. They are given, for propagation in one vertical direction only, by

$$D_o = R \left[\cos^{-1} \left(\frac{R}{r_o} \cos \Delta \right) - \Delta \right] \quad (5.21)$$

and

$$P'_{no} = \sqrt{r_o^2 - R^2 \cos^2 \Delta} - R \sin \Delta \quad . \quad (5.22)$$

The contributions to D and P'_n from passage of the ray through segment i are then given, by substitution of (5.20) into (5.16) and (5.17) respectively, as

$$D_i = f_n^2 R^2 \cos \Delta \int_{r_{i-1}}^{r_i} \frac{dr}{r \sqrt{ar^2 + br + c}} \quad (5.23)$$

and

$$P'_{ni} = f_n \int_{r_{i-1}}^{r_i} \frac{r \, dr}{\sqrt{ar^2 + br + c}} \quad (5.24)$$

where

$$\left. \begin{aligned} a &= f_n^2 - A_i \\ b &= B_i \\ c &= -f_n^2 R^2 \cos^2 \Delta \quad . \end{aligned} \right\} \quad (5.25)$$

Both these integrals are standard forms, evaluating analytically to

$$D_i = R \left[\sin^{-1} \left(\frac{br + 2c}{r \sqrt{b^2 - 4ac}} \right) \right]_{r_{i-1}}^{r_i} \quad (5.26)$$

and

$$P'_{ni} = f_n \left[\frac{\sqrt{ar^2 + br + c}}{a} + \frac{b}{2a \sqrt{-a}} \sin^{-1} \left(\frac{2ar + b}{\sqrt{b^2 - 4ac}} \right) \right]_{r_{i-1}}^{r_i} \quad (5.27)$$

Thus if these expressions can be evaluated for all segments i from 1 up to the segment n , at the upper boundary r_n of which the ray with frequency f_n is reflected, then the total ground range and group path are available in closed form as

$$D = 2 D_o + 2 \sum_{i=1}^n D_i \quad (5.28)$$

and

$$P'_n = 2 P'_{no} + 2 \sum_{i=1}^n P'_{ni} \quad (5.29)$$

where the factor 2 indicates upward and downward propagation through each segment. These equations can of course only be evaluated for known (or assumed) values of take-off angle Δ and base radius r_o .

5.3.2 Application of the Theory

From these basic ideas can be derived a number of other relations which aid in the more rigorous Rao analysis :

- (i) At reflection (at $r = r_n$), $\phi = \frac{\pi}{2}$, i.e. the ray is horizontal, so from Bouger's Rule (5.11),

$$R \cos \Delta = \mu r_n \quad (5.30)$$

so that the reflection level r_n is given by

$$r_n = \frac{R \cos \Delta}{\mu} = \frac{R \cos \Delta}{\sqrt{1 - f_{N_n}^2 / f_n^2}} \quad (5.31)$$

where f_{N_n} is the plasma frequency at $r = r_n$.

(ii) At $r = r_n$ also,

$$\sin^{-1} \left(\frac{br + 2c}{r \sqrt{b^2 - 4ac}} \right) = \frac{\pi}{2} \quad (5.32)$$

i.e. the upper limit for D_n in (5.26) for $i = n$ is $\frac{R\pi}{2}$. This result can be derived from (5.31) by substituting (5.20), and it has the following two important consequences -

(iii) r_n can now be found in terms of a, b, c ; i.e. in terms of the segment constants A_n and B_n and take-off angle Δ . From (5.32),

$$r_n = \frac{2c}{-b + \sqrt{b^2 - 4ac}} \quad (5.33)$$

(iv) D_n , the ground range corresponding to the ray path through the n th segment, is given by (5.26) with $i = n$ and (5.32) substituted. Then

$$D_n = R \left[\frac{\pi}{2} - \sin^{-1} \left(\frac{br_{n-1} + 2c}{r_{n-1} \sqrt{b^2 - 4ac}} \right) \right] \quad (5.34)$$

(v) At the lower boundary of the n th segment ($r = r_{n-1}$), continuity of the profile gives, from (5.20)

$$A_n = f_{N_{n-1}}^2 + \frac{B_n}{r_{n-1}} \quad (5.35)$$

and substitution of this and the expressions for a, b, c (equations

(5.25) into (5.34) leads to a solution for B_n in terms of only D_n , f_n , Δ and the profile co-ordinates at the previous point

$(f_{N_{n-1}}^2, r_{n-1})$. In fact

$$B_n = 2f_n^2 R \cos \Delta \cdot \left[\frac{R \cos \Delta}{r_{n-1}} + \sqrt{1 - \frac{f_{N_{n-1}}^2}{f_n^2} - \left(\frac{R \cos \Delta}{r_{n-1}} \right)^2} \cdot \cot \frac{D_n}{2R} \right] \quad (5.36)$$

This then suggests that, given (f_{N_i}, r_i) and (A_i, B_i) for all $i = 1$ to $n - 1$ as well as r_0 and Δ , we can use the oblique ionogram point (f_n, P'_n) to determine the parameters of segment n as follows :

- (i) find D_i for $i = 1 \dots n - 1$ from (5.26) and D_0 from (5.21)
- (ii) find D_n from (5.28) using the known D
- (iii) determine B_n from (5.36)
- (iv) determine A_n from (5.35)
- (v) compute a trial value of P'_n from (5.29), using (5.22) for P'_{no} and (5.27) for P'_{ni} , $i = 1, \dots, n$
- (vi) compare this value with the true value (from the ionogram), increment Δ and repeat the entire procedure until the desired agreement is obtained
- (vii) determine r_n from (5.33)
- (viii) determine $f_{N_n}^2$ from (5.20) at $r = r_n$

- the segment is then completely specified. This is the procedure followed in the Rao method.

The Smith formulation is appreciably simpler; here we use (5.31) and an approximate relation due to Maliphant and Muldrew (1963, unpublished) relating group path P'_n to the other ray parameters,

$$P'_n = \frac{r_n D}{R \cos \Delta} \quad (5.37)$$

to give an (approximate) expression for f_{N_n} directly from the ionogram point (f_n, P'_n) :

$$f_{N_n}^2 = f_n^2 \left(1 - \frac{D^2}{P_n'^2} \right) \quad (5.38)$$

Rewriting (5.37) we also have an explicit relation for r_n , viz.

$$r_n = \frac{P'_n R \cos \Delta}{D} \quad (5.39)$$

Then from (5.20) evaluated at the upper (r_n) and lower (r_{n-1}) boundaries of the segment n , we can obtain the segment constants

$$A_n = \frac{f_{N_n}^2 r_n - f_{N_{n-1}}^2 r_{n-1}}{r_n - r_{n-1}} \quad (5.40)$$

and

$$B_n = r_{n-1} \left(A_n - f_{N_{n-1}}^2 \right) \quad (5.41)$$

again assuming that all the underlying segment parameters as well as r_0 and Δ are already known. In practice we can compute a value of D for a given trial Δ from (5.28), using (5.21) for D_0 and (5.26) for D_i , $i = 1, \dots, n$. This D can then be compared with the known true value, Δ incremented and the procedure repeated until the two are within a specified allowable error.

In the following three sections we consider the specific problems of

- (i) the range of possible elevation angles allowed (section 5.3.3);
- (ii) the determination of the base radius r_0 and the parameters of the first segment (5.3.4);
- (iii) the profile peak (5.3.5).

5.3.3 Allowed Elevation Angles

It might at first appear that when the elevation (take-off) angle Δ of a ray is not measured we will simply have to make an arbitrary guess as to its value. In fact however, it turns out that fairly close limits can be placed on the range of possible values of Δ for a given frequency. Gething (1962) first drew attention to the fact that, given two of the three quantities P' , D and Δ , rather close limits may be placed on the third. (This problem of course only arises for a curved earth and ionosphere; in the plane earth and ionosphere case the three are related directly by the Breit and Tuve (1926) theorem). George (1970) utilizes this in his oblique ionogram reduction method, and gives an expression involving an empirical correction for a curved ionosphere. The uncorrected expression is easily derived from the geometry (Figure 3.2) as

$$\Delta = \cos^{-1} \left[\frac{2R \sin \left(\frac{D}{2R} \right)}{P'_n} \right] - \frac{D}{2R} \quad (5.42)$$

George adds a positive correction to P'_n which is proportional to the difference between P'_n and the minimum group path on the oblique ionogram to obtain an estimate of Δ directly from P'_n .

In the Smith and Rao methods the process of interpolation for the true Δ is considerably aided by the close limits which can be placed on the range of possible values for the ray with frequency f_n to be reflected at a level $r_n > r_{n-1}$. These limits are (Smith, 1970) :

- (i) Minimum angle Δ_{\min} : at this take-off angle the ray just reaches the lower boundary r_{n-1} of the segment n . This is given exactly from (5.31) evaluated at $(f_{N_{n-1}}^2, r_{n-1})$ (determined in the previous segment calculation), by

$$\Delta_{\min} = \cos^{-1} \left[\frac{r_{n-1}}{R} \sqrt{1 - \frac{f_{N_{n-1}}^2}{f_n^2}} \right] \quad (5.43)$$

A value of Δ greater than this usually avoids reflection in all segments below the n th; to ensure no such prior reflection, however,

one requires to calculate the right-hand side of (5.43) at all points $(f_{N_i}^2, r_i)$, $i = 1, \dots, n - 1$ and take the largest of these as Δ_{\min} .

- (ii) Maximum angle Δ_{\max} : for the given value of P'_n and within the approximation of (5.37) there is clearly a maximum angle such that Δ greater than this will give $r_n < r_{n-1}$:

$$\Delta_{\max} = \cos^{-1} \left(\frac{D r_{n-1}}{R P'_n} \right) \quad (5.44)$$

Evaluation of these two equations in real profiles shows that the possible values of Δ for a given segment are restricted to a narrow range (e.g. 5.88° to 7.55° in a 2F profile), making the interpolation process very efficient. The first two trial values used in practice were 1% of the range $(\Delta_{\max} - \Delta_{\min})$ above the minimum and below the maximum. Subsequent values were generated by successive linear interpolation - a process which was surprisingly efficient. Normally only 3 - 5 iterations were required to give the ground range D (in the Smith method) or group path P'_n (Rao method) to an accuracy of 0.05 km or 0.001 % !

5.3.4 The First Segment

In the first segment we have the problem that r_{n-1} , i.e. r_0 the base radius, is unknown, and a double interpolation has to be performed, using the data from the first two points on the oblique ionogram as follows :

- (i) An upper limit for r_0 is found by putting $\Delta_{\min} = \Delta_{\max}$, where for the first segment Δ_{\min} is now the take-off angle which gives a "mirror" (thin-layer approximation) reflection from the base of the ionosphere :

$$\Delta_{\min} = \tan^{-1} \left[\frac{r_0 \cos \left(\frac{D}{2R} \right) - R}{r_0 \sin \left(\frac{D}{2R} \right)} \right] \quad (5.45)$$

(derived from the geometry of Figure 3.2); and Δ_{\max} is given approximately by (5.44) with $n = 1$. This yields (in the approximation)

$$r_{\text{omax}} = R \cos \left(\frac{D}{2R} \right) + R \sin \left(\frac{D}{2R} \right) \sqrt{\frac{P_1'^2}{D^2} - 1} . \quad (5.46)$$

In the simple, rapid George method this upper limit is used as the true value of r_0 .

- (ii) A lower limit for r_0 can be arbitrarily set at, for example, $R + 90$ km. For a given trial r_0 between these two limits we can perform the interpolation in Δ outlined in section 5.3.2 to give the "true" Δ and segment parameters from the first ionogram point (f_1, P_1') .
- (iii) We then use the segment constants A_1 and B_1 determined in (ii), and assume that the second segment ($r_1 \leq r \leq r_2$) has the same constants. Then, using the second ionogram point (f_2, P_2') and Smith's approximations (5.37) and (5.38) as well as (5.20), we can calculate a take-off angle Δ_2 such that the ray with frequency f_2 and this Δ has the correct group path P_2' : we have, from (5.38) at (f_2, P_2') ,

$$f_{N_2}^2 = f_2^2 \left(1 - \frac{D^2}{P_2'^2} \right) \quad (5.47)$$

and from (5.20),

$$r_2 = \frac{B_1}{A_1 - f_{N_2}^2} \quad (5.48)$$

and hence, from (5.37),

$$\Delta_2 = \cos^{-1} \left(\frac{Dr_2}{RP_2'} \right) \quad (5.49)$$

- (iv) In the Smith method the ground range D covered by the ray with frequency f_2 and take-off angle Δ_2 is then computed, as outlined in section 5.3.2, so that for each trial r_0 a value of D is generated. Successive trial values of r_0 are generated by linear

interpolation between the two previous (r_o, D) points for the true value of D . This double interpolation is continued until the trial D approaches the true D within a specified accuracy.

- (v) In the Rao method, Δ_2 from (5.49) is used as an initial estimate in a Newton-Raphson iteration procedure (e.g. Dahlquist and Björck, 1974) using an equation implicit in Δ_2 derived as follows :
From (5.34) with $n = 1$

$$D_1 = R \cos^{-1} \left(\frac{br_o + 2c}{r_o \sqrt{b^2 - 4ac}} \right) \quad (5.50)$$

where now

$$\left. \begin{aligned} a &= f_2^2 - A_1 \\ b &= B_1 \\ c &= -f_2^2 R^2 \cos^2 \Delta_2 \end{aligned} \right\} \quad (5.51)$$

and substituting this and D_o from (5.21) into (5.28) we obtain the total ground range

$$D = 2R \left[\cos^{-1} \left(\frac{br_o + 2c}{r_o \sqrt{b^2 - 4ac}} \right) + \cos^{-1} \left(\frac{R}{r_o} \cos \Delta_2 \right) - \Delta_2 \right] \quad (5.52)$$

which cannot be solved explicitly for Δ_2 . The root calculated by the Newton-Raphson technique converges rapidly however, and once it has done so to a specified accuracy we can use this Δ_2 and f_2 to calculate P_2' , following the same procedure as that for obtaining P_1' in the first interpolation (section 5.3.2). Thus each trial r_o generates a value of P_2' ; successive trial values of r_o are generated by linear interpolation for the true value of P_2' from the ionogram. As in the Smith method, this process may be repeated until the trial P_2' is within some specified error of the true value; the value of r_o which generates this P_2' is then taken as the true base radius.

5.3.5 The Profile Peak

As in the vertical incidence case (section 5.2) the last point visible on the oblique ionogram does not represent the value of the maximum electron density. This is largely because of heavy absorption on the high-angle ray. Thus in order to obtain values for the peak parameters N_{\max} and h'_{\max} , the maximum electron density and the real height at which this maximum is attained, some extrapolation is necessary.

We again assume that the profile in the vicinity of the peak is parabolic and fit a parabola through the last three calculated (N, h) points on the profile. This is done by the standard method known as Cramer's Rule (see for example Dahlquist and Björck (1974); this is still an efficient process for the 3×3 case). We require to solve for a, b, c the system of equations

$$\left. \begin{aligned} ar_{N-2}^2 + br_{N-2} + c &= f_{N-2}^2 \\ ar_{N-1}^2 + br_{N-1} + c &= f_{N-1}^2 \\ ar_N^2 + br_N + c &= f_N^2 \end{aligned} \right\} \quad (5.53)$$

where $(f_{N_i}^2, r_i), i = N-2, N-1, N$ are the last 3 points on the calculated profile. Then

$$a = \frac{\begin{vmatrix} f_{N-2}^2 & r_{N-2} & 1 \\ f_{N-1}^2 & r_{N-1} & 1 \\ f_N^2 & r_N & 1 \end{vmatrix}}{\begin{vmatrix} r_{N-2}^2 & r_{N-2} & 1 \\ r_{N-1}^2 & r_{N-1} & 1 \\ r_N^2 & r_N & 1 \end{vmatrix}}, \text{etc.} \quad (5.54)$$

and the profile peak is at

$$\frac{df_N^2}{dr} = 2ar + b = 0 \quad (5.55)$$

so that $r_{\max} = -\frac{b}{2a}$ (5.56)

and $f_{N_{\max}}^2 = ar_{\max}^2 + br_{\max} + c$ (5.57)

5.4 Evaluation of the Methods

The oblique ionograms from which we wish to derive $N(h)$ profiles by these methods must meet certain basic requirements. These are :

- (i) The ionogram must be continuous.
- (ii) The ionogram must be monotonic - that is, successive ionogram data points must refer to higher points on the profile; this is a natural property of the ordered data set.
- (iii) The group path P' at any frequency is known absolutely.

In practice these requirements are easily met by digitizing (Chapter 4) an oblique ionogram into typically 20 - 30 points starting at the LLOF, proceeding in short steps up to the JF and then up the high-angle ray to the HLOF. If the offset on the ionogram is known, then all the above are satisfied.

The derived profiles have the following properties :

- (i) They are continuous and defined for all heights up to the peak, and their derivatives $\frac{dN}{dh}$ are also continuous. This is an important requirement for our purposes, in particular for use in the ray tracing program (Chapter 7).
- (ii) They are monotonic - "valleys" in the profiles where N decreases with increasing h are not catered for. The "re-entrant profile" approximation of Smith (1970) is not included. For our purposes this is satisfactory, as lower E- and F1-layer traces continuous with F2 traces are very rarely observed on the oblique ionograms.

The fact that only F2 region information is provided by the oblique ionograms means that considerable information on lower ionization in daytime profiles will be lacking. At night the position may be satisfactory as generally only a single F layer is observed on vertical ionograms then also. For daytime profiles to be realistic, some artificial correction or incorporation of lower-lying ionization will have to be made. Methods of performing this are discussed in section 7.3.

In the absence of any such correction, the base height derived by the Smith and Rao methods is critically dependent on the first two points on the oblique ionogram. These two points are used in the double interpolation technique described in section 5.3.4 and in effect define an initial slope for extrapolation back to zero density. Variation of the P' values of these two points relative to each other, even by only the small amount allowed in terms of the uncertainty to which P' can be read from the ionogram (typically 3 km, or 1.5 km per "hop" for the 2F mode), leads to appreciable alterations in the computed base height.

In the next chapter we shall be comparing directly profiles from oblique (using the above methods) and vertical ionograms (using the method of section 5.2.2). In view of the above remarks about lower lying ionization it is perhaps as well to ask at this stage whether such a comparison is valid. In the nighttime case where only F region traces are observed on both oblique and vertical ionograms, it probably is. During the day at lower frequencies it will of course be invalid, although the peak determination for the oblique profile should be little affected by the inclusion or exclusion of underlying ionization, so that comparison of peak densities (but perhaps not peak heights) may be quite valid (section 7.3).

The next question to be considered is - what does the oblique profile represent? Any profile derived from an oblique ionogram is in some way representative of conditions over some appreciable distance, particularly in our case where the angles of elevation are low and the rays cover very large ground ranges in traversing the ionosphere. An example from the ray tracing studies of Lambert (1977) will serve to illustrate the distances involved. For two equal hops through an "effective" normal daytime profile, a 15 MHz ray was above the ionospheric base height of 124 km for a ground range of 997 km on each hop out of the total hop length of 2235 km. [Even a simple calculation using equation (5.42) to

give Δ from the measured P' , then equation (5.21) for D_0 , whence the required ground range is $D - 2D_0$, gives for this example 952 km. This is essentially a lower limit as equation (5.42) gives the minimum Δ for given P' .] Thus there is no means by which we can obtain a realistic $N(h)$ profile at a particular point along the path, particularly when two or more hops are involved.

However, from the point of view of ray tracing and prediction of transmission frequencies, the "effective profile" derived from the oblique ionogram by the above methods "may often be precisely what is required" (George, 1970). In fact, "although the effective profile derived from the oblique data does not, and indeed cannot in general be expected to lie near the mid-point profile when the layer is known to be other than concentric, nevertheless ray tracing of this effective profile under the assumption of concentricity must produce the experimentally observed $P'(f)$ data at the given range since the process is reciprocal" (George, 1970). This is a justification for using "oblique profiles" as a means of reproducing oblique ionograms by ray tracing methods; it is confirmed in Chapter 7.

In view of the formulations of the methods in the previous sections, we would expect the profile computed by the Rao method to be the most accurate within the assumed approximations (no magnetic field and spherically stratified ionosphere), since it involves fewer simplifying approximations and is in fact, within the above limitations, almost exact. Thus, this profile, if any, should be considered the "true" profile derived from the oblique ionogram, and any later reference simply to an "oblique profile" will be taken to mean the profile derived from the oblique ionogram by the Rao method.

FORTTRAN programs for the Smith and Rao reduction methods were written directly from the formulations given in Appendix E. They were first tested on 4 simple "nighttime" oblique ionograms obtained during the R.S.A. great circle cruise discussed in the next chapter. Some points which arose in the practical implementation of the methods are :

- (i) The base heights derived by the Smith method were always lower than those calculated by the Rao method, apparently because the take-off angle Δ_2 calculated by Newton-Raphson iteration from

equation (5.52) in the latter method (section 5.3.4) was greater than the approximate Smith value from equation (5.49).

- (ii) The peak extrapolation (section 5.3.5) appeared to be more reliable in the Rao method than the Smith method. The peak of the latter profile was generally considerably more extended in both height and density from the last calculated point on the profile than either the Rao profile or that obtained indirectly via the equivalent vertical ionogram. There is no obvious reason for this as the same parabolic extrapolation technique was used.
- (iii) The interpolation in Δ was fairly efficient, convergence to the required accuracy generally being obtained in 3 - 5 trials. The interpolation in r_0 for the first segment double interpolation was not as efficient however, and in some cases Lagrangian interpolation had to be resorted to when D or P' had not converged to the required accuracy after 10 trials.
- (iv) The arrays were dimensioned 50, i.e. they could handle oblique ionograms with up to 50 points. Both programs required 14K of core on the ICL 1902T computer. A typical 28 point profile was reduced in 265 mill seconds by the Smith method and 375 mill seconds by the Rao method. A typical output is given in Table 5-1 and listings of the two programs NHSMITH and NHRAO are given in Appendix E.

Table 5-1 : Sample output N(h) profile from program NHRAO (for the oblique ionogram of 1977 day 043 1340 UT, 2F mode).

N(H) PROFILE FROM OBLIQUE IONOGRAM 1977 DAY 043 1540 SAST 2 HOP TRACE

BASE HEIGHT HO : MIN = 100.00 MAX = 237.73 KM EARTH RADIUS RE = 6371.35 KM DISTANCE D = 2235.42 KM

INTERPOLATED BASE HEIGHT HO = 202.59 KM RAO METHOD WITH SEGMENTS OF THE FORM FN2 = A - B/R WHERE R = RE + H

H (KM)	NE (CM-3)	SEGMENT	PARAMETERS A(N),B(N)	N	FN (MHZ)	F (MHZ)	P' (KM)	DELTA (DEG)
219.97	2.1399E 05	6.5452E 03	4.3028E 07	1	4.1534	14.81	2323.00	6.7793
221.21	2.2930E 05	6.5411E 03	4.3001E 07	2	4.2995	15.25	2324.50	6.9056
222.06	2.4116E 05	7.4335E 03	4.8884E 07	3	4.4092	15.60	2325.00	6.9475
222.97	2.5531E 05	8.2977E 03	5.4582E 07	4	4.5368	16.01	2325.50	6.9878
223.66	2.6647E 05	8.6408E 03	5.6845E 07	5	4.6349	16.32	2326.00	7.0294
224.30	2.7719E 05	8.9319E 03	5.8764E 07	6	4.7271	16.61	2326.50	7.0701
225.05	2.8888E 05	8.2994E 03	5.4592E 07	7	4.8258	16.90	2327.50	7.1539
225.71	2.9981E 05	8.8819E 03	5.8435E 07	8	4.9163	17.18	2328.00	7.1952
226.54	3.1325E 05	8.5903E 03	5.6511E 07	9	5.0253	17.50	2329.00	7.2783
227.27	3.2438E 05	8.2251E 03	5.4102E 07	10	5.1138	17.75	2330.00	7.3612
227.93	3.3424E 05	7.8631E 03	5.1713E 07	11	5.1909	17.96	2331.00	7.4449
228.83	3.4332E 05	5.4556E 03	3.5825E 07	12	5.2609	18.06	2334.00	7.6981
229.51	3.4815E 05	3.7722E 03	2.4714E 07	13	5.2978	18.03	2337.50	7.9912
229.89	3.4968E 05	2.1847E 03	1.4236E 07	14	5.3095	17.88	2342.00	8.3704
230.70	3.5286E 05	2.1272E 03	1.3856E 07	15	5.3335	17.76	2346.50	8.7437
231.11	3.5412E 05	1.6340E 03	1.0600E 07	16	5.3430	17.60	2351.00	9.1166
232.81	3.6024E 05	1.9452E 03	1.2654E 07	17	5.3890	17.51	2356.00	9.5198
233.67	3.6269E 05	1.5468E 03	1.0024E 07	18	5.4073	17.29	2362.50	10.0441
234.35	3.6451E 05	1.4619E 03	9.4625E 06	19	5.4208	17.16	2366.50	10.3620
237.06	3.7257E 05	1.6121E 03	1.0455E 07	20	5.4804	17.00	2374.00	10.9384
238.26	3.7588E 05	1.5067E 03	9.7584E 06	21	5.5048	16.86	2379.00	11.3208
239.67	3.7919E 05	1.2774E 03	8.2431E 06	22	5.5289	16.57	2388.00	11.9991
241.79	3.8428E 05	1.3125E 03	8.4748E 06	23	5.5659	16.39	2395.00	12.5078
244.17	3.8991E 05	1.2899E 03	8.3251E 06	24	5.6066	16.19	2403.00	13.0744
247.07	3.9672E 05	1.2863E 03	8.3015E 06	25	5.6553	16.00	2411.50	13.6570
249.44	4.0195E 05	1.2098E 03	7.7953E 06	26	5.6925	15.78	2420.50	14.2616
288.28	4.4354E 05	PARABOLIC FIT FOR PROFILE PEAK			5.9797			
PEAK PARAMETERS A,B,C	-2.2223E-03	2.9599E 01	-9.8525E 06	WHERE FN2 = A*R2 + B*R + C				

CHAPTER 6

RESULTS FROM THE R.S.A. "GREAT CIRCLE CRUISE"

FEBRUARY 1977

6.1 Introduction

As mentioned in Chapter 1, the research ship R.S.A. followed the SANAE - Grahamstown great circle path as far as 36°S on its return voyage from Antarctica in February 1977 (Figure 6.1). The vertical incidence ionosonde "Minibal" was operated on board and recorded vertical ionograms at 5 minute intervals for virtually the entire cruise (Haggard, 1977). The SANAE - Grahamstown sounding schedule (Table 2-1) was changed so that additional oblique soundings were made at 10, 25, 40 and 55 minutes in the hour for the duration of the cruise. Simultaneous oblique and vertical ionograms were thus obtained, allowing comparison of the two for different points along the path.

The first analysis of results, involving reduction of 2F oblique data to equivalent vertical ionograms (section 6.2), etc., was again carried out under the assumption of equal hops. The R.S.A. reached the 2F "reflection points" (Table 2-3) on 10 February (day 041) at 1915 UT and 19 February (day 050) at 0055 UT respectively; it cruised at typically 10 knots, thus covering about 450 km per day (Figure 6.1).

GREAT CIRCLE ROUTE FEBRUARY 1977

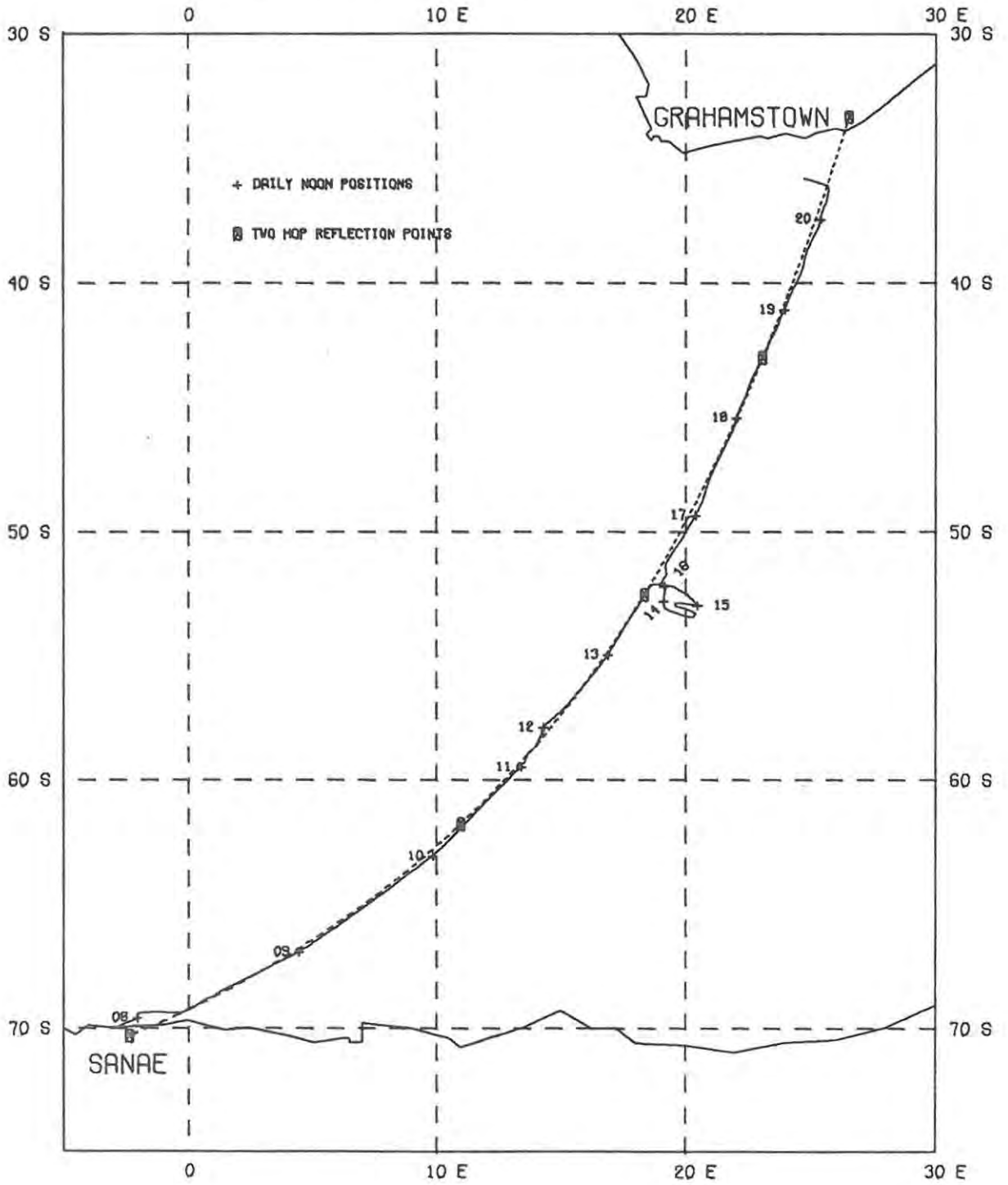


Figure 6.1 : The course of the research ship R.S.A. (solid line) 8 - 20 February 1977 along the SANAE - Grahamstown great circle (dashed line).

6.2 First Analysis : Nighttime Ionograms

6.2.1 Nighttime Equivalent Vertical Ionograms and N(h) Profiles

Two nighttime oblique ionograms and simultaneous R.S.A. vertical ionograms from the evening of 10 February, when the ship was near the first hop reflection point, and two from the night of 18 - 19 February, when it was near the second reflection point, were selected according to the following criteria :

- (i) low minimum frequency on both oblique and vertical records;
- (ii) continuous, well-defined and monotonic traces up to large P' or h' respectively;
- (iii) no intermediate cusps or spread-F conditions visible on the traces.

The times of the ionograms selected are listed in Table 6-1, together with the position of the R.S.A.

Table 6-1 : Nighttime oblique and simultaneous R.S.A. vertical ionograms selected.

<u>No.</u>	<u>Day</u>	<u>Time (UT)</u>	<u>R.S.A. Position</u>	<u>Distance (km)</u>
1.	041 (10 Feb)	1925	61°45'S 11°09'E	+ 9
2.	041 (10 Feb)	1955	61°40'S 11°14'E	+18
3.	049 (18 Feb)	2025	43°48'S 22°40'E	-97
4.	050 (19 Feb)	0320	42°33'S 23°17'E	+50

(The distance from the appropriate reflection point is given as negative if the ship is south of it, positive if north).

In each of these four cases the oblique ionogram was reduced to the equivalent vertical one, by the techniques described in section 3.1.2, and compared with the simultaneous R.S.A. vertical ionogram, as shown in the (A) sections of Figures 6.2 - 6.5. It is clear that the equivalent vertical ionogram is very similar to the R.S.A. ionogram in the vicinity of the first

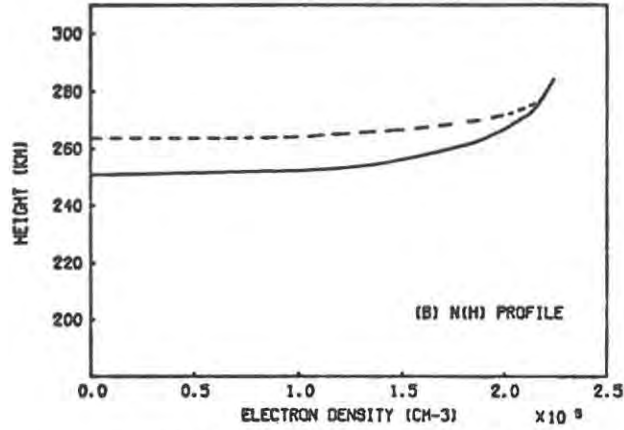
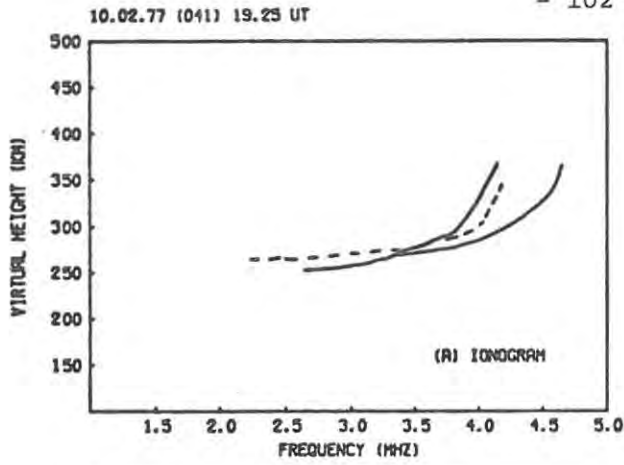


Figure 6.2 : Day 041 1925 UT.

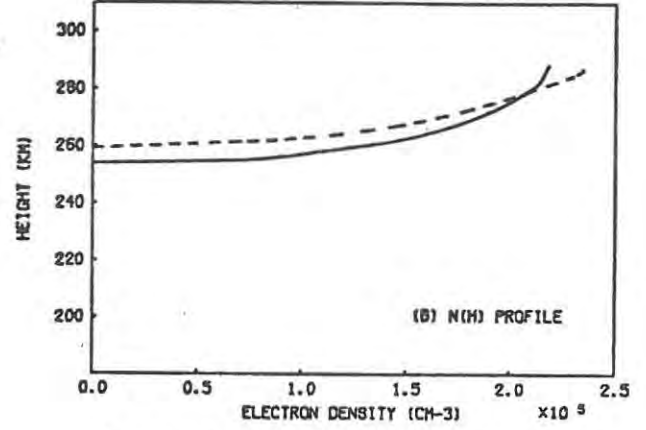
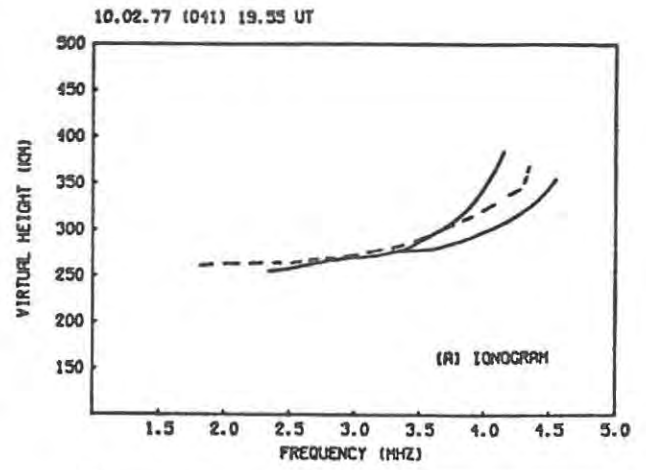


Figure 6.3 : Day 041 1955 UT.

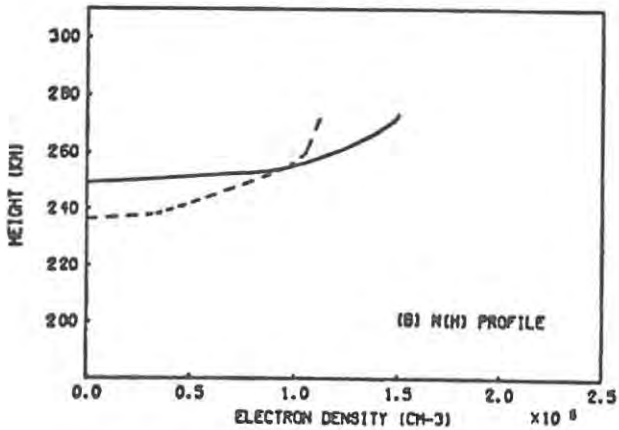
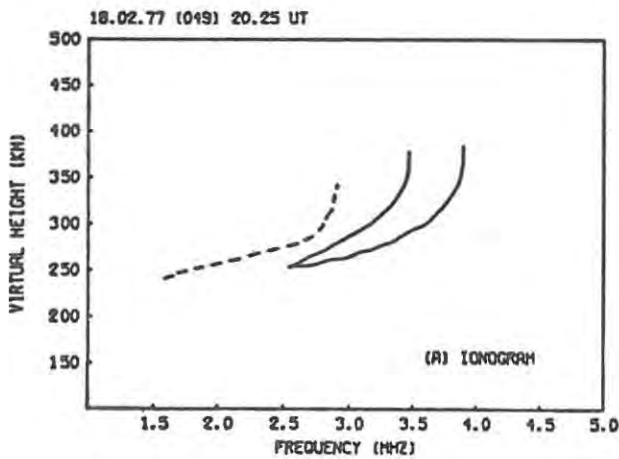


Figure 6.4 : Day 049 2025 UT.

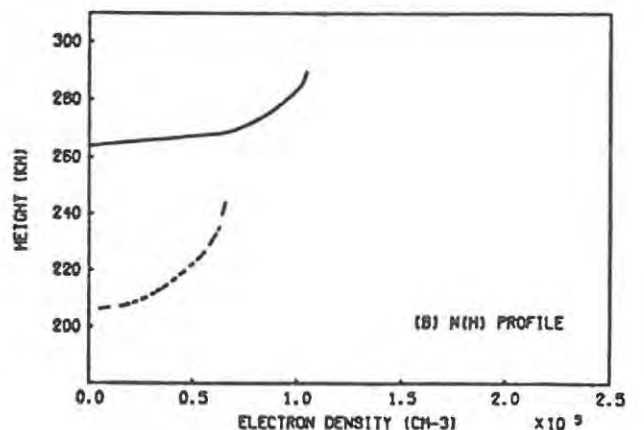
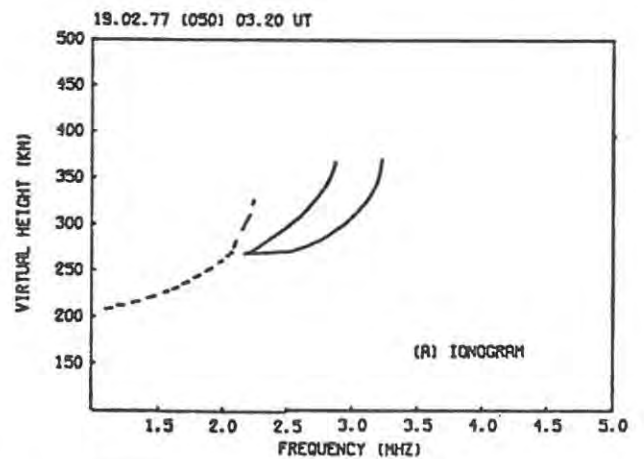


Figure 6.5 : Day 050 0320 UT.

Figures 6.2 - 6.5 : Nighttime ionograms (A) and derived N(h) profiles (B) from the R.S.A. (solid lines) and equivalent vertical ionogram (dashed lines).

reflection point (Figures 6.2(A) and 6.3(A)), but the two are quite dissimilar in the vicinity of the second reflection point (Figures 6.4(A) and 6.5(A)). This constituted the first direct evidence that the first hop region was in fact the "control" area for the 2F oblique mode.

These vertical ionograms were all reduced to $N(h)$ profiles, by the techniques described in section 5.2.2, and these profiles plotted and compared, as shown in the (B) sections of Figures 6.2 - 6.5. In the first two cases (Figures 6.2(B) and 6.3(B)) the two profiles are very similar in all respects (base height, peak height, peak density), whereas in the second two cases the R.S.A. profiles have considerably greater base heights and peak electron densities than the corresponding equivalent vertical profiles.

In order to check to what extent the resultant profile depended on the absolute group path and virtual height measurements, i.e. on the offset, etc., the base height of the equivalent vertical profile was set equal to that of the R.S.A. profile and the analysis repeated (Figures 6.6 - 6.9). It was then possible to obtain very good agreement between the two profiles in the vicinity of the first reflection point (Figures 6.6(B) and 6.7(B)), but not in the vicinity of the second (Figures 6.8(B) and 6.9(B)).

The above analysis was performed by a FORTRAN program OVIO (for Oblique and Vertical Incidence Ionograms) on the ICL computer; the repetition with equal base heights and plotting of ionograms and/or profiles, by calls to the subroutine AMGRAPH (Terry, 1975), were optional. A listing of the updated version OVIP of this program is given in Appendix E.

6.2.2 Discussion

Nighttime ionograms were used in this first analysis because of their simplicity : only F traces were present in all cases, so that derived F region profiles could be directly compared. The results of the above analysis indicated that, at least at night, the $N(h)$ profile derived from the 2F oblique ionogram via the equivalent vertical one is a good representation of the profile derived from the vertical ionogram obtained in the vicinity of the first reflection point, but this representation does not hold in the vicinity of the second reflection point.

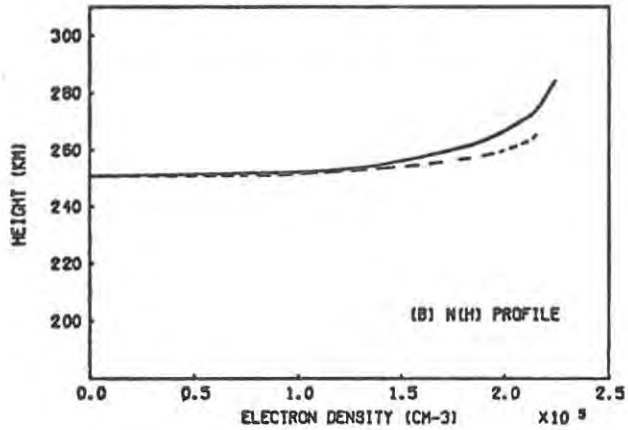
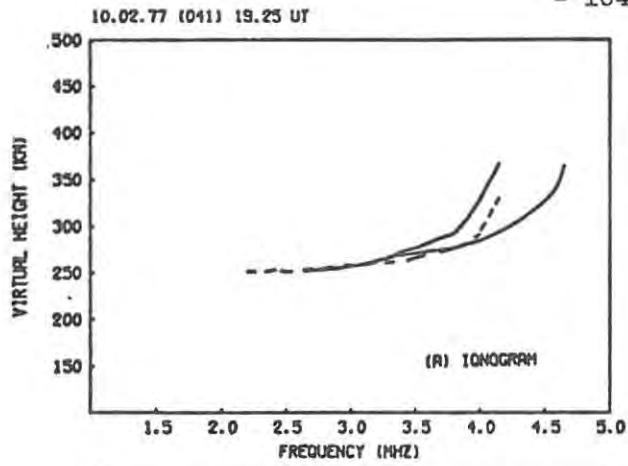


Figure 6.6 : Day 041 1925 UT.

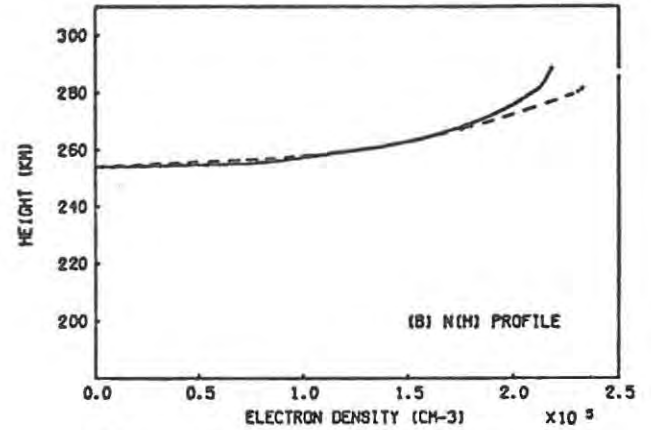
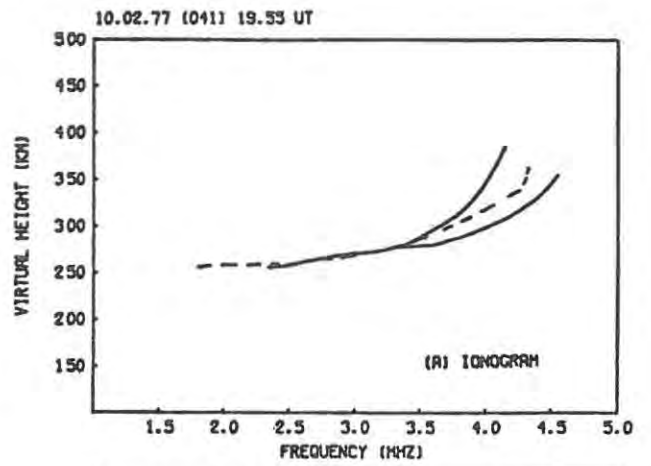


Figure 6.7 : Day 041 1955 UT.

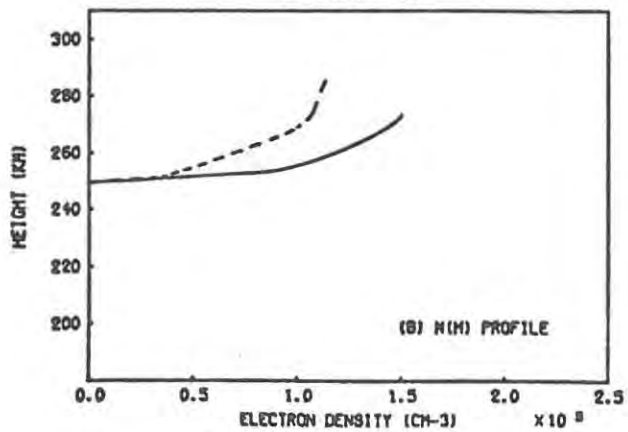
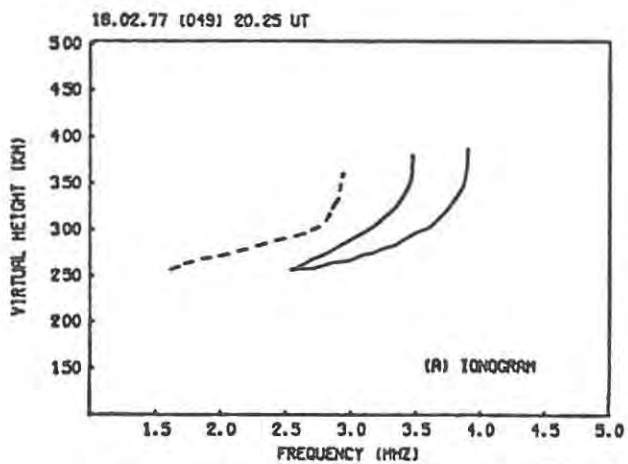


Figure 6.8 : Day 049 2025 UT.

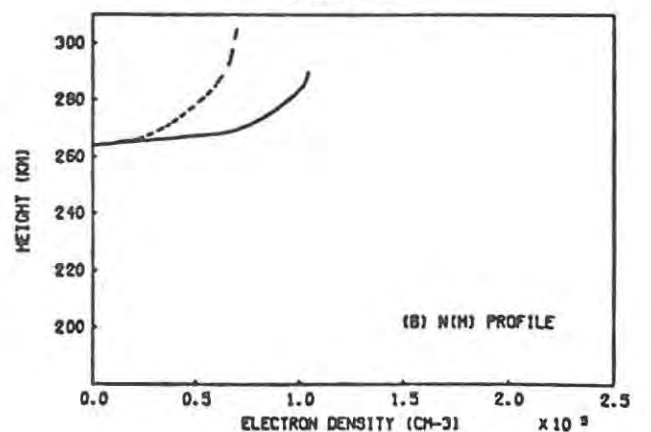
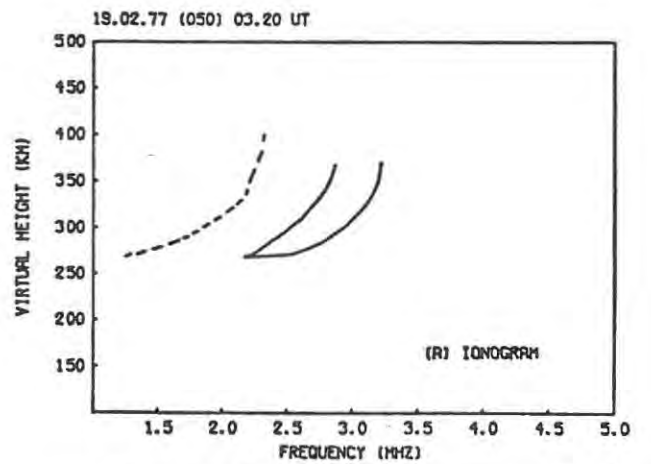


Figure 6.9 : Day 050 0320 UT.

Figures 6.6 - 6.9 : The nighttime ionograms (A) and derived N(h) profiles (B) of Figures 6.2 - 6.5, with equal base heights (solid lines, R.S.A.; dashed lines, equivalent vertical ionogram).

Further, the fact that the peak electron density N_{\max} of the equivalent vertical profile is smaller than that of the R.S.A. profile in the latter case seemed to indicate that, at night, N_{\max} at the first reflection point is less than that at the second, and that the former is the "control" point limiting the observed MOF. This was an important first result and was presented in a preliminary paper at an S.A.I.P. conference (Rash and Haggard, 1977). We would expect this if the ionosphere varies in some regular monotonic way between SANAE and Grahamstown since foF2 is generally lower at SANAE than at Grahamstown (e.g. the linear latitude dependent model of Lambert (1977)).

Figure 6.3(B) shows N_{\max} of the equivalent vertical profile to be greater than that of the R.S.A. profile, which cannot be accounted for in terms of the above. The idea that this could be due to tilts or gradients in N developed later; at the time (Rash and Haggard, 1977) it was thought that it could be due to one or more of the following causes :

- (i) the x- instead of the o- trace could have been measured on the oblique ionogram; the two modes are not normally separable. The difference between the ordinary and extraordinary JF's is generally less than the value $f_B/2$ observed between the corresponding critical frequencies on vertical ionograms (Davies, 1965, p. 181);
- (ii) absorption and spread traces could have caused inaccuracies;
- (iii) the ionospheric curvature correction factor k (section 3.1.3) could have been incorrect;
- (iv) the offset of the oblique ionogram may have been in error.

Another point to note is that the base heights, and in fact the heights at which N has a particular value, are practically the same for all four R.S.A. profiles, i.e. these heights are the same for the first hop and second hop region nighttime profiles, although this is perhaps fortuitous as they are at different values of UT. Thus a ray with a particular frequency would be reflected at almost the same height on both hops, apparently supporting our assumption of two equal hops.

6.2.3 Diurnal Variation in Vertical Critical Frequencies

In order to check how typical the conditions described in the previous section were, the diurnal variations in foF2 from the R.S.A. and EVFO (2F) when the ship was in the vicinity of each of the reflection points in turn were compared. The days used were day 041, during which the R.S.A. sailed from 65°S 7°E to 61°S 12°E (from 400 km south to 100 km north of the first reflection point), and day 050, during which it sailed from 43°S 23°E to 39°S 25°E (from 20 km south to 450 km north of the second reflection point).

The diurnal variations in the critical frequencies foF2 (R.S.A.) and EVFO (2F) as well as MOF (2F) for each of these two days are shown in Figures 6.10 and 6.11 respectively. The times of ground sunrise and sunset at the first and second reflection points are indicated by the lower and upper pairs of up-arrows respectively. Examination of these frequency plots reveals several features :

- (i) On day 041 (Figure 6.10) the oblique MOF and EVFO show normal quiet day variation, except that values for the morning hours after sunrise are missing due to absorption.
- (ii) The value of foF2 (R.S.A.) is less than that of EVFO (2F) throughout day 041 except during the evening hours after sunset at the second reflection point (~ 2000 - 2200 UT), when foF2 is greater. Sunset occurs almost two hours later at the first reflection point, so that during this period the lower nighttime N_{\max} at the second reflection point limits the MOF, while the daytime ionization levels at the first reflection point (as measured by foF2 (R.S.A.)) are maintained to a later UT.
- (iii) On day 050 (Figure 6.11) loss of oblique data because of absorption is considerably less. However, conditions appear to be slightly disturbed compared with day 041, with all three frequencies increasing more rapidly after sunrise to show enhancements of MOF and EVFO in the late morning and depressions in the early afternoon.
- (iv) foF2 (R.S.A.) is greater than EVFO (2F) from the late morning onwards on day 050.

1977 DAY 041 : RSA + OBLIQUE 2F

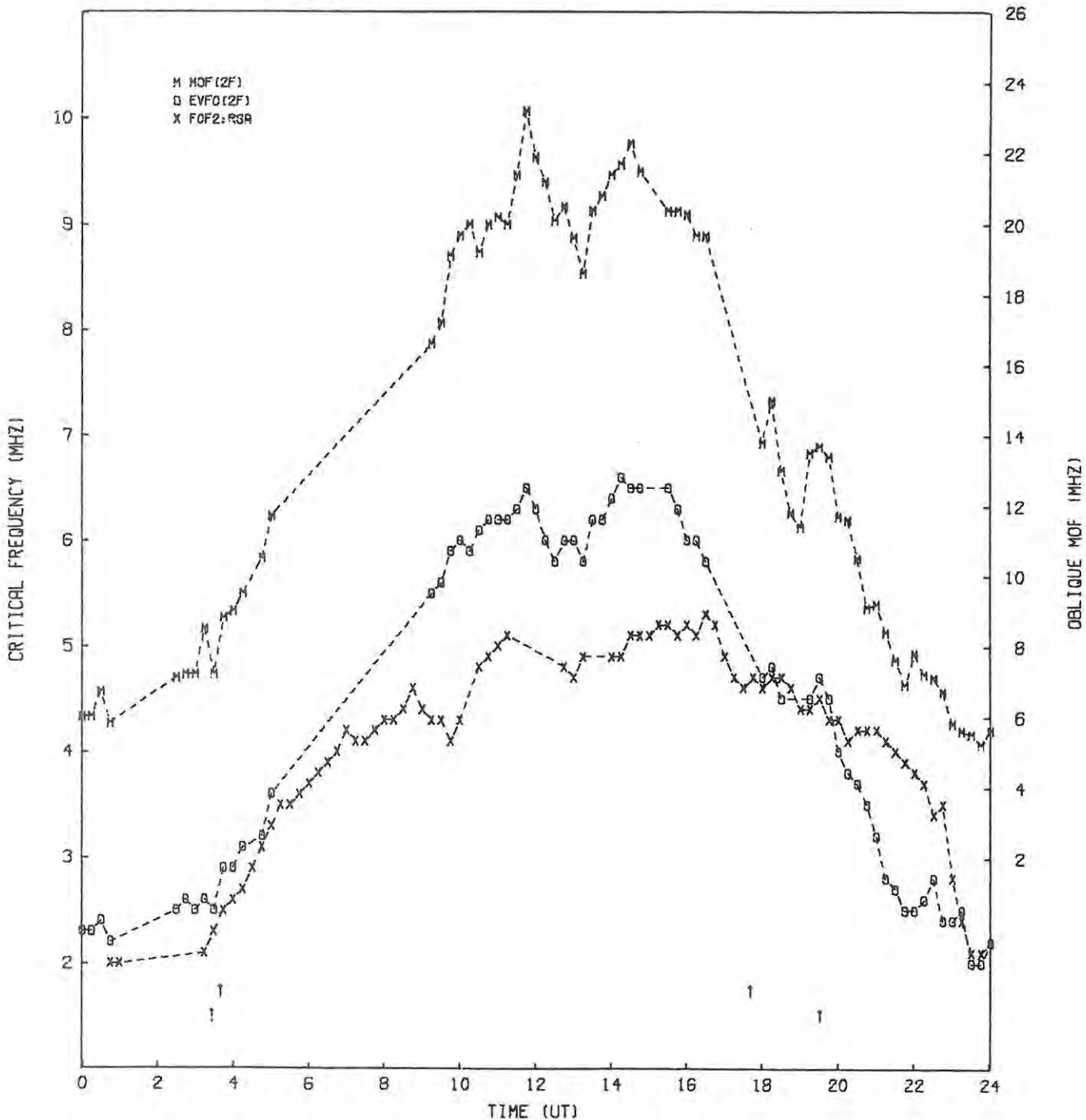


Figure 6.10 : Diurnal variation of foF2 (R.S.A.), EVFO (2F) and MOF (2F) for day 041.

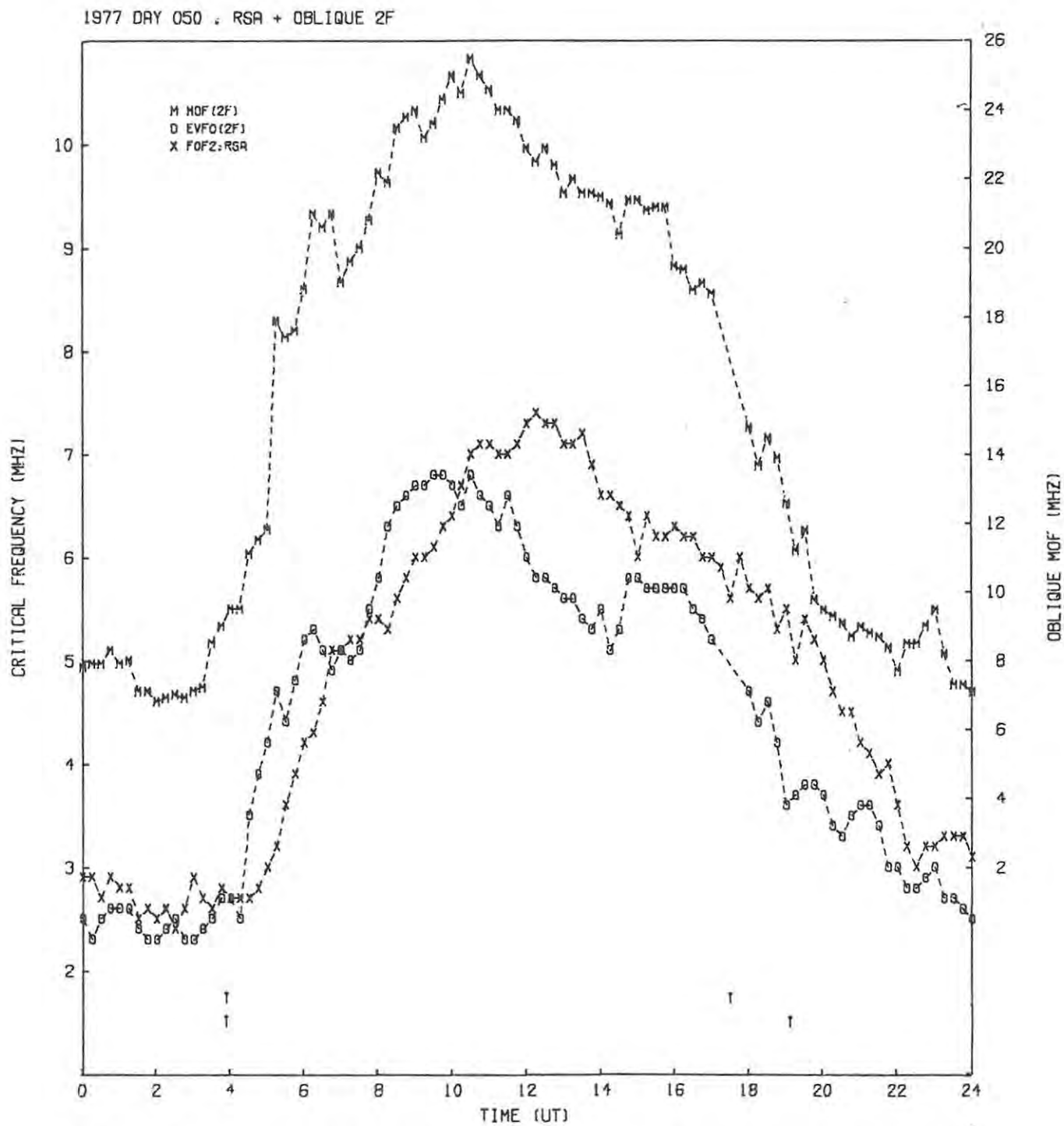


Figure 6.11 : Diurnal variation of foF2 (R.S.A.), EVFO (2F) and MOF (2F) for day 050.

If these critical frequencies represent the approximate value of N_{\max} then we would expect EVFO (2F) to be at most equal to the lower of the two values of foF2 at the reflection points. We cannot, in terms of the above, explain the observation (Figure 6.10) that EVFO is greater than foF2 at the first reflection point. It was suggested (Rash and Haggard, 1977) that this "discrepancy" might be due to an overestimation of EVFO obtained using the inverse transmission curves (section 3.1.4). The positioning of the latter on the h' scale, and therefore the value of EVFO, depend on the offset of the oblique ionogram, which could be in error. At 1100 UT, for instance, EVFO (2F) = 6.2 MHz and foF2 (R.S.A.) = 5.0 MHz; to make the two equal would require the offset to be reduced by 0.34 msec (103 km group path). Such an error is unlikely since the offset was calibrated (section 2.3.2) on the following day, and the above reduction would decrease EVH'F from 257 to 159 km - an unreasonable value (section 3.1.5).

A much more likely explanation of the observed behaviour is that the two hops are not of equal length, as a result of longitudinal tilts. Möller (1964) shows how the effects of tilts are "one sided", in that only increases in MOF over the untilted values are observed whether the tilt is positive or negative along the transmission path. This is discussed in section 7.5.

Between about 1100 UT and 1400 UT on day 050 (Figure 6.11) foF2 (R.S.A.) is significantly greater than EVFO (2F). This is simply explained in terms of the first reflection point being the control in the absence of strong tilt effects. However, this difference persists through the late afternoon and early evening; we would expect foF2 (R.S.A.) to fall more rapidly during this period on this day than on day 041 (Figure 6.10) because of the earlier sunset in this region.

6.2.4 Nighttime Profiles Directly from Oblique Ionograms

The four nighttime oblique ionograms of Table 6-1 were next reduced directly to N(h) profiles by each of the Smith and Rao methods described in section 5.3, and these profiles compared with the corresponding equivalent vertical and R.S.A. profiles (section 6.2.1). This served as a useful first test of these methods (see section 5.4). These N(h) profiles, for cases 1-4, are shown in Figures 6.12 - 6.15 respectively, on the same scales.

N(H) PROFILES 10.02.77 1925 UT

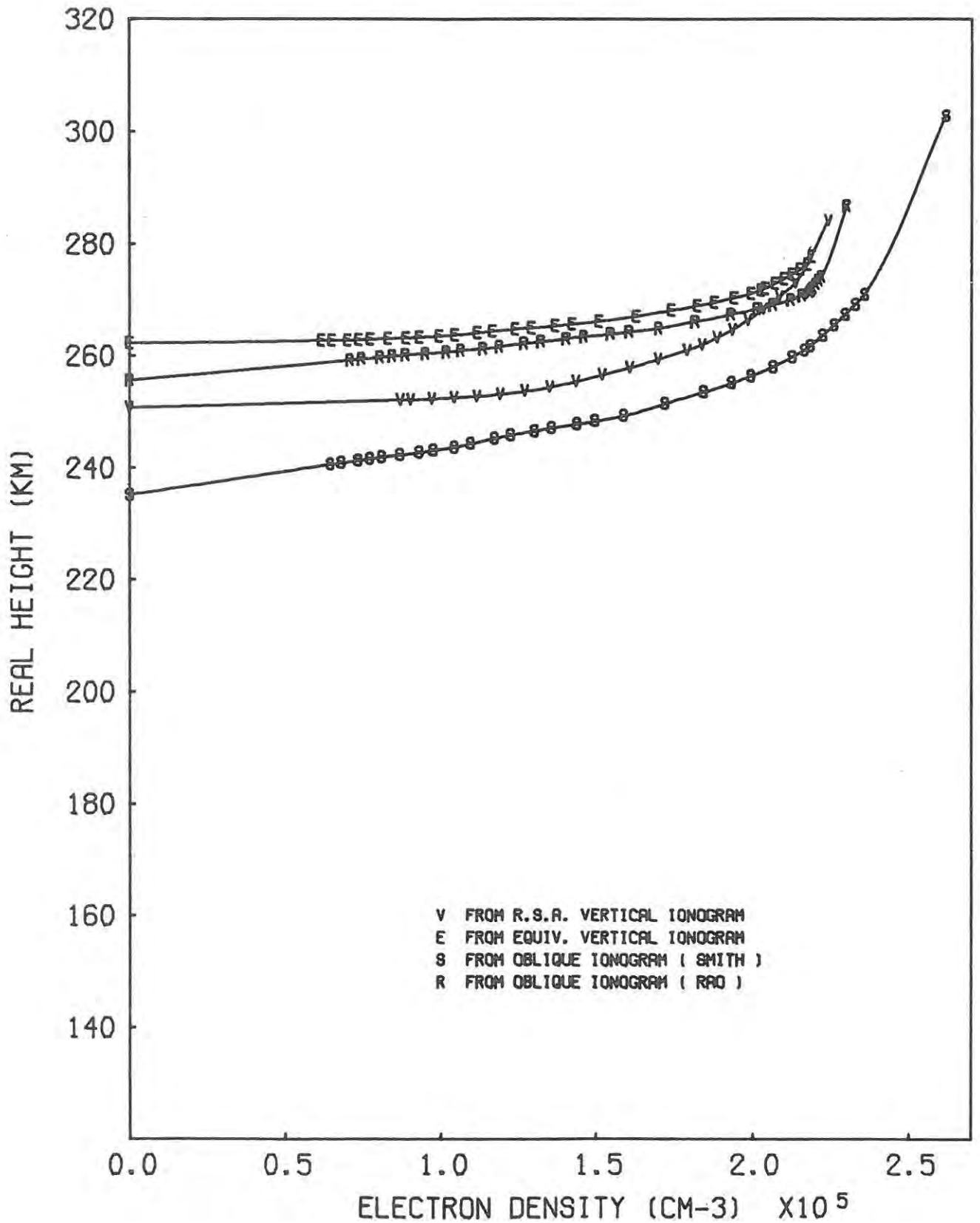


Figure 6.12 : Nighttime N(h) profiles for day 041 1925 UT.

N(H) PROFILES 10.02.77 1955 UT

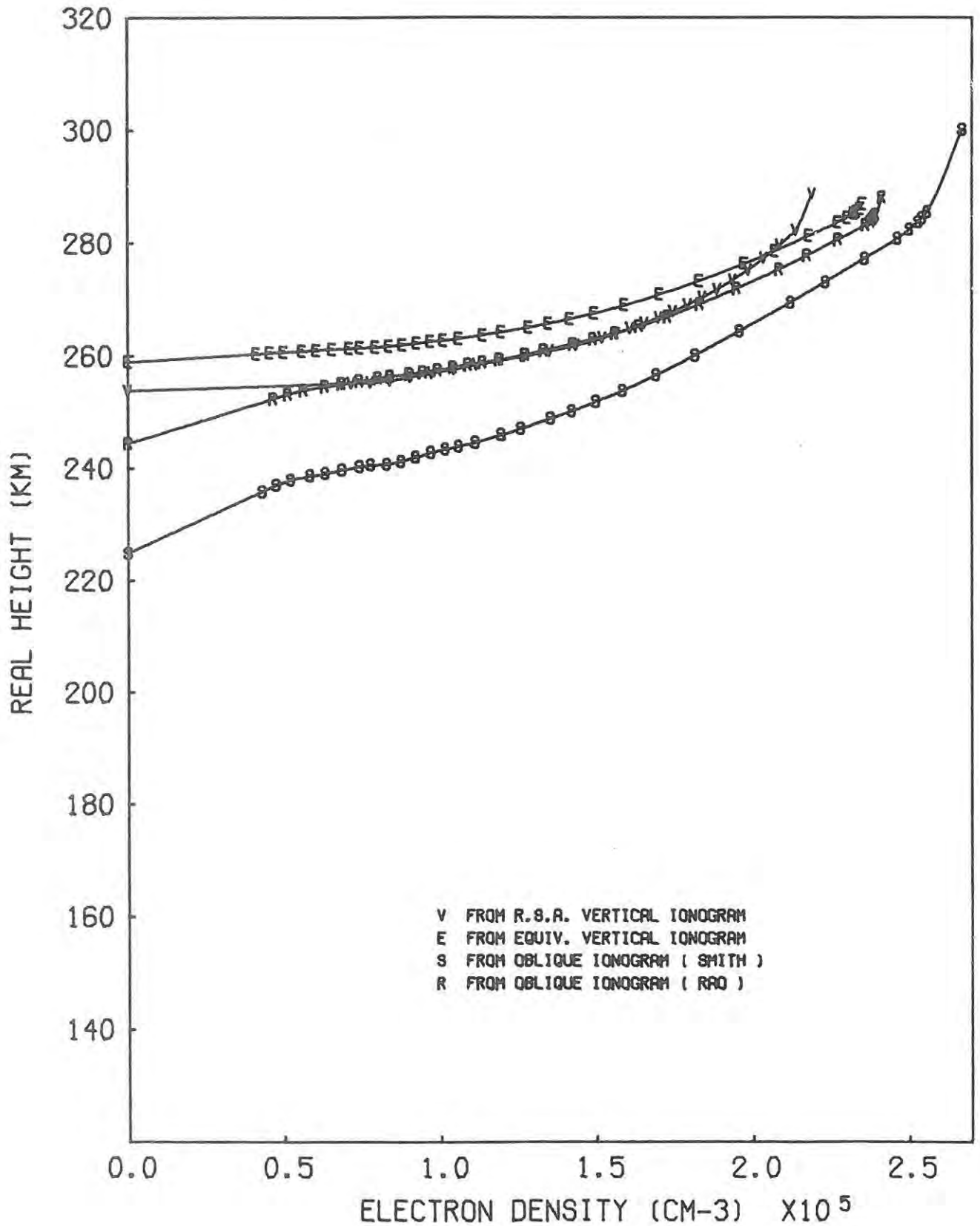


Figure 6.13 : Nighttime N(h) profiles for day 041 1955 UT.

N(H) PROFILES 18.02.77 2025 UT

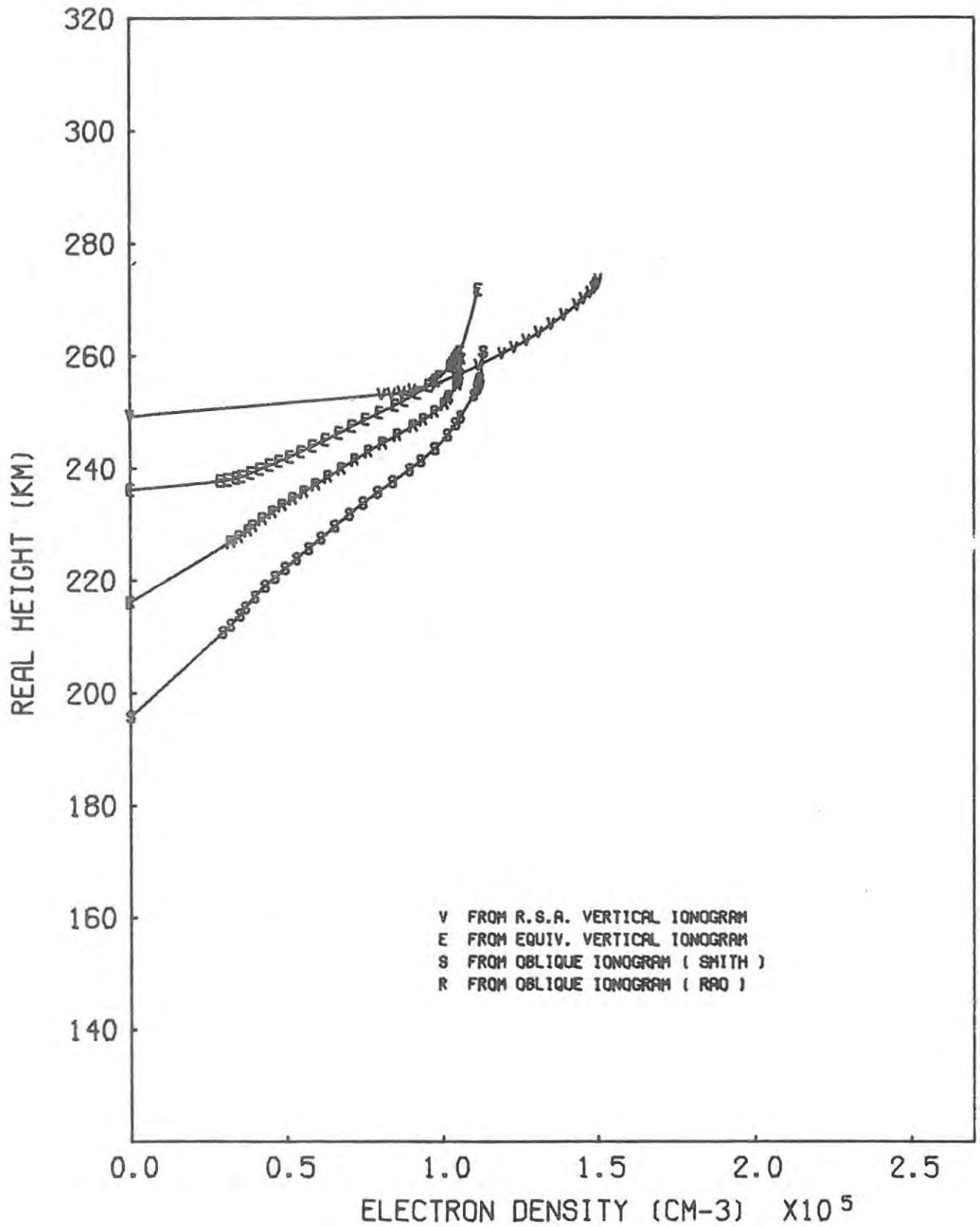


Figure 6.14 : Nighttime N(h) profiles for day 049 2025 UT.

N(H) PROFILES 19.02.77 0320 UT

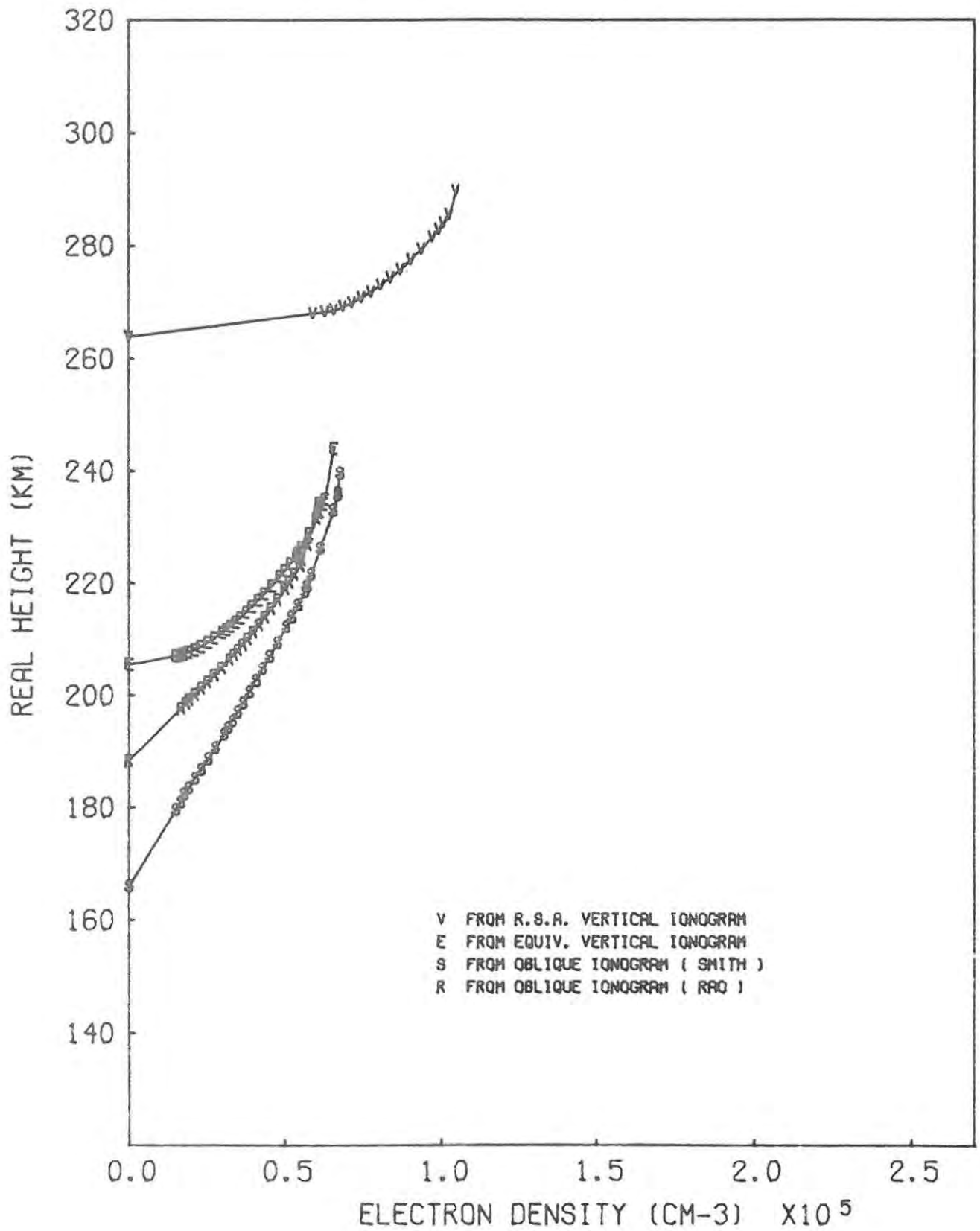


Figure 6.15 : Nighttime N(h) profiles for day 050 0320 UT.

The Rao oblique profile is the profile which agrees most closely with the R.S.A. profile in the vicinity of the first reflection point (Figures 6.12 and 6.13). The Smith oblique profile has considerably lower h_o and greater N_{max} in both cases. While the oblique and R.S.A. profiles are similar in this region, they differ markedly in the second hop reflection region (Figures 6.14 and 6.15). In the latter cases, however, the three "oblique profiles" are reasonably consistent. The equivalent vertical and Rao profiles are remarkably similar in all four cases, showing that within the same approximations (no magnetic field, spherically stratified ionosphere) the two give comparable results. The various profile parameters are compared in Table 6-2 .

It is again clear that the oblique profiles have smaller N_{max} than the R.S.A. in the second reflection region, apparently supporting the idea that the first hop is the "control", limiting MOF (2F). However, this is later (section 6.3) shown to be a somewhat simplistic explanation and perhaps only applies to this particular time of day. There are obvious shortcomings in attempting to compare cases 1 to 4, in that they are not at the same UT, and three of the four are near sunset when conditions are changing rapidly and may be too early to represent true nighttime profiles. Similar shortcomings were avoided in the daytime analysis presented in the next section.

Table 6-2 : Parameters of the nighttime profiles.

<u>No.</u>	<u>Day</u>	<u>Time</u>	<u>R.S.A.</u>	<u>Equiv. vert.</u>	<u>Rao</u>	<u>Smith</u>
(a) Base height (km)						
1.	041	1925 UT :	251	262	256	235
2.	041	1955 UT :	254	259	244	225
3.	049	2025 UT :	249	236	216	196
4.	050	0320 UT :	264	205	188	166
(b) Peak height (km)						
1.	041	1925 UT :	284	278	287	303
2.	041	1955 UT :	289	287	288	300
3.	049	2025 UT :	273	272	259	261
4.	050	0320 UT :	290	244	234	240
(c) Peak electron density ($\times 10^5 \text{ cm}^{-3}$)						
1.	041	1925 UT :	2.24	2.19	2.30	2.62
2.	041	1955 UT :	2.19	2.35	2.41	2.67
3.	049	2025 UT :	1.50	1.12	1.06	1.13
4.	050	0320 UT :	1.05	0.656	0.610	0.676

6.3 Analysis of Daytime Ionograms

6.3.1 Selection of Ionograms

The explanation of observed daytime oblique ionograms required consideration of a number of factors :

The vertical ionograms now have E traces and structured F traces (F1 and F2 portions) instead of the simple F trace observed at night. The oblique ionograms, however, still have only simple F traces. While modes involving E layer reflection may be visible at times (Chapter 3), these are almost certainly due to sporadic E layers, and no continuous E-F1-F2 trace is ever obtained. In obtaining N(h) profiles from daytime oblique ionograms, therefore, there is a major lack of information, viz. evidence of underlying ionization below the F2 region (see also sections 5.4 and 7.3).

In view of the large ground distances covered by an oblique ray while within the ionosphere (section 5.4), the period of data considered was extended to include the two days before and after the R.S.A. passed each of the 2F reflection points (Table 2-3), although the ship was probably within the region where the 2F ray is within the ionosphere for only one day on either side.

For these 8 days of data (040-043 for the first reflection region and 048-051 for the second) a fixed time of day was chosen so that the effect of the diurnal variation would be reduced, and instead the day-to-day variability at a given UT could be checked. The time of day was chosen such that the ionosphere could be considered stable, and not varying rapidly, as near sunrise and sunset. The early afternoon hours are the most suitable for this purpose.

The criteria listed at the beginning of section 6.2.1 were satisfied wherever possible for oblique and simultaneous R.S.A. vertical ionograms, as well as vertical ionograms from SANAE and Grahamstown obtained on the quarter-hour immediately before or after the oblique record. The latter were included in order to (a) check on the day-to-day consistency; (b) observe how the R.S.A. ionogram was related to those from the endpoints; (c) allow comparative ray-tracing studies with a linear electron density vs. latitude gradient using profiles derived from these endpoint ionograms (Lambert, 1977).

In practice it was impossible to satisfy all these conditions, but the ionograms listed in Table 6-3 below were eventually selected. No SANAE ionogram was available for day 042 because of heavy absorption. The position of the R.S.A., as well as its distance from the appropriate "reflection point", is also given.

Table 6-3 : Daytime oblique and vertical ionograms selected for analysis.
The times of the ionograms are given in UT.

<u>No.</u>	<u>Day</u>	<u>Oblique</u>	<u>R.S.A.</u>	<u>SANAE</u>	<u>Grahamstown</u>	<u>Kp</u>	<u>R.S.A. Position</u>	<u>Distance</u> (km)
"First hop" :								
5.	040	1335	1335	1330	1330	4+	66°39'S 04°55'E	-615
6.	041	1340	1335	1345	1345	3	62°44'S 10°11'E	-114
7.	042	1335	1335	-	1330	3+	59°20'S 13°28'E	+303
8.	043	1340	1330	1345	1345	1+	57°40'S 14°28'E	+496
"Second hop" :								
9.	048	1335	1335	1330	1345	2	49°02'S 20°32'E	-700
10.	049	1335	1335	1345	1330	2+	45°04'S 22°09'E	-244
11.	050	1340	1345	1345	1345	2	40°46'S 24°02'E	+258
12.	051	1335	1345	1330	1330	1	37°11'S 25°26'E	+674

6.3.2 Preliminary Analysis : Equivalent Vertical Ionograms

As in the preliminary nighttime analysis (section 6.2.1) each of the oblique ionograms was first reduced to the equivalent vertical one and compared with the simultaneous vertical ionogram from the R.S.A. In addition the vertical ionograms from SANAE and Grahamstown were plotted on the same graphs for comparison. All these vertical ionograms, at ~ 1335 UT on each of the 8 days, are shown in Figures 6.16 - 6.23.

Referring to Figures 6.16 - 6.19 for the 4 days in the first hop reflection region (040 - 043), in each case the equivalent vertical ionogram is seen to have lower virtual height for a given frequency than the F2 traces of the

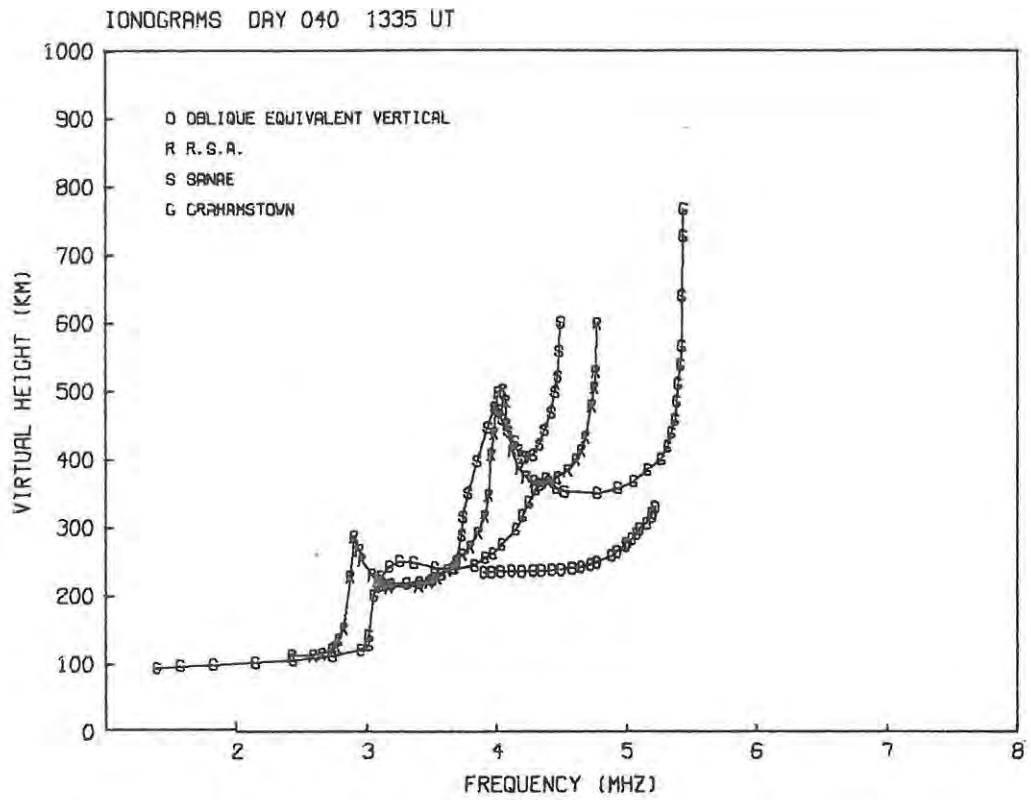


Figure 6.16 : Daytime vertical ionograms for day 040 1335 UT.

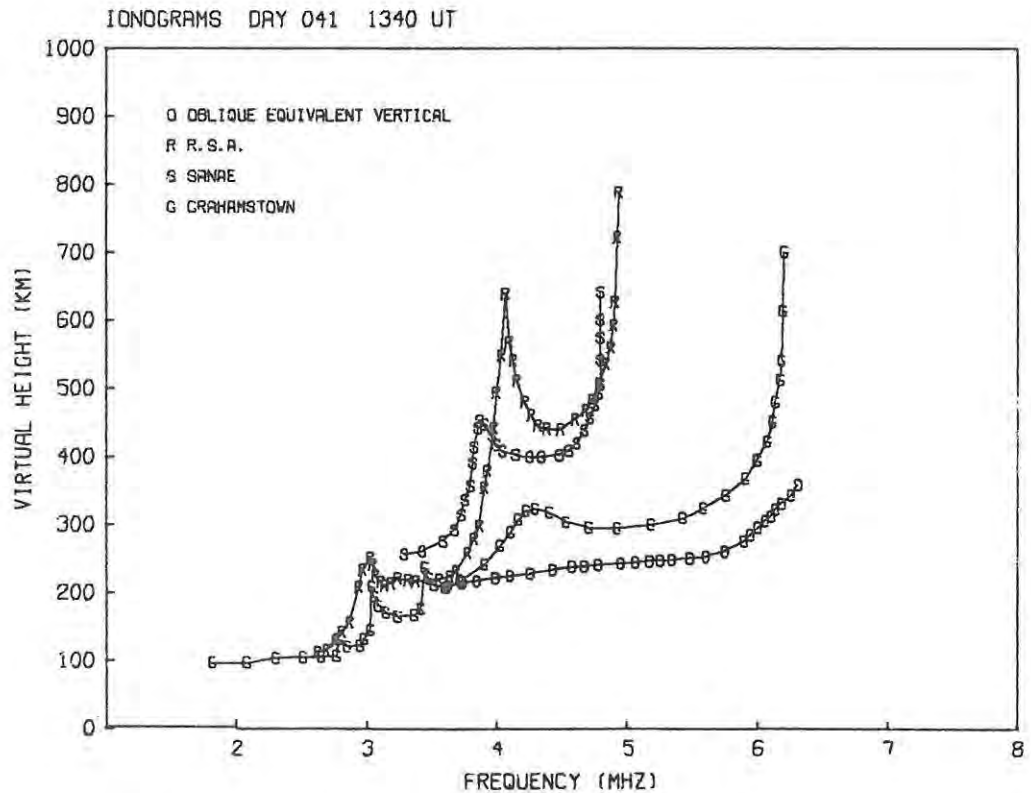


Figure 6.17 : Daytime vertical ionograms for day 041 1340 UT.

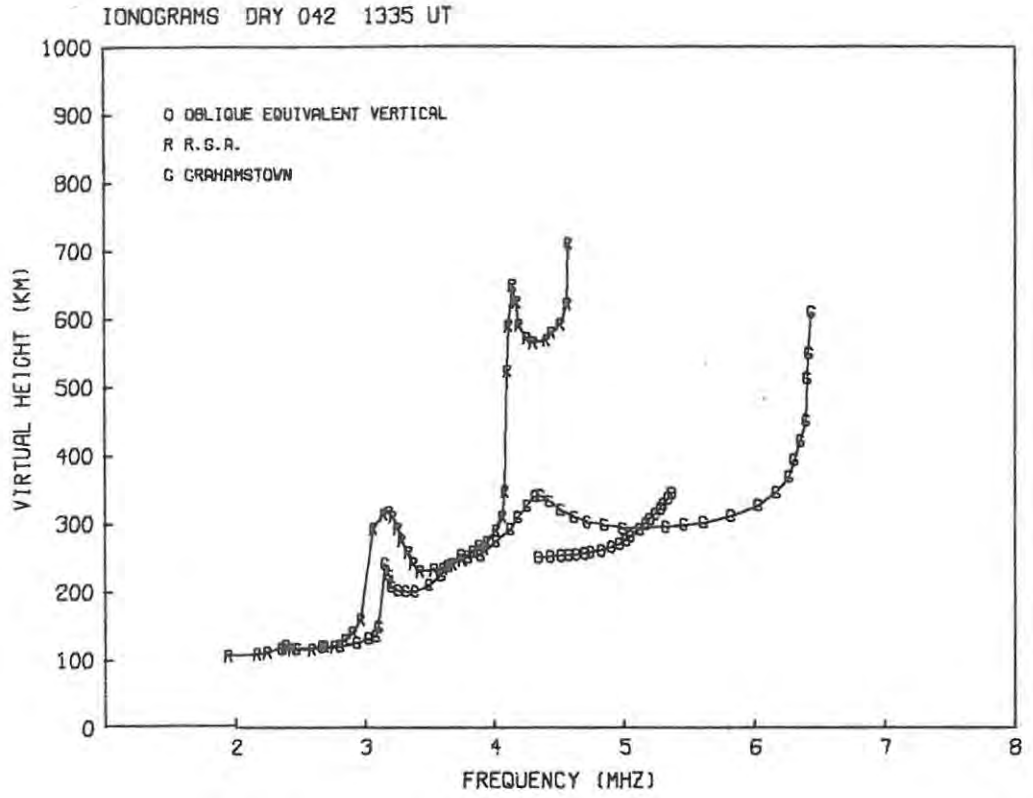


Figure 6.18 : Daytime vertical ionograms for day 042 1335 UT.

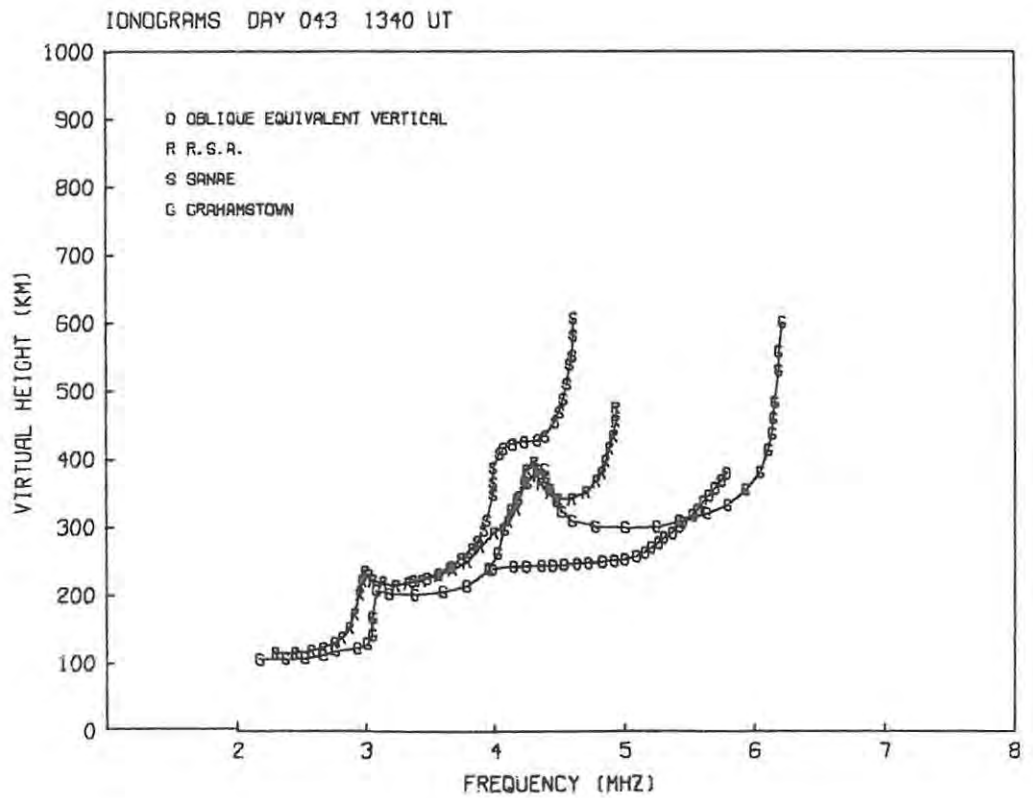


Figure 6.19 : Daytime vertical ionograms for day 043 1340 UT.

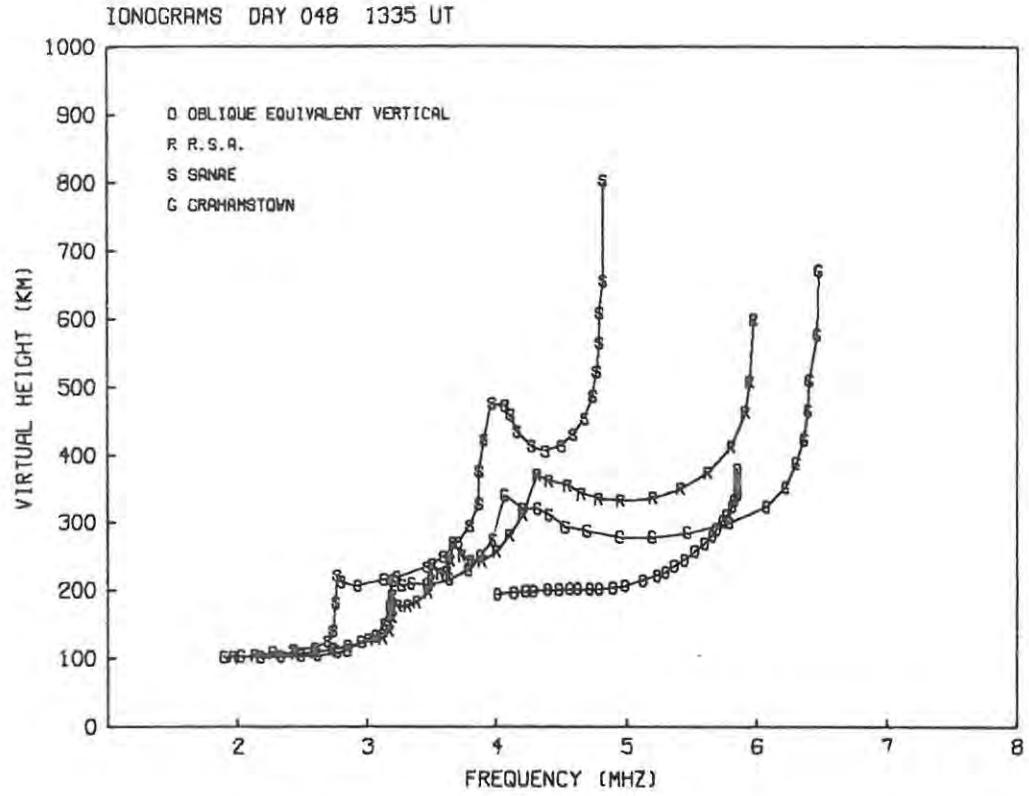


Figure 6.20 : Daytime vertical ionograms for day 048 1335 UT.

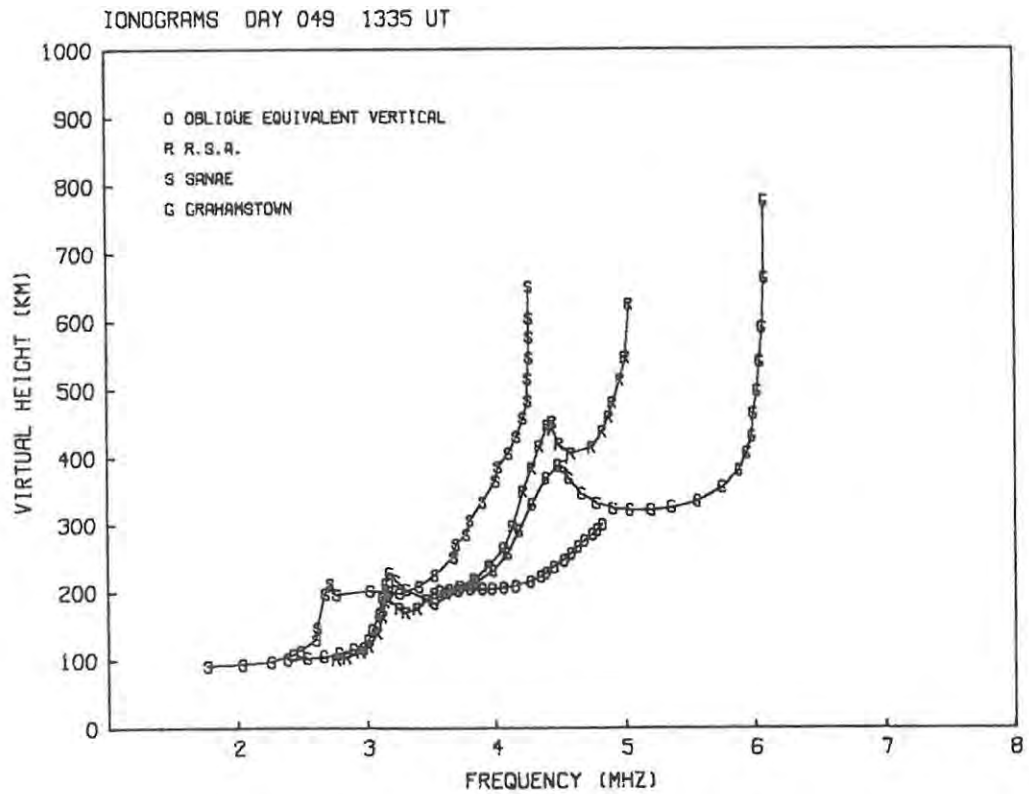


Figure 6.21 : Daytime vertical ionograms for day 049 1335 UT.

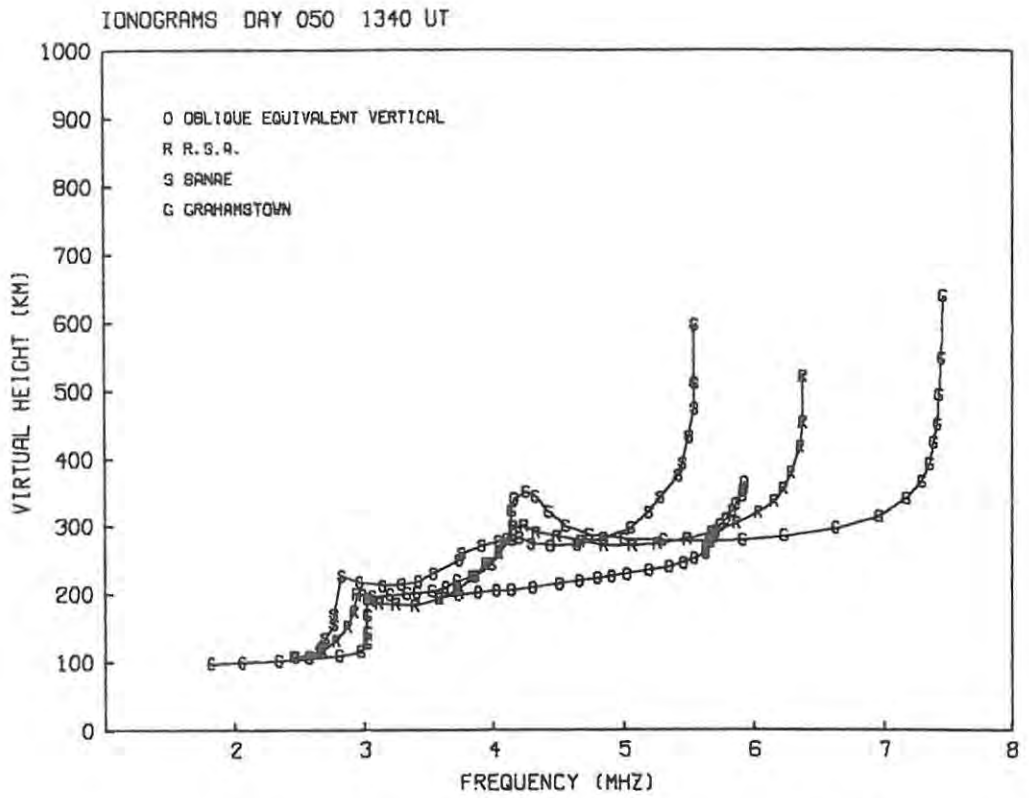


Figure 6.22 : Daytime vertical ionograms for day 050 1340 UT.

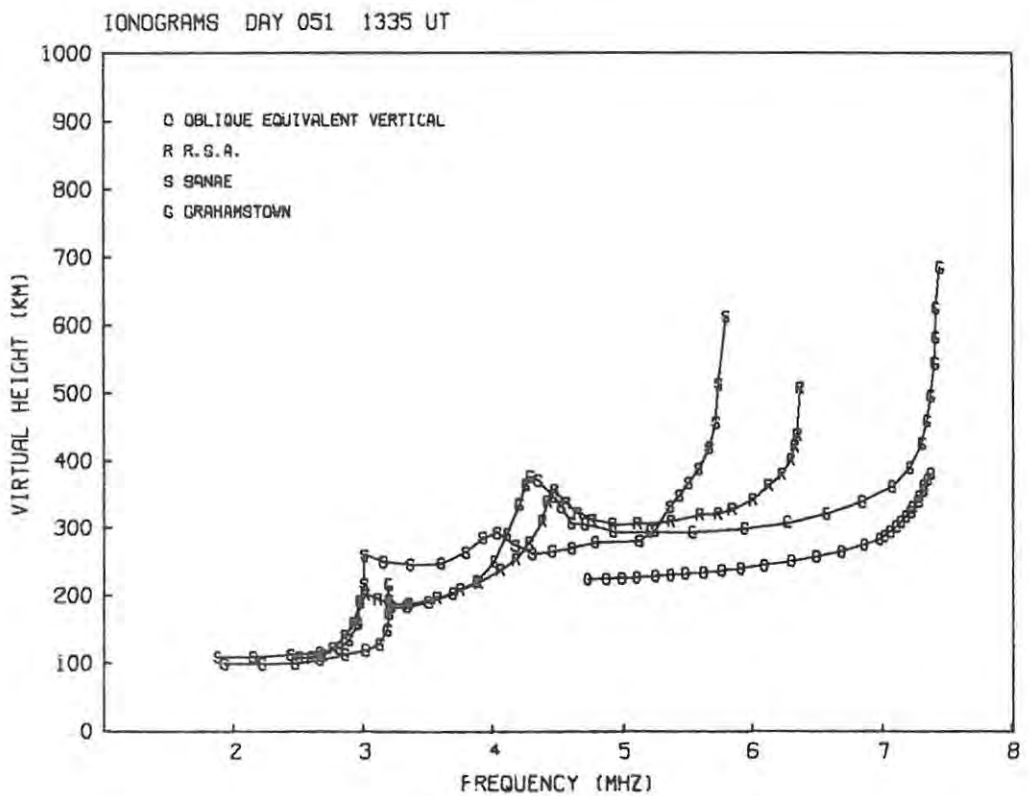


Figure 6.23 : Daytime vertical ionograms for day 051 1335 UT.

vertical ionograms. This may be due to an under-estimation of the group path P' , in turn due to too low a value of the offset being used. It is also evident that EVFO is greater than foF2 (R.S.A.) on all four occasions, and on day 041 (Figure 6.17) it is greater than foF2 at Grahamstown.

(The values of the critical frequencies are given in Table 6-4.) As in section 6.2.3, such an observation is difficult to explain in terms of the simple equal hop model, and must be due to considerable ionization gradients (e.g. Möller, 1964) over the path. These gradients would appear to be regularly present during the day in view of the consistent positive difference between EVFO and foF2 (R.S.A.).

On days 040 and 043 in particular (Figures 6.16 and 6.19), apparently normal quiet conditions, the R.S.A. F-trace lies between the SANAE and Grahamstown traces, supporting the idea that the ionospheric parameters vary in some regular monotonic way between the two end points.

The ionograms for the four days while the R.S.A. was in the second reflection region, Figures 6.20 - 6.23, show EVFO to be less than or equal to foF2 (R.S.A.) in three of the four cases. On day 051 however (Figure 6.23), EVFO is again greater than foF2 at Grahamstown. There appears to have been widespread enhancement of electron densities on this day; the values of foF2 at both SANAE and Grahamstown (Table 6.4) are considerably greater than the monthly median values. (The R.S.A. was, incidentally, probably outside the region where the 2F ray was within the ionosphere.) As EVFO was approximately equal to foF2 (R.S.A.) on the other three apparently normal days, we might draw the conclusion that this second reflection region is now the control in limiting MOF (2F) during the day. This is unexpected and opposite to the nighttime case (section 6.2.3).

Table 6-4 : Daytime ionogram critical frequencies (in MHz)

<u>No.</u>	<u>Day</u>	<u>Oblique</u>		<u>foF2</u>	<u>foF2</u>	<u>foF2</u>
		<u>JF</u>	<u>EVFO</u>	<u>R.S.A.</u>	<u>SANAE</u>	<u>Grahamstown</u>
5.	040	17.3	5.22	4.77	4.49	5.43
6.	041	20.2	6.31	4.93	4.79	6.20
7.	042	17.0	5.36	4.57	-	6.43
8.	043	18.1	5.78	4.93	4.60	6.21
9.	048	20.4	5.85	5.97	4.81	6.47
10.	049	16.9	4.82	5.03	4.26	6.07
11.	050	19.9	5.94	6.38	5.54	7.45
12.	051	23.2	7.80	6.36	5.79	7.43
Monthly medians :					4.65	6.45

6.3.3 Further Analysis : Daytime N(h) Profiles

As in the nighttime cases (sections 6.2.2 and 6.2.4), the oblique ionograms were reduced to N(h) profiles, by both the indirect (section 5.2) and direct (section 5.3) methods. The simultaneous vertical ionograms from SANAE, Grahamstown and the R.S.A. were also reduced to N(h) profiles by the usual technique. The resultant sets of six profiles for each of the 8 days are shown in Figures 6.24 - 6.31 on the same scales.

In all cases the oblique profiles are very "thin", i.e. there is a small increase in height for a large increase in electron density. It is also evident that the day-to-day variability is considerable; some of the profile parameters are given in Table 6-5.

Considering the first four sets of profiles, those for days 040 - 043 (Figures 6.24 - 6.27) when the R.S.A. was in the first hop reflection region, we can discern a number of features :

N(H) PROFILES DAY 040/77 1335 UT

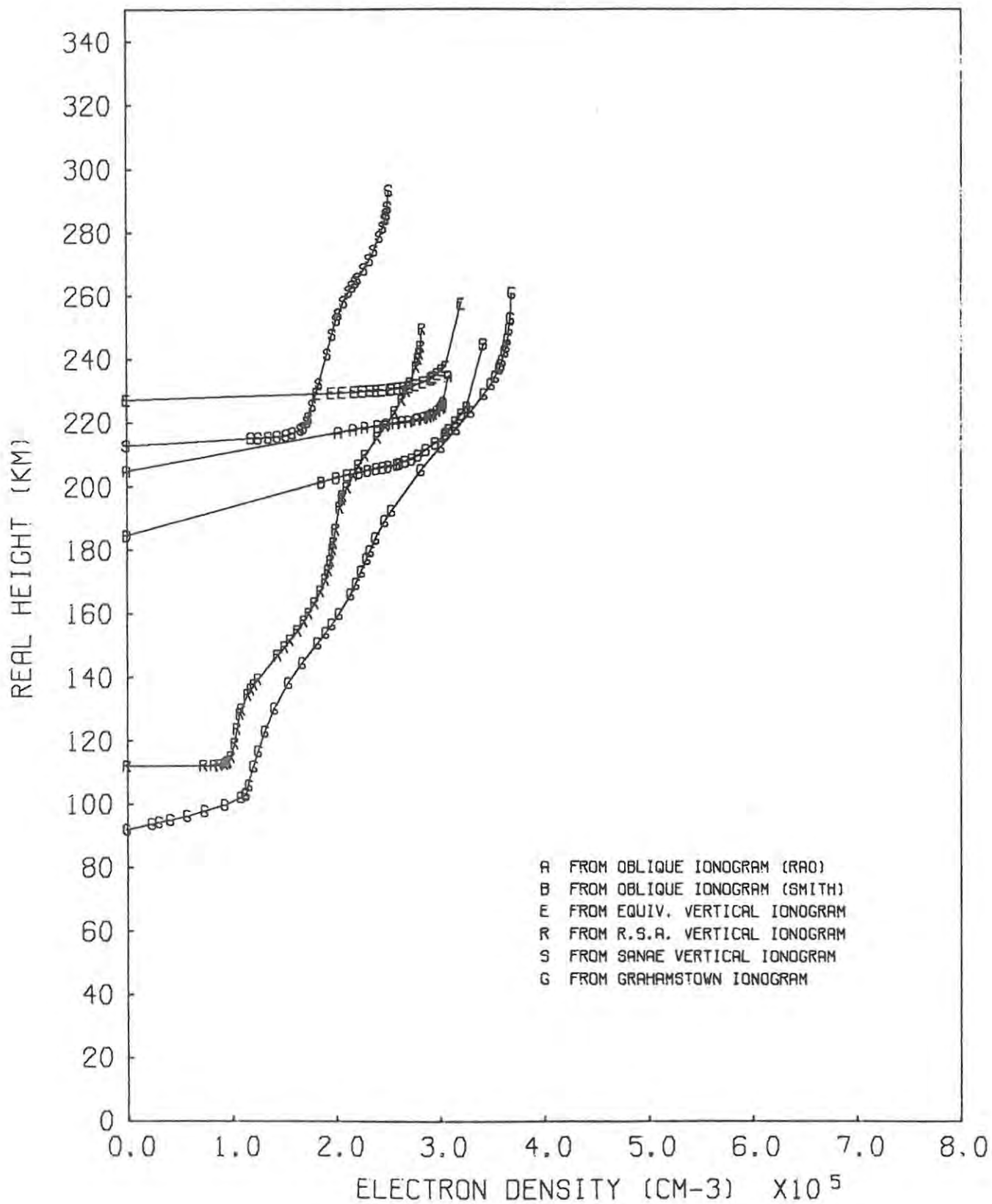


Figure 6.24 : Daytime N(h) profiles for day 040 1335 UT.

N(H) PROFILES DAY 041/77 1340 UT

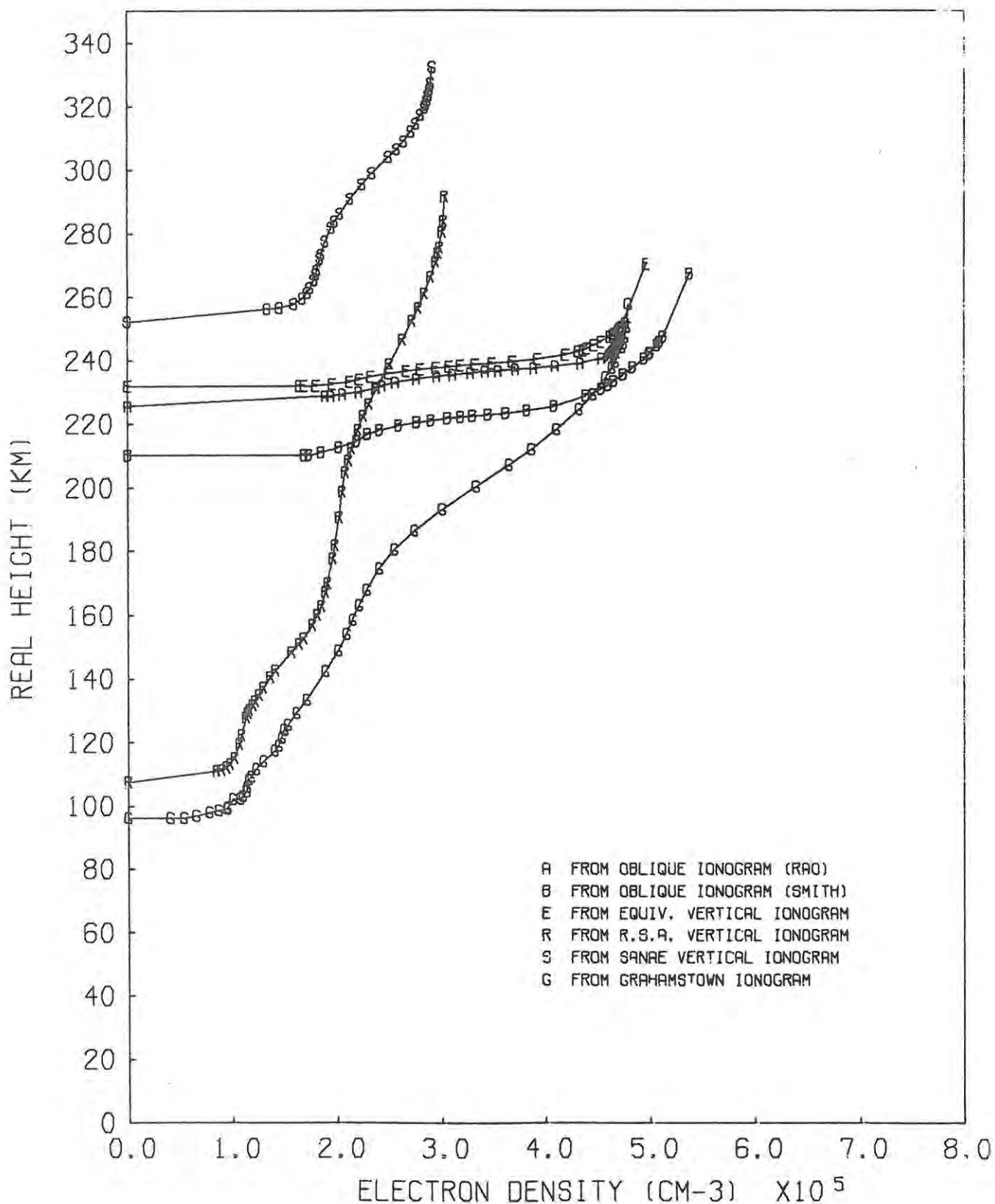


Figure 6.25 : Daytime N(h) profiles for day 041 1340 UT.

N(H) PROFILES DAY 042/77 1335 UT

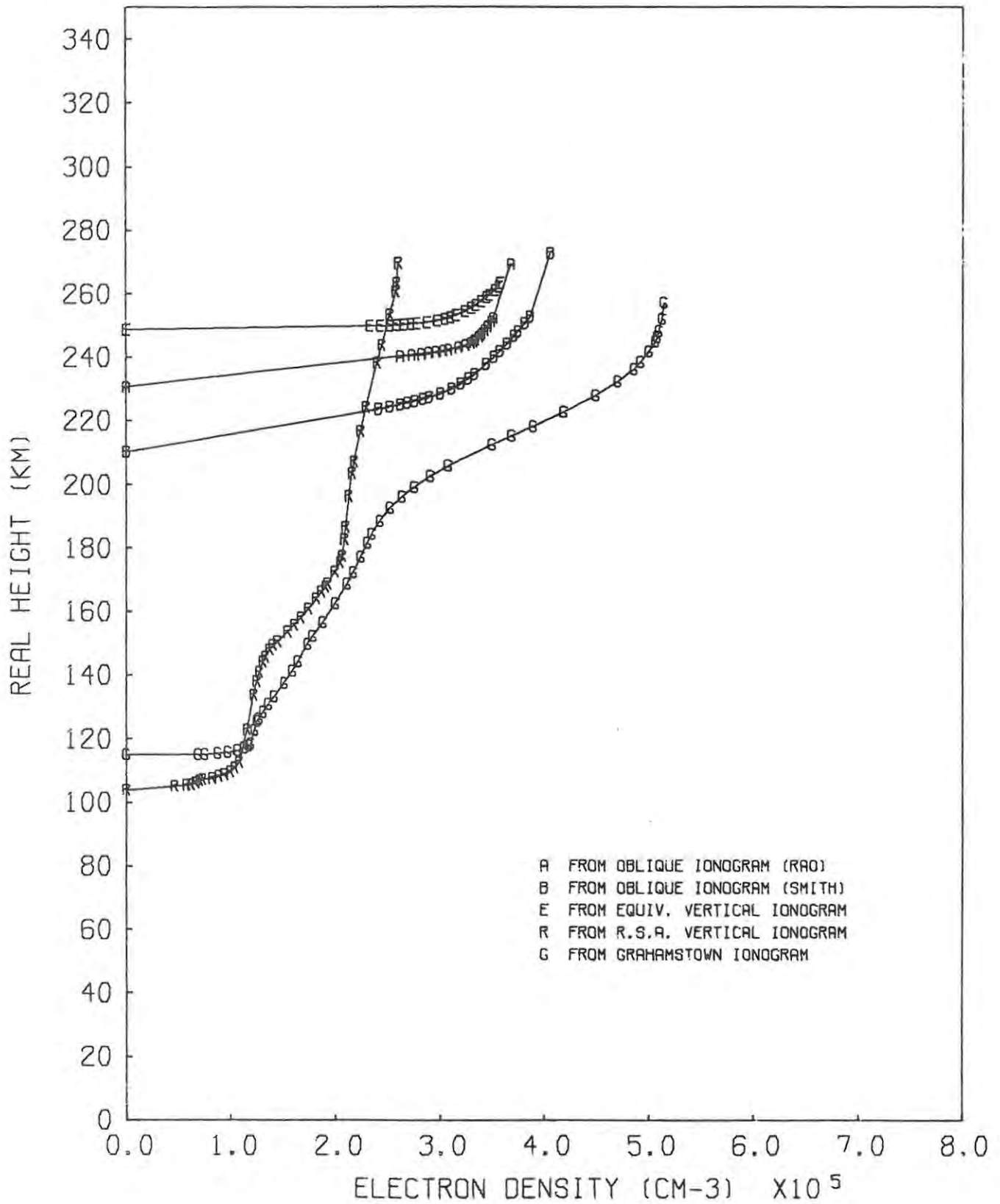


Figure 6.26 : Daytime N(h) profiles for day 042 1335 UT.

N(H) PROFILES DAY 043/77 1340 UT

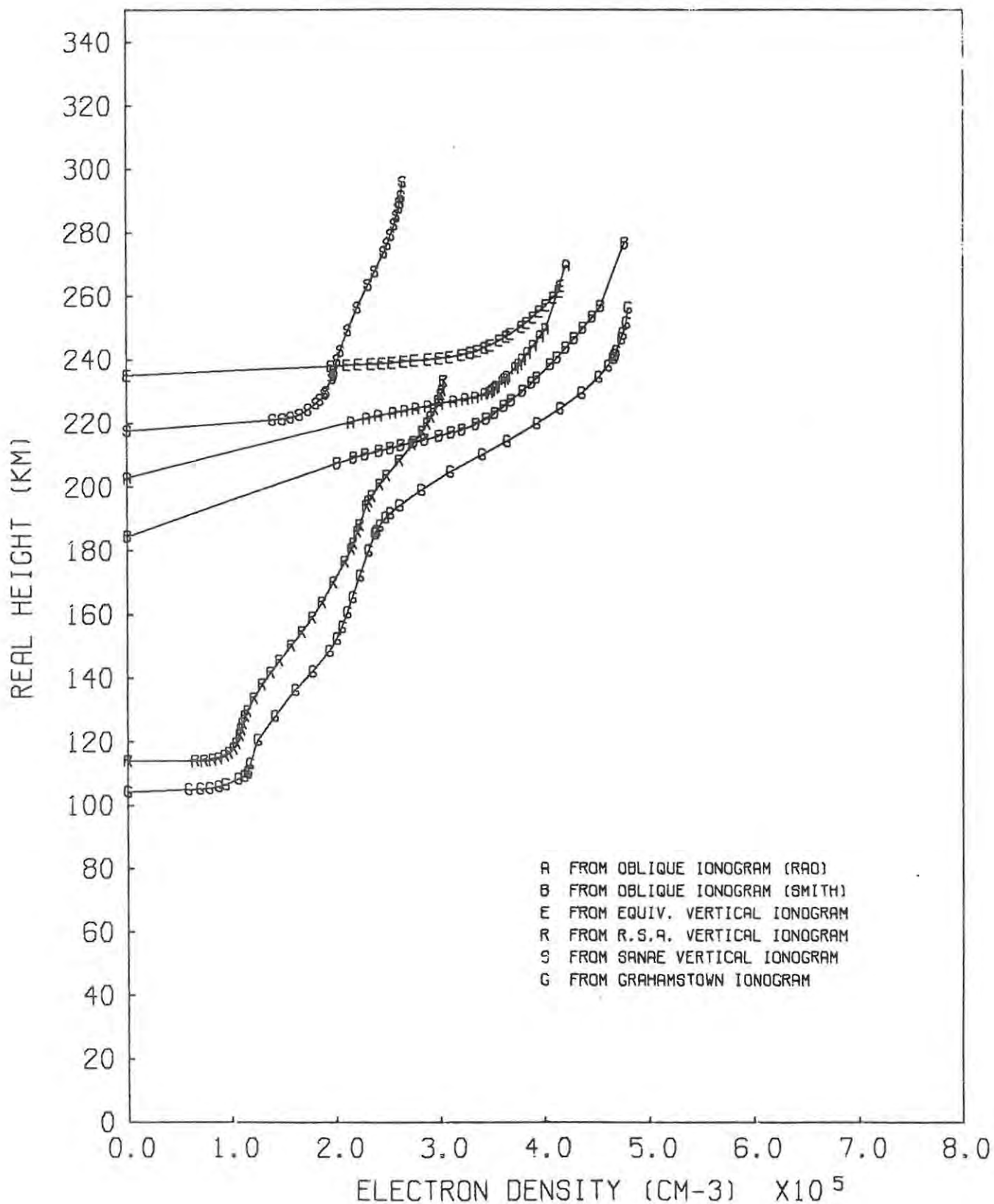


Figure 6.27 : Daytime N(h) profiles for day 043 1340 UT.

- (i) The F2 peak at SANAE has a consistently greater h_{\max} and smaller N_{\max} than at Grahamstown; N_{\max} of the R.S.A. profile lies between the values at SANAE and Grahamstown but in two of the cases (Figures 6.24 and 6.27) h_{\max} at the R.S.A. is lower than at either of the end points.
- (ii) The E region sections of the SANAE profiles (as well as those of the oblique profiles) are not determined as no E traces are visible on the ionograms.
- (iii) The base heights of the oblique profiles are, however, consistent with those of the F2 layers at the R.S.A. and Grahamstown.
- (iv) The values of N_{\max} for the oblique profiles obtained by all three methods lie between those at the R.S.A. and Grahamstown, except for the equivalent vertical and Smith profiles on day 041 (Figure 6.25). The peak heights are all consistent with those of the R.S.A. and Grahamstown, except for day 043 (Figure 6.27), when all three oblique profiles have h_{\max} greater than at either the R.S.A. or Grahamstown.

The second four sets of profiles, those for days 048 - 051 (Figures 6.28 - 6.31) when the R.S.A. was in the second hop reflection region, show that :

- (i) Because of a decrease in absorption the E region at SANAE is now determined; the base heights of all three "vertical profiles" are within 10 km of each other in all four cases.
- (ii) There is greater day-to-day variability in the vertical profiles than for the first four days, with considerable F layer depletion on day 049 (when h_{\max} at SANAE is also unusually low) and enhancement on day 051.
- (iii) The R.S.A. peak density still lies between the values at SANAE and Grahamstown, although there is no longer a regular decrease in peak heights.

N(H) PROFILES DAY 048/77 1335 UT

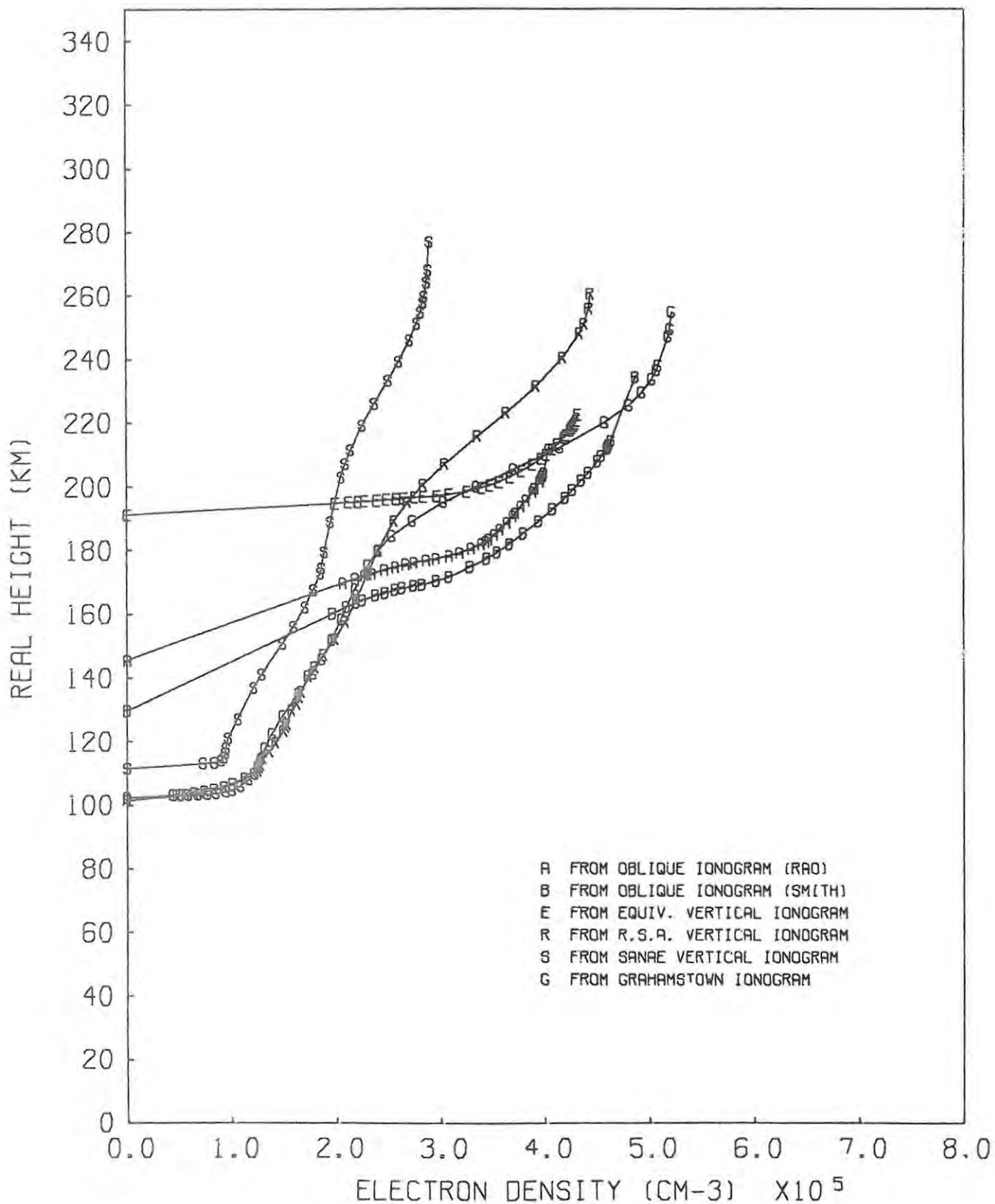


Figure 6.28 : Daytime N(h) profiles for day 048 1335 UT.

N(H) PROFILES DAY 049/77 1335 UT

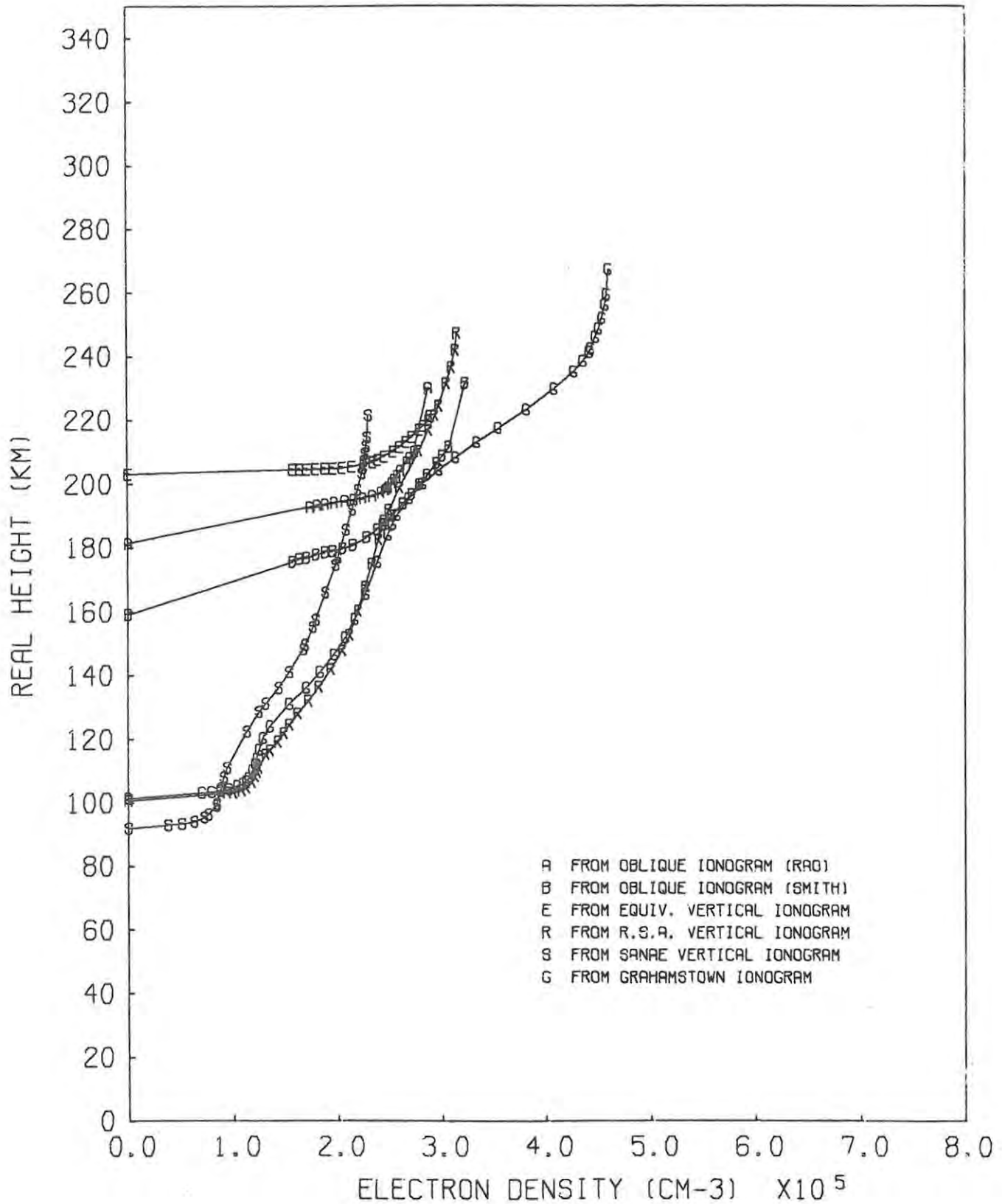


Figure 6.29 : Daytime N(h) profiles for day 049 1335 UT.

N(H) PROFILES DAY 050/77 1340 UT

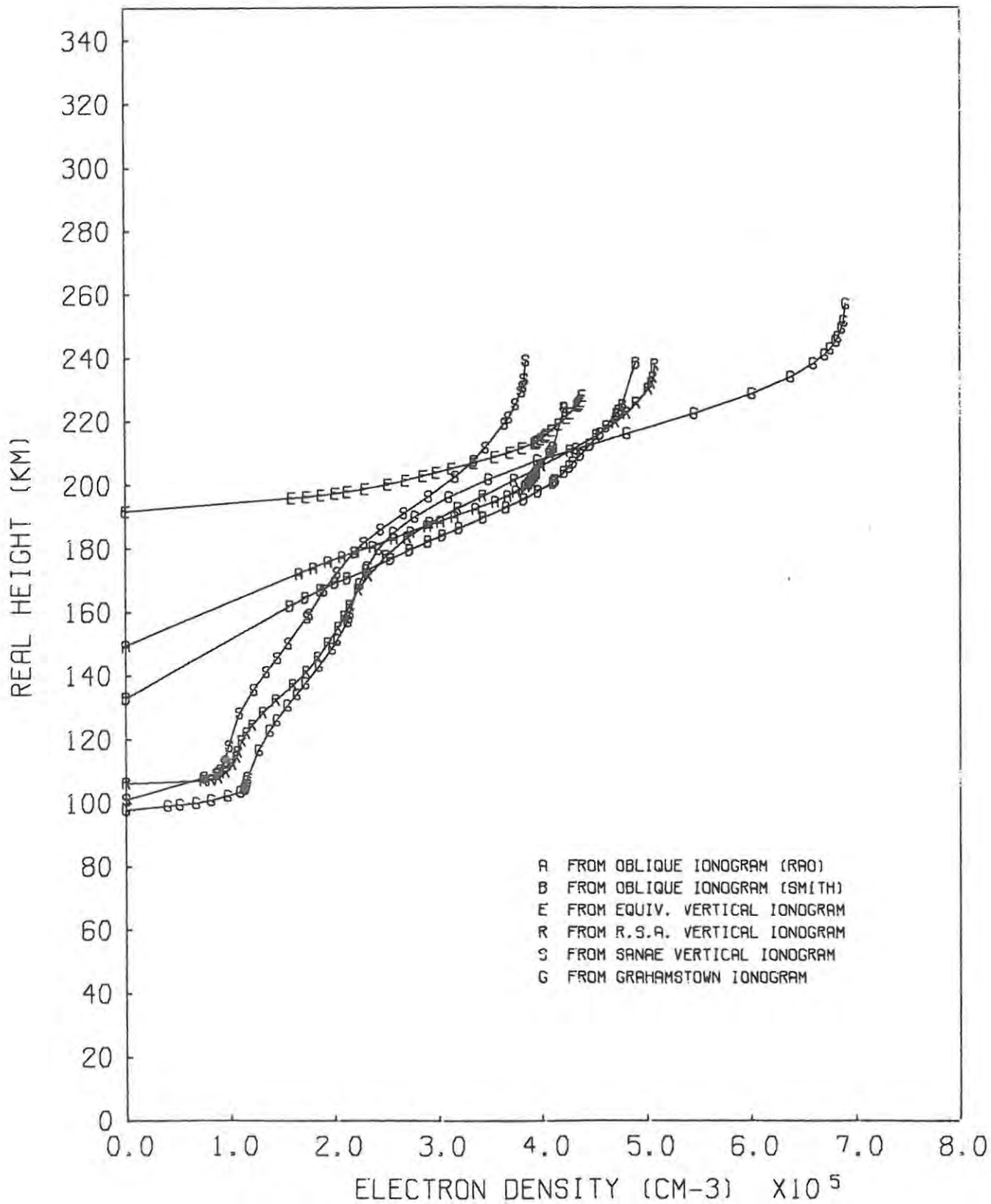


Figure 6.30 : Daytime N(h) profiles for day 050 1340 UT.

N(H) PROFILES DAY 051/77 1335 UT

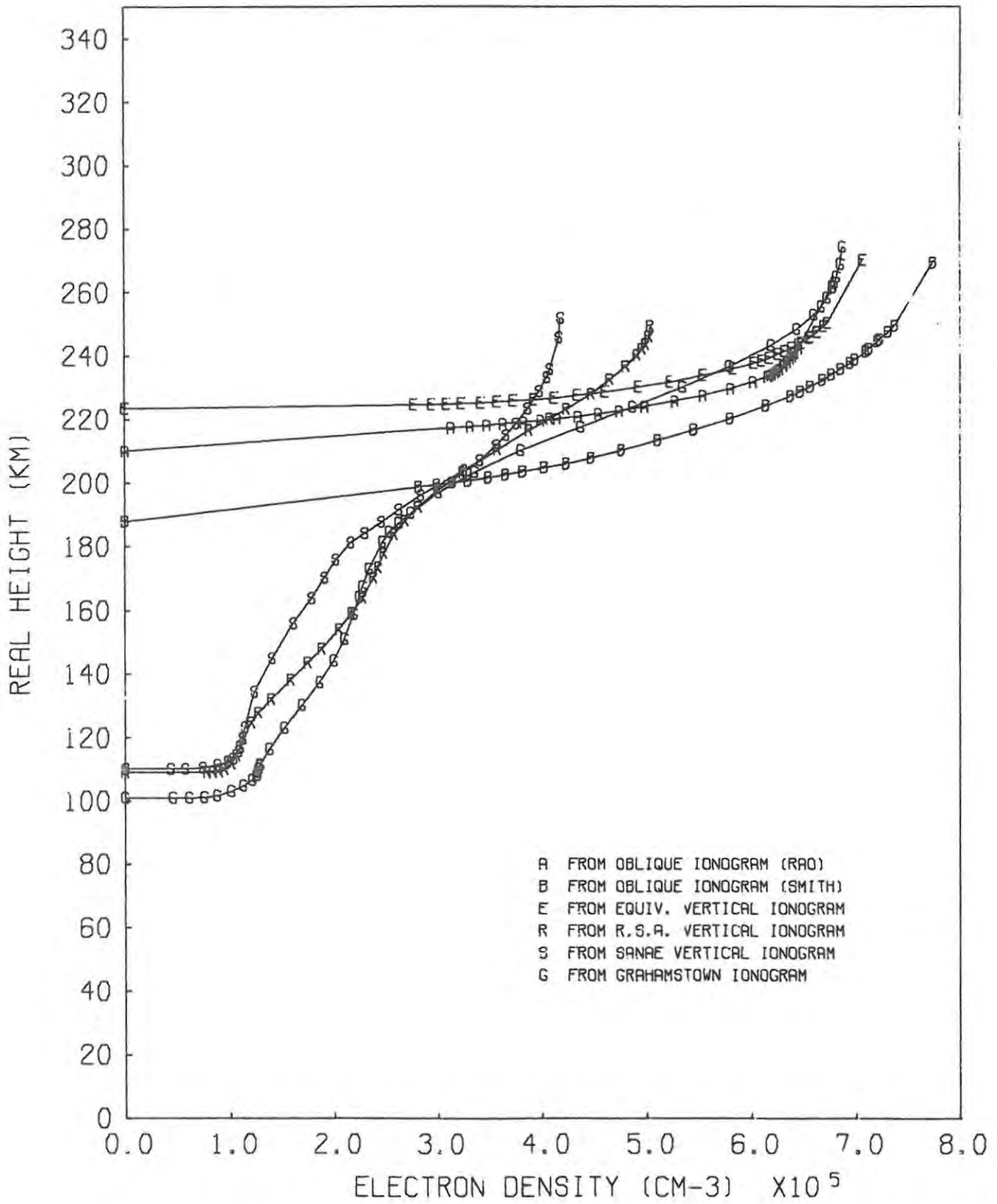


Figure 6.31 : Daytime N(h) profiles for day 051 1335 UT.

- (iv) The oblique profiles are all less "thin" in the first three cases (days 048 - 050); the low heights obtained, especially on day 048 (Figure 6.28), may however be due to the offset on the ionogram being too low. Otherwise the heights of the oblique profiles are again consistent with those of the F2 layers of the vertical profiles.
- (v) The values of N_{\max} for the oblique profiles are all fairly close to the R.S.A. values except for day 051 when they are close to the Grahamstown value.

Table 6-5 : Parameters of the daytime profiles (~ 1335 UT)

<u>No.</u>	<u>Day</u>	<u>Oblique</u>		<u>Equiv. vert.</u>	<u>R.S.A.</u>	<u>SANAE</u>	<u>Grahamstown</u>
		<u>Rao</u>	<u>Smith</u>				
(a) <u>Base height</u> (km)							
5.	040	205	184	227	112	213	92
6.	041	225	210	232	107	252	96
7.	042	231	210	248	104	-	115
8.	043	203	184	235	114	218	104
9.	048	145	130	191	101	111	102
10.	049	181	159	203	101	92	101
11.	050	149	133	191	106	101	98
12.	051	210	188	223	109	110	101
(b) <u>Peak height</u> (km)							
5.	040	234	244	257	249	293	261
6.	041	252	267	270	291	332	258
7.	042	269	273	263	269	-	257
8.	043	269	277	263	233	296	257
9.	048	212	234	222	261	277	255
10.	049	230	231	221	247	221	267
11.	050	224	238	228	237	239	257
12.	051	262	269	270	249	252	274
(c) <u>Peak density</u> ($\times 10^5 \text{ cm}^{-3}$)							
5.	040	3.09	3.43	3.21	2.83	2.51	3.70
6.	041	4.76	5.37	4.96	3.03	2.91	4.78
7.	042	3.68	4.06	3.58	2.60	-	5.14
8.	043	4.22	4.77	4.16	3.04	2.65	4.80
9.	048	4.04	4.86	4.32	4.44	2.89	5.21
10.	049	2.88	3.23	2.90	3.15	2.30	4.60
11.	050	4.22	4.90	4.39	5.08	3.85	6.90
12.	051	6.77	7.73	7.06	5.03	4.17	6.87

6.4 Conclusions

The day-to-day variability of ionospheric conditions in the region is undoubtedly the major problem in attempting to compare data from successive days. The idea of using R.S.A. vertical incidence data for a given UT on successive days to build up a model of the variation of profile parameters with latitude is simply not feasible, at least with this set of data. Data obtained during a similar great circle voyage of the R.S.A. in February 1978 were not examined in detail, but a cursory inspection indicated that absorption was generally lower and ionogram quality better than for the 1977 voyage, so that this may constitute a better set of data for further examination.

In order to settle the problem of which was the "control point", an attempt was made to find two occasions during the cruise when the following rather stringent set of conditions was satisfied :

- (i) the R.S.A. was near (within a few hundred km) each of the first and second reflection points in turn;
- (ii) the R.S.A. vertical ionograms, at the same UT, were both of good quality (e.g. the criteria of section 6.2.1 or those of Lambert (1977), Chapter 3);
- (iii) the oblique ionograms simultaneous with these ionograms were similar (i.e. the two values of each of the parameters P'_{min} , LLOF, JF and HLOF were approximately equal) and of reasonable quality;
- (iv) the SANAE and Grahamstown vertical ionograms approximately simultaneous with the above ionograms each satisfied similar conditions, viz. ionograms with parameters (particularly foF2) approximately equal and of reasonable quality.

The last two conditions were imposed in order to check that ionospheric conditions were similar for the two occasions. It was, however, not possible to find two such occasions in this set of data.

Conclusions which can be drawn from the results presented in this chapter are :

- (i) The simple 2 hop model where the first reflection point is the "control" point appears to be valid at night;
- (ii) During the day this simple picture may no longer hold, and the second reflection point would appear to be the "control"; there may also be seasonal differences (see section 3.3);
- (iii) Ionospheric gradients are obviously of considerable importance, particularly during the day; these are discussed further in section 7.5.

Ray tracing, of course, provides the means of testing the validity of any model profile, and is described and used in the next chapter for this purpose.

CHAPTER 7

RAY TRACING AND THE REAL IONOSPHERE

7.1 The Ray Tracing Program

The three-dimensional ray tracing program used is that described by Lambert (1977); it was written by Dr. P.D. Terry and solves the Haselgrove (1955) equations for the ray path in "geophysical" spherical polar co-ordinates (Terry, 1974). Such quantities as phase, real height, group path (or "delay time") and geographic position are determined for a ray of given frequency and initial direction, with given electron density distribution and magnetic field models.

Lambert (1977) modified and extended the original program by

- (i) adapting it to allow multi-hop propagation;
- (ii) adding a homing feature to determine the take-off angles required for the ray to reach a specified end point;
- (iii) incorporating a version of the subroutine NHPR (section 5.2.2) to compute one or two N(h) profiles from given vertical ionograms;
- (iv) allowing different profiles to be used for each hop or the electron density to vary linearly with latitude between two given profiles;
- (v) adding a tilted dipole magnetic field model.

These improvements allowed realistic simulations of 2F mode propagation between SANAE and Grahamstown to be performed (Lambert, 1977).

The ray tracing described in this chapter is partly an extension of Lambert's work, and partly a test of the oblique N(h) profile reduction methods. Three further minor modifications of the program were introduced :

- (i) Another version of NHPR was written which allows the reading of an N(h) profile (N and h values, segment coefficients A_n and B_n and peak parameters and coefficients) directly from a disc file and so avoids recomputation when the same profile is used for a number of different frequencies and take-off angles. This N(h)

profile could be derived from either a vertical or an oblique ionogram.

- (ii) Another version of the subroutine NEDNE, which simply determines N and $\frac{dN}{dh}$ at a given height h in the given profile, was written to cater for the different form of the segments in the profiles derived from oblique ionograms (section 5.3). In this case we have, from (5.20), if n is such that $h_{n-1} \leq h \leq h_n$,

$$N = 1.24 \times 10^4 \left(A_n - \frac{B_n}{R+h} \right) \quad (7.1)$$

$$\text{and } \frac{dN}{dh} = 1.24 \times 10^4 \frac{B_n}{(R+h)^2} \quad (7.2)$$

- (iii) A new magnetic field subroutine (Terry and Gagliardini, 1977), based on that of Jones and Stephenson (1975), was incorporated. This allowed the use of either a tilted dipole model or a spherical harmonic expansion of the field up to a maximum of 6 terms. The best compromise between accuracy of the model parameters in the South Atlantic region and computer time required to calculate them was found to be a 3rd order expansion (Terry and Gagliardini, 1977).

7.2 Ray Tracing through Nighttime Profiles

Both as a test of the accuracy of the Rao oblique ionogram reduction method (Chapter 5) and as a means of comparing oblique ionograms that would be obtained if rays travelled through the R.S.A. profiles, the following ray tracing analysis was performed. Two nighttime oblique ionograms, one each from when the R.S.A. was in the first and second hop reflection regions, were used. These were

- (i) "First hop" : Day 041 1925 UT
(ii) "Second hop" : Day 049 2025 UT

In each case the profiles (Figures 6.12 and 6.14 respectively) derived from the oblique ionogram by the Rao method (symbol R) and from the R.S.A.

vertical ionogram (symbol V) were used and two-hop rays of various frequencies traced through each of them. The results are shown in Figures 7.1 and 7.2 respectively. In each case the observed oblique ionogram is denoted by the solid curve and the synthetic ionograms derived from ray tracing through the "oblique profile" and "vertical profile" by the dashed curves with points O and Δ respectively.

- (i) In the first case (Figure 7.1) the O trace follows the actual ionogram surprisingly closely up to the JF. High angle rays through the oblique profile could not be made to converge, perhaps because of the thinness of the layer (Lambert, 1977), so strictly speaking the JF is not determined. The Δ trace low ray follows the actual ionogram reasonably closely (within 15 km group path), but the JF is 0.8 MHz lower (see Table 7-1 (a)).
- (ii) In the second case (Figure 7.2) the agreement between the "oblique profile" synthetic ionogram and the observed ionogram is again very close and the JF's (Table 7-1 (b)) are practically identical. The "vertical profile" synthetic ionogram now has a JF almost 1 MHz greater than the observed value. Again the agreement in P'_{min} in both cases is good.

Table 7-1 : Parameters of observed and synthetic nighttime oblique ionograms

	<u>JF</u> (MHz)	<u>P'_{min}</u> (km)
(a) <u>Day 041 1925 UT</u>		
Observed	12.85	4676
"oblique profile"	≥ 12.85	4681
"vertical profile"	12.05	4662
(b) <u>Day 049 2025 UT</u>		
Observed	9.05	4646
"oblique profile"	9.00	4646
"vertical profile"	10.00	4664

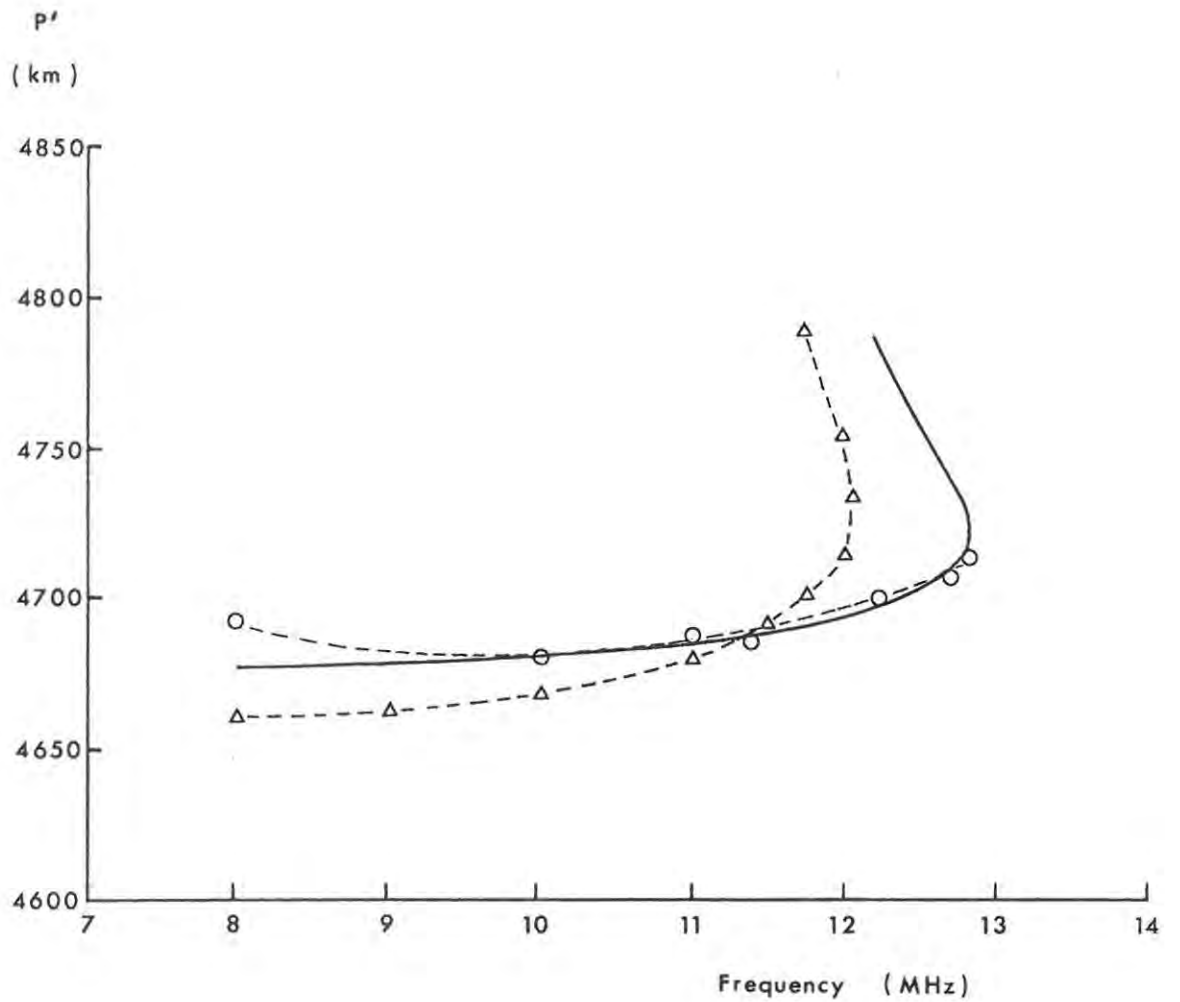


Figure 7.1 : 1977 Day 041 1925 UT : observed nighttime oblique ionogram (solid curve) and synthetic oblique ionograms (dashed curves) from ray tracing through oblique profile (O) and R.S.A. profile (Δ), the latter near the first reflection point.

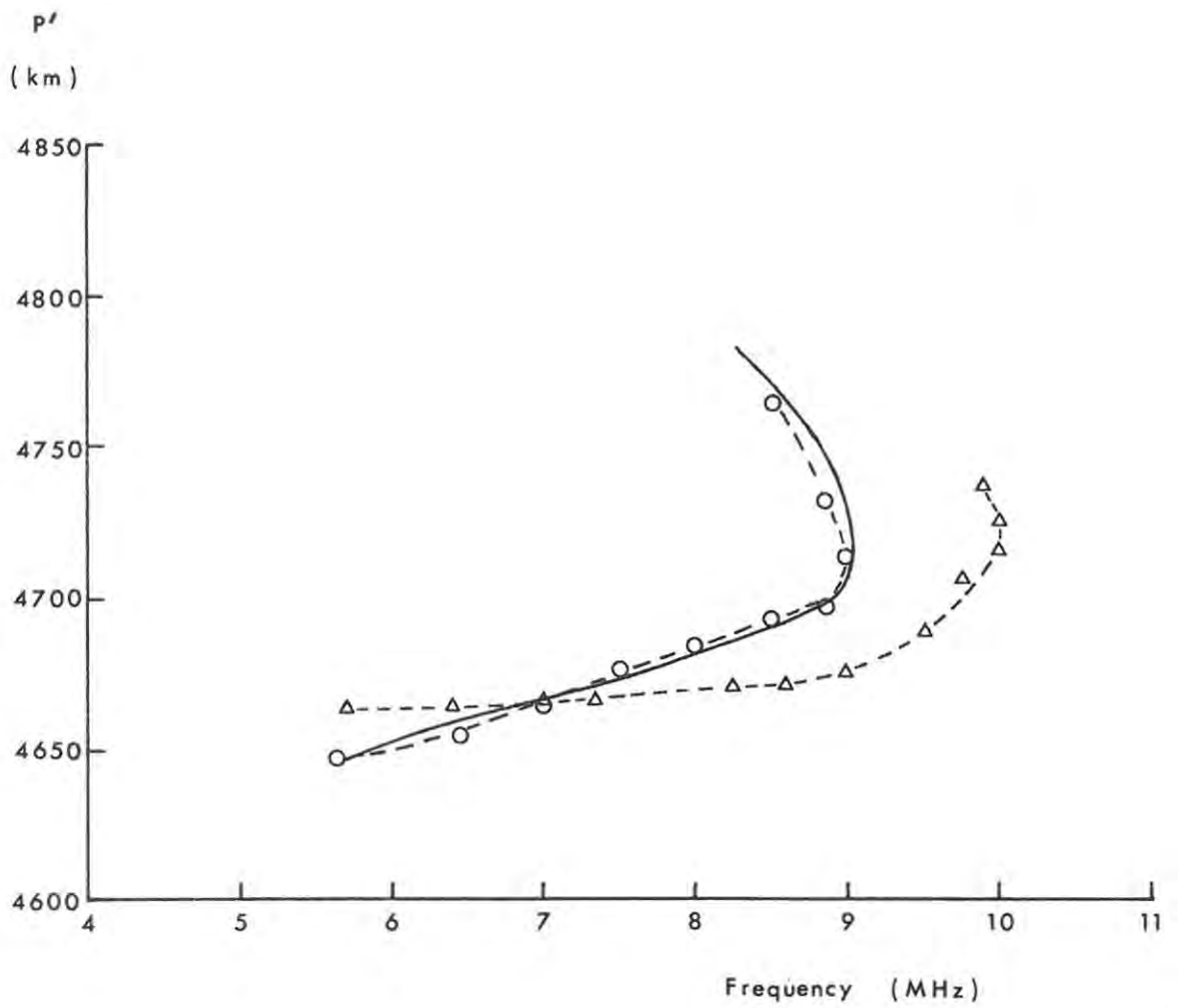


Figure 7.2 : 1977 Day 049 2025 UT : observed nighttime oblique ionogram (solid curve) and synthetic oblique ionograms (dashed curves) obtained from ray tracing through oblique profile (O) and R.S.A. profile (Δ), the latter near the second reflection point.

The results of (ii) (Figure 7.2) are again easily explained in terms of the simple idea that the first hop, having the smaller N_{\max} , is the "control", limiting the JF(2F) to a lower value than would be obtained for two hops through the "second hop profile" (the R.S.A. profile) which has a greater N_{\max} . However, the results of (i) (Figure 7.1), where the oblique ionogram has a JF greater than the value obtained through the R.S.A. profile (the "first hop profile"), cannot be explained without the assumption of a tilted ionosphere causing an increase in JF over the "predicted" (untilted) value.

The close agreement in both cases between the observed oblique ionogram and the synthetic one derived from the oblique (Rao) profile is extremely gratifying. It shows that

- (i) the assumption of two equal hops in deriving the profile from the oblique ionogram, if not accurately realistic, is at least self consistent, i.e. inversion of that profile by ray tracing through it for two equal hops will reproduce the original ionogram;
- (ii) the assumptions (section 5.3.1) of spherical symmetry (on each hop), and neglect of the earth's magnetic field, are apparently justified.

7.3 Ionization Below the F2 Region

As the daytime N(h) profiles derived from oblique ionograms presented in section 6.3 consist of an F2 layer only, some incorporation of lower lying ionization will have to be made if we wish to obtain a realistic representative profile. (The degree to which the profile is representative was discussed in section 5.4.) There are essentially three ways in which such an incorporation of E and F1 layers can be made :

- (i) by using profiles derived from vertical ionograms by the usual methods;
- (ii) by using model profiles generated from observed ionogram parameters (e.g. Bradley and Dudeney, 1973);
- (iii) by using predicted profiles or model profiles generated from predicted ionospheric characteristics (e.g. Haydon and Lucas, 1968; Rawer *et al.*, 1975).

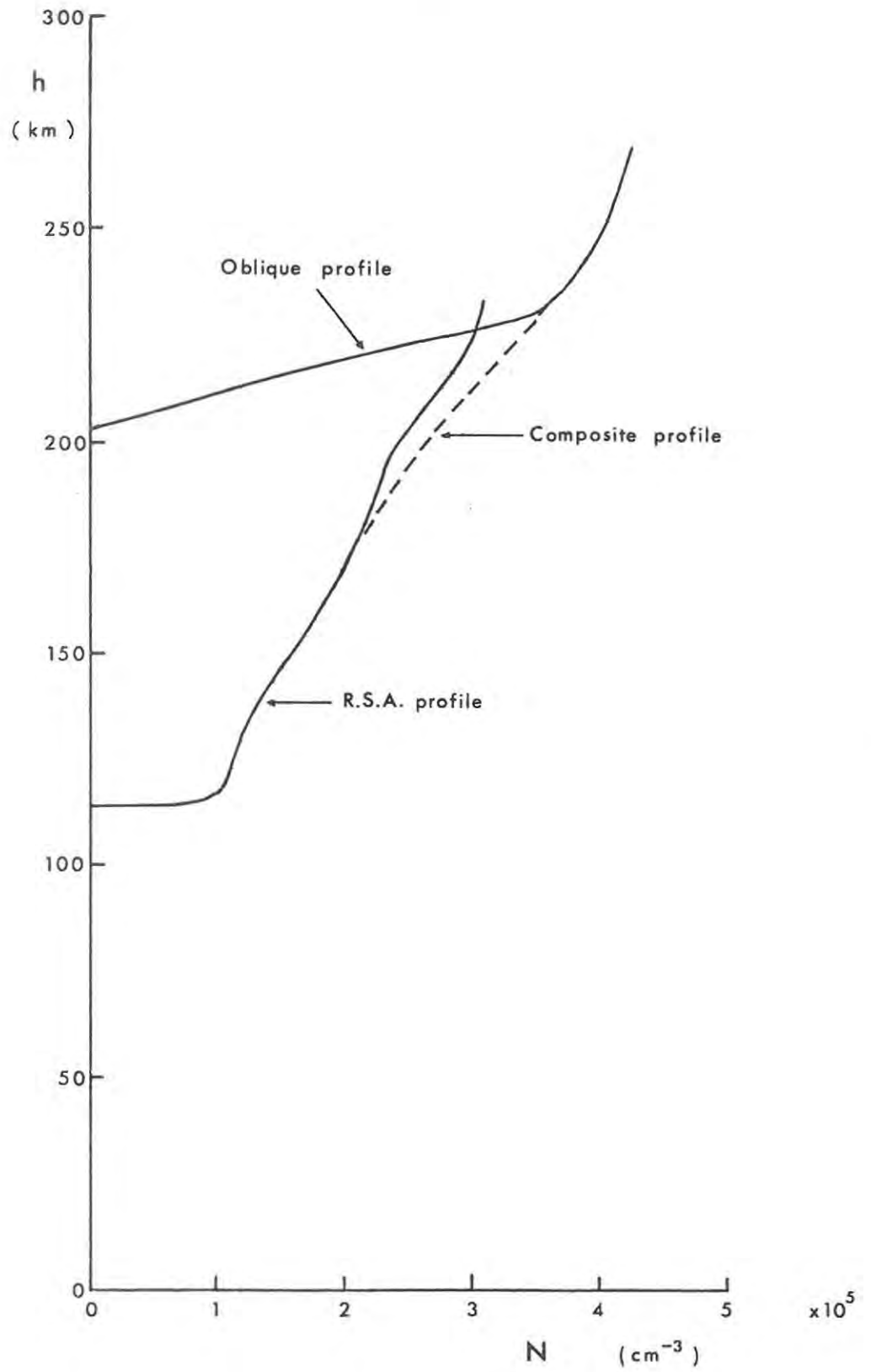


Figure 7.3 : "Composite profile", day 043 1340 UT.

The first of these methods can only be used in specific cases; as an example the (Rao) oblique profile for day 043, 1977 at 1340 UT, used for ray tracing in the next section, was examined. The peak of this F2 profile was arbitrarily joined to the F1 and E region sections of the profile from the simultaneous R.S.A. vertical ionogram (Figure 6.27) to generate a "composite profile" as illustrated in Figure 7.3. If such a profile (of up to 50 (N,h) points) is to be used for ray tracing, however, N(h) must be continuous (section 5.4). The same segment model used in the Smith and Rao reduction methods, equation (5.20), may be conveniently used here also : if two successive points (N_{n-1}, h_{n-1}) and (N_n, h_n) defining segment n are converted to $(f_{N_{n-1}}^2, r_{n-1})$ and $(f_{N_n}^2, r_n)$ using (5.1) and (5.2), then the segment constants A_n and B_n are simply given by equations (5.40) and (5.41), derived from the conditions of continuity at $r = r_{n-1}, r_n$.

The second method could prove useful in future work. The Bradley and Dudeney (1973) model is widely used, although it has some limitations. Dudeney (1978) has recently published an improved model which overcomes these limitations. This requires as input parameters foF2, foF1, foE, hmF2, hmE, ymF2 and ymE; the first three of these may be obtained from tabulated characteristics, the peak height hmE and semi-thickness ymE of the E layer may be given arbitrary values of, say, 110 km and 20 km respectively, and the corresponding F2 parameters hmF2 and ymF2 calculated from scaled characteristics such as M(3000)F2 by the method described by Dudeney (1974). Rush and Edwards (1975) compared the propagation characteristics (i.e. MUF, etc.) of several model profiles, including the Bradley - Dudeney model; they concluded that the effect of the different models on, say, the MOF, was considerably outweighed by the effects of the day-to-day variability of, in particular foF2 (Rush *et al.*, 1974). Likewise Dudeney (1974) states that any convenient model may be used to correct for underlying ionization in determining, say, N_{max} and h_{max} ; the profile shape below the F2 layer is not important as long as the total electron content $\int Ndh$ is approximately correct. However, joining such a model profile on to an observed oblique F2 profile may present problems of continuity. Relations for exact ray tracing through the Bradley-Dudeney model ionosphere have recently been published by Milsom (1977).

It might also prove interesting to investigate the use of model profiles derived from routinely scaled oblique ionogram characteristics in a similar manner to the vertical ionogram models mentioned above. The major difficulty, however, will probably be the determination of hmF2. How well the F2 profile calculated from the equivalent vertical ionogram may be represented by a parabolic layer may be conveniently checked by the method of Appleton and Beynon (1940). For a parabolic layer

$$h' = h_o + \frac{y_m}{2} \frac{f}{f_o} \ln \left(\frac{f_o + f}{f_o - f} \right) \quad (7.3)$$

so that the semi-thickness y_m and base height h_o may be obtained as the slope and intercept respectively of the best-fit straight line on a graph of

$$h' \text{ vs. } \frac{f}{2f_o} \ln \left(\frac{f_o + f}{f_o - f} \right)$$

An example of such a graph, for the equivalent vertical ionogram of 1977 day 050 at 1340 UT is shown in Figure 7.4. The fit of the straight line with $h_o = 173$ km, $y_m = 57$ km is remarkably good; the maximum deviation in h' is 20 km, and the deviation in real height would be considerably less. Similar graphs for each of the layers on the simultaneous vertical ionograms from the R.S.A., Grahamstown and SANAE are shown in Figure 7.5.

The parameters of these "equivalent parabolic layers" for the equivalent vertical ionogram and the F2 layers of the three vertical ionograms are compared in Table 7-2.

Table 7-2 : Parabolic layer parameters for the F2 layer, 1977 day 050 1340 UT.

<u>Parameter</u>	<u>Equiv. vertical</u>	<u>R.S.A.</u>	<u>Grahamstown</u>	<u>SANAE</u>
y_m (km)	57	60	98	71
h_o (km)	173	250	189	319
$\gamma = y_m/h_o$	0.33	0.24	0.52	0.22

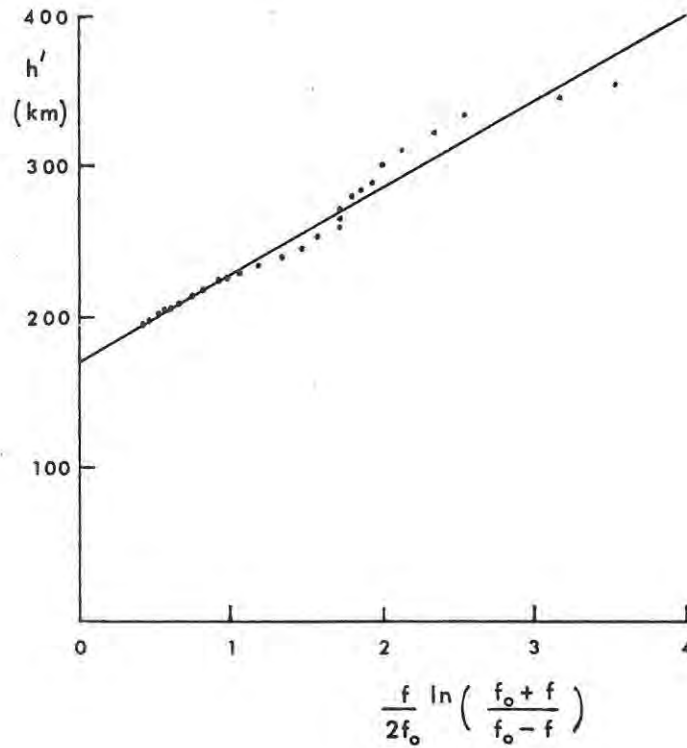


Figure 7.4 : "Appleton plot" of the function $\frac{f}{2f_o} \ln \left(\frac{f_o + f}{f_o - f} \right)$ versus h'

for the equivalent vertical ionogram of day 050 1340 UT. The equivalent parabolic layer has the base height $h_o = 173$ km and semithickness $y_m = 57$ km given by the intercept and slope respectively of the best-fit straight line shown ($\gamma = y_m/h_o = 0.33$).

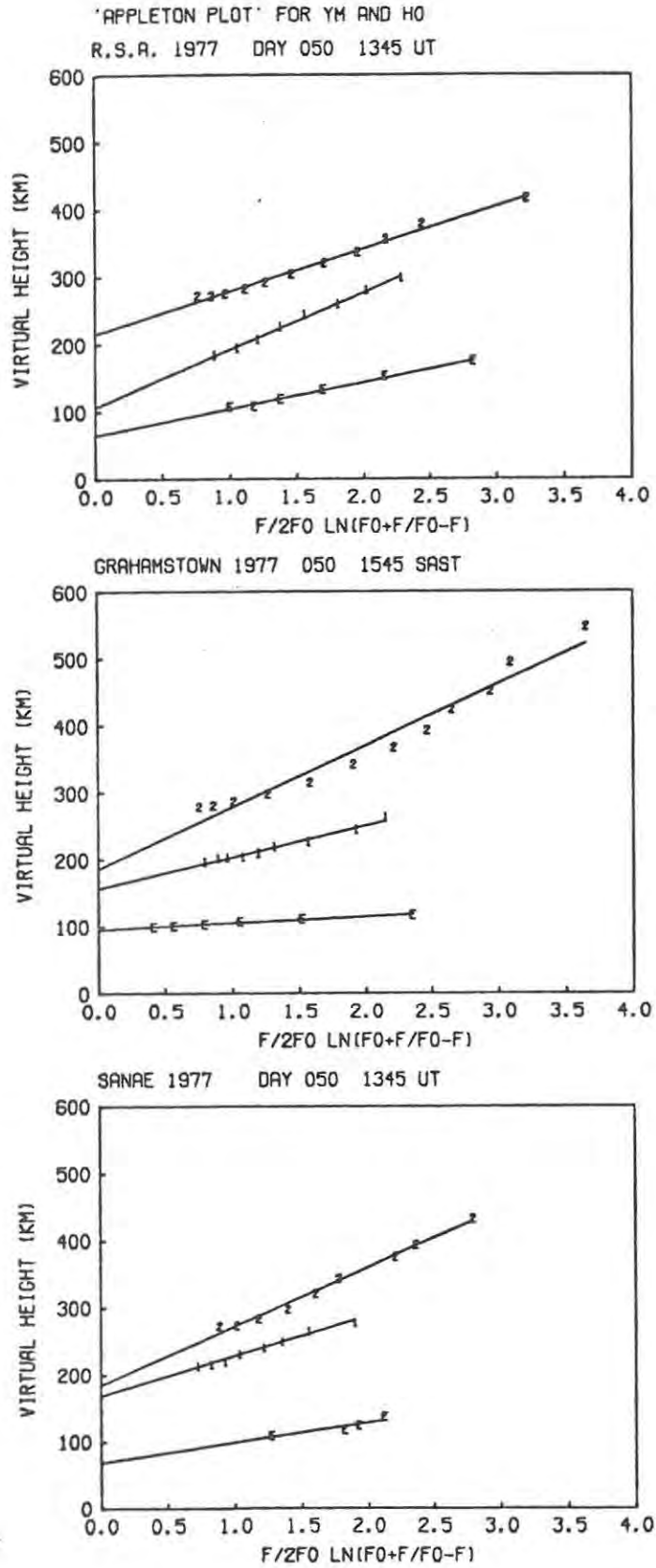


Figure 7.5 : "Appleton plots" for the parameters of the equivalent parabolic layers for R.S.A., SANAE and Grahamstown vertical ionograms for day 050 1340 UT (E = E layer, 1 = F1 layer, 2 = F2 layer).

7.4 Ray Tracing through Daytime Profiles

The daytime profiles chosen for analysis were those of day 043 1340 UT (Figure 6.27) because there was a clearly defined gradation in peak electron density, with

$$N_{\max}(\text{SANAE}) < N_{\max}(\text{R.S.A.}) < N_{\max}(\text{oblique}) < N_{\max}(\text{Grahamstown}) .$$

Unfortunately, time did not permit ray tracing through all these profiles, or other models, such as the latitude dependent model of Lambert (1977), as originally envisaged.

The synthetic oblique ionogram obtained by ray tracing at different frequencies through the oblique (Rao) profile is compared with the observed oblique ionogram in Figure 7.6. As in the nighttime cases (Figures 7.1 and 7.2) the agreement between the two is remarkably good; the nose frequencies differ by less than 0.1 MHz, the limit of accuracy to which JF is read, and the minimum group paths by less than 10 km, the limit of accuracy used in the homing routine for ray tracing (see Table 7-3).

Again the self consistency of the oblique profile is shown, as in the nighttime case (section 7.2). Further, however, the neglect of underlying ionization is also self consistent, i.e. the profile deduced from only the information on the oblique ionogram can again be inverted to reproduce the original ionogram, even though that profile is physically unrealistic. The neglect of underlying ionization, as discussed in the previous section, does not appear to matter in this regard.

Table 7-3 : Parameters of observed and synthetic daytime oblique ionograms :
Day 043 1340 UT

	<u>JF (MHz)</u>	<u>P'_{min} (km)</u>
Observed	18.05	4657
"oblique profile"	18.00	4648

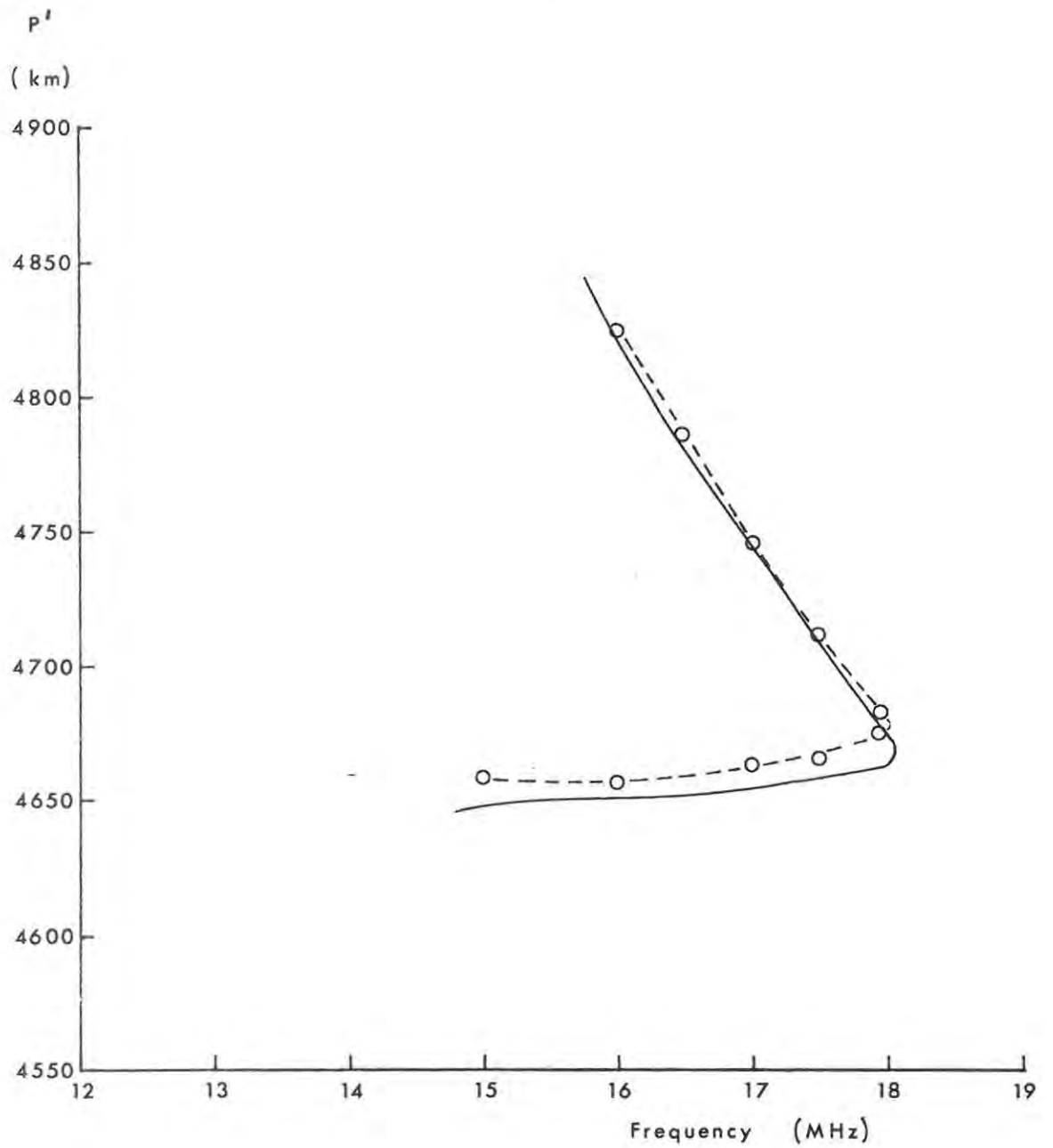


Figure 7.6 : 1977 Day 043 1340 UT : observed daytime oblique ionogram (solid curve) and synthetic oblique profile (dashed curve) obtained from ray tracing through the oblique profile.

Further, these results, together with the nighttime results (section 7.2), provide confirmation of our earlier assertion (section 5.4) that the processes of oblique ionogram reduction to an "effective" $N(h)$ profile and ray tracing through this profile are reciprocal (George, 1970). The Rao (1973) reduction method is seen to be a remarkably accurate means of producing such a profile (the inaccuracies inherent in the ray tracing procedure are considered to be negligible in comparison with those of the oblique ionogram reduction methods). The assumptions (section 5.3.1) of

- (i) no magnetic field;
 - (ii) spherical symmetry on each hop;
 - (iii) equal ionospheric parameters on each hop and therefore equal hops;
- are seen to be justified.

It was also argued in section 5.4 that, since the Rao method was almost exact within the above assumptions, this should be the "best" reduction method. While ray tracing through the profiles computed by the Smith, George and 'indirect' (equivalent vertical) methods in order to obtain synthetic oblique ionograms from these profiles for comparison, has not been undertaken, these ionograms clearly could not give as good agreement with the observed ionogram as does the Rao profile. The differences in form of the profiles produced from the same oblique ionogram by the different methods are evident in Figures 6.12 - 6.15 and 6.24 - 6.31.

Reduction of 1F mode daytime oblique ionograms, frequently observed during the current period of increased solar activity, to $N(h)$ profiles could also prove instructive. Inversion of this profile by one hop ray tracing could then help explain why this mode is in fact observed over the large SANAE - Grahamstown distance (c.f. Muldrew and Maliphant, 1962). Reduction of different order (2F, 3F, etc.) modes on the same oblique ionogram could prove useful in the determination of tilts and/or gradients, as discussed in the next section. Some of the difficulties sometimes experienced in obtaining convergence of rays traced through the various profiles could perhaps be explained by the focussing or de-focussing effects of ionization between the layers (Croft, 1967) and/or the low angles of elevation (Bradley, 1970).

7.5 Ionospheric Tilts

The $N(h)$ profile derived from an oblique ionogram assuming spherical symmetry (sections 6.2 and 6.3) appears to be an accurate model for the purposes of reproducing the ionogram by ray tracing (Figures 7.1, 7.2 and 7.6). However if we wish to derive a profile representing the actual profile at a particular point along the path, some incorporation of ionospheric tilts will have to be made. With the advent of reliable angle of arrival measurements this is a topic which is generating renewed interest (Gething, 1978, Chapter 13).

The "tilted mirror" model is often useful as a first approximation (Gething, 1978, p. 235); Croft and Fenwick (1963) published charts for different tilt angles, etc. using this model. For multi-hop propagation over a curved earth the "mirror" is often extended into a spherical shell not concentric with the earth. This geometry is similarly used for a tilted thick layer (Folkestad, 1968). Thick layers may be considered to have tilts (e.g. the height at which N has a particular value increases or decreases) or gradients (e.g. N_{\max} increases or decreases) depending upon the particular application. Nielson (1968) and Gething (1978, Appendix 7) have given formulations of the effective tilt of a parabolic layer; the latter, however, is largely concerned with transverse rather than longitudinal tilts. It is, of course, possible to have a gradient in, say, N_{\max} , without tilt effects. This appeared to be the case in the nighttime profiles presented in section 6.2 where the base heights h_o of the R.S.A. profiles at the first and second reflection points were approximately equal and the increases of N with h similar, even though the N_{\max} 's and h_{\max} 's were substantially different.

As shown by Lambert (1977), and the work presented here, during the day we are mainly concerned with longitudinal (north-south) tilts along the SANAE-Grahamstown path; the effects of transverse tilts in causing lateral deviations from the great circle are slight, except perhaps at sunrise and sunset. However, the assumption of a constant tilt over such a long path is probably unreasonable (Kopka and Möller, 1968; Gething, 1978).

If several multiple-F modes are present, data from them can in principle be used to provide information on tilts. Mather *et al.* (1965) suggested the use of " ΔMUF ", i.e. the difference in JF between successive modes, in

determining gradients in N_{\max} . As yet, however, no "thick layer" formulation utilizing P' and angle of arrival measurements has been developed (Gething, 1978).

Kopka and Möller (1968) showed that if large gradients are present over a long path then no high angle ray is observed on the oblique ionograms; the absence of a Pedersen ray could, then, in certain circumstances, be used as an indication of the presence of tilts.

Another approach with multi-hop propagation is to assume approximate spherical stratification on each hop, while allowing different profile parameters (h_o , N_{\max} , h_{\max} , etc.) on each (e.g. Kuriki *et al.*, 1974; Lambert, 1977, model e). However, it is apparent from the discussion in section 6.3 that such a model cannot account for an observed JF greater than that predicted through the profile with the smallest value of N_{\max} , unless possibly the heights of reflection are vastly different, i.e. the hops are of very different lengths. In terms of the above model Kuriki *et al.* (1974) and Lambert (1977) showed that for the two-hop mode the hop having the profile with the smaller N_{\max} generally has the greater reflection height.

In this connection it is of interest to examine our assumption of equal hops; in the nighttime case (section 6.2) mentioned above, this assumption is apparently justified. In general, if the heights of reflection are significantly, but not vastly, different, the "equivalent hop" theorems of Chernov (1968) may be useful. Using the parabolic layer formulation of Appleton and Beynon (1940), Chernov showed how a multi-hop mode with unequal hops could be considered equivalent to one with equal "equivalent hops". Allowing for variations in, say, h_o and the ratio $x = f/f_o$ where f is the ray frequency and f_o the layer critical frequency, the total ground range D_{Σ} for n unequal hops may be expanded as a double Taylor series in the deviations Δh_o and Δx from the respective arithmetic means h_{oav} and x_{av} . Then Chernov's Theorem 4 states that, provided the Δx_i are $\lesssim 20\%$ of x_{av} so that second and higher order terms may be neglected, approximately the same ground range D_{Σ} is obtained assuming n equal hops, on each of which $h_o = h_{oav}$ and $x = x_{av}$. While not explicitly stated by Chernov, a similar theorem must hold for the group path; it could also be stated in terms of h_{\max} rather than h_o , so that the ratio $\gamma = y_m/h_o$,

rather than y_m , is assumed constant (see Table 7-2). Nielson (1968) and Folkstad (1968) presented ray path equations for tilted parabolic and "quasi-parabolic" (Croft and Hoogasian, 1968) layers respectively.

In addition to large scale tilts there may be more localised ones caused by travelling ionospheric disturbances (TID's). Kopka and Möller (1968), Kerblay and Kovalevskaya (1967), Georges and Stephenson (1969) and others have deduced the effects of model disturbances (e.g. a localised increase in h_o) by means of ray tracing. However, more work appears to have been done on their effects on backscatter measurements (e.g. Hunsucker and Tveten, 1967; Georges and Stephenson, 1969) than on their effects on oblique ionograms. With the incorporation of angle of arrival and Doppler measurements (Georges, 1968), some interesting observations of TID's over the SANAE - Grahamstown path could perhaps be made (see for example Bartning, 1978).

CHAPTER 8

CORRELATIONS OF OBLIQUE INCIDENCE PARAMETERS
WITH ELECTRON PRECIPITATION MEASUREMENTS

8.1 The Satellite Data

Low energy precipitating electron flux data measured by the DMSP satellite over the Southern Ocean during March and April 1975 were made available to us by the National Geophysical and Solar-Terrestrial Data Centre (NGSDC) and the U.S. Air Weather Service. In this chapter the correlation analysis performed between some of these data and simultaneously measured oblique incidence parameters is described. Some of these results were presented at an S.A.I.P. conference (Rash, 1977).

The polar-orbiting DMSP (or DAPP) satellite number 9532 (Dickinson *et al.* 1974; NGSDC, 1975) counts precipitating electrons in six channels in the energy range 0.2 - 20 keV (Table 8-1). The power FWHM of each channel is 10% of the centre energy and the integral channel sensor steps through all six channels in one second. The sensor is directed towards the zenith at all times. The data printout consists of 1 second counts in each of the six channels, with the satellite position, altitude and time given every 8 seconds. The precipitating electron flux, in units of electrons $\text{cm}^{-2} \text{s}^{-1} \text{sr}^{-1} \text{keV}^{-1}$, in the channel with centre energy E keV is given by

$$\text{Flux} = \frac{\text{counts/sec}}{G E} \quad (8.1)$$

where the geometrical factor $G = 2.46 \times 10^{-5}$

Table 8-1 : Channel energies (keV)

Channel no.	:	1	2	3	4	5	6
Centre Energy E	:	0.200	0.502	1.261	3.170	7.962	20.00
$\log_{10} E$:	-0.70	-0.30	0.10	0.50	0.90	1.30

DMSP SATELLITE PASSES

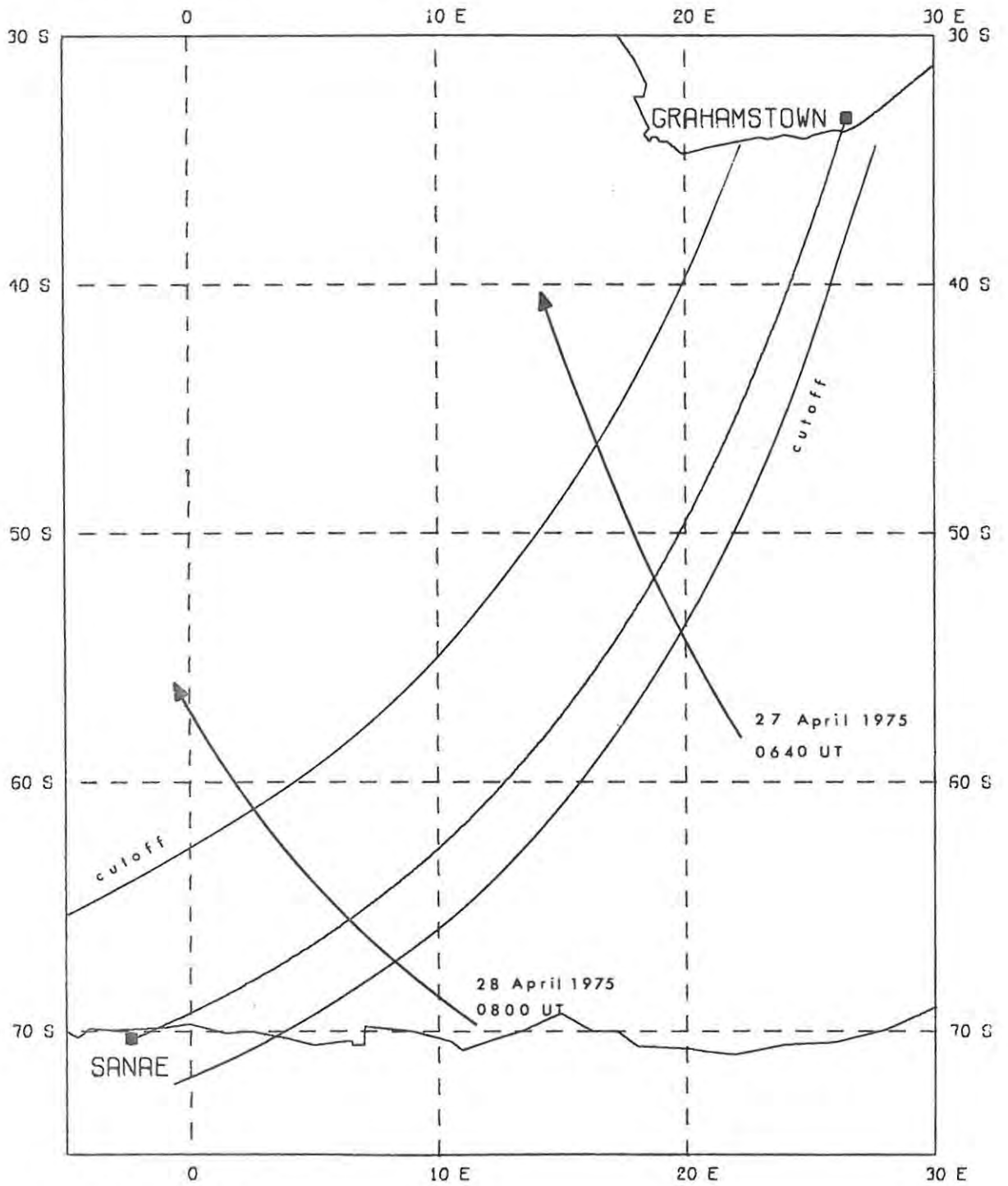


Figure 8.1 : Two typical passes of the DMSP satellite over the SANAE - Grahamstown great circle path.

The data set contained 54 passes of the satellite over the SANAE - Grahamstown great circle between 8 March and 30 April 1975 (the first two months of operation of the oblique incidence experiment). The passes were over different points along the path, but all occurred between about 0600 and 0900 UT, which is unfortunate in view of the gradients and rapid changes which occur in the ionosphere after sunrise. The direction of motion of the satellite in all these cases was within a few degrees of geomagnetic north, and its altitude approximately 830 km. Figure 8.1 shows two typical passes, on 27 and 28 April 1975. The data set for each pass was restricted to 8 second-averaged fluxes in each channel between the arbitrary limits 200 km geomagnetic south and 500 km geomagnetic north of the great circle (Figure 8.1). This yielded on average approximately 15 sets of flux and position data for each pass (i.e. covering a period of approximately 2 minutes). There was a cutoff at 40° S (northwards) in the original data set.

Using the average flux in each channel for each pass, the observed energy spectra, an example of which is shown in Figure 8.2, obeyed a power law of the form

$$J = J_0 E^{-\gamma} \quad (8.2)$$

where $-\gamma$ is the slope of the straight line in the log - log plot. γ had the mean value 0.907 ± 0.025 for the 54 passes. J_0 , the flux at 1 keV, was typically $\sim 10^7$.

The IDH integral flux in the energy range E_1 to E_2 is given by (from (8.2)),

$$I(E_1 \leq E \leq E_2) = 2\pi \int_{E_1}^{E_2} J dE$$

$$= \begin{cases} 2\pi \left[\frac{J_0}{1-\gamma} E^{1-\gamma} \right]_{E_1}^{E_2}, & \gamma \neq 1 \\ 2\pi \left[J_0 \log E \right]_{E_1}^{E_2}, & \gamma = 1 \end{cases} \quad (8.3)$$

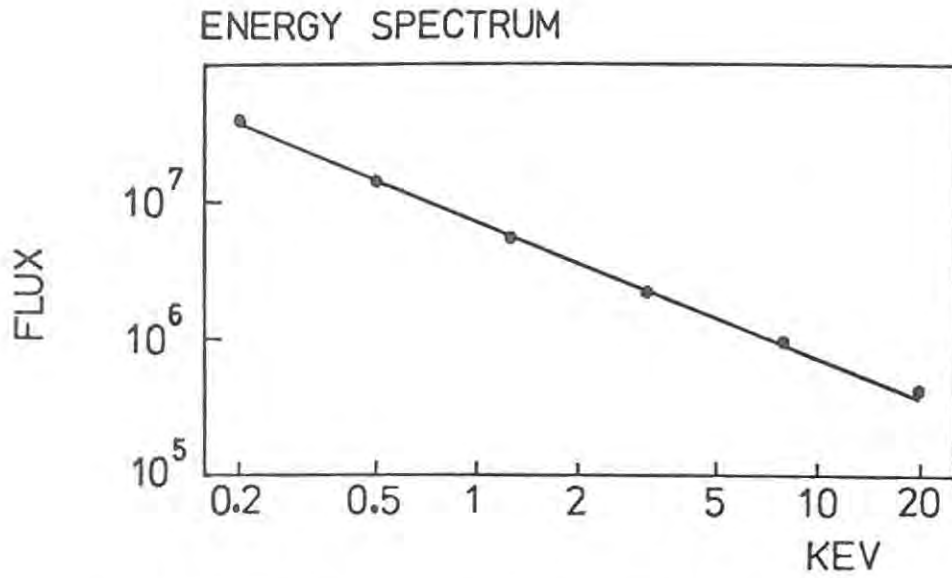


Figure 8.2 : A typical observed energy spectrum showing average flux J in each channel versus channel energy in keV (for the satellite pass on 15 March 1975 at 0730 UT) obeying the power law $J = J_0 E^{-Y}$.

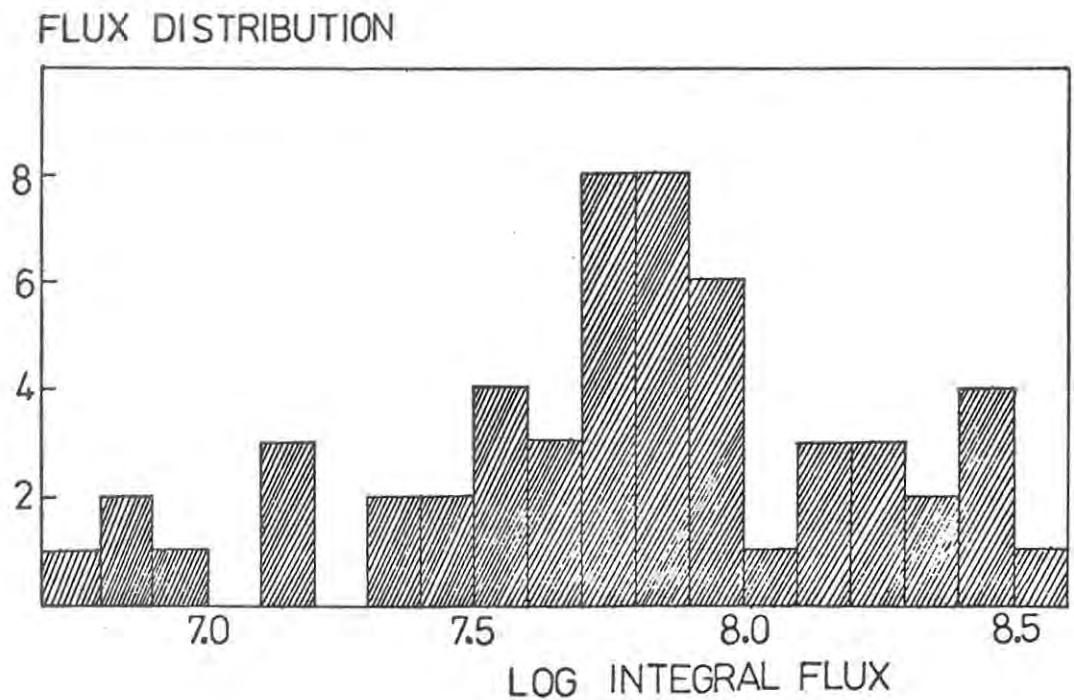


Figure 8.3 : Distribution of measured integral fluxes I for the 54 satellite passes.

in units of electrons $\text{cm}^{-2} \text{ s}^{-1}$. Before performing any correlation analysis, the flux data was examined to check that its distribution did not deviate markedly from normal. The integral flux I ($0.2 \leq E \leq 20 \text{ keV}$) had the distribution shown in the histogram of Figure 8.3, where frequency is plotted against $\log_{10} I$.

The total IDH energy flux F is given by

$$F = 1.6 \times 10^{-9} \times 2\pi \int_{E_1}^{E_2} J E \, dE$$

$$= \begin{cases} 1.6 \times 10^{-9} \times 2\pi \left[\frac{J_0}{2-\gamma} E^{2-\gamma} \right]_{E_1}^{E_2}, & \gamma \neq 2 \\ 1.6 \times 10^{-9} \times 2\pi \left[J_0 \log E \right]_{E_1}^{E_2}, & \gamma = 2 \end{cases} \quad (8.4)$$

in units of $\text{erg cm}^{-2} \text{ s}^{-1}$ ($= 10^3 \mu\text{W m}^{-2}$).

The "raw" satellite data (counts per 8 seconds, position and time) and ionogram data were used as input for a FORTRAN program FLUX which

- (i) computed the fluxes and determined averages for each pass
- (ii) determined the value of γ for the best straight line on the log - log graph
- (iii) computed the IDH integral flux and energy flux using (8.3) and (8.4)
- (iv) output the data for each pass in the format of Table 8-2.

8.2 The Correlation Analysis

For each of the 54 satellite passes the oblique ionogram obtained at the time closest to the time of crossing of the SANAE - Grahamstown great circle was scaled to obtain the LLOF and MOF of all visible multiple-F

Table 8-2 : Typical computed precipitating electron fluxes for a pass of the DMSP satellite over the SANAE - Grahamstown great circle path (output of program FLUX).

SATELLITE PASS NO. 18 DATE 20.3.75 TIME 0753.05 UT

CROSSES G.C.PATH AT 64.8 S 7.8 E 746 KM FROM SANAE

FLUX IN ELECTRONS CM-2 SEC-1 STER-1 KEV-1

ENERGY =	0.200	0.502	1.261	3.170	7.962	20.000	KEV
	3.78E 07	1.44E 07	5.64E 06	2.34E 06	9.42E 05	3.97E 05	
	4.87E 07	1.84E 07	7.20E 06	2.87E 06	1.15E 06	4.91E 05	
	5.71E 07	2.04E 07	8.57E 06	3.48E 06	1.36E 06	5.91E 05	
	6.28E 07	2.44E 07	9.86E 06	3.98E 06	1.49E 06	6.18E 05	
	6.30E 07	2.52E 07	1.03E 07	4.05E 06	1.62E 06	6.77E 05	
	6.89E 07	2.53E 07	1.04E 07	4.07E 06	1.66E 06	6.75E 05	
	6.34E 07	2.45E 07	1.01E 07	3.92E 06	1.60E 06	6.85E 05	
	6.65E 07	2.40E 07	9.54E 06	3.69E 06	1.51E 06	6.22E 05	
	5.81E 07	2.15E 07	8.48E 06	3.39E 06	1.34E 06	5.81E 05	
	5.18E 07	1.89E 07	7.88E 06	2.99E 06	1.21E 06	5.06E 05	
	4.51E 07	1.65E 07	5.83E 06	2.39E 06	9.55E 05	4.19E 05	
	4.15E 07	1.45E 07	5.32E 06	1.96E 06	8.35E 05	3.40E 05	
	3.72E 07	1.33E 07	4.34E 06	1.67E 06	7.12E 05	2.93E 05	
	3.21E 07	1.26E 07	4.13E 06	1.54E 06	6.08E 05	2.58E 05	
AVERAGES :	5.24E 07	1.96E 07	7.69E 06	3.02E 06	1.21E 06	5.11E 05	
INTEGRAL FLUX =	2.87E 08 ELECTRONS CM-2 SEC-1 (IDH) , 0.2 < E < 20 KEV						
ENERGY FLUX =	1.96E 03 UWATT M-2 (10-3 ERG CM-2 S-1) 0.2 < E < 20 KEV						
(ENERGY SPECTRUM : GAMMA = 1.006 ; VARIANCE OF FIT = 0.01)							

IONOGRAM DATA AT 0750 UT	MODE	MOF	LLOF	KP = 2+
	2	138	124	
	3	106	096	

modes. Nine of these ionograms showed complete absorption and four were unavailable due to equipment faults. (There was no apparent correlation between high fluxes and complete absorption). This left 41 passes for which approximately simultaneous ionogram parameters were available; correlation analyses between these sets of data was then performed. As "correlation" is a term often used somewhat loosely, the quantities calculated in each correlation analysis between n pairs of values of two variables x and y (assumed to have approximately normal distributions) are first defined. (The FORTRAN subroutine CORR used is listed in Appendix F).

- (i) The *correlation coefficient* r is defined in the usual way (e.g. Dixon and Massey, 1969) as

$$r = \frac{\sum_{i=1}^n (x_i - \bar{x})(y_i - \bar{y})}{\sqrt{\sum_{i=1}^n (x_i - \bar{x})^2 \sum_{i=1}^n (y_i - \bar{y})^2}} \quad (8.5)$$

$$\text{where } \bar{x} = \frac{\sum_{i=1}^n x_i}{n} \quad \text{and} \quad \bar{y} = \frac{\sum_{i=1}^n y_i}{n} \quad .$$

- (ii) The *significance level* α of r is such that the probability is $< \alpha$ that the population coefficient ρ is zero; this requires

$$\frac{r}{\sqrt{(1 - r^2) / (n - 2)}} > t_{1-\frac{\alpha}{2}}(n - 2) \quad (8.6)$$

where $t_{1-\frac{\alpha}{2}}(n - 2)$ is the value of "Student's t " for probability level $1-\frac{\alpha}{2}$ and $n-2$ degrees of freedom (Dixon and Massey, 1969).

- (iii) Equivalent to (8.6), a "*critical r* ", r_c , exists for a given α and n such that if $|r| > |r_c|$ then r is "significant at the α level". For $n > 30$ (Naiman *et al.*, 1972),

$$r_c = \frac{t}{\sqrt{t^2 + n - 2}} \quad (8.7)$$

where again $t = t_{1-\frac{\alpha}{2}}(n-2)$.

- (iv) The *confidence interval* for r at probability level P is obtained assuming a normal distribution for the variable

$$z = \frac{1}{2} \ln \left(\frac{1+r}{1-r} \right) \quad (8.8)$$

with standard deviation $\sigma_z = 1 / \sqrt{n-3}$ (Dixon and Massey, 1969).

The 95% and 99% confidence intervals for z are then $z \pm 1.960 \sigma_z$ and $z \pm 2.576 \sigma_z$ respectively. The corresponding values of r are obtained from the inverse transformation

$$r = \frac{e^{2z} - 1}{e^{2z} + 1} \quad (8.9)$$

In this analysis the levels $\alpha_i = 0.5, 0.2, 0.1, 0.05, 0.01$ and 0.001 (i.e. 50%, 20%, 10%, 5%, 1% and 0.1% respectively, in order of increasing significance) are used. For a given n , r_{c_i} for each of these levels ($i = 1$ to 6) is defined by (8.7) and is larger for smaller α_i . If $r_{c_i} \leq r < r_{c_{i+1}}$ then r is taken to have significance level α_i ; i.e. we reject the "*null hypothesis*", that r is in fact zero, at that significance level. If $r < r_{c_1}$ then r is not at all significant. The 95% and 99% confidence intervals (CI's) for r are also calculated in each case.

In the first tests the correlation analysis was performed between the average integral flux I and each of the following variables in turn :

- (i) LOF, the overall lowest observed frequency on the corresponding oblique ionogram;
- (ii) LLOF (2F);
- (iii) MOF, the overall maximum observed frequency (equal to MOF (2F) in all cases);
- (iv) the southern latitude at which the satellite crossed the great circle; and

- (v) the magnetic index Kp (Solar Geophysical Data, NGSDC, March and April 1975).

The results are given in Table 8-3. Scatter diagrams for cases (i), (iii) and (iv) are shown in Figure 8.4.

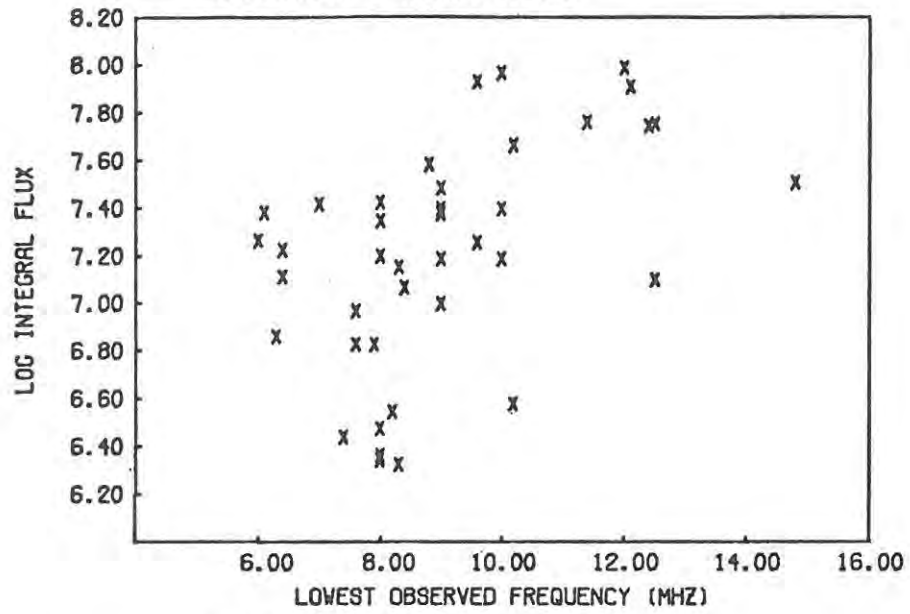
Table 8-3 : Correlation of Integral Flux I vs.

		<u>r</u>	<u>α</u>	<u>95% CI</u>
(i)	LOF	: 0.550	.001	0.292 to 0.734
(ii)	LLOF (2F)	: 0.338	.05	0.033 to 0.584
(iii)	MOF	: 0.018	-	-0.291 to 0.324
(iv)	Latitude S	: 0.532	.001	0.308 to 0.700
(v)	Kp	: 0.165	-	-0.108 to 0.414

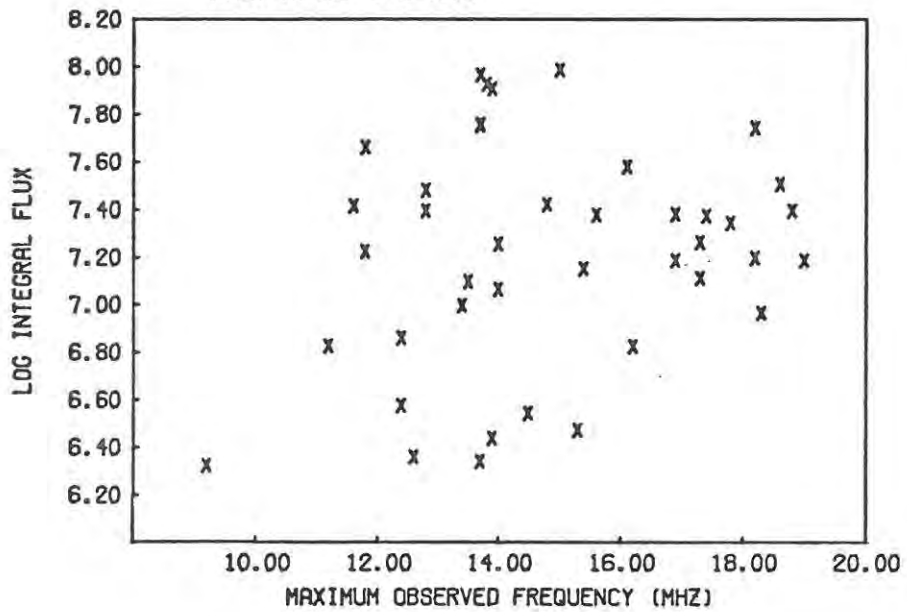
The integral flux is seen to have a highly significant ($\alpha = .001$) positive correlation with both LOF and southern latitude, a less significant ($\alpha = .05$) positive correlation with LLOF (2F), and no significant correlation with either MOF or Kp. Control analyses, such as between the LOF and the satellite latitude, and between flux and a set of random numbers, showed no significant correlation. Although one might expect F region parameters such as the MOF to be influenced by fluxes of low energy electrons, the effects of normal fluxes such as these are probably insignificant during the day (Gledhill and Huang, 1977; Huang, 1977).

As the latitude dependence was obviously important, data obtained on two passes of the satellite during this period in a direction approximately "parallel" to the SANAE - Grahamstown great circle were used. Figure 8.5 shows log I vs. latitude for these two cases. In both, the flux reaches a peak between 55° and 60° S, the centre of the "Southern Radiation Anomaly" (Chapter 1), (Ginzburg *et al.*, 1962).

Attempts were made to understand the correlations with LOF and MOF by determining whether restriction of the data to certain subsets caused the correlation to increase or decrease significantly; this could only be done to a limited extent in view of the size of the data set.



FLUX VS MOF : $R=.018$



FLUX VS LATITUDE : $R=.532$ (.001)

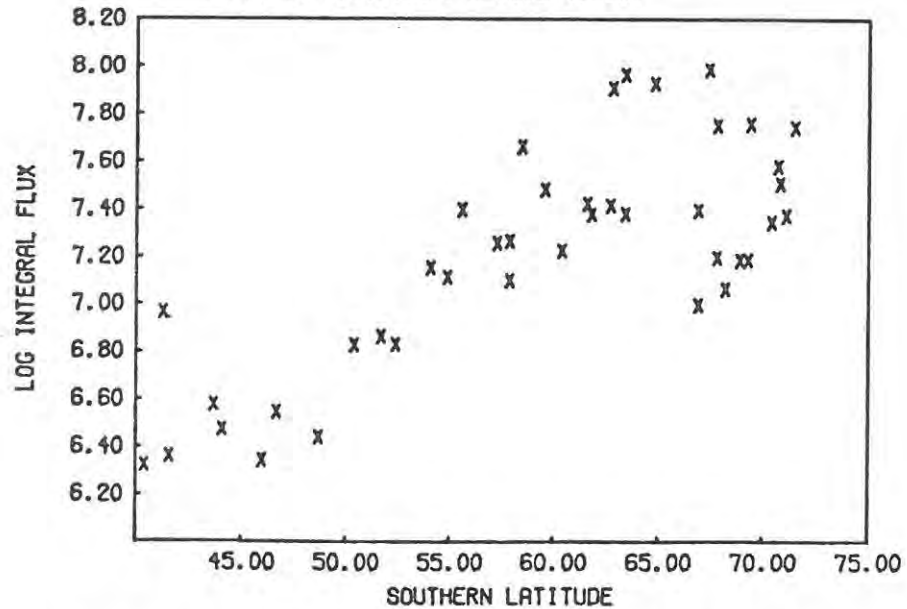


Figure 8.4 : Scatter diagrams of integral flux I versus (a) LOF, (b) MOF, (c) latitude.

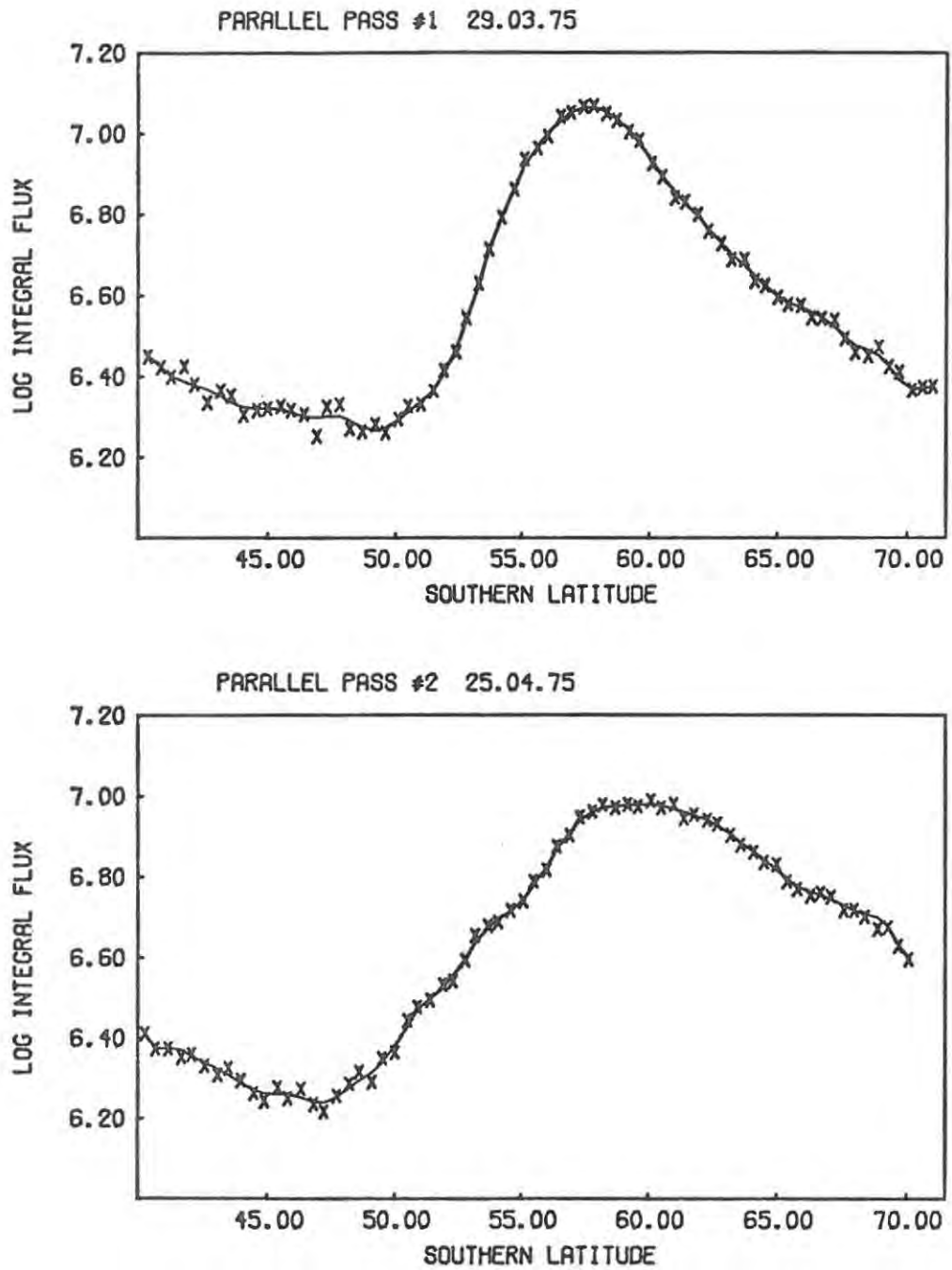


Figure 8.5 : Variation of log I with latitude for two passes of the satellite approximately parallel to the SANAE - Grahamstown great circle.

8.3 Further Analysis

8.3.1 Energy Dependence

The energy dependence of the correlation between flux and LOF was first examined by determining r for the average flux in each channel *vs.* LOF. The results of this are shown in Table 8-4.

Table 8-4 : Correlation of average flux J in each energy channel *vs.* LOF :

<u>Ch1</u>	<u>E(keV)</u>	<u>r</u>	<u>α</u>	<u>95% CI</u>
1	0.200	0.562	.001	0.307 - 0.741
2	0.502	0.538	.001	0.276 - 0.726
3	1.261	0.506	.001	0.235 - 0.704
4	3.170	0.426	.01	0.136 - 0.649
5	7.962	0.408	.01	0.115 - 0.636
6	20.00	0.366	.05	0.066 - 0.606

The correlation decreases with increasing channel energy, which is perhaps rather curious. The higher energy fluxes would be expected to influence the LOF more since electrons with higher energy (> 20 keV) penetrate lower into the ionospheric D region (Rees, 1963; Berger *et al.*, 1970), where most absorption occurs (Davies, 1965; Rush and Elkins, 1975). The improved correlation at lower energies may possibly be caused indirectly by high energy particles (with energies of the order of MeV) causing increased count rates in the low energy channels, as has been found in other cases (Gledhill, 1978).

8.3.2 "Area" Dependence

In order to try and determine whether the fluxes were in fact influencing the D or F region, the passes were divided into two subsets according to the criteria outlined below.

From the ray tracing studies of Lambert (1977) for the 2F mode, an approximate factor was found representing the proportion of the total ground range per hop that was traversed while the ray was below the ionosphere, i.e. D_0/D , where D_0 is given by equation (5.21).

With a base height of 90 km this ratio had the value 0.18. The assumption was then made that this ratio held for higher order modes as well. For each pass the highest order mode (always that on which the LOF was measured) was used to generate "latitude limits" along the great circle between which the multi-hop ray would be alternately above or below the ionosphere. All the sections of the great circle where the ray was below the base height were collectively defined as "area D" and all those where it was within the ionosphere were defined as "area F".

The latitude at which the satellite crossed the great circle on each pass was then used to determine into which of these two areas that pass fell. 18 passes were then through "area D" and 23 through "area F". The results of the correlation analysis between flux and LOF for each of the two subsets are given in Table 8-5.

Table 8-5 : Correlation of average flux in each channel J (Ch1) and integral flux I vs. LOF

Ch1	"Area D"		"Area F"	
	<u>r</u>	<u>α</u>	<u>r</u>	<u>α</u>
1	0.694	.001	0.443	.05
2	0.609	.01	0.472	.05
3	0.550	.05	0.472	.05
4	0.413	.1	0.475	.05
5	0.358	.2	0.498	.05
6	0.182	.5	0.610	.01
Integral	0.500	.05	0.491	.05

The most significant ($\alpha = .001$) correlation is obtained for the flux in the lowest energy channel in "area D". If the electron fluxes were influencing the D region, those at the higher energies would be expected to show better correlation with LOF. It is curious that the correlation falls off rapidly with increasing energy.

Attempts were also made to divide the passes into two subsets according to whether the satellite crossed the great circle south or north of the mid-point in order to try and determine whether the first or second hop of the 2F mode was being influenced. However this division placed 30 passes south of the mid-point and only 11 north of it. Thus it was felt that nothing meaningful could be learned from comparison of the two subsets.

8.3.3 "Height" Dependence

Instead of using the fluxes averaged over the period that the satellite was between the imposed cutoff limits, the analysis was repeated using the fluxes at each satellite position (i.e. every 8 seconds) between these limits. Each such position could be considered to define a field line which subsequently crossed the ray path at a specific height (Figure 8.6). This height could be determined from the known position, altitude and geomagnetic field parameters of the satellite (NGSDC, 1975).

11 "height ranges" were then defined (Table 8-6) and the above analysis repeated using the fluxes for the satellite positions appropriate to each height range. The satellite was assumed to provide spatial rather than temporal resolution. There were on average 40 pairs of values for each correlation in the "all passes" case. The results for the correlation of LOF with integral flux for each of these height ranges, for all passes and for the two areas "D" and "F", are given in Table 8-6. There is reasonably significant ($\alpha = .01$) positive correlation in all height ranges when all passes are considered; in "area D" there is no significant correlation in any height range; and in "area F" there is significant ($\alpha = .01$) positive correlation in the lowest height range, this correlation decreasing steadily with increasing height (i.e. increasing proximity of the satellite to the great circle).

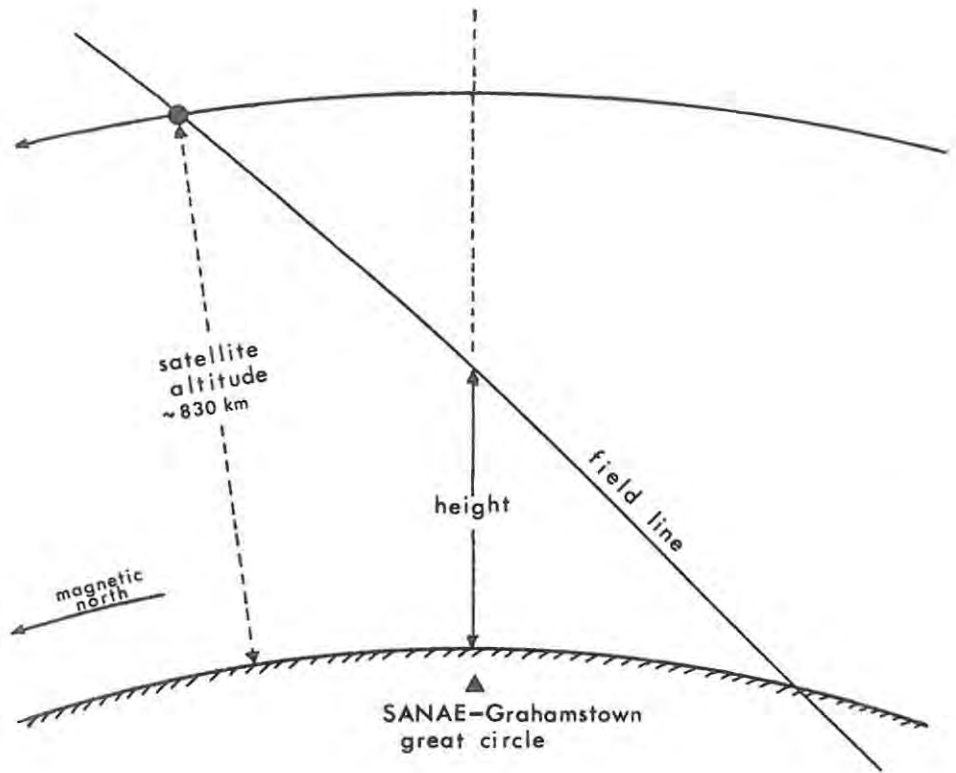


Figure 8.6 : Cross section showing the height above the great circle defined by the field line on which the satellite is positioned.

Table 8-6 : Correlation of LOF vs. integral flux I in various "height ranges"

No.	Height Range	<u>All passes</u>		<u>"Area D"</u>		<u>"Area F"</u>	
		r	α	r	α	r	α
1	-20 - 65 km	0.365	.05	0.043	-	0.604	.01
2	75 - 140 km	0.420	.05	0.001	-	0.573	.05
3	160 - 225 km	0.435	.01	-0.060	-	0.541	.05
4	260 - 320 km	0.468	.01	-0.027	-	0.457	.05
5	355 - 410 km	0.465	.01	0.055	-	0.404	.1
6	445 - 500 km	0.462	.01	0.056	-	0.348	.2
7	540 - 590 km	0.459	.01	0.069	-	0.293	.5
8	630 - 680 km	0.449	.01	0.022	-	0.250	.5
9	720 - 775 km	0.422	.01	0.077	-	0.190	.5
10	815 - 865 km	0.387	.05	-0.008	-	0.187	.5
11	910 - 955 km	0.351	.05	-0.107	-	0.117	-

The fluxes in each energy channel (Table 8-7) show similar trends : there is highly significant ($\alpha = .001$) correlation for heights between 160 and 680 km in channel 1 ($E = 0.2$ keV) when all passes are considered (Table 8-7 (a)); the correlation decreases somewhat with increasing channel energy. In "area D" no significant correlation was found in any channel or any height range. In "area F" the correlation was again most significant at the lowest heights, decreasing steadily in significance with increasing height; there was a slight, but not really significant, decrease in correlation with increasing energy.

A similar analysis for flux vs. MOF (using two-hop "D" and "F" areas) revealed no significant correlation in any subset.

Table 8-7 : Correlation of LOF vs. flux J (chl)

(a) All passes

Channel:	1		2		3		4		5		6	
Height range	r	α	r	α	r	α	r	α	r	α	r	α
1	0.45	.01	0.39	.05	0.36	.05	0.34	.05	0.32	.1	0.32	.1
2	0.51	.01	0.46	.01	0.41	.05	0.37	.05	0.38	.05	0.40	.05
3	0.54	.001	0.47	.01	0.41	.05	0.39	.05	0.40	.05	0.40	.05
4	0.58	.001	0.51	.01	0.46	.01	0.42	.01	0.42	.05	0.42	.01
5	0.58	.001	0.52	.001	0.46	.01	0.41	.05	0.39	.05	0.40	.05
6	0.59	.001	0.52	.01	0.48	.01	0.39	.05	0.40	.05	0.39	.05
7	0.55	.001	0.54	.001	0.48	.01	0.38	.05	0.40	.05	0.39	.05
8	0.58	.001	0.53	.001	0.48	.01	0.36	.05	0.36	.05	0.37	.05
9	0.51	.01	0.50	.01	0.46	.01	0.34	.05	0.35	.05	0.37	.05
10	0.41	.05	0.43	.01	0.43	.01	0.34	.05	0.32	.1	0.33	.05
11	0.41	.05	0.42	.01	0.40	.05	0.32	.05	0.26	.2	0.20	.5

(b) "Area D"

No significant correlation in any channel.

(c) "Area F"

1	0.63	.01	0.60	.01	0.61	.01	0.59	.01	0.60	.01	0.56	.05
2	0.58	.05	0.58	.05	0.58	.05	0.57	.05	0.56	.05	0.55	.05
3	0.58	.01	0.54	.05	0.55	.05	0.53	.05	0.53	.05	0.50	.05
4	0.47	.05	0.47	.05	0.46	.05	0.46	.05	0.45	.1	0.40	.1
5	0.42	.1	0.42	.1	0.40	.1	0.41	.1	0.39	.2	0.36	.2
6	0.37	.2	0.36	.2	0.34	.2	0.35	.2	0.34	.2	0.31	.2
7	0.33	.2	0.30	.5	0.29	.5	0.29	.5	0.27	.5	0.26	.5
8	0.26	.5	0.26	.5	0.25	.5	0.25	.5	0.24	.5	0.23	.5
9	0.23	.5	0.19	.5	0.19	.5	0.18	.5	0.18	.5	0.14	-
10	0.24	.5	0.22	.5	0.17	.5	0.18	.5	0.15	-	0.12	-
11	0.19	.5	0.14	-	0.11	-	0.08	-	0.08	-	0.07	-

8.4 Discussion

The initial result (Table 8-3) of a significant positive correlation between precipitating electron flux and LOF on the corresponding oblique ionogram was promising and prompted the more detailed analysis. The latter indicated that LOF was most significantly correlated with the flux in the lowest energy channel (0.2 keV) at the lowest "height" (i.e. at the position furthest geomagnetic north from the great circle crossing point) in the "area" where the path of the ray on which the LOF was measured was above 90 km.

The fact that the fluxes measured furthest north and west from the great circle show the most significant correlation could be because electrons precipitating further west are actually influencing the LOF. The results could possibly have been improved by the subtraction of a latitude-dependent "background", using for instance the data shown in Figure 8.5, from the measured flux, in order to gain a measure of how much the flux exceeds the normal level at that latitude. Likewise corrections could be applied to both sets of data to allow for the different times of observation, different solar zenith angles and therefore different levels of ionization. Clearly, from Figures 8.4(c) and 8.5, there is normally a maximum of the precipitating electron flux in the vicinity of 60°S , the centre of the Southern Radiation Anomaly, which is also the first "reflection point" of the 2F ray. Large fluxes might well produce observable ionospheric effects at night, such as increased MOF, "spread F" conditions or increased non-deviative absorption. If the first reflection region remains the "control" in the 2F mode, then these effects should be observable on the oblique ionograms from measurements of MOF, MOF-JF and JF-HLOF respectively.

In addition to the above difficulties, other factors may account for the inconclusiveness of the results. These are

- (i) lack of accurate simultaneity between the flux and ionogram measurements, as well as the usual problem of ionogram interpretation in terms of conditions at one of several reflection points
- (ii) the small size of the data base preventing division into subsets of significant size.

It may be that too narrow a correlation was attempted, and that a wider and longer term correlation, such as the "disturbed days" type of analysis carried out by Gledhill *et al.* (1967) using vertical incidence data, should be attempted. Piggott and Hurst (1976) found some correlation between f_{min} from vertical ionograms and particle precipitation at eight high-latitude stations.

CHAPTER 9

FURTHER OBSERVATIONS OF PARTICLE PRECIPITATION EFFECTS

9.1 The Event of 26 March 1976

9.1.1 AE-C Satellite Observations

The ionospheric-magnetospheric event of 26 March 1976 has already been the subject of a considerable amount of investigation (Coffey and McKinnon, 1977) as it occurred during STIP Interval II; our interest in it was aroused because it also fell within the first ASHAY Period (Gledhill, 1975, 1976) of 21 March - 3 April 1976. Atmosphere Explorer C (AE-C) satellite data for this period were made available to us by Dr. D.G. Torr. This set of data included a pass of the satellite over the Southern Ocean, passing close to SANAE and Marion Island (47°S , 38°E) between about 2015 and 2030 UT on 26 March (Figure 9.1) at an altitude of 300 ± 10 km. These results were presented by Gledhill and Rash (1978).

Details of the experiments and instrumentation on board AE-C may be found in Dalgarno *et al.* (1973) and following papers. The variations of total electron and proton energy fluxes in the energy range 0.2 - 25 keV over the pass are shown in Figure 9.2(a). This indicates intense precipitation of electrons between about 66 and 54°S (between 59 and 57°S invariant latitude Λ) and of protons between about 68 and 58°S (approximately 58.5°S invariant latitude). Such levels of precipitation, $\sim 10^{-1}$ erg cm^{-2} s^{-1} , at these latitudes is extremely unusual (Torr *et al.*, 1976); similar plots for other passes over this region show normal fluxes $\sim 10^{-4}$ erg cm^{-2} s^{-1} . The auroral oval is normally well to the south of SANAE (Bond and Thomas, 1971).

The electron and ion densities are shown in Figure 9.2(b) (with the same horizontal scale as 9.2(a)), which displays the characteristics of the nighttime *mid-latitude trough* (Muldrew, 1965; Sharp, 1966; Rycroft and Thomas, 1970; Rycroft and Burnell, 1970; Wrenn and Raitt, 1975) : the electron density N_e and major ion density N_{O^+} show pronounced minima, with less well defined minima in the minor constituent ion densities $N_{O_2^+}$, N_{NO^+} and $N_{N_2^+}$. (N_{O^+} appears to be greater than N_e at about 50°S due to instrumental inaccuracies). The electron temperature T_e (Figure 9.2(a)) shows a pronounced peak coinciding with the trough.

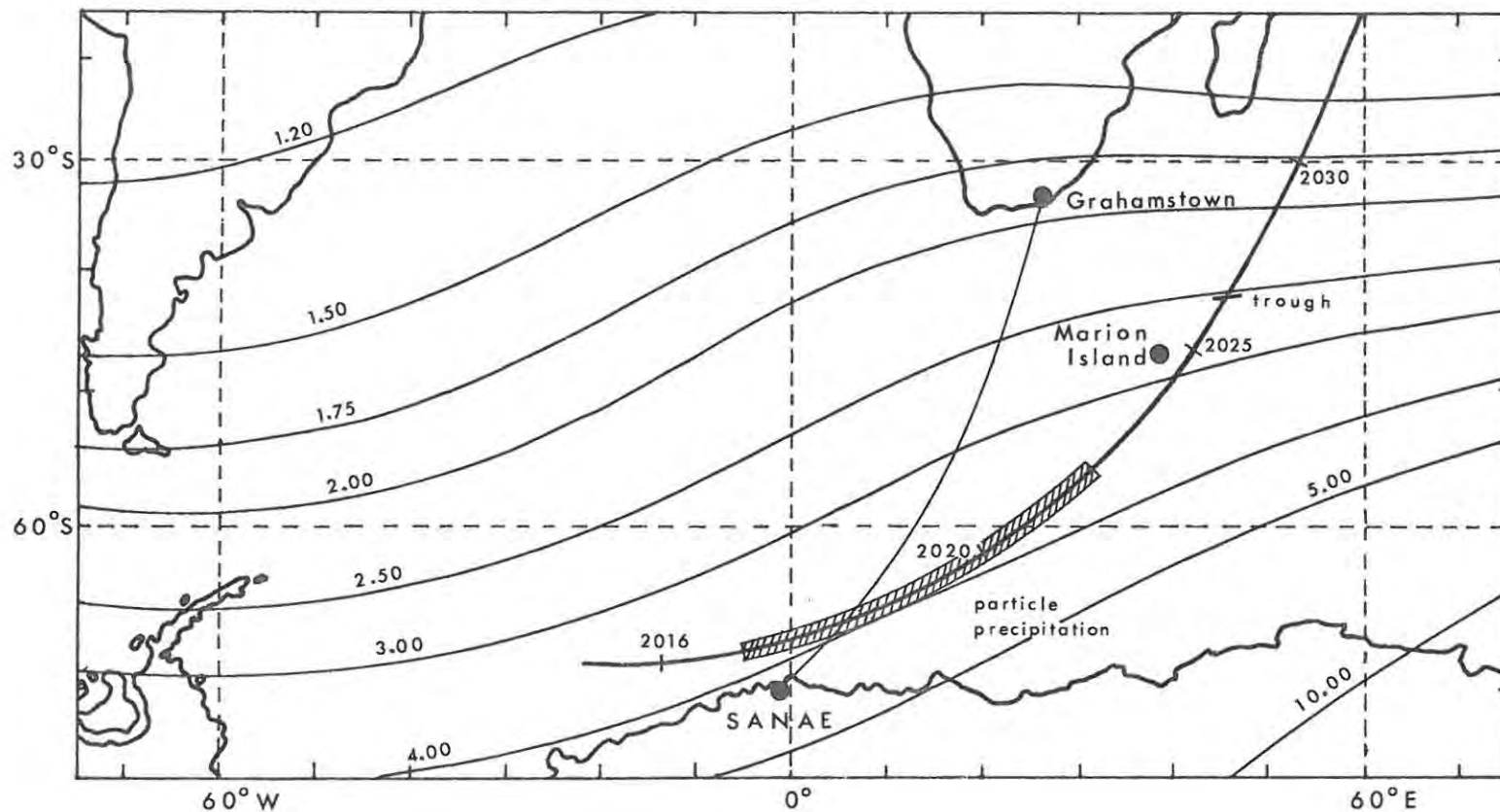


Figure 9.1 : Path of satellite AE-C (bold curve) over the Southern Ocean on 26 March 1976; the time in UT is indicated at several points along the path. The positions of observed particle precipitation and the mid-latitude trough are also indicated. L values at 300 km are from Roederer *et al.* (1965).

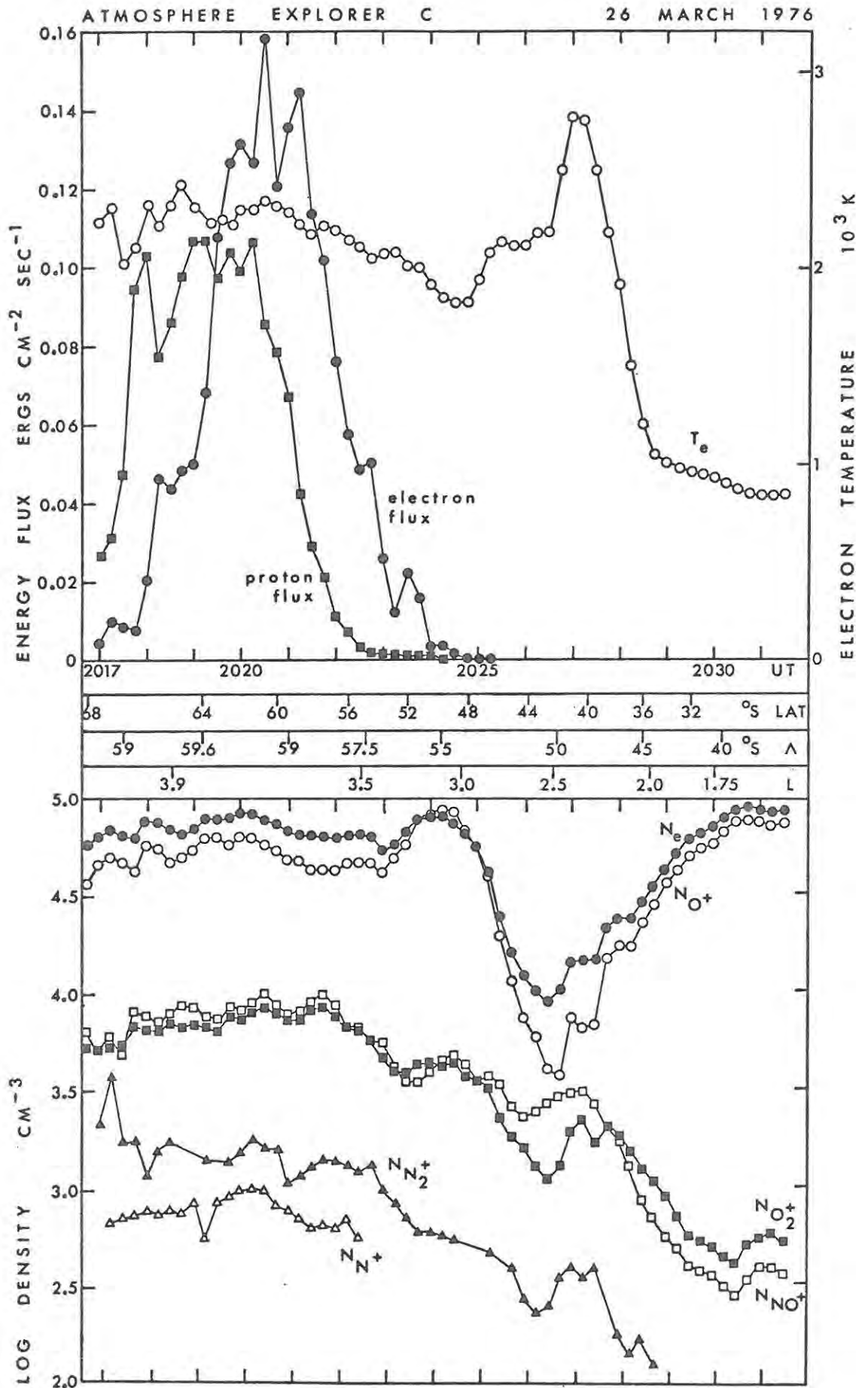


Figure 9.2 : AE-C measurements over the pass : (a) electron and proton energy fluxes and electron temperature T_e , (b) electron density N_e and densities of the ions O^+ , O_2^+ , NO^+ , N_2^+ and N^+ .

Rycroft and Burnell (1970) gave a relation for the invariant latitude Λ_T of the trough in terms of magnetic index K_p and local time t statistically derived from Alouette satellite observations. Köhnlein and Raitt (1977) have given a similar relation from ESRO 4 observations. The two relations are :

$$\text{Rycroft and Burnell : } \Lambda_T = 62.7^\circ - 1.4 K_p - 0.7t \pm 3.5^\circ \quad (9.1)$$

$$\text{Köhnlein and Raitt : } \Lambda_T = 65.2^\circ - 2.1 K_p - 0.7t \pm 2^\circ \quad (9.2)$$

where t is in hours and is counted negative before 0 hours LT. Substituting the appropriate values $K_p = 7$ (Solar - Geophysical Data, March 1976) and $t = -0.6$ (i.e. 23.4 hours LT) yields the values

$$\Lambda_T = 53.3^\circ \pm 3.5^\circ$$

$$\text{and } \Lambda_T = 50.8^\circ \pm 2^\circ$$

respectively. The observed value of 50.4° S (L value at 0 km = 2.46) agrees closely with that predicted by Köhnlein and Raitt, and is one of the lowest reported. (c.f. Tulunay and Hughes, 1973; Brace *et al.* 1976).

The positions of the region of particle precipitation (L at 300 km = 3.95 to 3.5) and the mid-latitude trough (L at 300 km = 2.58) are indicated in Figure 9.1. The former lies just north of SANAE and the latter just north of Marion Island at these times (2017 - 2023 UT and 2026 UT respectively). Ionogram data from the places indicated were examined in the hope of observing effects due to the northward movement of the trough and particle precipitation belt.

9.1.2 Oblique Incidence Data

Figure 9.3 shows graphs of the MOF of each individual mode, as well as the overall LOF on the oblique ionogram, plotted against time in UT, for 25 and 26 March 1976; the name "F-plot" is suggested for such a graph, analogous to the "f-plot" (Piggott and Rawer, 1972) used for vertical incidence frequencies. Multiple-F modes are indicated. The F-plot of the 25th shows normal quiet day behaviour, while beginning at about 0130 UT on the 26th a nose extension, probably due to scattering (Möller, 1964), develops on the 3F trace, and MOF (3F) increases rapidly to a maximum at 0230 UT. Shortly afterwards the 2F mode behaves similarly to peak at 0300 UT.

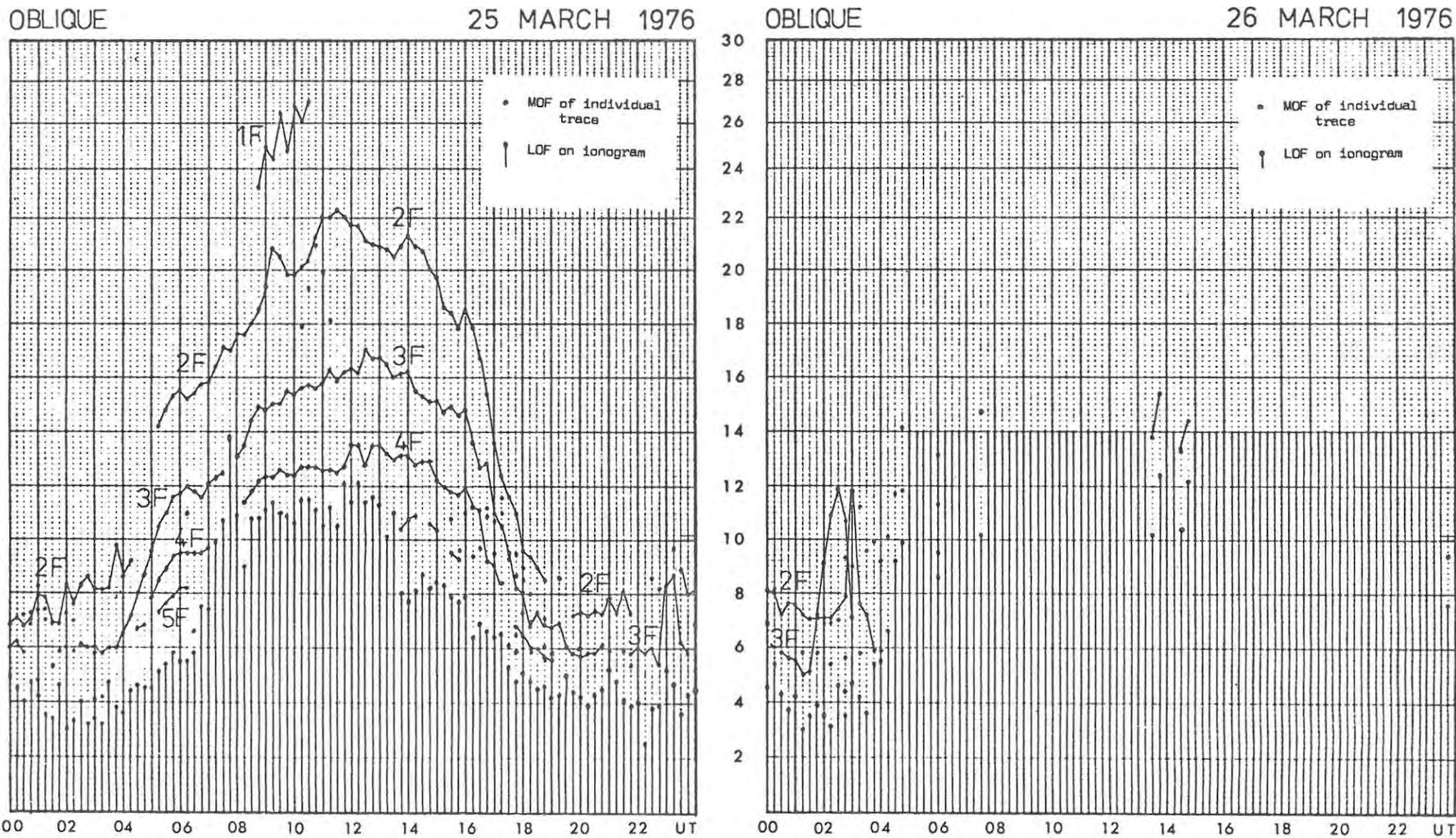


Figure 9.3 : Oblique frequency "F-plots" for 25 and 26 March 1976. (Frequency in MHz *versus* Time in hours UT.)

If, as usual (Chapter 6), the first reflection points of the respective modes are assumed to be the control points, then this behaviour could be interpreted as being caused by a northward-propagating disturbance. These two points (Table 2-3) are approximately 370 km apart; a propagation time of 30 minutes yields a velocity component of approximately 200 ms^{-1} . This is within the normal range of velocities ($100 - 250 \text{ ms}^{-1}$) of medium-scale travelling ionospheric disturbances (TID's) (Francis, 1975).

9.1.3 Vertical Incidence Data

Quarter-hourly vertical incidence ionograms from SANAE, Grahamstown and Marion Island (the latter provided by the N.I.T.R., Johannesburg) were scaled. The "f-plots" for 25 and 26 March at SANAE are shown in Figure 9.4; disturbed conditions appear to commence before 0215 UT, when a sporadic-E layer and spread-F condition are observed. This is followed from 0315 UT by blackout conditions for most of the day. From 1630 UT, however, there is intense blanketing "auroral-type" sporadic-E (Piggott and Rawer, 1972), with foEs reaching a maximum of 11.2 MHz at 2000 UT, shortly before the time of the satellite pass.

Some earlier and later SANAE ionograms have reasonably regular Es traces, allowing reduction to N(h) profiles by the method of section 5.2.2. Four such profiles, for 1800, 1900, 2015 and 2100 UT are shown in Figure 9.5. This suggests an initial large influx of high energy particles (1800 UT), a secondary influx of lower energy particles (1900 UT, when the height of maximum ionization $h_{\text{max}} = 150 \text{ km}$), and a further less intense influx of higher energy particles ($h_{\text{max}} = 120 \text{ km}$ at 2100 UT). No such reduction was possible for the 2000 UT ionogram owing to the irregular and diffuse nature of the Es trace. The ionograms do, however, suggest intense auroral particle precipitation over SANAE. No airglow or auroral observations were made as this occurred during twilight (sunset was at 1902 UT).

The f-plots for Marion Island for the same two days are shown in Figure 9.6; this shows the onset of disturbed conditions at 0615 UT on the 26th. The time of this onset is consistent with our earlier (section 9.1.2) postulation of a TID, which we suggested was at the 2F first reflection point at 0300 UT with a roughly NE velocity component of 200 ms^{-1} . The distance from this point to Marion Island is 2400 km (and the bearing is within 20°) so that at this velocity the disturbance should reach the island $3\frac{1}{4}$ hours later, in agreement with the observed time.

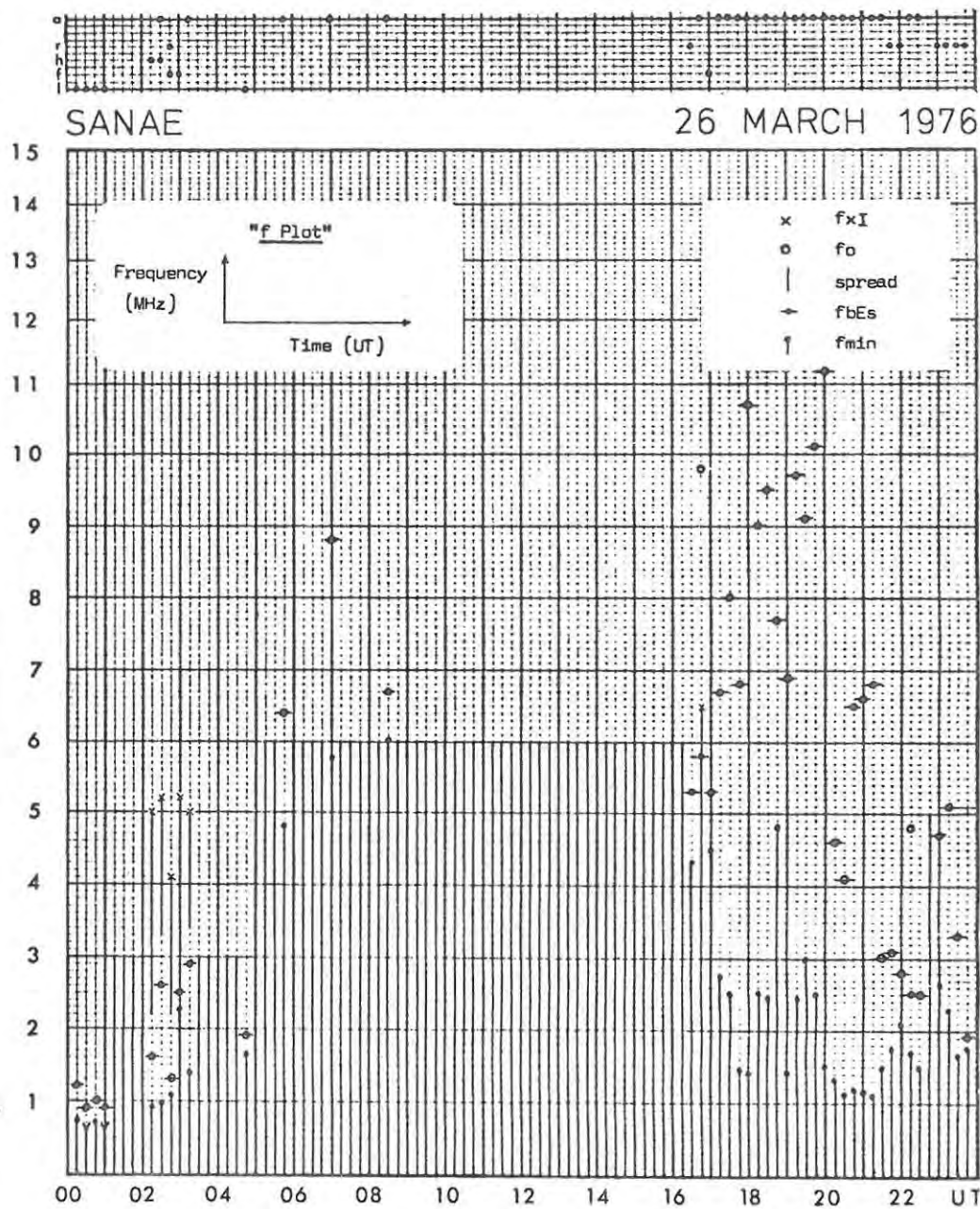
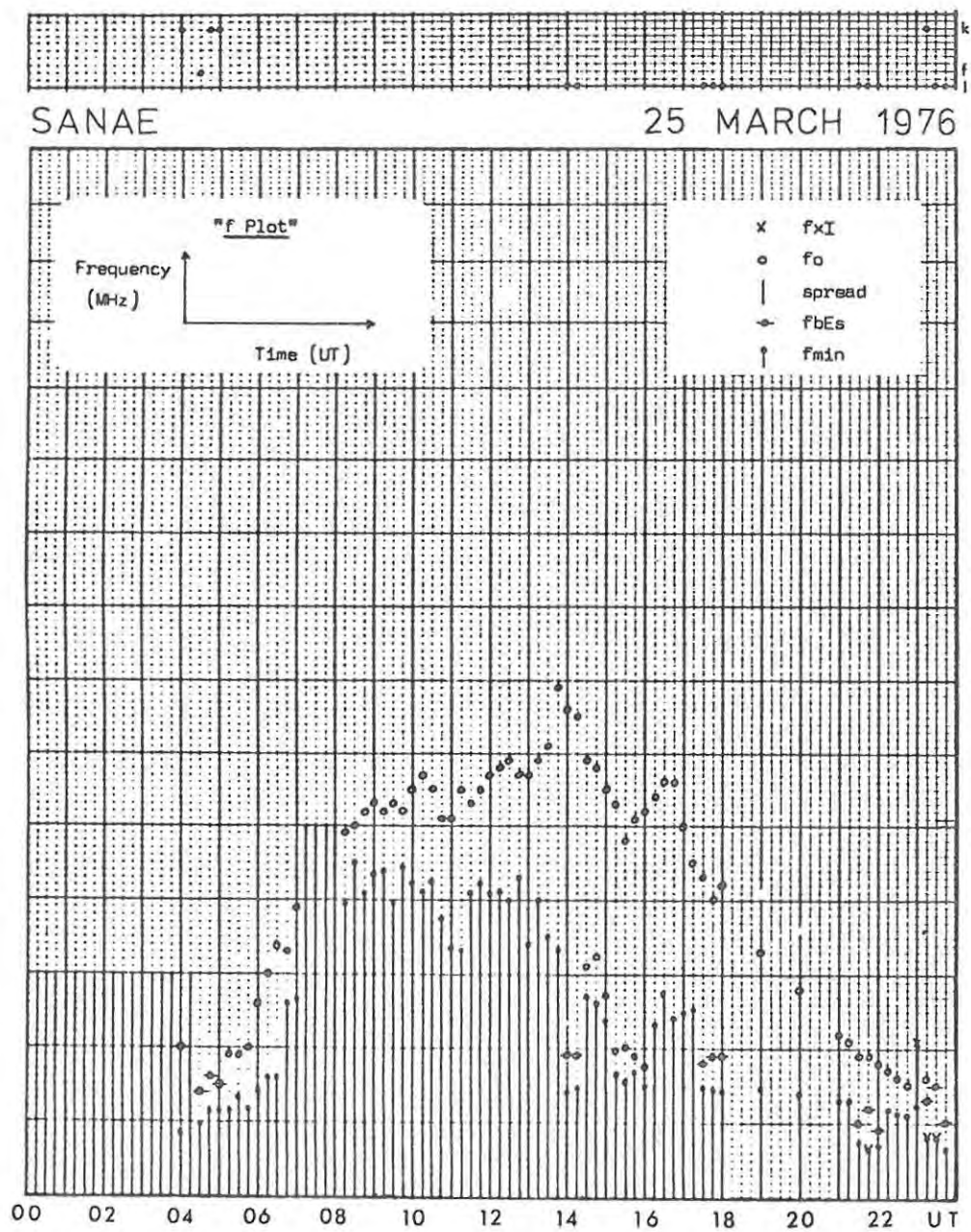


Figure 9.4 : f-plots for SANAE for 25 and 26 March 1976.

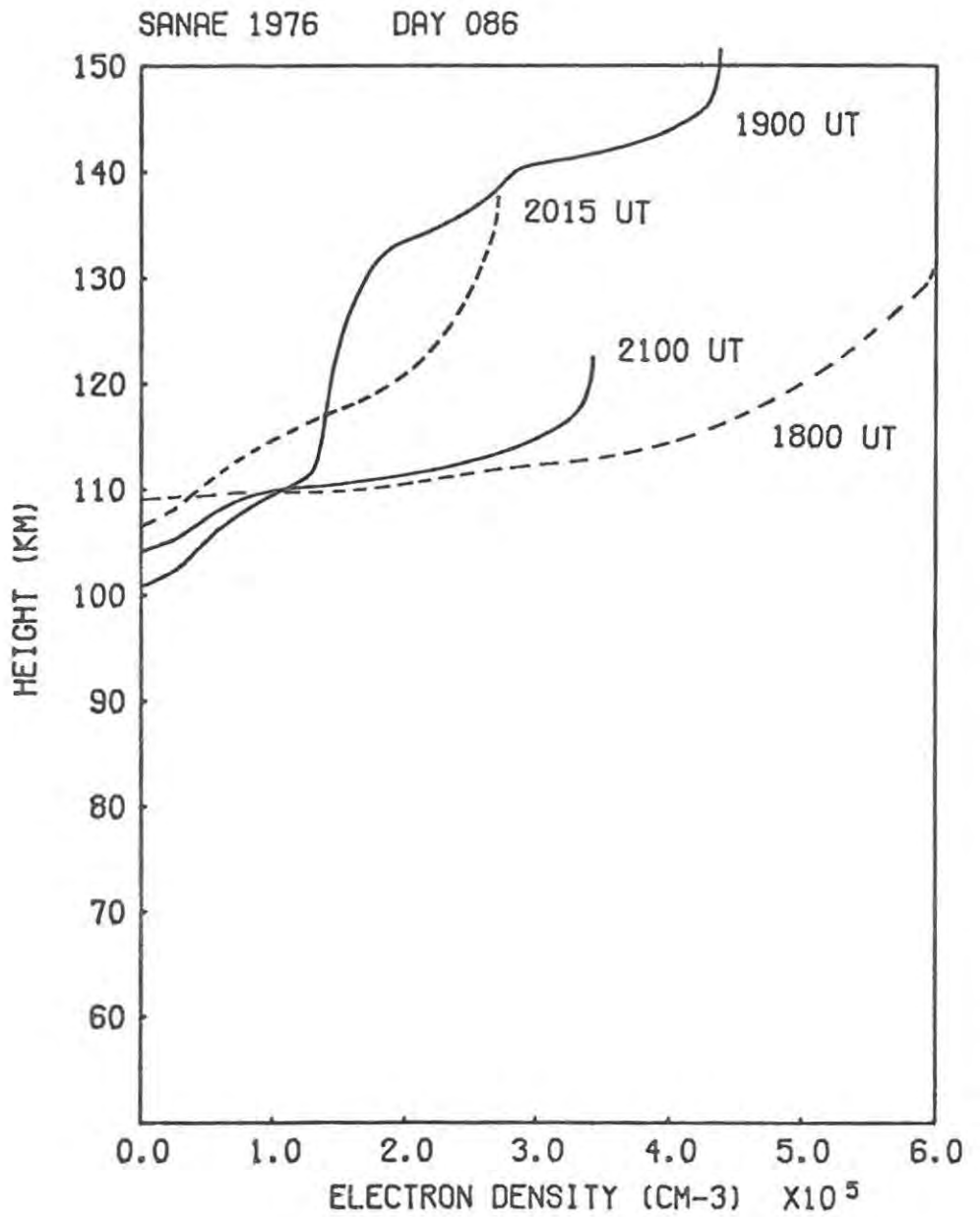
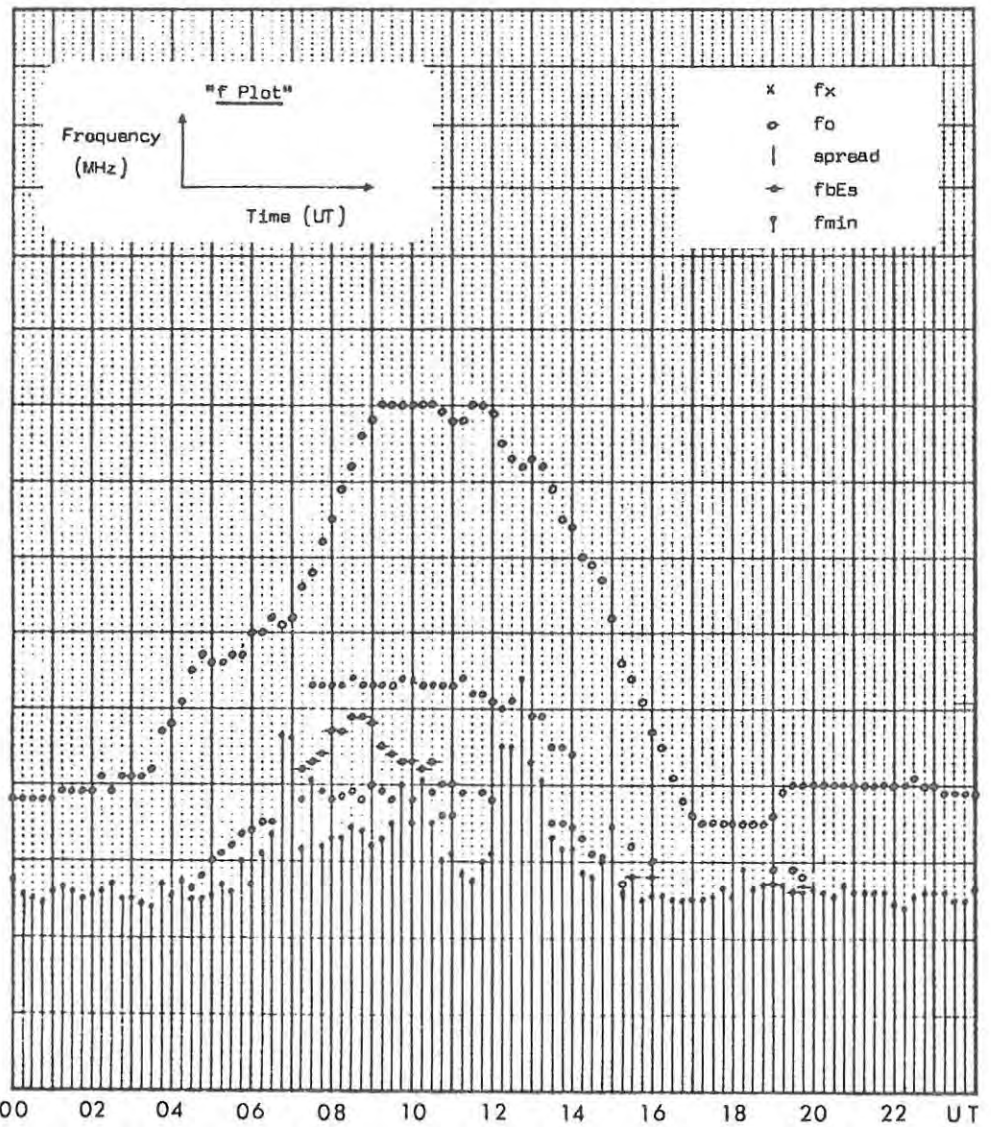


Figure 9.5 : $N(h)$ profiles at SANAE, 1800 - 2100 UT on 26 March 1976.



MARION ISLAND 25 MARCH 1976



MARION ISLAND 26 MARCH 1976

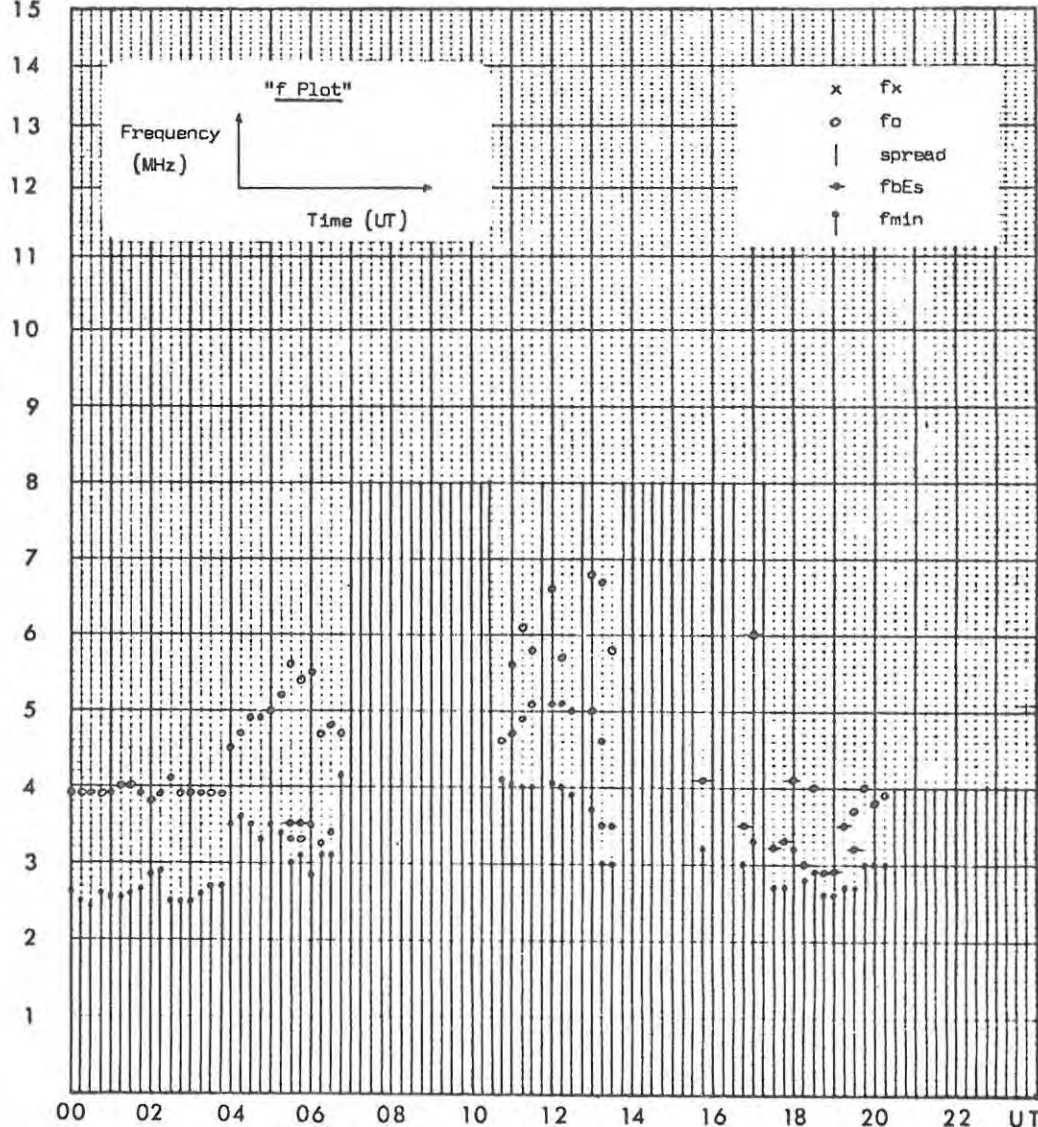


Figure 9.6 : f-plots for Marion Island for 25 and 26 March 1976.

Thereafter, as at SANAE, blackout conditions persist for the better part of the day. There is some sporadic-E activity prior to the time of the satellite pass (approximately 2030 UT); no evidence could be detected of the passage overhead of the mid-latitude trough (Bowman, 1969), which must have occurred at some time before 2030 UT.

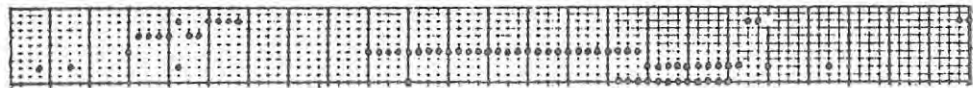
The Grahamstown f-plots for 25 and 26 March are shown in Figure 9.7; there is evidence of disturbed conditions on the 26th here too. F2 ionization is enhanced around noon and depleted in the evening. The most interesting feature, however, is sporadic-E activity from about 1700 UT (including the period of the satellite pass) of the type known as "particle-E" (Piggott and Rawer, 1978); this is characterised by the retardation on the high frequency end of the Es trace and on the low frequency end of the F trace. Such activity is extremely unusual in Grahamstown, and this is, we believe, the first evidence of particle precipitation at these latitudes.

9.1.4 Discussion

Four main features of this event in the Southern Ocean region have been identified. These are :

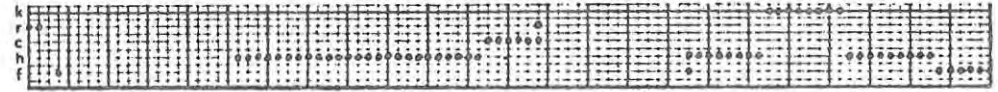
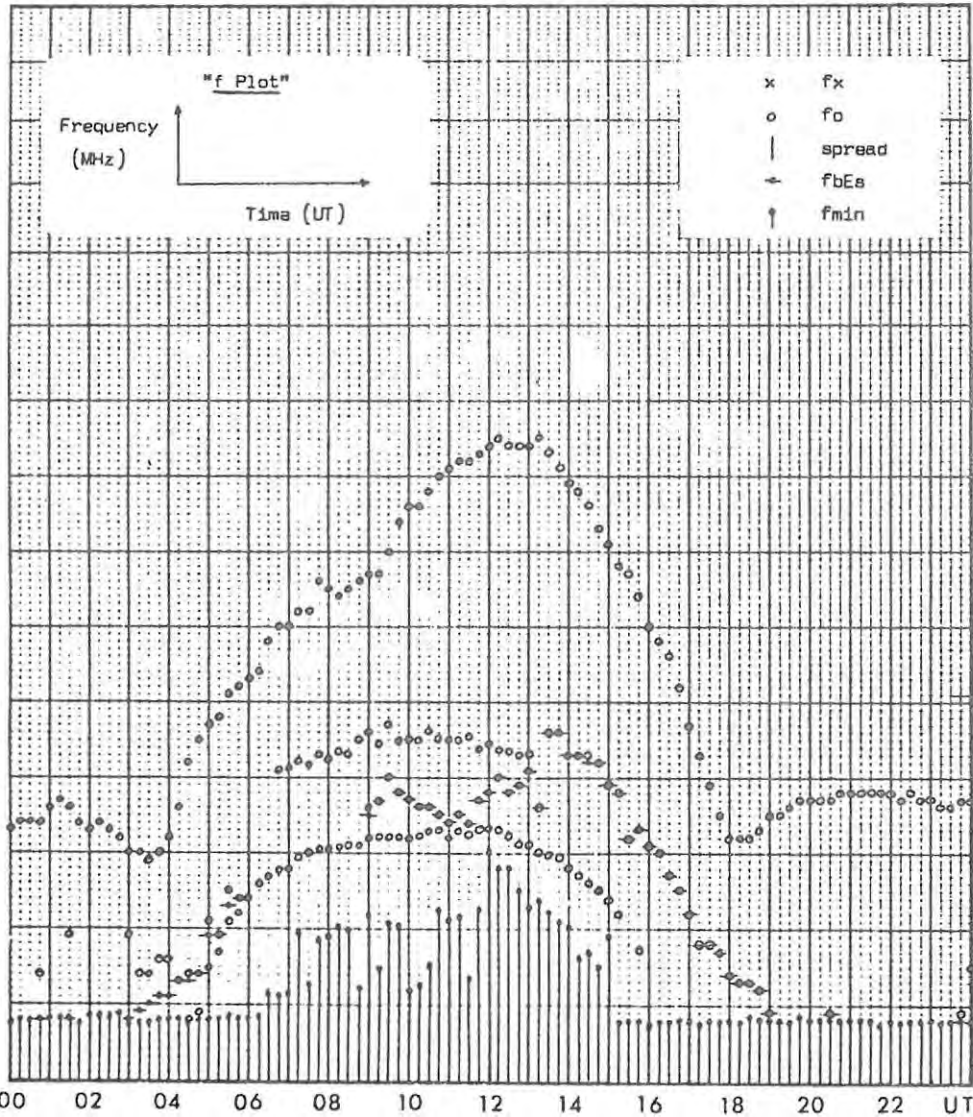
- (i) the apparent north-eastward propagation of a medium-scale TID with a velocity component of 200 ms^{-1} between 0200 and 0600 UT;
- (ii) the equatorward movement of the mid-latitude trough in response to intense magnetic activity to at least $L = 2.5$ ($\Lambda = 50.4^\circ\text{S}$, geographic latitude 42°S) as observed at 2025 UT;
- (iii) intense low energy particle precipitation between $L = 4$ and $L = 3.5$, possibly associated with the northward movement of the auroral oval;
- (iv) evidence of particle precipitation effects in the ionosphere as far north as Grahamstown.

Unfortunately, southern hemisphere precipitating electron data from the DMSP satellite (Chapter 8) were not available during this period (Kroehl *et al.*, 1977); those from the northern hemisphere were used (Kroehl and Henning, 1977) to identify and follow the equatorward boundary of the



GRAHAMSTOWN

25 MARCH 1976



GRAHAMSTOWN

26 MARCH 1976

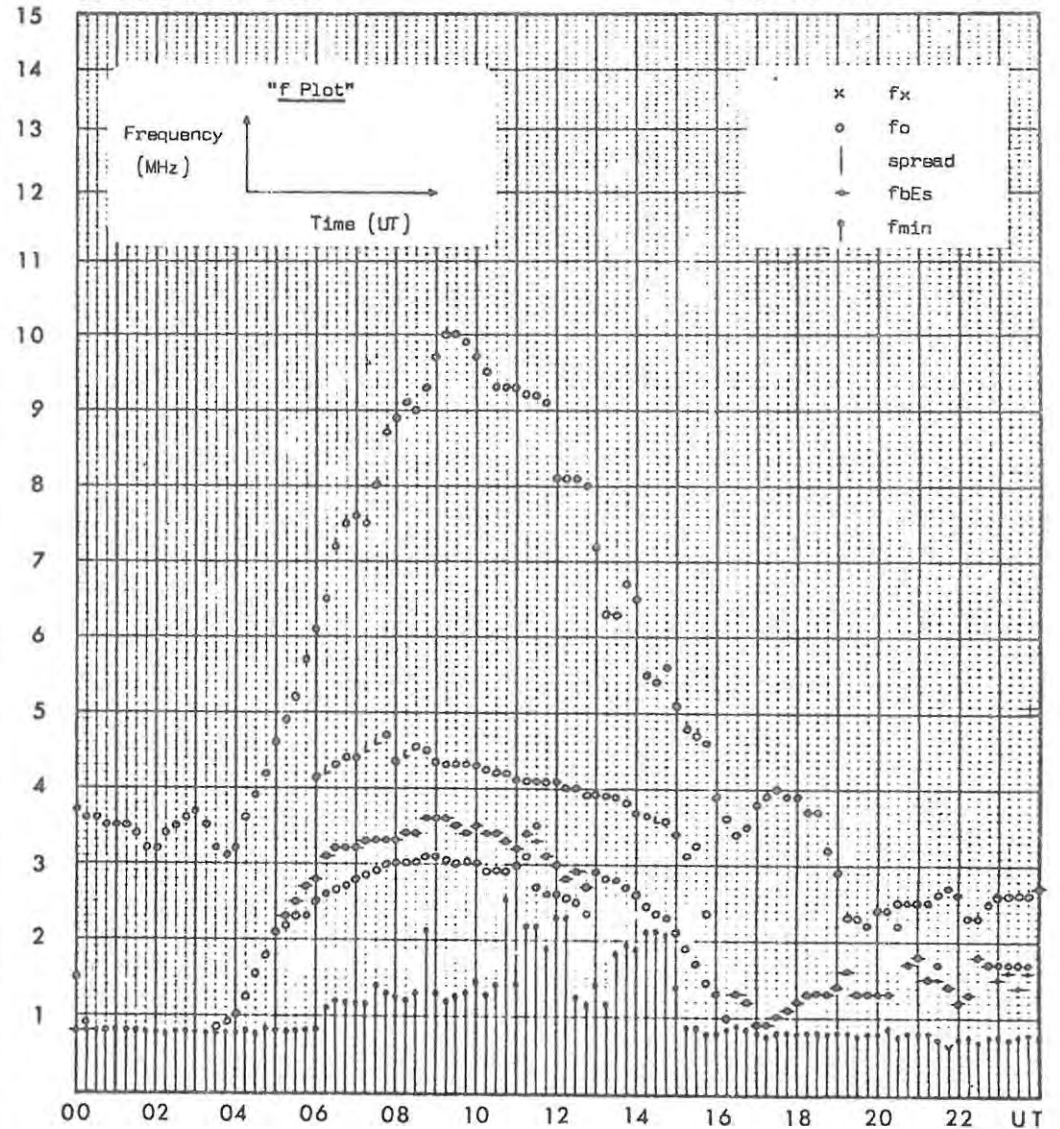


Figure 9.7 : f-plots for Grahamstown for 25 and 26 March 1976.

northern auroral oval. This reached the low corrected geomagnetic latitude of 53.2°N at 1436 UT. An analysis such as this, or that of Kamide and Winningham (1977), for the austral auroral oval would be extremely useful.

The above constitute merely some preliminary observations; an event of this magnitude clearly warrants further, more detailed, study.

9.2 The Events of 19 and 24 September 1977

These events were examined because of the interest shown in them by numerous workers; reports on data for the period 7 - 24 September and 22 November 1977 are to be published shortly in a UAG report, including a report by Gledhill *et al.* (1978) incorporating some of the results presented here.

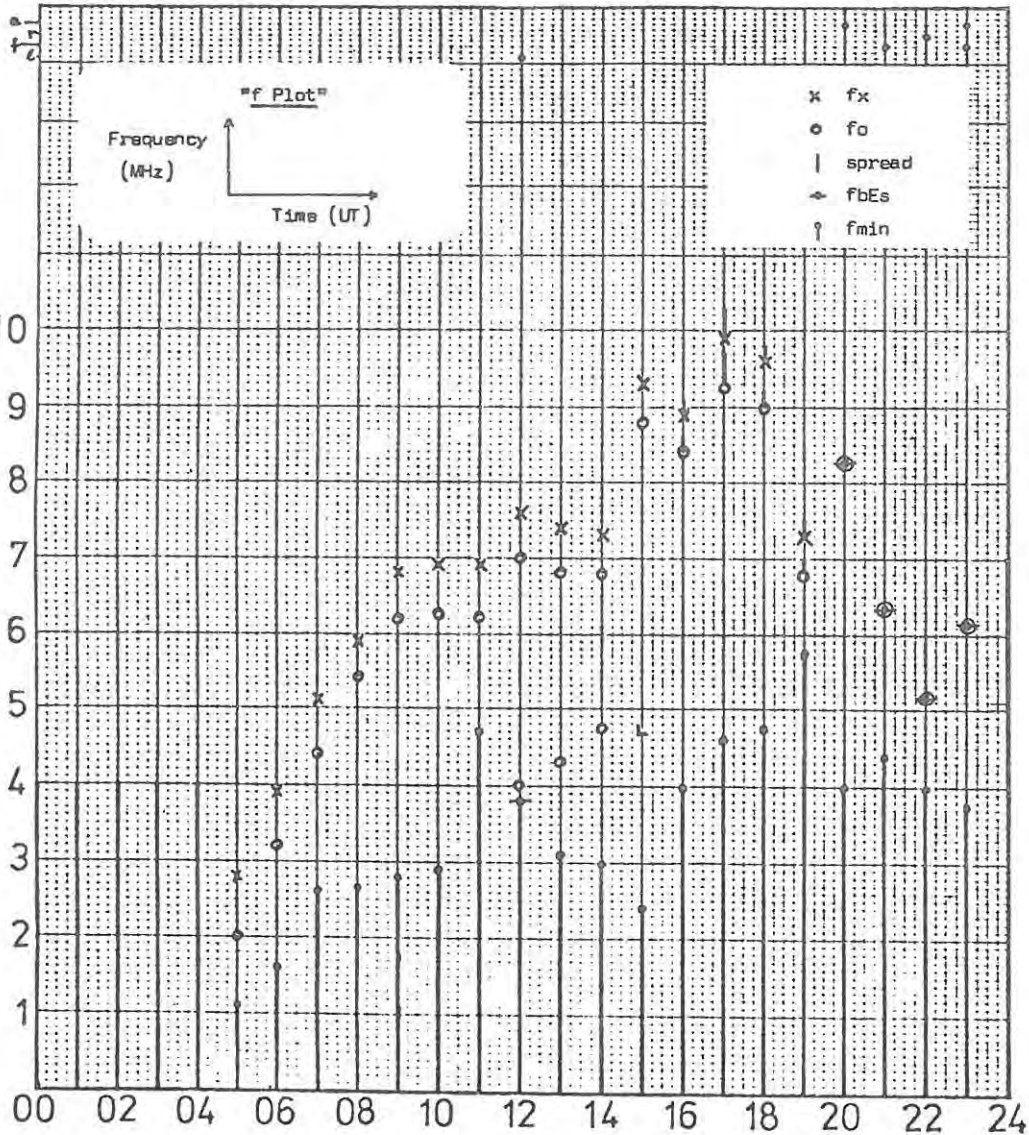
9.2.1 19 September

The hourly-value vertical incidence f-plots for SANAE and Grahamstown for 19 September 1977 are given in Figure 9.8. Both show high absorption ($f_{\text{min}} = 4.7$ MHz and B condition respectively) at 1100 UT, followed by appreciable F2 ionization enhancement between approximately 1500 and 2000 UT. f_oF_2 at SANAE reached a peak value of 9.25 MHz, with spread-F conditions, at 1700 UT; the monthly median and upper quartile values for this time in September 1977 are 5.4 and 5.6 MHz respectively. This represents a threefold increase in the peak electron density N_{max} above the median value (from 3.6×10^5 to $1.1 \times 10^6 \text{ cm}^{-3}$).

Absorption, as indicated by f_{min} , also increases considerably to peak at 5.75 MHz at 1900 UT (the monthly median value is 2.8 MHz). Blackout conditions occurred from 0000 to 2200 UT on the following day (20 September) and for most of the two days after that. Blanketing a- and r-type sporadic-E, with foEs reaching a maximum of 8.3 MHz at 2000 UT, probably due to auroral particle precipitation, occurred between 2000 and 2300 UT.

At Grahamstown the maximum value of f_oF_2 during the period of enhancement, 6.9 MHz, is attained at 1700 UT, the same time as the SANAE maximum, while f_{min} does not show any appreciable increase.

SANAE 19 SEPT 1977



GRAHAMSTOWN 19 SEPT 1977

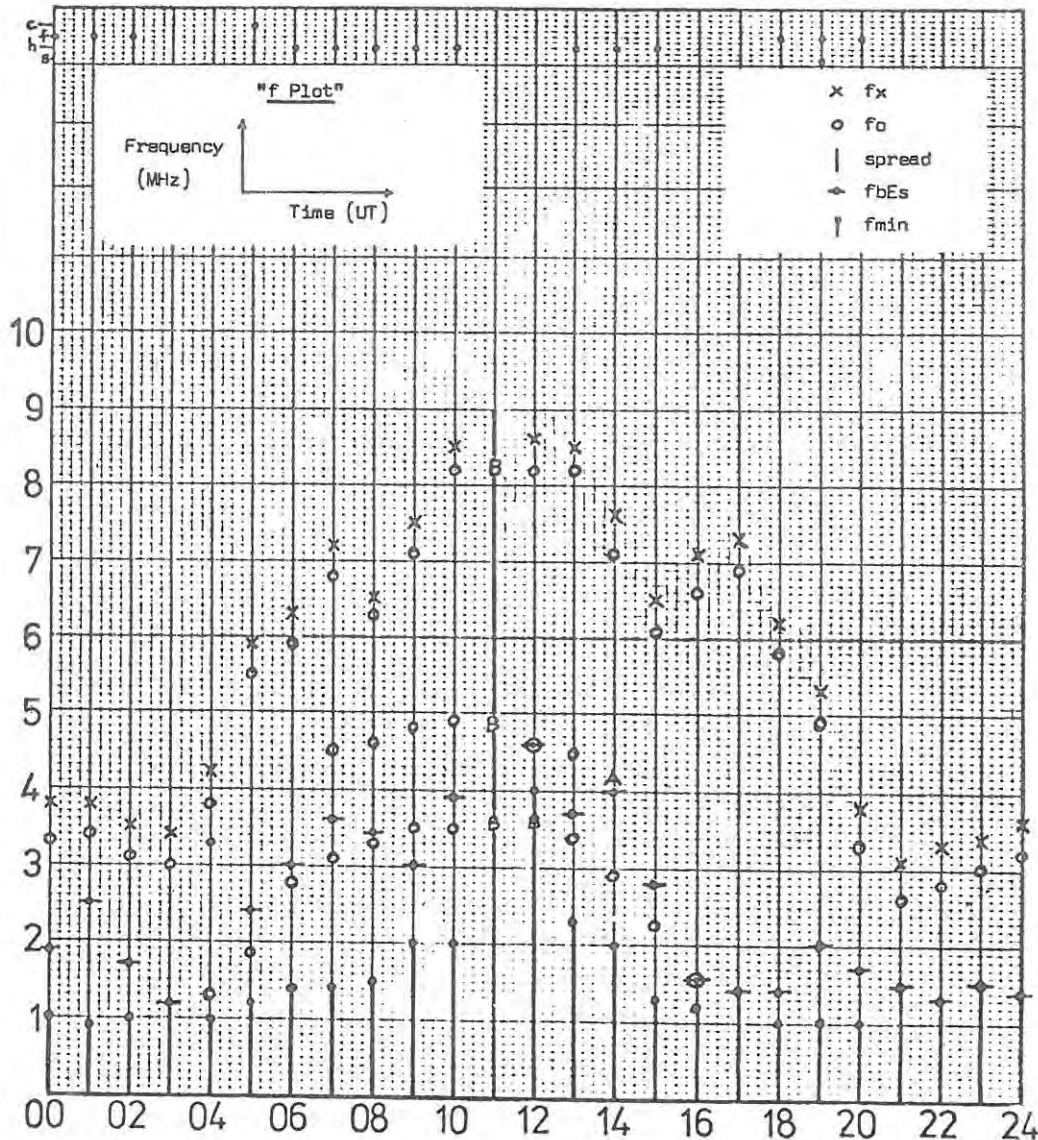


Figure 9.8 : f-plots for SANAE and Grahamstown for 19 September 1977.

The oblique "F-plot" of hourly values for 19 September is shown in Figure 9.9. The LOF, a measure of absorption, is high from 0900 UT onwards, with a maximum of 18 MHz at 1100 UT, when only the 2F mode is present. This coincides with the SANAE and Grahamstown absorption maxima. Both the 2F and 3F modes show the effects of F2 ionization and absorption enhancements similar to those observed at the end points, with maxima at approximately 1700 UT. The MOF (2F) value at 1800 UT is 21.5 MHz, compared with values of 9.2 and 10.8 MHz for the preceding two days.

Using data from the quarter-hourly records (not shown in the Figures), the onset of the enhancement appears to have occurred at approximately 1415 UT at SANAE, 1435 UT on the 2F mode, 1450 UT on the 3F mode, and 1530 UT at Grahamstown. If we interpret the increase in MOF (2F) as being due to an increase in F2-region ionization at the 2F first reflection point ("control point") (Table 2-3), and that of MOF (3F) as being due to a similar increase at the 3F second reflection point, then this onset can be interpreted as the front of a large-scale TID (Francis, 1975) propagating northwards from SANAE. (Such a front would of course enhance the ionization at the 3F first reflection point earlier than at the second but MOF (3F) could then be limited by the lower N_{\max} at the second reflection point, so that the increase in MOF could only be observed when the front reached the latter).

Using the times of onset given above and the appropriate distances from SANAE (Table 2-3), a velocity of 3600 km/hr or 1000 ms^{-1} (Figure 9.10) is obtained; this is equal to the upper limit of the range of velocities of large scale TID'S ($400 - 1000 \text{ ms}^{-1}$) given by Francis (1975). Such a gravity wave propagates equatorwards from the auroral region in response to auroral heating (Francis, 1975; Chiu, 1976). (If its direction were approximately perpendicular to the L contours (Figure 9.1), its actual velocity would be considerably less than the above figure).

After this onset the foF2's and MOF's increase rapidly to an initial maximum at 1515 UT at SANAE, at 1535 UT on both the 2F and 3F modes, and at 1545 UT at Grahamstown, with several minor fluctuations thereafter. (Sudden enhancements of foF2 at high latitudes have been described by Hill (1963)).

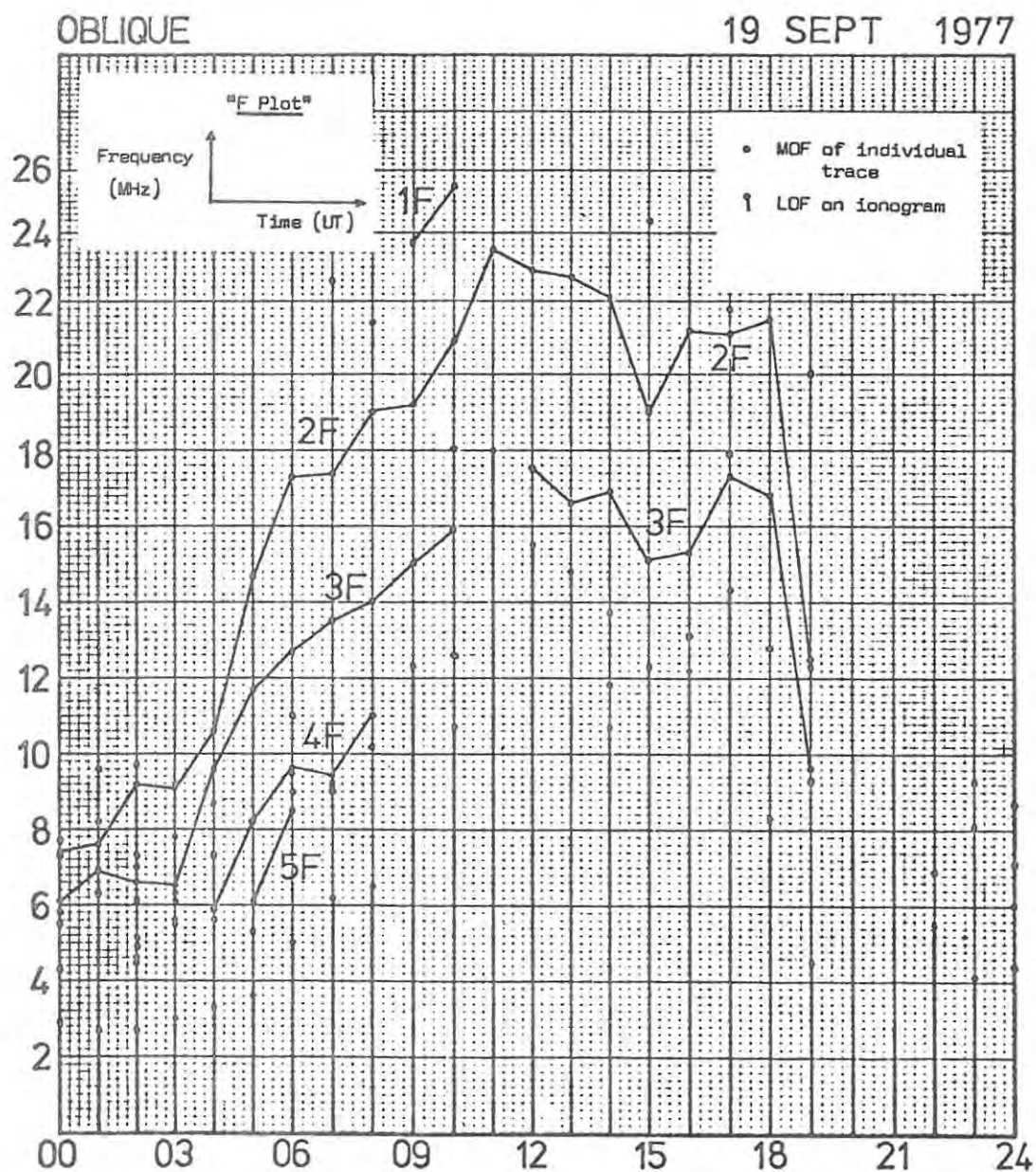


Figure 9.9 : Oblique frequency "F-plot" for 19 September 1977.

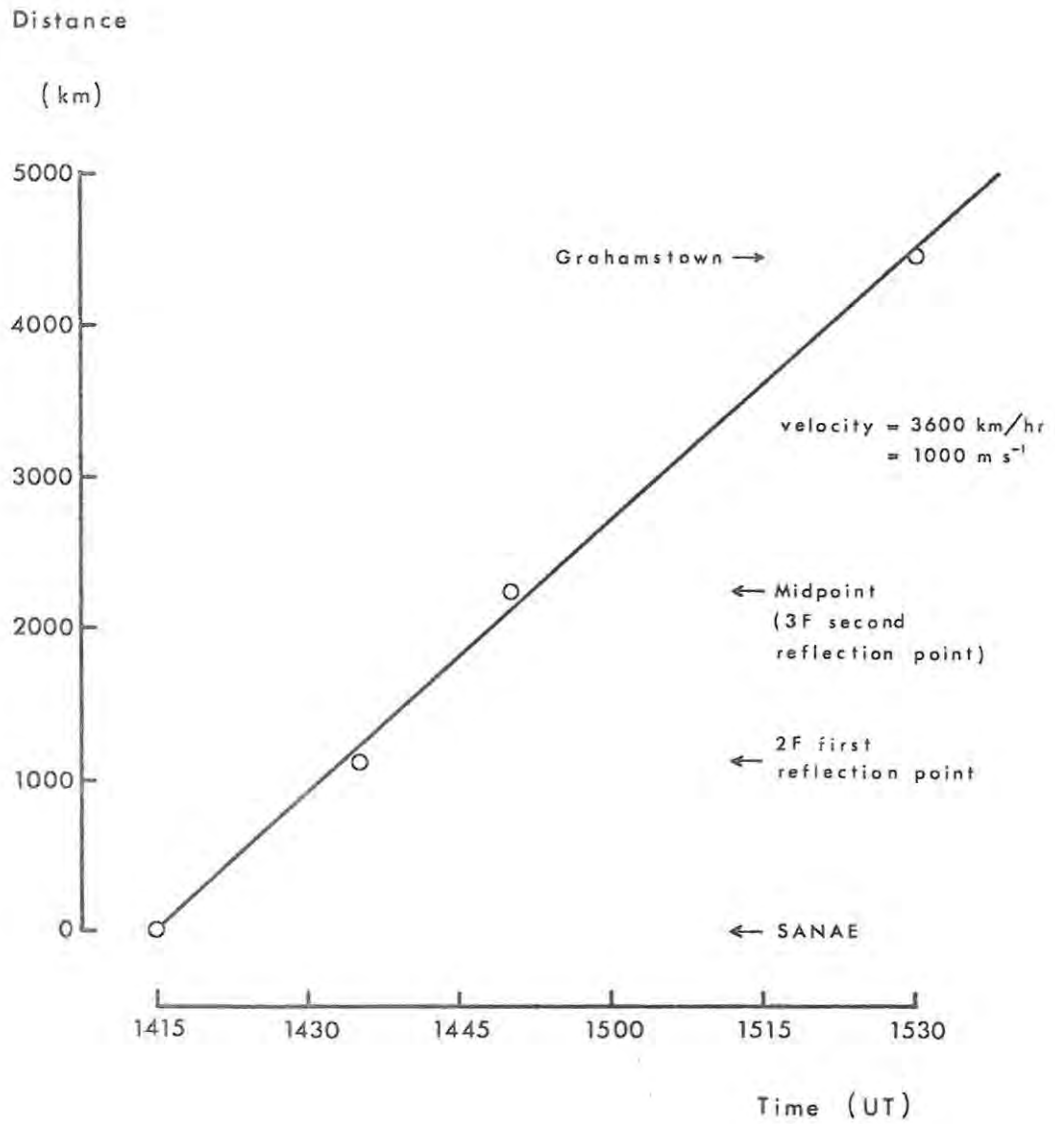


Figure 9.10 : Propagation of onset of ionization enhancement over the SANAE - Grahamstown path 19 September 1977.

9.2.2 24 September

The SANAE and Grahamstown hourly value f-plots for 24 September 1977 are shown in Figure 9.11. SANAE shows complete blackout from 0400 to 1200 UT. (The previous day, 23 September, showed fairly normal absorption, $f_{min} \sim 3$ MHz, after 3 days of almost total blackout following the event of 19 September.) f_{min} remains high, between 4 and 5 MHz, throughout the afternoon but falls to the low value of 1 MHz at 2100 UT. Blackout conditions return from 2200 UT. f_oF_2 , visible between 1300 and 2100 UT, is fairly normal; the values at 1300 - 1600 UT are within the monthly quartile ranges, while there is a slight enhancement, peaking at 1700 UT, followed by increased absorption at 1800 UT.

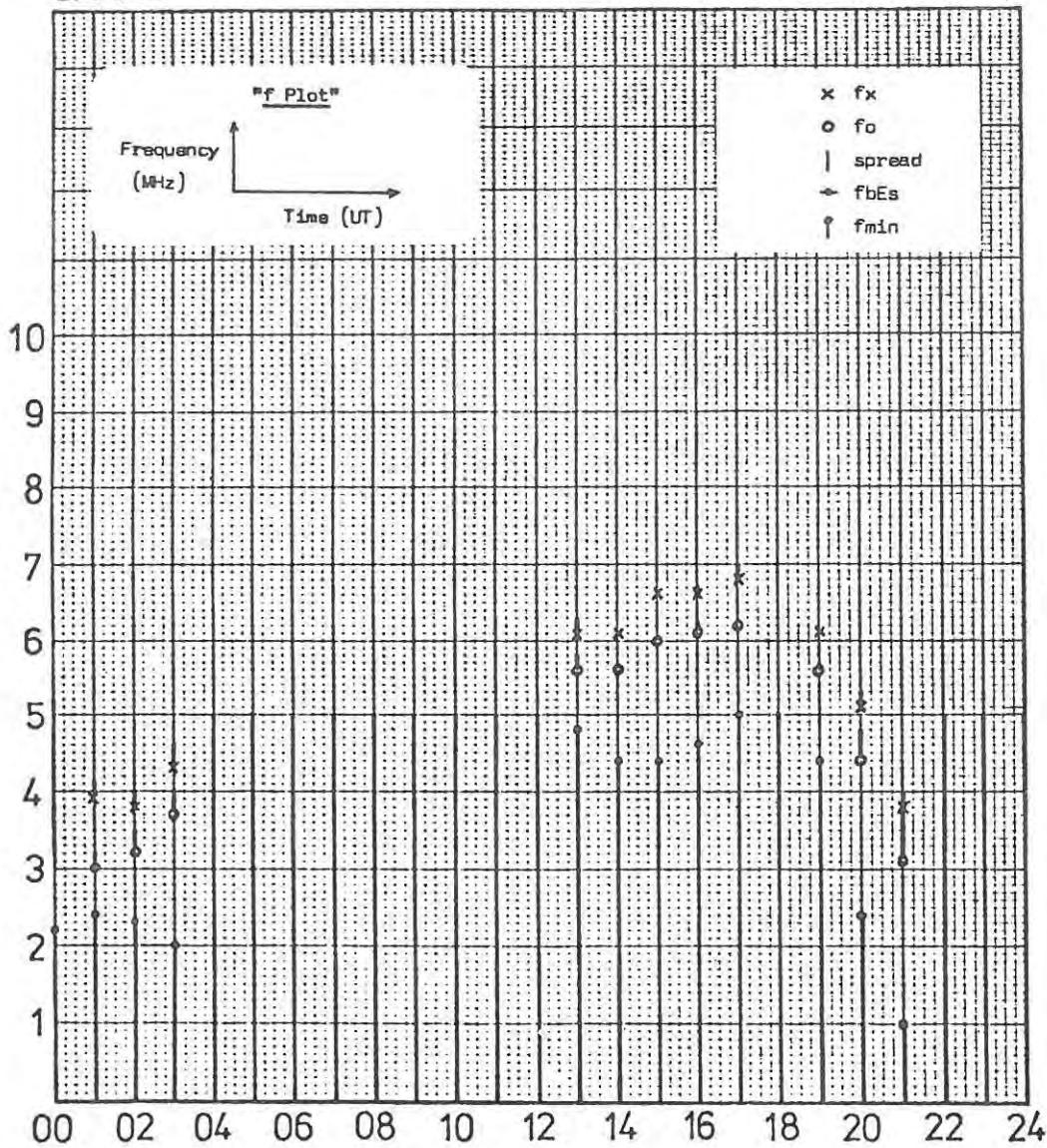
Grahamstown conditions are normal apart from a noticeable increase in f_{min} , from 2 to 3 MHz, at 1100 UT, and a depression of f_oF_2 at 1200 UT by about 1 MHz.

The oblique "F-plot", Figure 9.12, shows high absorption (high LOF or complete blackout) between 0500 and 1800 UT. When the 2F and 3F modes are visible around midday their MOF's are normal. After 1900 UT, however, the MOF's and LOF all fall to unusually low values, the LOF reaching 2MHz, the oblique sweep lower limit, at 2400 UT.

This event was clearly different from that of 19 September. It is a more typical absorption or PCA event (Davies, 1965); such events regularly cause complete blackout on both the SANAE vertical records and the oblique ones.

SANAE

24 SEPT 1977



GRAHAMSTOWN

24 SEPT 1977

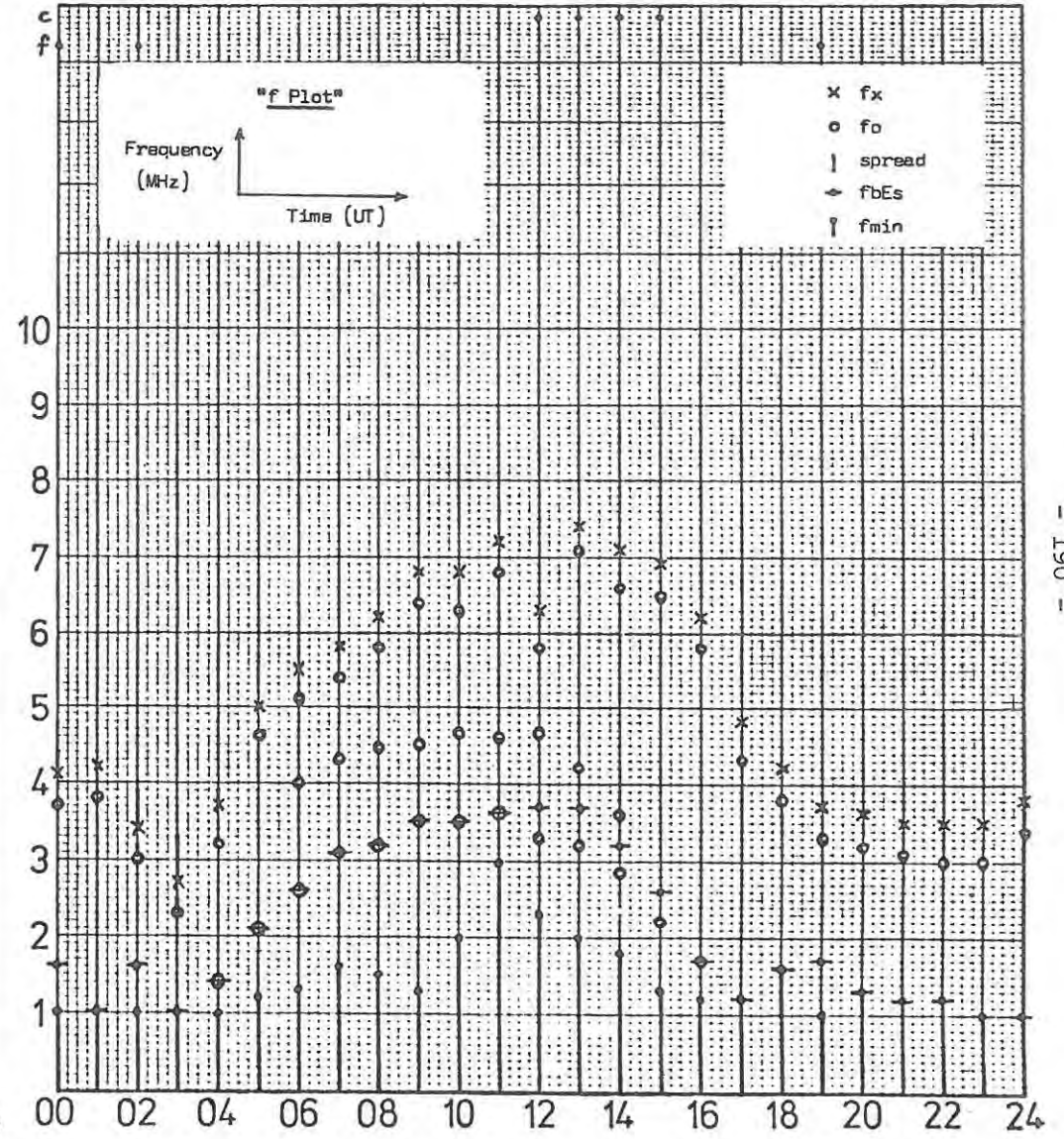


Figure 9.11 : f-plots for SANAE and Grahamstown for 24 September 1977.

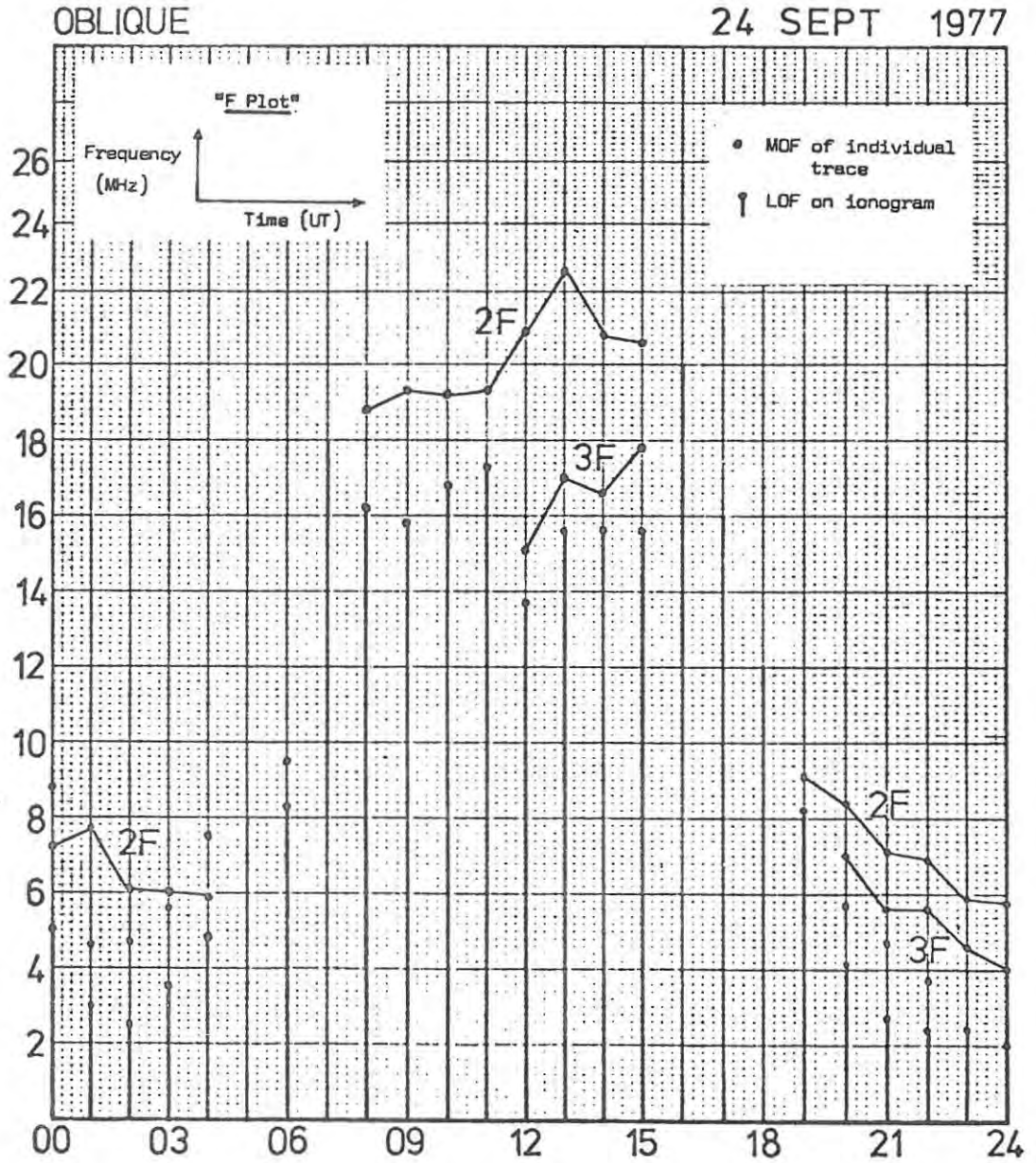


Figure 9.12 : Oblique frequency "F-plot" for 24 September 1977.

CHAPTER 10

CONCLUSIONS

10.1 Summary of Results

In any first 'overview' of this kind, some of the avenues of research opened up will prove more worthwhile following than others; likewise some of the topics examined in detail here have proved more fruitful than others. The following outlines some of the results so far obtained.

Problems of oblique ionogram interpretation, in particular mode identification, have been largely overcome and this interpretation is now believed to be reasonably reliable, although in individual cases it may be suspect.

The simple techniques of the equivalent vertical ionogram and the assumption of equal hops give surprisingly consistent results in routine scaling; the parameters EVFO and EVH'F appear to be consistent and fairly reliable, although the behaviour of the latter does appear to be puzzling at times. This is probably due to unreliable values of P' derived from the assumed offset.

Particularly with the development of the computer-assisted scaling techniques, the production of synoptic median oblique data has been shown to be viable and worthwhile. The data handling techniques developed have been proved to be adequate and reliable.

The solar minimum winter and summer monthly median data obtained show a number of features :

- (i) during the day the 2F, 3F and 4F modes are generally present in winter but only the 2F and 3F in summer, with a 1F high angle ray and other intermediate modes sometimes present;
- (ii) the diurnal variations of the MOF's and EVFO's follow the trend of foF2 at SANAE;
- (iii) while the variability in the values of a particular parameter at a particular hour of the day, as indicated by the range, is often large, the consistency of the data, as indicated by the quartile ranges, is generally good.

These median data and results from the R.S.A. 'great circle cruise' in February 1977 also established that in the quiet, untilted nighttime ionosphere the first reflection point, i.e. that nearer SANAE, of the 2F mode is the 'control point' limiting the MOF on that mode, on account of its smaller maximum electron density. In this case also, because the heights at which the electron density has a particular value are equal on the two hops, the assumption of an untilted ionosphere, and therefore of two equal hops, is apparently justified.

During the day the situation is more complex with tilts playing an important role. The effective longitudinal tilt should be 'downwards' from SANAE to Grahamstown; the first hop, on account of its greater reflection height, has a greater hop length. Some of the evidence does suggest, however, that the second hop may in this case be the control.

The derivation of N(h) profiles from oblique ionograms by 3 methods, the 'indirect method' (e.g. Gething, 1969) and the 'direct methods' of Smith (1970) and Rao (1973) has been shown to be a viable procedure with the 2F mode oblique ionograms obtained. The Rao method in particular has been shown by ray tracing to be remarkably accurate insofar as inversion to reproduce the original oblique ionogram is concerned, in spite of the assumption of a spherically stratified ionosphere, neglect of the earth's magnetic field and ignoring of underlying ionization.

The correlation analysis performed between oblique incidence parameters and low energy precipitating electron fluxes established a significant correlation between the LOF on an oblique ionogram and the integral flux. More detailed analysis showed the 'best' correlation to be with the flux in the lowest energy channel, in the 'area' where the oblique ray path was within the ionosphere, and for the satellite position furthest geomagnetic north from its crossing point with the SANAE - Grahamstown great circle. No physical explanation of this correlation has been forthcoming; the LOF is generally accepted to be determined by absorption in the D region, and F region absorption is considered negligible in comparison (e.g. Rush and Elkins, 1975).

The studies of individual ionospheric events, particularly with the aid of satellite observations, have proved promising, although only a preliminary analysis has been undertaken so far. The apparent detection of TID's or

atmospheric gravity waves from the oblique records, while not based on solid evidence, suggests that this would be a profitable avenue of further investigation.

10.2 Equipmental Improvements

While the Barry Research Chirpsounders have proved to be reliable instruments capable of adequately performing the routine observations required, several improvements and extensions to the equipment could be introduced.

In order to obtain more reliable group path measurements, better clocks, with improved timing stability, could be incorporated. The variation of clock rate of the quartz oscillators has proved erratic at times and the assumption of a linear drift rate over a period of a week is not always reliable. Otherwise, more frequent calibrations should be performed, particularly during periods when the drift rate is large or varying.

Because of the frequent loss of data due to high absorption or 'blackout' over the path, the present transmitter, with its output power of 8W, is considered to be inadequate. A transmitter with an output power of ~ 100 W, which is shortly to be installed at SANAE, will improve matters considerably.

During the current period of increasing solar activity the upper frequency limit of the oblique sweep, 28.56 Mhz, is often below the MOF of the least-delayed modes during the day. Thus the resetting of this limit to 30 MHz, or its possible increase above this value, should be investigated in order to reduce this loss of data.

Various improvements are scheduled to be implemented shortly in terms of the overall 'digitization project' under the supervision of A.W.V. Poole. While one of the aims of this project is the production, and scaling, of digital ionograms, this is clearly a very long term goal for oblique ionograms. However, the introduction of angle arrival measurements, as noted earlier, would be of considerable benefit in mode identification and the measurement of tilts. In addition, the envisaged greater flexibility of the system under microcomputer control should permit such possibilities as Doppler shift measurements and automatic calibrations, amongst others.

10.3 Future Work

A clear need now is the development of a reasonable data base of monthly median data, which should preferably not be based on the sometimes arbitrary identification of modes, but rather approached from a 'communications' viewpoint. Such a project is in fact proposed and should prove valuable for comparison with, and thereby possible improvement of, predictions, as well as being a foundation for other later work.

The data from the February 1978 'great circle cruise' of the R.S.A. could prove more useful than the 1977 data examined here in providing a picture of the variation of ionospheric parameters over the transmission path. In addition it might be possible to obtain ionograms satisfying the criteria listed in section 6.4 in order to resolve conclusively the model of the two-hop mode. The only better experiment for this purpose would require two shipborne ionosondes to be in the areas of the first and second reflection points simultaneously.

The determination of longitudinal ionospheric tilts is clearly an important matter over this path, and the possible use of angle of arrival measurements (Gething, 1978) could be investigated. The determination of N(h) profiles, etc. for different order modes on the same oblique ionogram, and such measurements as those of Mather *et al.*, (1965) also present possibilities in this regard.

Observation of TID's offers exciting prospects, particularly utilizing Doppler shift measurements. Bartning (1978) has recently published such observations using oblique group path and Doppler measurements. Considerations of phase path as discussed by Gething (1965, 1974, 1978) may prove useful in this regard.

The use of model profiles to correct for underlying ionization in 'oblique profiles', and the development of profile models from scaled oblique parameters, as discussed in section 7.3, also warrant further investigation. For the purposes of 'inverting' such profiles rapidly for checking with the original ionogram, it would probably be very useful to have available a simpler, more rapid ray tracing program than that used here, based, for instance, on Bouger's Rule (i.e. the inverse of the Rao (1973) oblique ionogram reduction process of Chapter 5).

Satellite observations of low energy particles at ionospheric heights over the South Atlantic - Southern Ocean area are becoming increasingly available and present further interesting possibilities for the study of F region phenomena and individual ionospheric 'events'.

APPENDIX A

THE MANUAL "USER'S GUIDE TO IONOGRAM SCALING
USING THE GRAF PEN DIGITIZER"

USER'S GUIDE
TO
IONOGRAM SCALING
USING THE
GRAF/PEN DIGITIZER

Authors : Jon Rash
and Errol de Kock

Department of Physics
Rhodes University

January 1978

CONTENTS

	Page
Setting up Ionogram Scaling Program	1
Terminating the Program	2
Scaling Vertical Ionograms	3
Scaling Oblique Ionograms	6
Filing and Listing Ionogram Data	9
Transmitting Files to MAXIMOP	10
Scaling Program Description Summary	12
Descriptions of Control Commands	15
Variable Names in the Scaling Program	17
The Scaling Program "IONO"	20
The Transmitting Program "MAXI"	31

FOREWORD

It is assumed that the user is already familiar with normal scaling procedures as described in reference (1). Details of the interfacing and original programs are in reference (2). Parameter names etc. for oblique scaling are to be found in reference (3).

It is hoped that the programs will remain identical from the user's point of view when the digitizer is transferred to the new 6800 system shortly, and that only instructions peculiar to the NOVA will have to be altered. All criticisms, suggestions and queries concerning the contents of this manual will be welcomed and should be directed to the undersigned in the first instance.

Jon Rash

REFERENCES

- (1) W.R. Piggott and K. Rawer (eds.), URSI Handbook of Ionogram Interpretation and Reduction, Second Edition, November 1972.
 - (2) E.J. de Kock, "Computer Assisted Ionogram Scaling", Honours Project, Department of Physics, Rhodes University, 1977.
 - (3) K. Davies, "Ionospheric Radio Propagation", NBS, Washington, 1965, Chapter 4.
-

USER INSTRUCTIONS FOR SETTING UP IONOGRAM SCALING PROGRAM

=====

If the NOVA is on and in DDOS, i.e. invitation to type on the VDU is ':', and the DISK DRIVE unit is on, first switch off (steps 3 - 5 on page 2).

1. Insert disk no. 43 into DISK DRIVE 0 (upper), and the disk on which the ionogram data are to be filed (e.g. no. 34 or 42) in DRIVE 1 (lower).
2. Switch on ENLARGER lamp and fan.
3. Switch on GRAF PEN control box.
4. Switch on MEMORY box (below DISK DRIVE unit) and DISPLAY unit.
5. VDU REMOTE switch up (switch at upper left of keyboard).
6. VDU POWER switch on (switch at back of VDU).
7. VDU REMOTE switch down.
8. NOVA POWER key on.
9. DISK DRIVE POWER switch on.
10. BOOTSTRAPPING procedure : perform the following switch sequence

on the NOVA front panel :

DATA SWITCHES (octal)	ACTION SWITCH
000376	EXAMINE
060120	DEPOSIT
000377	DEPOSIT NEXT
000376	RESET then START

The response on the VDU should be 3190 DDOS REV 2 77600 : (invitation to type)

11. Type OPEN(1)USER(1) to open the disk in DRIVE 1 for reading & writing.
12. Type MTB to load the version of BASIC used.
 The response should be DATE: MM-DD-YY } which the user can provide
 then TIME: HH:MM } or omit (press RETURN)
 then * (invitation to type)
13. Type ENTER"IONO" to load the ionogram scaling program.
14. Type RUN to commence operation of the program.

All subsequent normal user responses will be from the digitizer table.

The first response of the program should be (in inverse video mode)

START AT DAY ? TIME (& TIME INTERVAL) ? YEAR/PLACE ?

to which the user responds by digitizing the appropriate points ...

See NOTES on page 2.

USER INSTRUCTIONS FOR TERMINATING SCALING PROGRAM AND CLOSING DOWN THE SYSTEM
=====

1. At the end of a scaling session (normally when the data from the last ionogram have been filed), return from the scaling program to MTB by pressing ESC on the VDU.
2. Type HOME to return from MTB to DDOS
(The invitation to type should then be ':').
3. Switch off DISK DRIVE POWER.
4. Switch off VDU POWER.
5. Switch off NOVA POWER key.
6. Switch off MEMORY box (below DISK DRIVE) and DISPLAY unit.
7. Switch off GRAF PEN control box.
8. Switch off ENLARGER lamp and fan.
9. Remove disks from DISK DRIVE and replace in appropriate boxes!
10. Have a happy day !!

(NOTE : If you are leaving the NOVA on for someone else to use,
steps 3 - 8 may be omitted.)

- NOTES :
1. Each typed instruction (steps 11 - 14 on page 1 and step 2 on page 2) is ended by pressing the RETURN button.
 2. If the NOVA is on and 'bombs out' when entering MTB, see page 11.
 3. The disks are inserted label down, 'groove' towards the rear.
 4. The DATA SWITCHES on the NOVA, apart from the first digit, are in groups of 3 for each digit, the right hand switch of each group being "1", the middle "2", and the left "4"; up is on, down is zero for each. Thus e.g. the digit 3 is ↓↑↑ (0+2+1) and 6 is ↑↑↓ (4+2+0).
 5. If the user makes a typing error, pressing SHIFT and DEL (together) will erase the last typed character, and this can be repeated as far back as the incorrect one. In the DDOS system (steps 11 and 12) the character is repeated on the VDU screen; in the MTB system (steps 13 and 14) the cursor backspaces and wipes out the character.
-

USER INSTRUCTIONS FOR NORMAL SCALING OF VERTICAL IONOGRAMS
=====

1. The first prompt from the program after typing RUN is
START AT DAY ? TIME (& TIME INTERVAL) ? YEAR/PLACE ?
The user response to this is to
 - (i) digitize the day number of the first ionogram to be scaled, e.g. 115, using the numbers in column 2 of the control area, then the control block DAY in column 4. The program response is then
DAY NUMBER 115
 - (ii) digitize the time of the first ionogram, and if the time interval between ionograms is to be other than 60 minutes, this time interval as well. The time is digitized as HHMM e.g. 0600 using the numbers in column 2 of the control area, then if necessary the time interval in minutes* e.g. 15, then the control block TIME in column 4. The program response is then
TIME IS AT PRESENT 06:00
TIME INTERVAL IS 15
 - (iii) digitize the year and place code of the first ionogram as 2 numbers e.g. 76 (in column 2) and one letter* e.g. G (in column 1), then the control block YEAR/PLACE in column 4. The program response is then
YEAR IS 1976 PLACE IS G
1976 G DAY NUMBER 115 TIME 06:00
DEFINE AXES

- the ionogram i.d. information is now defined and the program prompts the user to define the axes of the first ionogram. If the place code is given as other than G, S or O the program requests the electron gyrofrequency, which the user types in on the VDU, and presses RETURN.
2. The user defines the axes by digitizing the 3 ionogram points*
(1 MHz, 1000 km) , (1MHz, 100 km) , (10 MHz, 100 km) in order, then the control block AXES in column 4 of the control area. The program response is
AXES DEFINED
3. The user then proceeds to scale the necessary parameters on the ionogram by digitizing first the point on the ionogram (e.g. the lowest frequency on the ionogram), then the appropriate parameter name in column 3 of the control area. Exceptions to this "one point, parameter name" rule are
 - (i) "MUF" which requires 3 ionogram points around the curve of the F2 trace;
 - (ii) "Es type" which requires one or more letters e.g. H from columns 1 or 2 of the control area;
 - (iii) "All values" which requires one letter e.g. B.
(The latter can be used without defining the axes.)

* For 'Minibal ionograms, see notes on page 5.

If any qualifying and descriptive letters are required, e.g. EB, these should be digitized (in column 1) after the ionogram point but before the parameter name block. One (descriptive letter only) or two (qualifying and descriptive) letters may be given.

If the qualifying letter J is digitized for a frequency parameter the program automatically subtracts half the electron gyrofrequency (ordinary ray frequency deduced from extraordinary).

If a parameter cannot be ascribed a value, i.e. the appropriate point is not visible on the ionogram because of e.g. absorption, the appropriate single replacement letter, e.g. B, is digitized, followed by the parameter name block.

The program prints out on the VDU the parameter name and value immediately the name block is digitized, e.g. FMIN 1.57 MHz (see PROGRAM DESCRIPTION SUMMARY for other examples). The order in which the parameters are scaled is arbitrary. Errors may be corrected using the RUBOUT and DELETE commands (see page 14).

If the table is bumped or the film moved at any stage during the scaling of an ionogram (after the axes have been defined), the user must digitize the RESTART command in column 4. The program will then print the day and time information again and prompt the user to define the axes (as for the END command except that the time is not incremented). The axes cannot be defined a second time unless a RESTART (same ionogram) or END (new ionogram) command is given.

4. After all the parameters for the ionogram have been scaled, the user digitizes the END command in column 4. The program then checks that the four parameters FOF2, H'F, FMIN and MUF have been scaled, and if any of them have not gives a warning message e.g. FMIN NOT SCALED, to which the user should respond by digitizing the appropriate points or simply digitizing END again if he/she is not worried about the missing parameter.

The program then gives the name of the data file in which the data from this ionogram are to be stored, e.g. FILED IN G76:115

and then lists the data in the form in which it is filed, e.g.

```

YR DAY TIME FOF2 H'F2 FOF1 H'F  FOF  H'E  FOF2 H'ES FBES FMIN  etc
G76 115 0600 039DR 273  293  214EA 207  103  036  125  022  103  etc

```

This takes a few seconds to print and write to disk so the user can utilize this time by winding on the film to the next ionogram to be scaled.

The program meanwhile prints out on the VDU the year, place, day and time of this new ionogram (using the time interval supplied or the default value of 60 minutes if this was omitted), and prompts the user to define the axes of this new ionogram, in our example

```

1976 G   DAY NUMBER 115   TIME 06:15
DEFINE AXES

```

5. The user then proceeds with steps 2 - 4 above for each ionogram to be scaled. When the last required ionogram has been scaled and ENDED, the user terminates the program and closes down the system as outlined on page 2.

ADDITIONAL NOTES FOR SCALING OF MINIBAL IONOGRAMS

1. If the time interval between ionograms is 5 minutes, this must be digitized as 05 (see 1(ii) page 3 and the TIME command page 15.)
 2. The place code letter R should be used for Minibal ionograms (see 1(iii) page 3 and the YEAR/PLACE command page 15.)
 3. To define the axes of the non-linear Minibal ionograms, the first two axes points defined are (1 MHz, 900 km) and (1 MHz, 100 km). Each of the frequency markers 2 MHz, 3 MHz, etc. along the 100 km height marker is then digitized in turn, followed by the top frequency of the ionogram (if this does not coincide with a frequency marker), and finally the AXES control block.
 4. If the height/frequency marker grid is 'wavy' or the required ionogram point does not digitize, the value of the parameter may be read off from the ionogram by eye and the value inserted using the numbers in column 2 (and possibly the letters in column 2) and then digitizing the required parameter name block in column 3. However note that for frequencies the value must be given in the format in which the data is filed. Thus e.g. a frequency of 4.3 MHz for FOF2 must be digitized as 043. All other frequency parameters except for FOF1, FOF and FMIN are given in this form, i.e. 3 digits in units of 0.1 MHz ; these three parameters are given as 3 digits in units of 0.01 MHz, e.g. a frequency of 1.35 MHz for FMIN must be digitized as 135. For heights the value in km is digitized e.g. 215. As for normal digitizing one or two letters may follow the parameter value; if one (descriptive letter only), the program will automatically insert a '-' for the qualifying letter.
-

USER INSTRUCTIONS FOR NORMAL SCALING OF OBLIQUE IONOGRAMS
=====

1. As for vertical ionograms, the first prompt from the program is
START AT DAY ? TIME (AND TIME INTERVAL) ? YEAR/PLACE ?
and the user response is to digitize the appropriate numbers and control
commands as in step 1 for the vertical case, except that the letter O
should be used for the place code in YEAR/PLACE. The program then prompts
OBLIQUE SCALING ? to which the user response should be to digitize the
OBLIQUE control block in column 4.

2. The program then prompts OBLIQUE SCALING INITIALIZATION
NEXT CALIBRATION DAY ?
and the user then types in on the VDU the day number of the next calibration
after the day number given in 1. The program then prompts
OFFSET AT 14:00 SAST ?
and after the value (in msec) has been typed in, the program first checks
that the day number and time of the calibration are greater than the day
and time given in 1. If not the message DAY/TIME CALIBRATION DAY/TIME
is output and the prompt NEXT CALIBRATION DAY ? is given again.
If the check is satisfied the output on the VDU is e.g.
OFFSET AT 14:00 ON DAY 210 IS 13.77 MSEC = 4131 KM
DRIFT RATE IN MSEC/WEEK ?
and after this value has been typed in, responds
DRIFT RATE IS - 0.31 MSEC/DAY = 93.86 KM/DAY
NUMBER OF TIMING SHIFTS ?
and the user then types in the number of timing adjustments made between
the starting day/time defined in 1 and the day/time of the calibration
defined above. If this number is greater than zero, for each shift the
program prompts e.g.
SHIFT 1 ON DAY ? then AT TIME ? then SHIFT ?
and when the required information has been typed in responds with e.g.
TIMING SHIFT ON DAY 207 AT 11:40 IS + 1.03 MSEC = + 309 KM
(N.B. the time is typed in as HHMM e.g. 1140 , and negative timing shifts,
i.e. those that advance the receiver clock, must be typed in as e.g. -0.96 ;
for positive timing shifts the + sign may be omitted.)
When this has been done for the number of shifts specified above, or if
this number is zero, the program then calculates the offset of the first
ionogram specified in 1, opens the appropriate file, and outputs on the VDU
1976 O DAY NUMBER 205 TIME 08:05 OFFSET 14.13 MSEC = 4239 KM
DEFINE AXES

- the ionogram i.d. information is now defined and the user is prompted to define the axes of the first ionogram.

3. The user defines the axes by digitizing the 3 ionogram points (3 MHz, 1000 km) , (3 MHz, 100 km) , (20 MHz, 100 km) in order, then the control block AXES. The program response is
AXES DEFINED
HOP/MODE OF FIRST TRACE ?
4. The user then defines the hop number (for normal multiple - F layer reflections) or mode (for other intermediate mode reflections) of the first trace to be scaled (the order of scaling is arbitrary). this is digitized as (i) for HOP, one number, e.g. 2, then the control block HOP (ii) for MODE, one or mode letters and/or numbers, e.g. M or 2F-E, then the control block MODE. The program response is e.g.

2F MODE or 2F+E MODE

and the user may now proceed with scaling the necessary parameters on that trace by digitizing the appropriate ionogram point, then the parameter name in column 3. Exceptions to this "one point - parameter name" rule are : (i) "EVFO" which requires 3 points from the high ray portion of the trace (only for multiple - F layer reflections, i.e. HOP traces) ; (ii) "S" which requires a number (column 2) between 1 and 5 signifying the user's estimate of the signal strength of the trace. Each parameter name and value is output on the VDU immediately the parameter name block is digitized; some examples are :

2F MODE
LLOF 9.5 MHz (lowest observed frequency on low ray)
MOF 15.2 MHz (maximum observed frequency)
EVFO 3.9 MHz (equivalent vertical critical frequency)
P' 4649 km (virtual path)
EVH' 237 km (this is computed by the program when P' is digitized)
S 3 (signal strength) etc...

As for the vertical case, any qualifying and descriptive letters required are digitized after the ionogram point but before the parameter name block, and if a single replacement letter is required, this is simply digitized (column 1) followed by the parameter name block. Again, mistakes may be corrected using the RUBOUT and DELETE commands. If the wrong mode has been digitized, digitizing DELETE then HOP or MODE will delete all the data for the current mode (this may be repeated for preceeding modes).

5. As in step 4 for the vertical case, when all the parameters for an ionogram have been scaled, the user digitizes the END command in column 4. The program response is as in the vertical case, e.g.

FILED IN 076:205 (the name of the file containing data for that day) followed by a list of all the data filed in the format in which it is filed, e.g.

YEAR	DAY	TIME	MODE	LLOF	MOF	JF	HLOF	EVFO	P'	EVH'	S	OFFSET
076	205	0805	2F	095	152	149UF	142	039-F	4649	237	3	4239
076	205	0805	2F+E	078	127				4691		1	4239

followed by the day/time information of the next ionogram and the prompt to define the axes of this new ionogram - in our example

1976 0 DAY NUMBER 205 TIME 08:20 OFFSET 14.13 MSEC = 4238 KM

DEFINE AXES

6. The user then proceeds with steps 3 - 5 above for each ionogram to be scaled. When the last required ionogram has been scaled and ENDED, the user terminates the program and closes down the system as outlined on page 2.



USER INSTRUCTIONS FOR FILING AND LISTING IONOGRAM DATA

1. The scaling program "ICNO" stores the ionogram data in files of the form e.g. G76:115, where G is the place code for Grahamstown, 76 is the year and 115 the day number. Thus a file contains all the data for one day and presupposes that the ionograms have been scaled in the correct order; if not, this can be corrected later. If the user stops scaling in the middle of a day and then starts up again where he/she left off, the new data will be appended onto the already existing data file.
The data will be written to such files on the disk in DISK DRIVE 1 (lower), assuming the user has specified OPEN(1)USER(1) at the start of the session, and the user should ensure that the correct disk has been inserted.
 2. Information concerning the files on the disk in DRIVE 1 may be obtained in the DDOS system (if in the MTB system type HOME) :
To check what files (i.e. what days' data) are on the disk, type FILES(I=0) (letter 'oh')
and a list will be output on the VDU (in the order in which the files were written), e.g. G76:098
G76:099
G76:100 etc.
To check the contents of a particular file (i.e. a particular day's data), type COPY(filename,\$TTO) (letter 'oh')
e.g. COPY(G76:100,\$TTO)
 3. A file or a series of consecutive data files may be transferred to a MAXIMQP subfile on the ICL by means of the program "MAXI" whose use is described on page 11. A number of such subfiles containing ionogram data may then be written to an Antarctic Research data file or magnetic tape using the FORTRAN program "FILE" (consult Jon Rash or Pete Mountfort for details).
 4. Points from an ionogram trace (vertical or oblique) as required for the determination of N(h) profiles may be filed as follows :
Specify the year/place, day and time of the ionogram by starting scaling at that day/time or by digitizing the appropriate DAY and TIME during a session. Define the axes in the usual way, and if oblique the HQP/MODE, then digitize the required number of points on the trace (up to 100). If the trace is the extraordinary ray, digitize the letter X (column 1); otherwise the trace is assumed to be the ordinary ray. Digitize the control block "h" and "f" (column 4). The coordinates of the points are then filed in a filename of the form e.g. G76:129:13:15H&F for the year 1976 at place G, day 129, time 13:15, and the data is listed on the VDU in the format in which it is filed.
-

USER INSTRUCTIONS FOR TRANSMITTING FILES TO MAXIMOP

NOTE : It is sometimes worthwhile to check that MAXIMOP is up before commencing this procedure !

1. Return to DDOS, i.e obtain a ':' invitation to type (if in MTB type HOME). Ensure that the system disk (no 43) is in DISK DRIVE 0 (upper) and the disk from which the required file(s) is/are to be read is in DRIVE 1 .
2. Type MIXBAS to load the version of BASIC used.
The response is (as for MTB) DATE: MM-DD-YY - press RETURN
then TIME: HH:MM - press RETURN
and MIXBAS then signs the user on and issues a '*' invitation to type.
3. Switch to HALF DUPLEX (switch at top left hand corner of keyboard).
Type RUN"MAXI" to load and commence operation of the program.
4. The following prompts are issued by the program
JOBNUMBER (provide your user code, e.g. CODE)
PASSWORD (provide your job password, e.g. PASS)
FILENAME CODEMAXIMOP (Y OR N) (answer Y or N for 'yes' or 'no' ;
if N the program asks WHAT THEN ?)
MAXIMOP SUBFILE NAME (provide name of MAXIMOP subfile, e.g. JUNK)
ICONOGRAM DATA FILES (Y OR N) (answer Y or N for 'yes' or 'no')
If the answer to this question is 'yes', the program prompts
FIRST DATA FILE (provide name of first file to be read, e.g. G76:060)
LAST DATA FILE (provide name of last file to be read, e.g. G76:071)
(N.B. All these files must exist and be on the disk in DRIVE 1 !)
If the answer is 'no' the program prompts
DISK FILE (provide name of file to be read, e.g. GUNK:02)
MAXIMOP SUBFILE HEADER (provide heading or simply press RETURN)
5. The program then logs in to MAXIMOP and displays JPNI— etc. (one '-' for each 'line' transferred, then, when the input is complete,
CONNECTED FOR X MINUTES etc. (you have now been logged out of MAXIMOP).
The program automatically FASTLISTs the subfile input.
Press CONTROL Q to terminate the program and return to MIXBAS.
To transfer a second file or series of files, type RUN and proceed from step 4.
6. To return to DDOS, type HOME (obtain a ':' invitation to type)
and switch back to FULL DUPLEX.

- NOTES :
1. Each typed instruction is ended by pressing the RETURN button.
 2. Typing errors are deleted by pressing CONTROL A (not SHIFT DEL).
 3. To abort the program press CONTROL Q (not ESC), then type CLOSE.
 4. It is usually worthwhile after ending a transmission and returning to DDOS, before proceeding further to type BOOT to re-bootstrap the NOVA, then OPEN(1)USER(1) to open the disk in DRIVE 1 for reading and writing.
 5. If, when logging in to MIXBAS during the above procedure, or at any other stage of the proceedings, the system goes 'dead', follow the 'bombout' procedure described below.
 6. To transmit the contents of a paper tape, switch on the paper tape reader, load the tape from the right hand side (sprocket holes towards the rear) and follow the procedure on the previous page, except that \$PTR must be used for the DISK FILE name.
-

'BOMBOUT' PROCEDURE

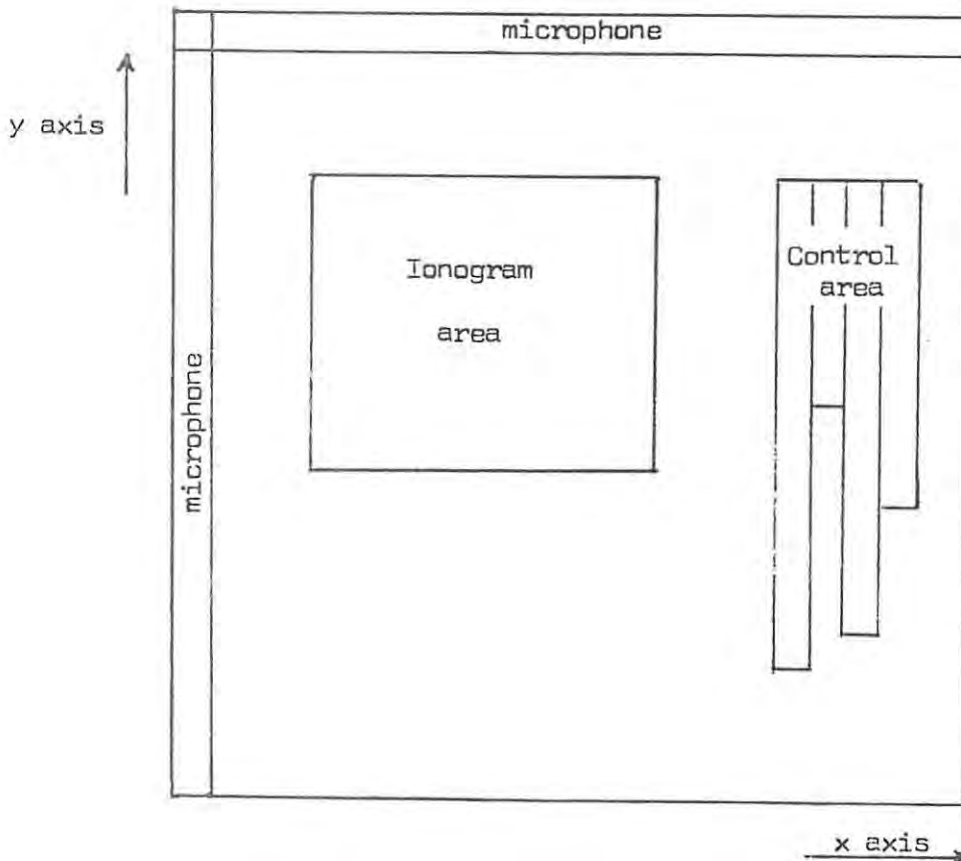
1. Press STOP switch on NOVA front panel.
 2. Switch on WRITE PROTECT switches on DISK DRIVES.
 3. Set DATA SWITCHES on NOVA front panel to 000002 (octal).
 4. Press RESET then START switches on NOVA front panel.
 5. Switch off WRITE PROTECT switches on DISK DRIVES.
 6. The prompt on the VDU should be DATE: MM-DD-YY to which the user response should be to press the RETURN button and proceed with the normal logging in to BASIC (MIXBAS or MTB).
 7. If there is no response on the VDU, it will be necessary to switch off the machine, switch on again and re-bootstrap. (See pages 2 and 1 resp.)
-

PROGRAM DESCRIPTION SUMMARY

The program to handle the data obtained from the digitizer has been written in MULTEX BASIC and has been designed in such a way as to give the scaler as many options as possible, but with as many of these defaulted as possible. This means that the system is versatile and yet not unduly difficult or complicated to use. Throughout the program, the procedure usually adopted in the scaling of ionograms has been borne in mind, although the program is versatile enough to be used in a way that differs from this.

A short description of some of the more complicated parts of the program will be given, in addition to the general description of operation of the system. A full listing of the program is given in the Appendix.

In order to make the system more convenient to use, certain areas of the digitizing table have been set aside as control blocks. These include alphabetic letters, numbers, the parameter names used in the scaling, and control names for controlling the program and requesting various options. In addition to the control area, an area has been set aside for the projection of ionograms. This means that the person scaling the ionograms never has to leave the digitizing table and yet has complete control of the program. A diagram of the layout of the digitizing table is given below :



The program has been designed to give as much feedback as possible to the scaler. For this purpose, use has been made of the VDU and the X-Y Display Unit. Messages are output to the terminal to prompt, remind or warn the scaler as the case may be. For the scaler's information the program also prints the values of the scaled parameters as they are scaled. The scaled points from the ionogram are displayed on the X-Y Display with the latest point marked with the cursor. The scaler is thus provided with a reasonable checking capability.

A typical output on the VDU may be as follows :

```
START AT DAY ? TIME (& TIME INTERVAL) ? YEAR/PLACE ?
DAY NUMBER 123                                after DAY command
TIME IS AT PRESENT 12:00
TIME INTERVAL IS 60                           after TIME command
YEAR IS 1975 PLACE IS G
1975 G DAY NUMBER 123 TIME 12:00
DEFINE AXES                                    after YEAR/PLACE command
AXES DEFINED                                  after AXES command
FMIN 1.48 MHz                                  after FMIN command
H1E 110 km                                    after H1E command
FOE 2.57 MHz                                  after FOE command
H1F 312 km                                    after H1F command
FOF1 3.30 UR MHz                              after FOF1 command
H1F2 442 km                                   after H1F2 command
FOF2 5.27 MHz                                 after FOF2 command
FILED IN G75:123
G75 123 1200 053 442 330UR 312 257 110        148
1975 G DAY NUMBER 123 TIME 13:00
DEFINE AXES                                    after END command
```

The comments on the right do not appear on the screen but are given to indicate what was done to obtain the response given on the left. The response for the other commands not included above is very similar and should be self explanatory. All error messages, which likewise should be self explanatory, as well as some of the more important prompts are preceded by a bell on the VDU. The last two lines indicated above are output every time an END or RESTART command is given.

Points from the Ionogram area and Control area are called Ionogram points and Control points respectively. On receiving the coordinates of a point, the program determines whether the point lies within either of these areas, and if not an error message is output to the VDU. In the case of an Ionogram point a matrix conversion of the coordinates is performed to produce the actual ionogram coordinates. These coordinates are then loaded into the storage buffer. If the point is a Control point, two control numbers I and J are found according to the position in the Control area. The values of I and J corresponding to the various positions are given in the table below :

J \ I	1	2	3	4
1	A	0	foF2	RUBOUT
2	B	1	h'F2	DELETE
3	C	2	foF1	RESTART
4	D	3	h'F	DOMAIN
5	E	4	foE	DISPLAY
6	F	5	h'E	h' and f
7	G	6	foEs	DAY
8	H	7	h'Es	TIME
9	I	8	fbEs	YEAR/PLACE
10	J	9	fmin	AXES
11	K	-	MUF	END
12	L	+	fxI	OBLIQUE
13	M	.	Es type	HQP
14	N		All values	MODE
15	C		LLOF	
16	P		MOF	
17	Q		JF	
18	R		HLOF	
19	S		EVfo	
20	T		P'	
21	U		S	
22	V			
23	W			
24	X			
25	Y			
26	Z			

DESCRIPTIONS OF CONTROL COMMANDS

The general operation of the system is Reverse Polish ; that is, any data relating to a command must be digitized before the command is digitized. The only commands that do not require any data at all are DISPLAY and OBLIQUE as these commands change the mode of operation. The effects of the various control commands and the data required by them are given below :

RUBOUT

The effect of this command is to erase the previous entry (ionogram point). The command does not require any specific data and can be used repeatedly. It is not possible to RUBOUT any entries once a command requiring the entries as data has been given. This command is thus used when the user realizes before digitizing the parameter name block or control block that he/she has digitized the wrong ionogram point or letter etc.

DELETE

This command can be used to erase the last parameter (name and value). It is thus used when the user realizes after digitizing the parameter name block or control block that the wrong ionogram point/letter and/or parameter name block has been digitized. The user digitizes DELETE followed by the parameter name he/she wishes to delete (not necessarily the last one scaled), e.g. FBES, and the command may be used repeatedly in this manner.

RESTART

The effect of this command is to erase all the previous entries (parameter names and data) up to the last END command ; that is all the entries referring to the present ionogram. Again no specific data are required. This command cannot be used repeatedly. It is used for instance when the film or table are moved after the axes of an ionogram have been defined.

DOMAIN

The effect of this command is to set up a matrix that will be used to determine more accurately the coordinates of a point within a smaller region of the ionogram. The data required is 3 points surrounding the region within which the point is required. The points must lie on the intersection of a frequency and a height marker and must form a right-angled triangle. The order in which the points are digitized is not important.

DISPLAY

This command can be used to enter the display mode and will allow the ionogram to be traced out with the pen, displaying the ionogram on the X-Y Display as this is done. To return to normal operation the DISPLAY command is digitized again.

hⁿ and f

The purpose of this command is to allow samples of ionogram points to be taken, e.g. to use as data to compute an N(h) profile, and to store the data in a separate file. The data required is a number of ionogram points,

followed by a single letter, O or X, to denote the ordinary or extraordinary mode. This letter can be omitted, in which case O is assumed by default. On giving the command the program lists the data in columns of f and h' on the VDU and files them in a file with a name of the form e.g. S77:289:14:15HGf.

DAY

The data required by this command is up to 3 numbers which will be interpreted as the day number of the ionogram.

TIME

The data required is 4 numbers that will be interpreted as the time of the ionogram in HHMM. An extra 2 numbers are optionally allowed and if included will be interpreted as the time interval between successive ionograms in minutes. This interval is set to 60 minutes by default.

YEAR/PLACE

This command is used to specify the year and place of the first ionogram to be scaled (or of course if these are changed during a scaling session). The data required is 2 numbers (tens and units of the year) and a letter (place code).

AXES

This command is used to define the axes of an ionogram. The data required is 3 specific ionogram points in a specific order. These points are for vertical ionograms (1 MHz, 1000 km) , (1 MHz, 100 km) , (10 MHz, 100 km) for oblique ionograms (3 MHz, 1000 km) , (3 MHz, 100 km) , (20 MHz, 100 km)

END

This command is used to indicate to the program that all the data for the present ionogram has been digitized. The program files the data and increments the time by the time interval that is currently set and outputs the day/time (and offset for oblique) of the next ionogram to be scaled.

OBLIQUE

This command initializes (on first call) or terminates (on second call) the scaling of oblique ionograms. It sets the oblique scaling flag and redefines the frequency axis. No data is required.

HOP

This requires as data one number. It will normally be used to denote a particular trace on an oblique ionogram which is a normal multiple - F layer reflection mode, e.g. 2 HOP. It must be specified before any data relating to that trace are digitized.

MODE

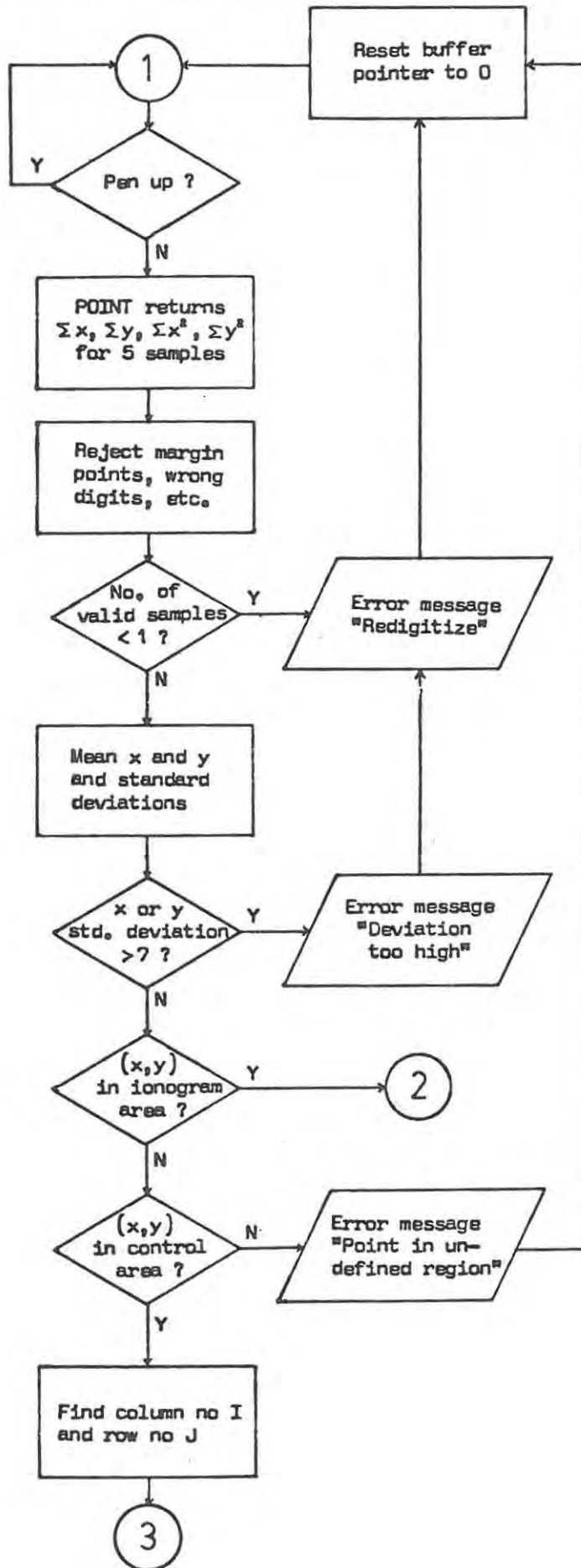
This command is similar to HOP but is used to denote intermediate modes on an oblique ionogram other than multiple - F layer reflections, such as e.g. M or M modes, or more specifically e.g. 2F+E. The data required is one or more letters and/or numbers.

APPENDIX B

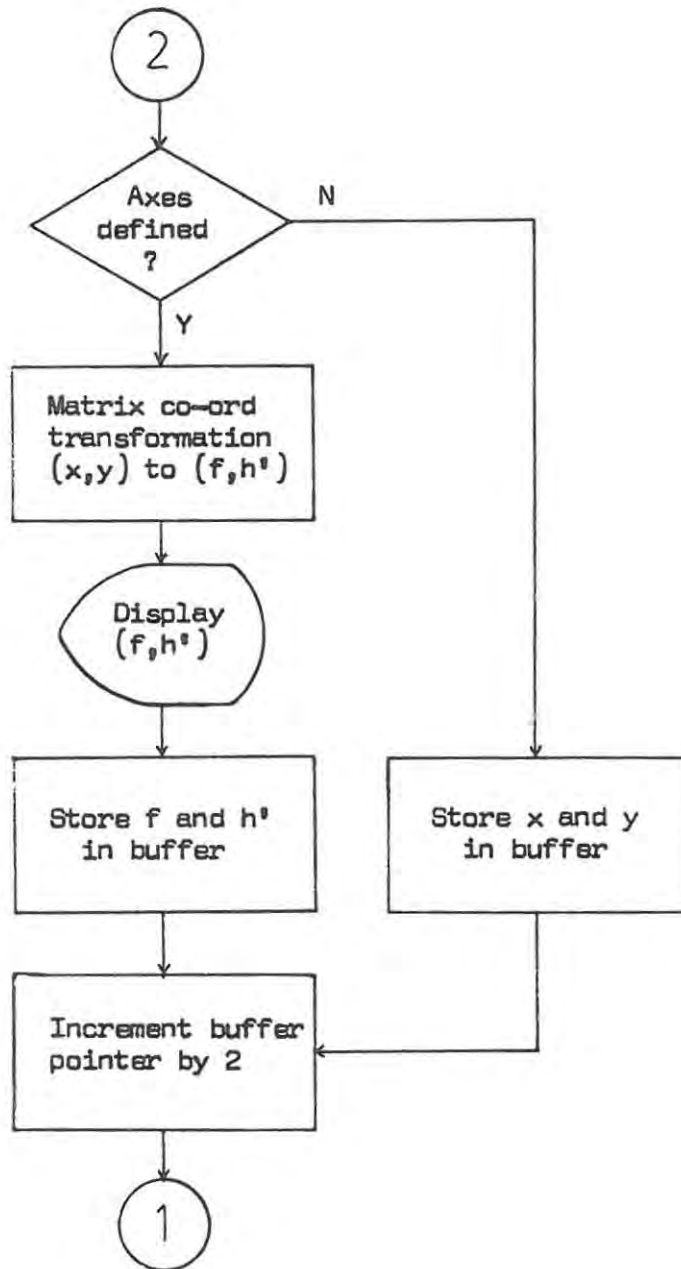
THE IONOGRAM SCALING PROGRAM "IONO"

1. Flowcharts.
2. List of variable names.
3. Listing.

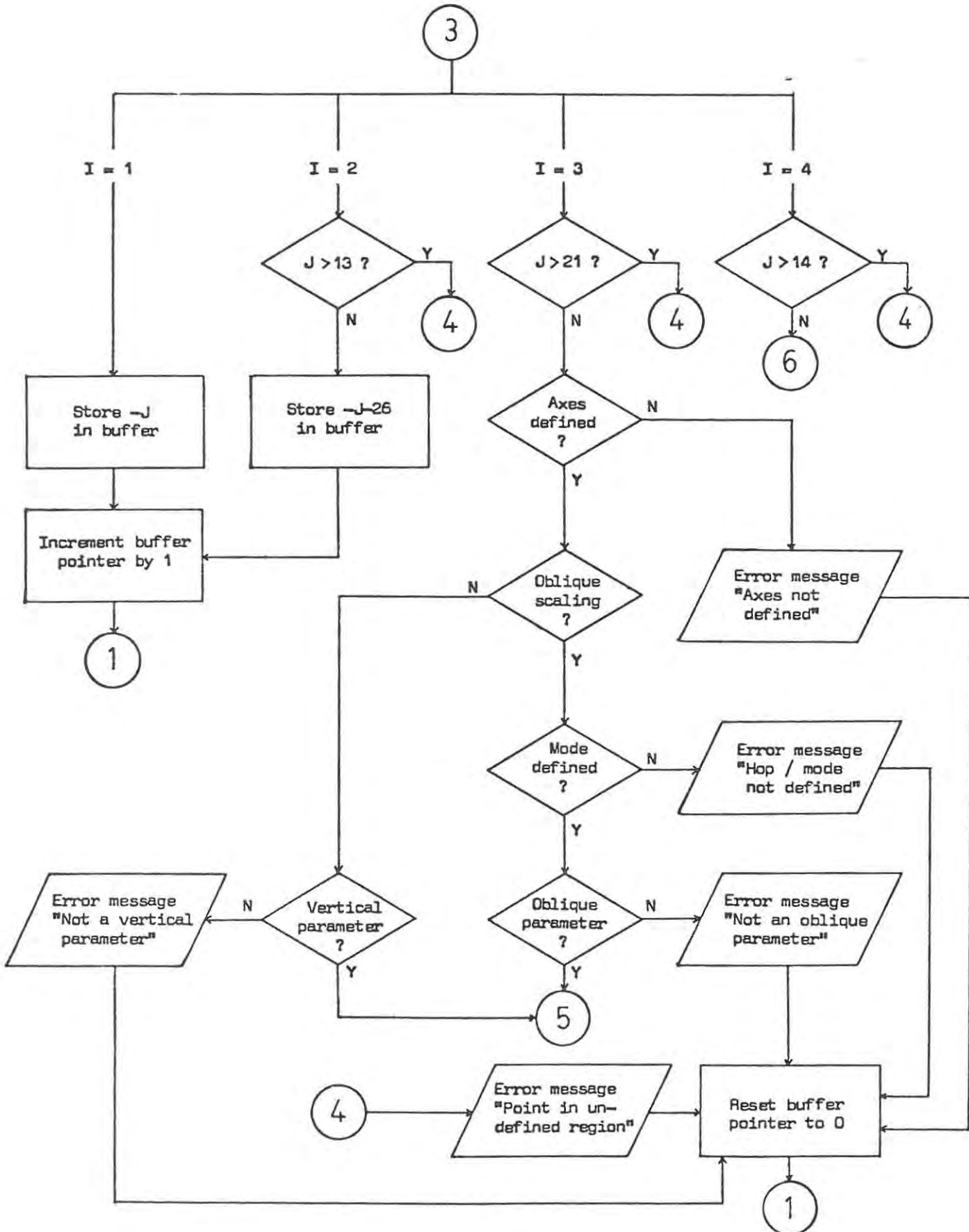
Flowchart 1 : Main program "DIGITIZE A POINT"



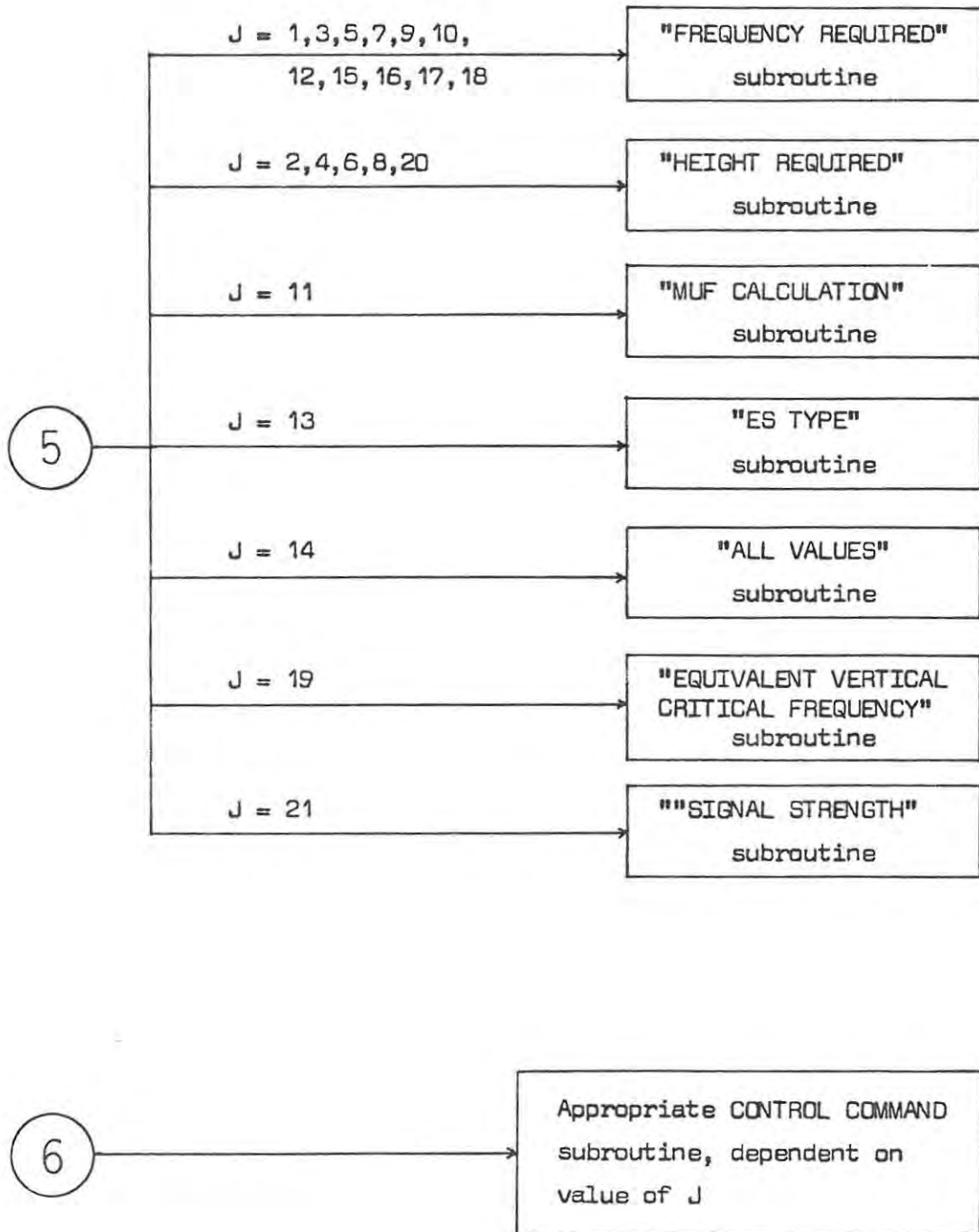
Flowchart 2 : "IONOGRAM POINT" subroutine



Flowchart 3 : "QUALIFYING LETTER (I=1)", "NUMBER (I=2)",
"SCALED PARAMETER (I=3)" and "CONTROL COMMAND (I=4)"
subroutines



Flowchart 4 : Scaled Parameter and Control Command subroutines



VARIABLE NAMES USED IN THE IONOGRAM SCALING PROGRAM

A Value of a parameter (frequency or height)
A1\$ Array containing A as a string
A2 Matrix A in ionogram coordinate transformation
A3 Matrix A2 in domain coordinate transformation
B Initial storage buffer
B1\$ Final storage buffer
B2 Matrix B in ionogram coordinate transformation
B3 Matrix B2 in domain coordinate transformation
C Matrix C in ionogram coordinate transformation
C1 Inverse of matrix C
C2 Matrix A1 in ionogram coordinate transformation
C3 Matrix A2 in ionogram coordinate transformation
C4 Matrix in domain coordinate transformation
C5 - ditto - ; array of frequencies in MUF calculation
C6 - ditto - ; array of heights in MUF calculation
C7 - ditto -
C8 - ditto -
C9 - ditto -
D Day number of ionogram
D\$ Day number of ionogram as a string
D1 Display buffer counter
D2 Domain set flag
D3 Day number of calibration
D4 Day number of timing shift
E Error word on return from POINT
F Matrix of frequencies of axes points
F1 Matrix $A2 \times X3$ in ionogram coordinate transformation
F1\$ String array containing the parameter names
F2 Matrix $F1 + B2$ in ionogram coordinate transformation
F3 Matrix in domain coordinate transformation
F4 - ditto -
F5 Array in frequency scale conversion for 'Minibal' ionograms
G Electron gyrofrequency
H Matrix of heights of axes points
H0 Offset on oblique ionogram
I Control number (column)
I0 Double RUBOUT flag
I1 Axes not defined flag
I2 Initialization flag

VARIABLE NAMES (continued)

I3 Oblique initialization flag
I4 Oblique scaling flag
I5 Hop/mode not defined flag
I6 Array of flags for foF2, h'F, fmin & MUF defined
J Control number (row)
K Pointer in buffer B, points to next place to load
L Number of valid data points
L1 Mode counter for oblique ionograms
M No. of samples containing margin points ; max h' in MUF calculation
M\$ Array containing letters and numbers etc as a string
N No. of samples per point
N\$ Name of file in which the data is to be stored
N1 Number of hops for mode on oblique ionogram
P No. of samples if pen lifted early ; EVh' from oblique pathlength
P\$ String array containing the place code of the ionogram
Q Counter for number of timing shifts
R For/next loop counter
R1 Pointer in final buffer B1\$, points to next place to load
S For/next loop counter
S0 Variance of x coordinates for point ; chord length in EVfo calculation
S1 Variance of y coordinates for point ; arc height in EVfo calculation
T Time of ionogram
T\$ Time of ionogram as a string
T0 Minutes of ionogram time
T0\$ Minutes of ionogram time as a string
T1 Hours of ionogram time
T1\$ Hours of ionogram time as a string
T2 Time interval between ionograms
T3 Offset at calibration in msec
T4 Drift rate in msec/week initially, then msec/day ; top frequency marker
T5 Time of timing shift for 'Minibal' ionograms
T6 Amount of timing shift in msec
W No. of samples with wrong digits ; determinant in MUF calculation
X Array of x coordinates on table
X0 Sum of x coordinates for point ; constant c in MUF calculation
X1 x coordinate of scaled point ; constant b in MUF calculation
X2 Sum of squares of x coordinates ; constant a in MUF calculation
X3 Matrix X in ionogram coordinate transformation
X4 x coordinate of latest point being displayed

VARIABLE NAMES (continued)

Y Array of y coordinates on table
Y\$ Year of ionogram as a string
Y0 Sum of y coordinates for point
Y1 y coordinate of scaled point
Y2 Sum of squares of y coordinates
Y3 Year of ionogram
Y4 y coordinate of latest point being displayed
Z Pen up flag

```
0810 GOTO 0850
0820 PRINT "<7>DEVIATION TOO HIGH - ";
0830 PRINT "<7>REDIGITIZE"
0840 GOTO 0870
0850 IF I><4 THEN LET IO=0
0860 ON I THEN GOSUB 0950, 0990, 1040, 1280
0870 NPT,Z
0880 IF Z><1 THEN GOTO 0870
0890 GOTO 0570
0900 REM
0910 REM
0920 REM
0930 PRINT "<7>POINT IN UNDEFINED REGION"
0940 GOTO 0870
0950 REM ***** QUALIFYING LETTER (I=1) *****
0960 LET B[K]=J
0970 LET K=K+1
0980 RETURN
0990 REM ***** NUMBER (I=2) *****
1000 IF J>13 THEN GOTO 1340
1010 LET B[K]=J-26
1020 LET K=K+1
1030 RETURN
1040 REM ***** SCALED PARAMETER (I=3) *****
1050 IF J>21 THEN GOTO 1340
1060 IF J=14 THEN GOTO 1160
1070 IF I1><0 THEN GOTO 1230
1080 IF I5><0 THEN GOTO 1260
1090 IF I4=1 THEN GOTO 1130
1100 IF J<15 THEN GOTO 1160
1110 PRINT "<7>NOT A VERTICAL PARAMETER"
1120 GOTO 1240
1130 IF J>13 THEN GOTO 1160
1140 PRINT "<7>NOT AN OBLIQUE PARAMETER"
1150 GOTO 1240
1160 IF K=0 THEN GOTO 1210
1170 ON J THEN GOSUB 1680, 2250, 1680, 2250, 1680, 2250, 1680, 2250
1180 ON J-8 THEN GOSUB 1680, 1680, 2800, 1680, 3530, 3740, 1680
1190 ON J-15 THEN GOSUB 1680, 1680, 1680, 3940, 2250, 4210
1200 RETURN
1210 PRINT "<7>NO POINTS SCALED"
1220 RETURN
1230 PRINT "<7>AXES NOT DEFINED"
1240 LET K=0
1250 RETURN
1260 PRINT "<7>HOP/MODE NOT DEFINED"
1270 GOTO 1240
1280 REM ***** CONTROL COMMAND (I=4) *****
1290 IF J>14 THEN GOTO 1340
1300 IF J><1 THEN LET IO=0
1310 ON J THEN GOSUB 4340, 4440, 4610, 4670, 8120, 6970, 6680, 6340
1320 ON J-8 THEN GOSUB 8410, 7690, 4950, 5820, 8680, 8880
1330 RETURN
1340 PRINT "<7>POINT IN UNDEFINED REGION"
1350 RETURN
1360 REM ***** IONOGRAM POINT *****
1370 LET IO=1
1380 IF Y1<Y[23] THEN GOTO 0930
1390 IF I1><0 THEN GOTO 1580
1400 LET X3[1,1]=X1
1410 LET X3[2,1]=Y1
1420 MAT F1=A2*X3
1430 MAT F2=F1+B2
1440 LET B[K]=F2[1,1]
1450 LET B[K+1]=F2[2,1]
1460 IF D2=1 THEN GOSUB 1620
1470 LET X4=(B[K]-.5)*25.5
1480 IF X4>255 THEN LET X4=255
1490 IF X4<0 THEN LET X4=0
1500 LET Y4=B[K+1]/3.92
1510 IF Y4>255 THEN LET Y4=255
1520 IF Y4<0 THEN LET Y4=0
1530 DISP,D1,Y4,X4
1540 CURS,X4,Y4
1550 LET D1=D1+1
1560 LET K=K+2
1570 GOTO 0870
1580 LET B[K]=X1
1590 LET B[K+1]=Y1
1600 LET K=K+2
```

```
1610 GOTO 0870
1620 MAT F3=A3*F2
1630 MAT F4=F3+B3
1640 LET B[K]=F4[1,1]
1650 LET B[K+1]=F4[2,1]
1660 LET D2=0
1670 RETURN
1680 REM ***** FREQUENCY REQUIRED *****
1690 LET K=K+1
1700 LET R1=J*6+8
1710 IF J=12 THEN LET R1=R1+4
1720 IF J>14 THEN LET R1=R1+21
1730 PRINT F1$(R1,R1+4);
1740 IF J>14 THEN LET R1=R1+(L1-2)*96
1750 IF B[K]=-99 THEN GOTO 4490
1760 IF K=0 THEN PRINT " ";
1770 IF K=0 THEN LET R1=R1+3
1780 FOR R=0 TO K
1790   IF B[R]>0 THEN GOTO 1960
1800   LET B1$(R1,R1)=M$[-B[R],-B[R]]
1810   PRINT B1$(R1,R1);
1820   LET R1=R1+1
1830 NEXT R
1840 IF K>0 THEN PRINT " MH<122> "
1850 IF K=0 THEN PRINT
1860 IF B[0]>0 THEN GOTO 1890
1870 IF K>3 THEN GOTO 1920
1880 GOTO 1900
1890 IF K<2 THEN GOTO 1920
1900 LET B1$(R1-1,R1-1)="-"
1910 LET R1$(R1,R1)=M$[-B[K],-B[K]]
1920 IF J=1 THEN LET I6[1]=1
1930 IF J=10 THEN LET I6[3]=1
1940 LET K=0
1950 RETURN
1960 IF P$="R" THEN GOSUB 2170
1970 IF B[K-1]=-10 THEN LET B[R]=B[R]-G/2
1980 IF J=3 THEN GOTO 2040
1990 IF J=5 THEN GOTO 2040
2000 IF J=10 THEN GOTO 2040
2010 LET A=INT(B[R]*10+.5)
2020 PRINT A/10;
2030 GOTO 2060
2040 LET A=INT(B[R]*100+.5)
2050 PRINT A/100;
2060 ABBA,A,A1$
2070 LET A1$[1,1]="0"
2080 LET A=LEN(A1$)-1
2090 LET A1$=A1$," "
2100 LET B1$(R1,R1+2)=A1$[1,3]
2110 IF A>3 THEN LET B1$(R1,R1+2)=A1$[2,4]
2120 IF A<3 THEN LET B1$(R1,R1)="0"
2130 IF A<3 THEN LET B1$(R1+1,R1+2)=A1$[1,2]
2140 LET R1=R1+3
2150 LET R=R+1
2160 GOTO 1830
2170 REM ***** FREQUENCY SCALE CONVERSION FOR MINIBAL IONOGRAMS *****
2180 LET A=(B[R]-1)/(F5[2]-F5[1])+1
2190 FOR S=1 TO 4
2200   IF B[R]>F5[S] THEN LET A=(B[R]-F5[S])/(F5[S+1]-F5[S])+S
2210   IF B[R]<F5[S+1] THEN GOTO 2230
2220 NEXT S
2230 LET B[R]=A
2240 RETURN
2250 REM ***** HEIGHT REQUIRED *****
2260 LET K=K+1
2270 LET R1=J*6+8
2280 IF J=20 THEN LET R1=150
2290 PRINT F1$(R1,R1+4);
2300 IF J>14 THEN LET R1=R1-1+(L1-2)*96
2310 IF B[K]=-99 THEN GOTO 4490
2320 IF K=0 THEN PRINT " ";
2330 IF K=0 THEN LET R1=R1+3
2340 FOR R=0 TO K
2350   IF B[R]>0 THEN GOTO 2670
2360   LET B1$(R1,R1)=M$[-B[R],-B[R]]
2370   PRINT B1$(R1,R1);
2380   LET R1=R1+1
2390 NEXT R
2400 IF K=0 THEN GOTO 2630
```

```
2410 IF K<2 THEN LET R1=R1+2
2420 IF B[0]>0 THEN GOTO 2460
2430 IF I4=1 THEN GOTO 2460
2440 IF K><3 THEN GOTO 2500
2450 GOTO 2470
2460 IF K><2 THEN GOTO 2500
2470 LET B1$[R1-1,R1-1]="-"
2480 LET B1$[R1,R1]=M$[-B[K],-B[K]]
2490 LET R1=R1+1
2500 PRINT "<107><109> ";
2510 IF I4><1 THEN GOTO 2630
2520 PRINT "(";INT(A-H0);")"
2530 IF N1=0 THEN GOTO 2640
2540 LET P=12743*SIN(4471/(12743*N1))
2550 LET P=SQR((A/N1)+2-P+2)/2-6371*(1-COS(4471/(12743*N1)))
2560 LET P=INT(P+.5)
2570 ABBA,P,A1$
2580 LET A1$[1,1]="0"
2590 LET A1$=A1$, " "
2600 LET R1$[R1+1,R1+3]=A1$[2,4]
2610 IF P<100 THEN LET B1$[R1+1,R1+3]=A1$[1,3]
2620 PRINT "EVH" ";P;" "<107><109>";
2630 PRINT
2640 IF J=4 THEN LET I6[2]=1
2650 LET K=0
2660 RETURN
2670 LET A=INT(B[R+1]+.5)
2680 IF I4=1 THEN LET A=INT(B[R+1]+H0+.5)
2690 PRINT A;
2700 ABBA,A,A1$
2710 LET A1$=A1$, " "
2720 LET B1$[R1,R1+2]=A1$[2,4]
2730 IF A<100 THEN LET B1$[R1,R1]="0"
2740 IF A<100 THEN LET B1$[R1+1,R1+2]=A1$[2,3]
2750 IF I4=1 THEN LET B1$[R1+3,R1+3]=A1$[5,5]
2760 LET R1=R1+3
2770 IF I4=1 THEN LET R1=R1+1
2780 LET R=R+1
2790 GOTO 2390
2800 REM ***** MUF CALCULATION *****
2810 LET K=K+1
2820 IF K=0 THEN GOTO 2850
2830 IF K<5 THEN GOTO 3470
2840 IF K>7 THEN GOTO 3470
2850 PRINT "MUF ";
2860 LET R1=74
2870 IF B[K]=-99 THEN GOTO 4490
2880 IF K=0 THEN GOTO 3490
2890 FOR R=1 TO 3
2900 IF B[2*(R-1)]<0 THEN GOTO 3470
2910 IF B[2*R-1]<0 THEN GOTO 3470
2920 LET C5[R,1]=B[2*(R-1)]
2930 LET C6[R,1]=B[2*R-1]
2940 IF P$<"R" THEN GOTO 2980
2950 LET B[R]=C5[R,1]
2960 GOSUB 2170
2970 LET C5[R,1]=B[R]
2980 LET S0=SQR(1+(.23326/(C6[R,1]/6371.35+.027586)))+2)
2990 LET C5[R,1]=C5[R,1]*1.114*S0
3000 NEXT R
3010 LET W=C6[1,1]+2*(C6[2,1]-C6[3,1])-C6[2,1]+2*(C6[1,1]-C6[3,1])
3020 LET W=W+C6[3,1]+2*(C6[1,1]-C6[2,1])
3030 LET X2=C5[1,1]*(C6[2,1]-C6[3,1])-C5[2,1]*(C6[1,1]-C6[3,1])
3040 LET X2=(X2+C5[3,1]*(C6[1,1]-C6[2,1]))/W
3050 LET X1=C6[1,1]+2*(C5[2,1]-C5[3,1])-C6[2,1]+2*(C5[1,1]-C5[3,1])
3060 LET X1=(X1+C6[3,1]+2*(C5[1,1]-C5[2,1]))/W
3070 LET X0=C6[1,1]+2*(C6[2,1]*C5[3,1]-C6[3,1]*C5[2,1])
3080 LET X0=X0-C6[2,1]+2*(C6[1,1]*C5[3,1]-C6[3,1]*C5[1,1])
3090 LET X0=(X0+C6[3,1]+2*(C6[1,1]*C5[2,1]-C6[2,1]*C5[1,1]))/W
3100 LET M=-X1/(2*X2)
3110 LET M=INT((X2*M+2+X1*M+X0)*10+.5)
3120 IF M<0 THEN GOTO 3470
3130 PRINT M/10;
3140 ABBA,M,A1$
3150 LET A1$[1,1]="0"
3160 LET A1$=A1$, " "
3170 LET R1$[R1,R1+2]=A1$[1,3]
3180 IF M>100 THEN LET B1$[R1,R1+2]=A1$[2,4]
3190 LET R1=R1+3
3200 IF K<6 THEN GOTO 3290
```

```
3210 FOR R=6 TO K
3220 IF B[R]>0 THEN GOTO 3470
3230 LET B1$[R1,R1]=M$[-B[R],-B[R]]
3240 PRINT B1$[R1,R1];
3250 LET R1=R1+1
3260 NEXT R
3270 IF K=6 THEN LET B1$[R1-1,R1-1]="-"
3280 IF K=6 THEN LET B1$[R1,R1]=M$[-B[K],-B[K]]
3290 PRINT "MH<122>"
3300 IF I4=1 THEN GOTO 3450
3310 IF I6[1]=1 THEN GOTO 3350
3320 PRINT "M3000?"
3330 PRINT "<7>FOF2 NOT SCALED"
3340 GOTO 3440
3350 IF K<6 THEN LET R1=R1+2
3360 IF K=6 THEN LET R1=R1+1
3370 LET A1$=B1$[14,16], " "
3380 IF A1$[1,1]=" " THEN GOTO 3440
3390 ABBA,A1$,A
3400 LET M=INT(M/A*100+.5)
3410 ABBA,M,A1$
3420 LET B1$[R1+1,R1+3]=A1$[2,4]
3430 PRINT "M3000";M/100
3440 LET I6[4]=1
3450 LET K=0
3460 RETURN
3470 PRINT "<7>MUF ERROR"
3480 GOTO 3450
3490 LET R1=R1+3
3500 LET R1$[R1,R1]=M$[-B[K],-B[K]]
3510 PRINT " ";B1$[R1,R1]
3520 GOTO 3440
3530 REM ***** ES TYPE *****
3540 LET K=K+1
3550 PRINT "ES TYPE ";
3560 LET R1=90
3570 IF B[K]=-99 THEN GOTO 4490
3580 FOR R=0 TO K
3590 IF B[R]>0 THEN GOTO 3720
3600 IF R=0 THEN GOTO 3650
3610 IF B[R]<=-26 THEN GOTO 3650
3620 PRINT " ";
3630 LET B1$[R1,R1]=","
3640 LET R1=R1+1
3650 LET B1$[R1,R1]=M$[-B[R],-B[R]]
3660 PRINT B1$[R1,R1];
3670 LET R1=R1+1
3680 NEXT R
3690 PRINT
3700 LET K=0
3710 RETURN
3720 PRINT "<7>INVALID QUALIFYING LETTER"
3730 GOTO 3700
3740 REM ***** ALL VALUES *****
3750 LET K=K+1
3760 IF K>0 THEN GOTO 3720
3770 PRINT "ALL VALUES ";
3780 IF B[K]=-99 THEN GOTO 4530
3790 PRINT M$[-B[K],-B[K]]
3800 IF I4=1 THEN GOTO 3860
3810 FOR R=0 TO 10
3820 LET R1=R*6+17
3830 LET B1$[R1,R1]=M$[-B[K],-B[K]]
3840 NEXT R
3850 GOTO 5150
3860 IF L1<1 THEN LET B1$[17,21]="ALL "
3870 IF L1=<0 THEN LET L1=1
3880 FOR R=0 TO 5
3890 LET R1=(L1-1)*96+R*6+26
3900 IF R=5 THEN LET R1=R1+1
3910 LET B1$[R1,R1]=M$[-B[K],-B[K]]
3920 NEXT R
3930 RETURN
3940 REM ***** EQUIVALENT VERTICAL CRITICAL FREQUENCY *****
3950 LET K=K+1
3960 IF K=0 THEN GOTO 3990
3970 IF K<5 THEN GOTO 4180
3980 IF K>7 THEN GOTO 4180
3990 IF N1=0 THEN GOTO 4180
4000 LET R1=143
```

```
4010 PRINT F1$(R1,R1+4);
4020 LET R1=R1+(L1-2)*96
4030 IF B[K]=-99 THEN GOTO 4490
4040 PRINT " ";
4050 IF K=0 THEN GOTO 3490
4060 LET S0=12742.7*SIN(4470.84/(12742.7*N1))
4070 LET S1=6371.35*(1-COS(4470.84/(12742.7*N1)))
4080 FOR R=1 TO 3
4090   IF B[2*(R-1)]<0 THEN GOTO 4180
4100   IF B[2*R-1]<0 THEN GOTO 4180
4110   LET C5[R,1]=B[2*(R-1)]
4120   LET C6[R,1]=B[2*R-1]+H0
4130   LET C6[R,1]=SQR((C6[R,1]/N1)2-S02)/2-S1
4140   LET C5[R,1]=C5[R,1]/(.2146/N1+.97)
4150   LET C5[R,1]=C5[R,1]/SQR(1+(S0/(2*(C6[R,1]+S1)))2)
4160 NEXT R
4170 GOTO 3010
4180 PRINT "<7>EVFO ERROR"
4190 LET K=0
4200 RETURN
4210 REM ***** SIGNAL STRENGTH *****
4220 LET K=K+1
4230 IF K>0 THEN GOTO 4320
4240 PRINT "S ";
4250 LET R1=(L1-1)*96+65
4260 IF B[K]=-99 THEN GOTO 4490
4270 IF B[K]>0 THEN GOTO 4320
4280 LET B1$(R1,R1)=M$[-B[K],-B[K]]
4290 PRINT B1$(R1,R1)
4300 LET K=0
4310 RETURN
4320 PRINT "<7>SIGNAL STRENGTH ERROR"
4330 GOTO 4300
4340 REM ***** RUBOUT COMMAND (J=1) *****
4350 IF IO><0 THEN LET K=K-1
4360 IF IO><0 THEN LET D1=D1-1
4370 LET K=K+1
4380 IF K<0 THEN GOTO 4400
4390 RETURN
4400 PRINT "<7>NO POINTS TO RUB OUT"
4410 LET D1=0
4420 LET K=0
4430 RETURN
4440 REM ***** DELETE (J=2) *****
4450 LET K=0
4460 LET B[K]=-99
4470 LET K=1
4480 RETURN
4490 PRINT B1$(R1,R1+5);" DELETED"
4500 LET B1$(R1,R1+5)=" "
4510 LET K=0
4520 RETURN
4530 LET L1=L1-1
4540 IF L1<=0 THEN LET B1$=" "
4550 IF L1<=0 THEN LET B1$=B1$," "
4560 IF L1<=0 THEN LET B1$=B1$," "
4570 IF L1>0 THEN LET B1$=B1$[1,L1*96]
4580 PRINT " DELETED"
4590 LET K=0
4600 RETURN
4610 REM ***** RESTART COMMAND (J=3) *****
4620 LET K=0
4630 LET D1=0
4640 DISP,0
4650 LET I1=1
4660 GOTO 5540
4670 REM ***** SMALLER DOMAIN BEING DEFINED (J=4) *****
4680 LET K=K+1
4690 IF K>=5 THEN GOTO 4930
4700 FOR R=1 TO 3
4710   FOR S=1 TO 2
4720     LET C4[R,S]=B[S-3+R*2]
4730     IF S=1 THEN LET C5[R,1]=INT(B[S-3+R*2]+.5)
4740     IF S=2 THEN LET C6[R,1]=INT((B[S-3+R*2]+50)/100)*100
4750   NEXT S
4760   LET C4[R,3]=1
4770 NEXT R
4780 MAT C7=INV(C4)
4790 MAT C8=C7*C5
4800 MAT C9=C7*C6
```

```
4810 FOR R=1 TO 2
4820 LET A3[1,R]=C8[R,1]
4830 NEXT R
4840 LET B3[1,1]=C8[3,1]
4850 LET B3[2,1]=C9[3,1]
4860 FOR R=1 TO 2
4870 LET A3[2,R]=C9[R,1]
4880 NEXT R
4890 PRINT "DOMAIN DEFINED FOR NEXT POINT"
4900 LET D2=1
4910 LET K=0
4920 RETURN
4930 PRINT "<7>DOMAIN ERROR"
4940 GOTO 4910
4950 REM ***** END OF IONOGRAM COMMAND (J=11) *****
4960 IF I4><1 THEN GOTO 5100
4970 LET A=71
4980 ABBA,HO,A1$
4990 IF HO<1000 THEN LET A1$[2,5]=" "
5000 LET A2$=PS,Y$[4,5]," ",DS," ",T1$,TOS
5010 IF L1=0 THEN GOTO 5080
5020 FOR R=1 TO L1
5030 LET R1=(R-1)*96
5040 LET B1$[R1+1,R1+14]=A2$
5050 LET B1$[R1+68,R1+71]=A1$[2,5]
5060 NEXT R
5070 GOTO 5220
5080 LET B1$[1,14]=A2$
5090 GOTO 5220
5100 IF I6[1]=0 THEN PRINT "<7>FOF2 NOT SCALED"
5110 IF I6[2]=0 THEN PRINT "<7>H'F NOT SCALED"
5120 IF I6[3]=0 THEN PRINT "<7>FMIN NOT SCALED"
5130 IF I6[4]=0 THEN PRINT "<7>MUF NOT SCALED"
5140 IF I6[1]+I6[2]+I6[3]+I6[4]=4 THEN GOTO 5190
5150 FOR R=1 TO 4
5160 LET I6[R]=1
5170 NEXT R
5180 RETURN
5190 LET A2$=PS,Y$[4,5]," ",DS," ",T1$,TOS
5200 LET B1$[1,12]=A2$
5210 LET A=95
5220 FOR R=1 TO LEN(B1$) STEP 96
5230 PRINT FILE[1],B1$[R,R+A]
5240 NEXT R
5250 PRINT
5260 PRINT "FILED IN "NS
5270 PRINT F1$[I4*96+1,I4*96+72]
5280 IF I4><1 THEN GOTO 5330
5290 FOR R=1 TO LEN(B1$) STEP 96
5300 PRINT B1$[R,R+71]
5310 NEXT R
5320 GOTO 5360
5330 PRINT B1$[1,72]
5340 PRINT F1$[73,96]
5350 PRINT B1$[73,96]
5360 LET I1=1
5370 LET D1=0
5380 DISP,0
5390 LET K=0
5400 LET T=T+T2
5410 IF T<1440 THEN GOTO 5540
5420 LET T=T-1440
5430 LET D=D+1
5440 IF D<366 THEN GOTO 5500
5450 IF INT(Y3)/4-INT(Y3/4)><0 THEN GOTO 5470
5460 IF D<367 THEN GOTO 5500
5470 LET D=1
5480 LET Y3=Y3+1
5490 ABBA,Y3,Y$
5500 CLOSE FILE[1]
5510 GOSUB 6890
5520 LET N$=PS,Y$[4,5],":",DS
5530 OPEN FILE[1,2],N$
5540 LET B1$=""
5550 LET B1$=B1$," "
5560 LET R1=1
5570 LET L1=0
5580 GOSUB 6600
5590 IF I4><1 THEN GOTO 5670
5600 IF D*1440+T>D3*1440+905 THEN GOTO 5980
```

```
5610 LET HQ=INT(T3*300+(D-D3+(T-840)/1440)*T4*300+.5)
5620 IF Q=0 THEN GOTO 5670
5630 FOR S=1 TO Q
5640 IF D*1440+T>D4[S]*1440+T5[S]-1 THEN GOTO 5660
5650 LET HQ=INT(HQ-T6[S]*300+.5)
5660 NEXT S
5670 PRINT
5680 PRINT Y3;PS;" DAY NUMBER ";D3;" TIME ";T3;
5690 IF I4>4 THEN GOTO 5740
5700 PRINT USING " OFFSET = ##.## MSEC = #### KM",HQ/300,HQ;
5710 LET I5=1
5720 LET N1=0
5730 GOTO 5780
5740 FOR R=1 TO 4
5750 LET I6[R]=0
5760 NEXT R
5770 IF PS="R" THEN LET I6[4]=1
5780 PRINT
5790 PRINT
5800 PRINT "<7>DEFINE AXES"
5810 RETURN
5820 REM ***** OBLIQUE SCALING INITIALIZATION (J=12) *****
5830 IF I4=1 THEN GOTO 6240
5840 LET I3=0
5850 LET I4=1
5860 LET I5=1
5870 LET F[1,1]=3
5880 LET F[2,1]=3
5890 LET F[3,1]=20
5900 PRINT
5910 PRINT "<7>OBLIQUE SCALING INITIALIZATION"
5920 PRINT
5930 INPUT "<7>NEXT CALIBRATION DAY ? ",D3
5940 INPUT "<7>OFFSET AT 14:00 SAST ? ",T3
5950 PRINT USING "OFFSET AT 14:00 ON DAY ### IS ##.## MSEC",D3,T3;
5960 PRINT USING " = #### KM",T3*300
5970 IF D*1440+T<D3*1440+905 THEN GOTO 6020
5980 PRINT
5990 PRINT "<7>DAY/TIME > CALIBRATION DAY/TIME"
6000 CLOSE
6010 GOTO 5920
6020 INPUT "<7>DRIFT RATE IN MSEC/WEEK ? ",T4
6030 LET T4=T4/7
6040 PRINT USING "DRIFT RATE IS +##.## MSEC/DAY",T4;
6050 PRINT USING " = +###.# KM/DAY",T4*300
6060 INPUT "<7>NUMBER OF TIMING SHIFTS ? ",Q
6070 IF Q=0 THEN GOTO 5510
6080 FOR R=1 TO Q
6090 PRINT "<7>SHIFT";R;
6100 INPUT "ON DAY ? ",D4[R];
6110 INPUT "<7> AT TIME ? ",T5[R];
6120 INPUT "<7> SHIFT ? ",T6[R];
6130 IF D4[R]>366 THEN GOTO 6200
6140 LET T5[R]=INT(T5[R]/100)*60+T5[R]-INT(T5[R]/100)*100
6150 IF T5[R]>1440 THEN GOTO 6200
6160 PRINT USING "TIMING SHIFT ## ON DAY ### ",R,D4[R];
6170 PRINT USING "AT ##:## ",INT(T5[R]/60),T5[R]-INT(T5[R]/60)*60;
6180 PRINT USING "IS +##.## MSEC = +#### KM",T6[R],T6[R]*300
6190 GOTO 6220
6200 PRINT "<7>TIMING SHIFT ERROR"
6210 GOTO 6090
6220 NEXT R
6230 GOTO 5510
6240 LET I3=1
6250 LET I4=0
6260 LET I5=0
6270 LET F[1,1]=1
6280 LET F[2,1]=1
6290 LET F[3,1]=10
6300 PRINT
6310 PRINT "<7>OBLIQUE SCALING TERMINATED"
6320 PRINT
6330 RETURN
6340 REM ***** TIME OF IONOGRAM (J=8) *****
6350 LET K=K+1
6360 IF K>5 THEN GOTO 6530
6370 IF K<3 THEN GOTO 6530
6380 FOR R=0 TO K
6390 IF B[R]=>0 THEN GOTO 6530
6400 IF ABS(B[R])<26 THEN GOTO 6530
```

```
6410 NEXT R
6420 LET TO#=(B[3]+27+(B[2]+27)*10)
6430 IF TO>59 THEN GOTO 6530
6440 LET T1#=(B[1]+27+(B[0]+27)*10)
6450 LET T=60*T1+TO
6460 IF T=>1440 THEN GOTO 6530
6470 IF K<4 THEN GOTO 6550
6480 LET T2=0
6490 FOR R=K TO 4 STEP -1
6500 LET T2=T2-(B[R]+27)*10+(K-R)
6510 NEXT R
6520 GOTO 6550
6530 PRINT "<7>TIME ERROR"
6540 LET T=0
6550 GOSUB 6600
6560 PRINT "TIME IS AT PRESENT ";T$
6570 PRINT "TIME INTERVAL IS";T2;"MINS"
6580 LET K=0
6590 RETURN
6600 ABBA,INT(T/60),T1$
6610 ABBA,T-INT(T/60)*60,T0$
6620 LET T1$[1,1]="0"
6630 LET T0$[1,1]="0"
6640 LET T1$=T1$[LEN(T1$)-2,LEN(T1$)-1]
6650 LET T0$=T0$[LEN(T0$)-2,LEN(T0$)-1]
6660 LET T$=T1$,":",T0$
6670 RETURN
6680 REM ***** DAY NUMBER OF IONOGRAM (J=7) *****
6690 LET K=K+1
6700 IF K>2 THEN GOTO 6790
6710 LET D=0
6720 FOR R=0 TO K
6730 IF B[R]=>0 THEN GOTO 6790
6740 IF ABS(B[R])=<26 THEN GOTO 6790
6750 LET D=D*10-(B[R]+27)
6760 NEXT R
6770 IF D>366 THEN GOTO 6800
6780 GOTO 6810
6790 LET D=1
6800 PRINT "<7>DAY NUMBER ERROR"
6810 GOSUB 6890
6820 PRINT "DAY NUMBER ";D$
6830 LET K=0
6840 IF I2=1 THEN RETURN
6850 CLOSE FILE[1]
6860 LET N$=P$,Y$[4,5],":",D$
6870 OPEN FILE[1,2],N$
6880 RETURN
6890 ABBA,D,D$
6900 LET D$[1,1]="0"
6910 IF D<10 THEN GOTO 6940
6920 LET D$=D$[LEN(D$)-3,LEN(D$)-1]
6930 RETURN
6940 LET A1$=D$[1,2]
6950 LET D$="0",A1$
6960 RETURN
6970 REM ***** H' AND F VALUES (J=6) *****
6980 LET K=K+1
6990 PRINT
7000 PRINT "H' AND F VALUES : ";INT((K+1)/2);"POINTS"
7010 PRINT
7020 IF K<101 THEN GOTO 7060
7030 PRINT "<7>MORE THAN 50 POINTS SCALED"
7040 LET K=0
7050 RETURN
7060 LET A1$="0"
7070 IF B[K]=24 THEN LET A1$="X"
7080 IF B[K]<0 THEN LET K=K-1
7090 PRINT P$;Y$," DAY ";D$;" TIME ";T$;" ";A1$;" RAY"
7100 LET N$=P$,Y$[4,5],":",D$,";",T1$,T0$,";H&F"
7110 OPEN FILE[0,2],N$
7120 IF I4=1 THEN GOTO 7340
7130 IF P$>"G" THEN GOTO 7180
7140 LET B1$="GRAHAMSTOWN",Y$," ",D$," ",T1$,T0$," SAST ",A1$
7150 LET L=33.3153
7160 LET M=26.5042
7170 GOTO 7310
7180 IF P$>"S" THEN GOTO 7230
7190 LET B1$="SANA",Y$," DAY ",D$," ",T1$,T0$," UT ",A1$
7200 LET L=70.3200
```

```
7210 LET M=-2 3722
7220 GOTO 7310
7230 IF PS><"R" THEN GOTO 7260
7240 LET B1$="R.S.A.",YS," DAY ",DS," ",T1$,TOS," UT ",A1$
7250 GOTO 7290
7260 INPUT "PLACE NAME ? ",B1$
7270 LET B1$=B1$," "
7280 LET B1$=B1$[1,11],YS," ",DS," ",T1$,TOS," UT ",A1$
7290 INPUT "LATITUDE ? ",L;
7300 INPUT "LONGITUDE ? ",M
7310 PRINT FILE[O],B1$
7320 PRINT FILE[O],G;" -60.0 ";L;M;" 0"
7330 GOTO 7390
7340 PRINT "OFFSET";HO;" ";N1;"HOP"
7350 PRINT FILE[O],"OBLIQUE";YS;" DAY ";DS;" ";T1$;TOS;" SAST ";HO
7360 PRINT FILE[O],"0 0 -1 32 12 15 19 16 23 11"
7370 PRINT FILE[O],"20 15 15 20 1 10 0 1000 0 1000000 0 500"
7380 PRINT FILE[O],N1;" 100 10 10 0 0 0 0 1 0"
7390 PRINT " H "
7400 IF B[1]>B[3] THEN LET B[1]=B[3]
7410 FOR R=0 TO K STEP 2
7420 IF I4=1 THEN GOTO 7460
7430 IF PS="R" THEN GOSUB 2170
7440 IF R=0 THEN GOTO 7460
7450 IF B[R]<B[R-2] THEN LET B[R]=B[R-2]
7460 LET B[R]=INT(B[R]*100+.5)/100
7470 PRINT USING "#### ##.##",INT(B[R+1]+.5);B[R]
7480 PRINT FILE[O],USING "#### ##.##",INT(B[R+1]+.5);B[R]
7490 NEXT R
7500 LET A=9999
7510 IF I4=1 THEN GOTO 7550
7520 PRINT FILE[O],USING "#### ##.##",A;B[K-1]
7530 PRINT "9999 FOF2 ";B[K-1]
7540 GOTO 7630
7550 FOR R=1 TO 3
7560 LET B[2*(R-1)]=B[K-7+2*R]
7570 LET B[2*R-1]=B[K-6+2*R]
7580 NEXT R
7590 PRINT "9999 ";
7600 LET K=5
7610 GOSUB 3940
7620 PRINT FILE[O],USING "#### ##.##",A;M/10
7630 CLOSE FILE[O]
7640 PRINT
7650 PRINT "FILED IN ";NS
7660 PRINT
7670 PRINT "<7>NORMAL SCALING RESUMED"
7680 GOTO 4610
7690 REM ***** AXES BEING DEFINED (J=10) *****
7700 LET K=K-1
7710 IF PS="R" THEN GOSUB 7980
7720 IF K><5 THEN GOTO 7960
7730 LET I1=0
7740 FOR R=1 TO 3
7750 FOR S=1 TO 2
7760 IF B[S-3+R*2]<0 THEN GOTO 7960
7770 LET C[R,S]=B[S-3+R*2]
7780 NEXT S
7790 LET C[R,3]=1
7800 NEXT R
7810 MAT C1=INV(C)
7820 MAT C2=C1*F
7830 MAT C3=C1*H
7840 FOR R=1 TO 2
7850 LET A2[1,R]=C2[R,1]
7860 NEXT R
7870 LET B2[1,1]=C2[3,1]
7880 LET B2[2,1]=C3[3,1]
7890 FOR R=1 TO 2
7900 LET A2[2,R]=C3[R,1]
7910 NEXT R
7920 PRINT "AXES DEFINED"
7930 IF I4=1 THEN PRINT "<7>HOP/MODE OF FIRST TRACE ?"
7940 LET K=0
7950 RETURN
7960 PRINT "<7>AXES ERROR - REDEFINE"
7970 GOTO 7940
7980 REM ***** FREQUENCY SCALE CONVERSION FOR MINIBAL IONOGRAMS *****
7990 IF K<9 THEN GOTO 7960
8000 LET F[3,1]=11.8
```

```
8010 LET H[1,1]=900
8020 LET F5[1]=1
8030 LET T4=(K-3)/2
8040 FOR S=2 TO T4
8050 LET F5[S]=(B[2*S]-B[2])*10.8/(B[K-1]-B[2])+1
8060 NEXT S
8070 LET F5[T4+1]=2*F5[T4]-F5[T4-1]
8080 LET R[4]=B[K-1]
8090 LET R[5]=B[K]
8100 LET K=5
8110 RETURN
8120 REM ***** DISPLAY REQUESTED (J=5) *****
8130 LET N=2
8140 PRINT "<7>DISPLAY MODE"
8150 NPT,Z
8160 IF Z=0 THEN GOTO 8150
8170 NPT,Z
8180 IF Z><0 THEN GOTO 8170
8190 POINT,N,E,X0,Y0,X2,Y2
8200 LET P=INT(E/65536)
8210 LET M=E-INT(E/256)*256
8220 LET W=INT((E-P*65536)/256)
8230 LET L=N-P/3-W-M
8240 IF L<0 THEN GOTO 8170
8250 LET X1=X0/L
8260 IF X1>7000 THEN GOTO 8370
8270 LET Y1=Y0/L
8280 LET X3[1,1]=X1
8290 LET X3[2,1]=Y1
8300 MAT F1=A2*X3
8310 MAT F2=F1+B2
8320 LET X1=(F2[1,1]-.5)*25.6
8330 LET Y1=F2[2,1]/3.92
8340 DISP,D1,Y1,X1
8350 LET D1=D1+1
8360 GOTO 8170
8370 LET N=5
8380 LET K=0
8390 PRINT "END OF DISPLAY MODE"
8400 RETURN
8410 REM ***** YEAR/PLACE (J=9) *****
8420 LET K=K+1
8430 IF K><2 THEN GOTO 8540
8440 IF B[K]>0 THEN GOTO 8540
8450 LET P$=M$[-B[K],-B[K]]
8460 LET Y3=0
8470 FOR R=K-1 TO 0 STEP -1
8480 IF B[R]>0 THEN GOTO 8540
8490 LET Y3=Y3-(B[R]+27)*10+(K-1-R)
8500 NEXT R
8510 LET Y3=1900+Y3
8520 ABBA,Y3,Y$
8530 GOTO 8550
8540 PRINT "<7>YEAR/PLACE ERROR"
8550 PRINT "YEAR IS";Y3;"PLACE IS ";P$
8560 IF P$="S" THEN LET G=1.18
8570 IF P$="G" THEN GOTO 8620
8580 IF P$="S" THEN GOTO 8620
8590 IF P$="O" THEN PRINT "OBLIQUE SCALING ?"
8600 IF P$="O" THEN GOTO 8620
8610 INPUT "<7>ELECTRON GYROFREQUENCY ? ",G
8620 IF I2=0 THEN CLOSE FILE[1]
8630 GOSUB 6890
8640 IF P$><"O" THEN GOSUB 5520
8650 LET I2=0
8660 LET K=0
8670 RETURN
8680 REM ***** NUMBER OF HOPS (J=13) *****
8690 LET K=K+1
8700 IF K>0 THEN GOTO 8860
8710 IF B[K]>0 THEN GOTO 8860
8720 IF B[K]=-99 THEN PRINT "MODE";
8730 IF B[K]=-99 THEN GOTO 4530
8740 IF L1>0 THEN LET B1$=B1$,"
8750 IF L1>0 THEN LET B1$=B1$,"
8760 IF L1>0 THEN LET B1$=B1$,"
8770 LET R1=L1*96+17
8780 LET B1$[R1,R1]=M$[-B[K],-B[K]]
8790 LET B1$[R1+1,R1+1]="F"
8800 LET N1=(B[K]+27)
```

```
8810 PRINT " ";B1$(R1,R1+1);" MODE"
8820 LET L1=L1+1
8830 LET I5=0
8840 LET K=0
8850 RETURN
8860 PRINT "<7>INVALID HOP NUMBER"
8870 GOTO 8840
8880 REM ***** INTERMEDIATE MODE (J=14) *****
8890 LET K=K+1
8900 IF B[K]=-99 THEN PRINT "MODE";
8910 IF B[K]=-99 THEN GOTO 4530
8920 FOR R=0 TO K
8930   IF B[R]>0 THEN GOTO 9120
8940 NEXT R
8950 IF L1>0 THEN LET B1$=B1$,"
8960 IF L1>0 THEN LET B1$=B1$,"
8970 IF L1>0 THEN LET B1$=B1$,"
8980 LET R1=L1*96+17
8990 PRINT " ";
9000 FOR R=0 TO K
9010   LET B1$(R1,R1)=M$[-B[R],-B[R]]
9020   PRINT B1$(R1,R1);
9030   LET R1=R1+1
9040 NEXT R
9050 PRINT " MODE"
9060 LET N1=0
9070 IF B1$(L1*96+18,L1*96+19)="E " THEN LET N1=- (B[0]+27)
9080 LET L1=L1+1
9090 LET I5=0
9100 LET K=0
9110 RETURN
9120 PRINT "<7>INVALID MODE DESIGNATION"
9130 GOTO 9100
9140 REM ***** TERMINATE *****
9150 CLOSE
9160 PRINT
9170 PRINT "<7>SCALING TERMINATED"
9180 PRINT
9190 PRINT "LAST DATA FILE USED ";N$;" TIME IS ";T$
9200 STOP
```

APPENDIX C

IONOGRAM DATA HANDLING PROGRAMS

1. The NOVA BASIC program MAXI (Transfers data from files on the NOVA floppy disk to MAXIMOP subfiles on the ICL 1902T.)
2. The ICL FORTRAN program FILE (Transfers data from MAXIMOP subfiles to a data file or magnetic tape.)
3. The ICL Find 2 program FIND (Lists selected vertical incidence data from a data file.)
4. The ICL Find 2 program FIDO (Lists selected oblique incidence data from a data file.)
5. The ICL Find 2/Direct Access Sorting program MEDI (Lists selected oblique incidence data from a data file ordered with respect to one of the parameters.)

1. Listing of Program MAXI

```
0010 REM "MAXI"
0020 REM
0030 REM THIS PROGRAM CALLS THE PROGRAMS "MIXPO" AND "MIXPN".
0040 REM ORIGINAL VERSION "MAXIN" CALLS "MIXPO" AND "MAXPN",
0050 REM AUTHOR PETE MOUNTFORT.
0060 REM AMENDMENTS IN "MIXPN" VERSION BY JON RASH.
0070 REM "MIXPO" ACTS AS 'RECEIVER' IN COMMUNICATING WITH
0080 REM MAXIMOP, "MIXPN" ACTS AS 'TRANSMITTER'.
0090 REM
0100 KILL,0
0110 EXECUTE,0,"LOAD'MIXPO'"
0120 CHAIN "MIXPN"
```

```
0010 REM "MIXPO"
0020 REM
0030 COM A$[130],B$[130],C$[130]
0040 COM A1,B1,C1,E1
0050 ON ESC THEN GOTO 0140
0060 ON ERR THEN GOSUB 0210
0070 PRINT A$;"<27>"
0080 LET A1=1
0090 LET C1=1
0100 INPUT "",B$;
0110 LET B1=1
0120 ON C1 THEN GOTO 0100, 0070
0130 GOTO 0100
0140 BUFR,0,B$
0150 ON E1 THEN GOTO 0170
0160 STOP
0170 LET B1=2
0180 SUSPEND
0190 IF A1=1 THEN GOTO 0190
0200 GOTO 0070
0210 ON E1 THEN GOTO 0240
0220 PRINT "ERR NO";SYS(7);
0230 STOP
0240 RETURN
```

```
0010 REM "MIXPN"
0020 REM
0030 COM A$[130],B$[130],C$[130],A1,B1,C1,E1
0040 DIM A1$[1],D$[130],D1$[5],E$[100],F$[100],F0$[12],F1$[10]
0050 DIM F2$[16],G2$[16],H1$[96],H2$[72],J1$[12],J2$[12]
0060 LET E1=0
0070 LET E=0
0080 LET C1=1
0090 LET F9=0
0100 LET L0=61
0110 LET L1=57
0120 LET L2=100
0130 LET L3=100
0140 LET D1=0
0150 LET E$=""
0160 READ H1$[1,48]
0170 READ H1$[49,96]
0180 READ H2$[1,48]
0190 READ H2$[49,72]
0200 DATA " YR DAY TIME FOF2 H'F2 FOF1 H'F FOF H'E "
0210 DATA " FOES H'ES FBES FMIN MUF M3000 FXI ESTYPE "
0220 DATA "YEAR DAY TIME MODE LLOF MOF JF HLOF EV"
0230 DATA "FO P' EVH' S OFFSET"
0240 KILL,0
0250 PRIORITY;10,E
0260 ON ESC THEN GOTO 2440
0270 IF E<0 THEN PRINT "PRIORITY ERR";E
0280 PRINT
0290 INPUT "JOBNUMBER ",J1$
0300 INPUT "PASSWORD ",J2$
0310 LET J1$=J1$,"MAXIMOP"
0320 PRINT "FILENAME ";J1$;
0330 INPUT "(Y OR N) ",F0$
0340 IF F0$="Y" THEN GOTO 0380
0350 LET F9=1
0360 INPUT "WHAT THEN? ",F0$
0370 LET J1$=J1$[1,4]
```

```
0380 INPUT "MAXIMOP SUBFILE NAME ",F1$
0390 INPUT "IONOGRAM DATA FILES (Y OR N) ",A1$
0400 IF A1$><"Y" THEN GOTO 0490
0410 INPUT "FIRST DATA FILE ",F2$
0420 INPUT "LAST DATA FILE ",G2$
0430 IF F2$[1,3]=G2$[1,3] THEN GOTO 0460
0440 PRINT "DATA FILE ERR"
0450 STOP
0460 LET D1$=F2$[5,7]
0470 ABBA,D1$,D1
0480 GOTO 0510
0490 INPUT "DISK FILENAME ",F2$
0500 INPUT "MAXIMOP SUBFILE HEADER ",ES
0510 OPEN FILE[F1,3],F2$
0520 REM LOGIN
0530 LET A$="#<27><1>"
0540 LET A1=#0
0550 LET B1=#0
0560 LET E1=#1
0570 LET C1=#1
0580 EXECUTE,0,"RUN",E
0590 IF E><0 THEN PRINT "RUN ERR",E
0600 IF A1=#0 THEN GOTO 0600
0610 LET B9=#0
0620 IF B1>0 THEN GOTO 0720
0630 LET B9=#B9+1
0640 IF B9<10000 THEN GOTO 0620
0650 KILL,0
0660 IF B1><2 THEN GOTO 0660
0670 LET B1=#0
0680 LET A1=#0
0690 RDY,0,E
0700 IF E><0 THEN PRINT "LOGIN RDY ERR";E
0710 GOTO 0600
0720 REM COME HERE ON FIRST RESPONSE
0730 LET B2=#B1
0740 LET B1=#0
0750 LET A$=J1$
0760 LET A1=#0
0770 IF B2=#2 THEN GOTO 0820
0780 IF B1=#0 THEN GOTO 0780
0790 LET B2=#B1
0800 LET B1=#0
0810 GOTO 0770
0820 REM THIS SHOULD BE JOBNUMBER REQUEST
0830 LET C$=B$
0840 RDY,0,E
0850 IF E><0 THEN PRINT "J# RDY ERR";E
0860 IF C$><"TYPE JOB NUMBE " THEN PRINT "JOB# ERR ";C$
0870 PRINT "J";
0880 IF B1=#0 THEN GOTO 0880
0890 LET B2=#B1
0900 LET B1=#0
0910 LET A$=J2$
0920 LET A1=#0
0930 IF B2=#2 THEN GOTO 0980
0940 IF B1=#0 THEN GOTO 0940
0950 LET B2=#B1
0960 LET B1=#0
0970 GOTO 0930
0980 REM THIS SHOULD BE PASSWORD REQUEST
0990 LET C$=B$
1000 RDY,0,E
1010 IF E><0 THEN PRINT "PW RDY ERR";E
1020 IF C$><" THEN PRINT "PW REQ ERR ";C$
1030 PRINT "P";
1040 ON ESC THEN GOTO 2400
1050 ON ERR THEN GOTO 2400
1060 REM NOW BREAK INTO NEWS
1070 IF B1=#0 THEN GOTO 1070
1080 LET B1=#0
1090 LET A$="#<1>"
1100 LET A1=#0
1110 IF B1=#0 THEN GOTO 1110
1120 LET C$=B$
1130 LET B1=#0
1140 IF C$[1,4]><"NEWS" THEN GOTO 1110
1150 LET C1=#2
1160 REM WAIT FOR INVITATION TO TYPE
```

```
1170 PRINT "N";
1180 IF B1><2 THEN GOTO 1180
1190 IF F9=0 THEN GOTO 1280
1200 LET A$="OPEN ",F0$
1210 LET A1=0
1220 LET B1=0
1230 RDY,O,E
1240 IF E><0 THEN PRINT "OPEN RDY ERR";E
1250 PRINT "O";
1260 IF B1><82 THEN GOTO 1260
1270 REM COME HERE IF FILE OPEN
1280 LET A$="INPUT ",F1$
1290 LET A1=0
1300 LET B1=0
1310 RDY,O,E
1320 IF E><0 THEN PRINT "INPUT RDY ERR";E
1330 REM DATA OUTPUT LOOP
1340 PRINT "I";
1350 LET E2=0
1360 ON ESC THEN GOTO 2160
1370 ON ERR THEN GOTO 2160
1380 IF A1$><"Y" THEN GOTO 1440
1390 REM HEADINGS
1400 IF F2$(1,1)><"O" THEN LET E$=H1$
1410 IF F2$(1,1)="O" THEN LET E$=H2$
1420 PRINT " FILE ",F2$;
1430 GOTO 1450
1440 IF E$="" THEN READ FILE[1],E$
1450 LET D$=E$
1460 ON ERR THEN GOTO 2160
1470 IF E2=1 THEN GOTO 1940
1480 READ FILE[1],F$
1490 LET F7=0
1500 IF EOF(1)=0 THEN GOTO 1530
1510 LET E2=1
1520 GOTO 1760
1530 LET F8=LEN(F$)
1540 IF F8=0 THEN GOTO 1480
1550 IF A1$><"Y" THEN GOTO 1570
1560 IF F8<71 THEN GOTO 1480
1570 LET L1=L1-1
1580 IF L1<0 THEN LET L1=L0
1590 LET L2=L2-3
1600 LET E$=""
1610 FOR J=1 TO F8
1620 IF F$(J,J)="$" THEN LET F$(J,J)="$"
1630 IF F$(J,J)=>" " THEN GOTO 1710
1640 IF F$(J,J)><"<9>" THEN GOTO 1690
1650 LET E3=LEN(E$)
1660 LET L=(INT(E3/8)+1)*8
1670 LET E$(E3+1,L)=" "
1680 GOTO 1720
1690 IF F$(J,J)="$<12>" THEN GOTO 1480
1700 GOTO 1720
1710 LET E$=E$,F$(J,J)
1720 NEXT J
1730 IF LEN(E$)+LEN(D$)=>L2 THEN GOTO 1760
1740 LET D$=D$,"<13>",E$
1750 GOTO 1480
1760 IF F7 THEN GOTO 1780
1770 LET L2=L3
1780 ON B1 THEN GOTO 1800, 1860
1790 GOTO 1760
1800 LET C$=B$
1810 LET B1=0
1820 IF C$="WAITING" THEN KILL,0
1830 IF LEN(C$)=0 THEN GOTO 1850
1840 PRINT C$
1850 GOTO 1760
1860 LET A$=D$
1870 LET B1=0
1880 LET A1=0
1890 IF LEN(B$)>4 THEN GOTO 2240
1900 RDY,O,E
1910 IF E><0 THEN PRINT "DATA RDY ERR";E
1920 PRINT B$;
1930 GOTO 1450
1940 REM COME HERE ON END OF NOVA FILE
1950 IF A1$><"Y" THEN GOTO 2160
1960 IF F2$=G2$ THEN GOTO 2160
1970 REM NEXT DATA FILE
```

```
1980 CLOSE FILE[1]
1990 LET D1=D1+1
2000 ABBA,D1,D1$
2010 LET D1$[1,1]="0"
2020 IF D1>9 THEN GOTO 2050
2030 LET F0$=D1$
2040 LET D1$="0",F0$
2050 LET F2$[5,7]=D1$[LEN(D1$)-3,LEN(D1$)-1]
2060 PRINT
2070 PRINT "FILE ";F2$;
2080 ON ERR THEN GOTO 2140
2090 OPEN FILE[1,3],F2$
2100 LET E2=0
2110 LET D$=""
2120 LET F$=""
2130 GOTO 1440
2140 IF SYS(7)=24 THEN PRINT " NOT FOUND"
2150 REM INPUT TERMINATOR
2160 IF B1><2 THEN GOTO 2160
2170 LET B1=0
2180 LET A$="****"
2190 LET A1=0
2200 RDY,0,E
2210 IF E><0 THEN PRINT "TERMINATOR RDY ERR";E
2220 IF B1><2 THEN GOTO 2220
2230 LET B1=0
2240 REM COME HERE IF DATE<137> RECEIVED
2250 ON ESC THEN GOTO 2310
2260 ON ERR THEN GOTO 2310
2270 LET A$="FAST ",F1$
2280 LET A1=0
2290 RDY,0,E
2300 IF E><0 THEN PRINT "FASTLIST RDY ERR"
2310 IF B1><2 THEN GOTO 2310
2320 LET B1=0
2330 IF LEN(B$)>10 THEN PRINT "<7>";B$;"<7>"
2340 LET A$="LOGO"
2350 LET A1=0
2360 RDY,0,E
2370 IF E><0 THEN PRINT "LOGO RDY ERR";E
2380 REM NOW COPY CLOSING COMMENTS ONTO VDU & CLOSE ON ESC
2390 ON ESC THEN GOTO 2440
2400 IF B1=0 THEN GOTO 2400
2410 LET B1=0
2420 PRINT "<7>";B$;"<7>"
2430 GOTO 2400
2440 CLOSE
2450 STOP
2460 DIM Z$[100],Y$[100]
2470 PRINT
2480 INPUT "FN ",Z$
2490 OPEN FILE[1,3],Z$
2500 READ FILE[1],Y$
2510 PRINT Y$
2520 IF EOF(1)=0 THEN GOTO 2500
2530 CLOSE
2540 STOP
```

2. Listing of Program FILE

JOB XA,ARJR,RASH
FORTRANCOMP FILE
EXECUTE FILE

DOC FORTRAN FILE
SHORTLIST
LIBRARY(CSCSRROUTINES)
PROGRAM (FILE)
COMPRESS INTEGER AND LOGICAL
COMPACT
TRACE 0
INPUT 5 = CRO
OUTPUT 6 = LPO
END

C ***** FILE

MASTER FILE IONO

C READS VARIABLE LENGTH ALPHA RECORDS FROM A MAXIMOP SUBFILE
C AND STORES THEM IN A DATA FILE, SPACE FILLED TO NCR CHARACTERS

INTEGER INB(128),OUTB(128),OUTA(128),B(25)
DIMENSION FILNAM(2),NAM(3)
COMMON /MAXICOM/ INB
DATA NO/128/,IN/128/,NCR/96/,NAM(1)/12H MAXIMOP /

C OPEN OUTPUT FILE

WRITE (6,6000)
READ (5,5000) FILNAM
WRITE (6,6005) FILNAM
CALL ASINFORT(2,OUTB(1),NO,FILNAM(1),1,1,-1,OUTA(1),128)
N=5
WRITE (6,6070)
READ (5,5040) IR
WRITE (6,6075) IR

C OPEN INPUT FILE

WRITE (6,6010)
READ (5,5010) IUSER
CALL COPY(4,NAM(1),1,IUSER,1)
WRITE (6,6015) NAM
CALL ASINFORT(1,INB(1),IN,NAM(1),2,1,-1,0,0)
WRITE (6,6050)
READ (5,5030) IANS
I=1
CALL COMP(I,IANS,1,1HO,1)
IF (I.EQ.1) NCR=72
IF (I.EQ.1) N=7
WRITE (6,6060) IANS

C READ SUBFILE NAME , AND SEARCH DIRECTORY

10 READ (5,5020) SFN
I=4
CALL COMP(I,SFN,1,4H####,1)
IF (I.EQ.4) GO TO 80
WRITE (6,6020)
CALL MAXIND(1,SFN,INS,NB)
IF (NB.GE.0) GO TO 20
WRITE (6,6024) SFN,INS,NB
GO TO 10
20 WRITE (6,6025) SFN,INS,NB
INCOUNT=0

C READ RECORDS SEQUENTIALLY FROM EACH BUCKET

DO 70 IB=1,NB
CALL READSR(1,INS+IB-1,1)
LB=MOD(INB(2),4096)
INW=3
30 LR=MINO((INB(INW)-1)*4,NCR)
IF (LR.LE.8) GO TO 60
INCOUNT=INCOUNT+1
CALL COPY(LR,B(1),1,INB(INW),5)
I=NCR-LR
IF (I.LE.0) GO TO 50
DO 40 J=1,I

```

40          CALL COPY(1,B(1),LR+J,1H,1)
50          IBUC=(IR-1)/N
          IREC=IR-IBUC*N
          IBUC=IBUC+1
          CALL WRITESR(2,IBUC,IREC,0)
          CALL WRITEST(2,NCR,B(1))
          IR=IR+1
60          INW=INW+INB(INW)
          IF (INW.LT.LB) GO TO 30
70  CONTINUE
WRITE (6,6040) INCOUNT,SFN
GO TO 10

80  CALL CLOSE(1)
CALL WRITESR(2,1,1,0)
CALL IWRITE(2,NCR)
CALL IWRITE(2,N)
CALL IWRITE(2,IR)
CALL CLOSE(2)
WRITE (6,6030) IR
STOP OK

```

```

5000 FORMAT(A8,A4)
5010 FORMAT(A4)
5020 FORMAT(A5)
5030 FORMAT(A1)
5040 FORMAT(IO)

```

```

6000 FORMAT(1H0,11HOUTPUT FILE)
6005 FORMAT(1H+,12X,A8,A4)
6010 FORMAT(1H0,15HINPUT FILE CODE)
6015 FORMAT(1H+,16X,3A4)
6020 FORMAT(1H0,7HSUBFILE)
6024 FORMAT(1H+,8X,A5,1X,9HNOT FOUND,2I4)
6025 FORMAT(1H+,8X,A5,1X,8HFOUND AT,15,2X,6HLENGTH,15)
6030 FORMAT(1H0,26HNEXT RECORD IN OUTPUT FILE,I7)
6040 FORMAT(1H,15,2X,25HRECORDS READ FROM SUBFILE,2X,A5)
6050 FORMAT(1H0,27HVERTICAL (V) OR OBLIQUE (O) )
6060 FORMAT(1H+,28X,A1)
6070 FORMAT(1H0,26HNEXT RECORD IN OUTPUT FILE)
6075 FORMAT(1H+,26X,I7)
END

```

C ***** MAXIND *****

```

SUBROUTINE MAXIND(ISTR,SFN,ISTRT,NBUC)
COMMON /MAXICOM/ IB(128)
DATA N/128/

DO 20 K=1,7
CALL READSR(ISTR,K,1)
IFRST=3
IF (K.EQ.1.OR.K.EQ.3.OR.K.EQ.5) IFRST=11
DO 10 J=IFRST,N,9
IF (IB(J).NE.9) GO TO 20
I=5
CALL COMP(I,SFN,1,IB(J+1),1)
IF (I.EQ.5) GO TO 30
10  CONTINUE
20  CONTINUE
ISTRT=-1
NBUC=-1
RETURN
30  ISTRT=IB(J+4)
NBUC=IB(J+5)
RETURN
END
FINISH

```

```

****
DOC DATA FILE
ARJRDATA02
860
ARJR
OBLIQUE
JAN1
JAN2
JAN3
###
****
FINISH

```

3. Listing of Program FIND

```

JOB XA<FIND>,ARJR,RASH
VOLUME 1000
RUN X63C,,,,1
****
DOC DATA X63C
#READ, ED,ARARATA03  ,,-1
#DICTIONARY
LENGTH C W0C0 4C
PLACE C W1C0 1C
YEAR C W1C1 2C
DAY C W2C0 3C
HOURS C W3C0 2C
MINUTES C W3C2 2C
FOF2 C W4C1 6C
H'F2 C W5C3 6C
FOF1 C W7C1 6C
H'F C W8C3 6C
FOE C W10C1 6C
H'E C W11C3 6C
FOES C W13C1 6C
H'ES C W14C3 6C
FBES C W16C1 6C
FMIN C W17C3 6C
MUF C W19C1 6C
M3000 C W20C3 4C
FXI C W21C3 6C
ESTYPE C W23C1 7C
#ENQUIRY
?ENQ1
(YEAR EQL '78' AND DAY BET '001','031')
#WRITE, ED, WORK1,0,0,0
#READ, ED, WORK1,0
#OPTION LP 120 LIST
#HEAD

```

VERTICAL INCIDENCE DATA FOR SANAE 1978

```

#SPACE 1
#PAGE
  YR DAY TIME FOF2 H'F2 FOF1 H'F FOE H'E FOES H'ES
  FBES FMIN MUF M3000 FXI ESTYPE
#SPACE 1
#CONTROL 1 DAY PAGE
#FORM
1A 2A 1B 3A 1B 2A 2A 1B 6A 6A 6A 6A 6A 6A 6A 6A 6A 6A 6A 4A 6A 7A
,PLACE
,YEAR
,DAY
,HOURS
,MINUTES
,FOF2
,H'F2
,FOF1
,H'F
,FOE
,H'E
,FOES
,H'ES
,FBES
,FMIN
,MUF
,M3000
,FXI
,ESTYPE
#STOP
****

```

4. Listing of Program FIDO

```

JOB XA<FIND>,ARJR,RASH
VOLUME 1000
RUN X63C,,,,1
****
DOC DATA X63C
#READ,ED,ARJRDATA02 ,,-1
#DICTIONARY
LENGTH C W0C0 4C
PLACE C W1C0 1C
YEAR C W1C1 2C
DAY C W2C1 3C
TIME C W3C2 4C
MODE C W5C0 6C
LLOF C W6C2 6C
MOF C W8C0 6C
JF C W9C2 6C
HLOF C W11C0 6C
EVFO C W12C2 6C
P' C W14C0 7C
EVH' C W15C3 5C
S C W17C0 3C
OFFSET C W17C3 5C
#ENQUIRY
?ENQ1
(YEAR EQL '76' AND DAY BET '001','031')
#WRITE,ED,WORK1,0,0,0
#READ,ED,WORK1,,0
#OPTION LP 120 LIST
#HEAD

```

```

SANAE - GRAHAMSTOWN OBLIQUE INCIDENCE DATA JANUARY 1976
#SPACE 1
#PAGE

```

```

YEAR DAY TIME MODE LLOF MOF JF HLOF EVFO P' E
VH' S OFFSET
#SPACE 1
#CONTROL 1 DAY PAGE
#FORM
1A 2A 2B 3A 2B 4A 2B 6A 6A 6A 6A 6A 6A 7A 5A 3A 5A
/PLACE
/YEAR
/DAY
/TIME
/MODE
/LLOF
/MOF
/JF
/HLOF
/EVFO
/P'
/EVH'
/S
/OFFSET
#STOP
****

```

5. The Program MEDI

(a) Use of the program MEDI

Submit as "JOB" :

% MEDI A, B, C, D, E, F, G, H, I, J

Where the parameters are :

A = JOB NAME e.g. FIND APR 78

Default = (SORT FIND)

B = VOLUME e.g. 1000

Default = (2000)

C = YEAR e.g. 78

Default = (76)

D = START DAY NUMBER e.g. 091

Default = (001)

E = END DAY NUMBER e.g. 120

Default = (031)

F = MODE e.g. 3F + E

Default = (2F)

G = WORD . CHARACTER of parameter to be ordered (see DICTIONARY)

e.g. 8.0 for MOF

Default = (2.1) (for DAY)

H = NUMBER OF CHARACTERS e.g. 4

Default = (3)

I = MONTH - YEAR HEADING e.g. APRIL 1978

Default = (JANUARY 1976)

J = LINES OR PAGE THROW e.g. 3 or PAGE

Default = (5)

(b) Listing of Program MEDI

```

JOB XA<SORT FIND>,ARJR,RASH
VOLUME XB<2000>
RUN X63C,,,,1
EXPECT HALTED HH
RUN XSDC,,,,1
EXPECT HALTED HH
RUN X63C,,,,1

```

```

****
DOC DATA X63C
#READ,ED,ARJRDATA02,,-1
#DICTIONARY
LENGTH C W0C0 4C
PLACE C W1C0 1C
YEAR C W1C1 2C
DAY C W2C1 3C
TIME C W3C2 4C
MODE C W5C0 6C
LLOF C W6C2 6C
MOF C W8C0 6C
JF C W9C2 6C
HLOF C W11C0 6C
EVFO C W12C2 6C
P' C W14C0 7C
EVH' C W15C3 5C
S C W17C0 3C
OFFSET C W17C3 5C

```

```

#ENQUIRY
?ENQ1
(YEAR EQL 'X<76>' AND DAY BET 'XD<001>', 'XE<031>')
?ENQ2
(MODE EQL 'XF<2F>' )
#WRITE,ED,WORK1,0,0,0
#STOP

```

```

****
DOC DATA XSDC
XSDC,KEYQ2(2,01D,XG<2.1>,XH<3>;1,01A,3.2,4),
XSDC,NUM01,
XSDC,INP(WORK1(0000))DA,
XSDC,WOR01(WORK2(0000)),
XSDC,WOR02(WORK1(0000)),
XSDC,OUT(WORK2(0000))DA,
XSDC,COR18000,
XSDC,END,

```

```

****
DOC DATA X63C
#READ,ED,WORK2,,-1
#DICTIONARY
LENGTH C W0C0 4C
PLACE C W1C0 1C
YEAR C W1C1 2C
DAY C W2C1 3C
TIME C W3C2 4C
MODE C W5C0 6C
LLOF C W6C2 6C
MOF C W8C0 6C
JF C W9C2 6C
HLOF C W11C0 6C
EVFO C W12C2 6C
P' C W14C0 7C
EVH' C W15C3 5C
S C W17C0 3C
OFFSET C W17C3 5C

```

```

#ENQUIRY
?ENQ1
(YEAR EQL 'X<76>' AND DAY BET 'XD<001>', 'XE<031>')
?ENQ2
(MODE EQL 'XF<2F>' )
#WRITE,ED,WORK1,0,0,0
#READ,ED,WORK1,,0
#OPTION LP 120 LIST ALL ENQ1,ENQ2
#HEAD

```

SANAE - GRAHAMSTOWN OBLIQUE INCIDENCE DATA JANUARY 1976
2F MODE
#PAGE

YEAR DAY TIME MODE LLOF MOF JF HLOF EVFO P' E

VH' S OFFSET COUNT

```
#SPACE 1
#CONTROL 1 TIME %J<5>
#FORM
1A 2A 2B 3A 2B 4A 2B 6A 6A 6A 6A 6A 7A 5A 3A 5A 3B 2X
#PLACE
#YEAR
#DAY
#TIME
#MODE
#LLOF
#MOF
#JF
#HLOF
#EVFO
#PI
#EVH'
#S
#OFFSET,///1
#COUNT,1
#STOP
****
```

APPENDIX D

MONTHLY MEDIAN OBLIQUE INCIDENCE DATA FOR WINTER
(AUGUST 1975) AND SUMMER (JANUARY 1976)

MONTHLY MEDIANS AUGUST 1975 2F MODE

TIME	COUNT	LLOF	MOF	EVFO	P'	EVH'F
0005	12	5.1	8.0	2.0	4622	216
0105	13	5.0	8.4	2.1	4627	220
0205	19	5.0	8.9	2.2	4625	218
0305	18	4.6	8.5	2.2	4641	233
0405	17	5.0	8.4	2.2	4640	232
0505	15	5.2	11.1	2.8	4628	221
0605	9	7.6	10.8	2.9	4658	247
0705	18	10.6	15.0	3.9	4639	231
0805	22	11.7	16.6	4.3	4637	229
0905	21	13.2	16.9	4.4	4641	233
1005	21	13.8	18.3	5.2	4676	262
1105	21	13.8	18.8	5.3	4670	257
1205	21	13.8	19.5	5.5	4674	260
1305	23	13.6	19.8	5.4	4661	250
1405	22	11.1	19.7	5.3	4650	240
1505	22	9.8	17.5	4.5	4637	229
1605	21	7.9	14.2	3.7	4638	230
1705	19	6.0	10.0	2.6	4647	238
1805	16	5.0	7.8	2.0	4647	238
1905	7	5.0	5.8	1.5	4637	229
2005	3	4.6	6.0	1.5	4642	233
2105	3	4.0	5.4	1.5	4690	273
2205	7	5.0	7.2	1.8	4639	231
2305	14	5.0	6.8	1.7	4633	226

TIME IN UT, FREQUENCIES IN MHZ, P' & EVH'F IN KM

MONTHLY MEDIANS AUGUST 1975 3F MODE

TIME	COUNT	LLOF	MOF	EVFO	P'	EVH'F
0005	10	4.3	5.8	1.7	4716	210
0105	15	4.0	5.9	1.8	4735	220
0205	17	4.0	5.9	1.8	4728	217
0305	13	3.6	5.8	1.8	4726	216
0405	15	4.0	6.0	2.0	4764	234
0505	13	4.2	6.9	2.2	4758	231
0605	16	6.4	9.6	3.3	4785	244
0705	21	6.4	11.0	3.6	4750	227
0805	20	8.8	12.2	3.9	4732	219
0905	19	10.0	12.7	4.1	4741	223
1005	19	10.6	14.1	5.1	4828	263
1105	17	10.7	14.5	5.2	4814	257
1205	20	10.7	15.0	5.3	4808	254
1305	21	10.2	15.1	5.2	4793	248
1405	20	9.7	14.9	4.9	4762	233
1505	23	7.7	13.8	4.4	4741	223
1605	20	6.3	11.0	3.5	4732	219
1705	18	5.0	7.5	2.4	4737	221
1805	11	4.5	6.3	2.0	4740	223
1905	5	3.6	4.9	1.5	4721	213
2005	2	4.3	5.7	1.8	4728	217
2105	3	3.9	5.7	1.7	4707	206
2205	7	4.5	5.9	1.8	4735	220
2305	8	4.6	6.2	1.9	4735	220

TIME IN UT, FREQUENCIES IN MHZ, P' & EVH'F IN KM

MONTHLY MEDIANS AUGUST 1975 4F MODE

TIME	COUNT	LLOF	MOF	EVFO	P'	EVH'F
0005	3	4.0	5.5	2.1	4888	224
0105	6	3.6	4.8	1.8	4869	219
0205	9	3.5	4.9	1.8	4855	214
0305	5	3.5	4.8	1.9	4890	225
0405	4	3.6	4.7	1.9	4919	234
0505	10	3.8	5.7	2.1	4855	214
0605	14	5.2	7.8	3.2	4945	241
0705	19	6.6	9.2	3.6	4885	223
0805	18	7.9	10.0	3.9	4893	226
0905	11	9.0	10.7	4.4	4938	239
1005	9	9.0	11.2	5.0	5024	264
1105	13	9.4	11.7	5.2	5019	262
1205	9	10.0	12.4	5.5	5010	260
1305	12	9.4	12.3	5.2	4964	247
1405	16	8.3	11.7	4.8	4925	236
1505	22	7.3	11.3	4.4	4885	223
1605	19	5.6	8.7	3.4	4873	220
1705	14	4.3	6.0	2.3	4883	223
1805	6	4.1	5.3	2.1	4907	230
1905	0	-	-	-	-	-
2005	0	-	-	-	-	-
2105	0	-	-	-	-	-
2205	3	3.0	3.9	1.4	4845	211
2305	2	3.8	5.9	2.2	4853	213

TIME IN UT, FREQUENCIES IN MHZ, P' & EVH'F IN KM

MONTHLY MEDIANS JANUARY 1976 2F MODE

TIME	COUNT	LLOF	MOF	EVFO	P'	EVH'F
0005	24	5.4	8.8	2.8	4672	259
0105	24	5.3	7.6	2.4	4697	279
0205	22	5.5	8.4	2.3	4667	256
0305	20	7.7	9.4	2.7	4677	264
0405	24	8.3	10.7	3.1	4660	249
0505	26	10.0	12.7	3.7	4658	248
0605	20	12.3	15.4	4.2	4663	252
0705	20	13.4	16.5	4.9	4674	261
0805	13	14.5	17.3	5.4	4692	275
0905	15	14.5	17.6	5.6	4692	275
1005	13	13.0	17.3	5.6	4727	302
1105	17	14.9	17.3	5.8	4708	288
1205	20	14.3	17.7	5.7	4692	275
1305	19	14.1	17.8	5.6	4686	271
1405	19	14.5	17.4	5.1	4679	265
1505	24	13.6	17.0	5.2	4687	271
1605	21	13.2	16.6	5.1	4697	279
1705	19	12.5	14.7	4.5	4675	262
1805	23	13.0	15.0	4.3	4684	269
1905	24	10.2	14.0	4.3	4676	262
2005	21	7.7	11.6	3.7	4669	257
2105	17	6.5	10.7	3.4	4667	255
2205	23	5.6	9.3	2.8	4671	259
2305	21	5.6	8.8	2.7	4662	251

TIME IN UT, FREQUENCIES IN MHZ, P' & EVH'F IN KM

MONTHLY MEDIANS JANUARY 1976 3F MODE

TIME	COUNT	LLOF	MOF	EVFO	P'	EVH'F
0005	23	4.9	6.7	2.5	4818	260
0105	19	4.8	6.7	2.3	4815	259
0205	13	5.4	7.2	2.8	4796	250
0305	17	7.5	8.4	2.8	4816	259
0405	21	8.0	10.5	3.9	4805	254
0505	23	9.3	11.5	4.2	4820	261
0605	25	10.0	12.3	4.6	4803	253
0705	23	10.2	12.8	4.7	4828	264
0805	20	10.0	13.2	5.1	4884	288
0905	15	11.3	13.2	5.4	4850	274
1005	13	10.9	14.1	5.3	4863	279
1105	11	11.4	15.1	5.7	4837	268
1205	11	11.5	14.1	5.4	4833	266
1305	13	11.3	14.4	5.1	4817	259
1405	10	12.1	13.8	5.2	4839	269
1505	15	11.2	13.3	5.1	4822	262
1605	18	11.0	13.0	5.1	4813	258
1705	19	10.9	13.3	4.5	4784	245
1805	16	11.4	13.8	4.9	4775	241
1905	16	7.9	11.6	4.6	4778	242
2005	18	7.3	9.5	3.8	4787	246
2105	17	5.5	8.7	2.9	4790	247
2205	19	5.0	7.3	3.1	4796	250
2305	19	4.6	6.9	2.5	4804	254

TIME IN UT, FREQUENCIES IN MHZ, P' & EVH'F IN KM

MONTHLY MEDIANS JANUARY 1976 4F MODE

TIME	COUNT	LLOF	MOF	EVFO	P'	EVH'F
0005	5	4.3	6.0	2.6	4882	222
0105	5	4.7	6.1	2.9	4903	229
0205	3	5.5	6.5	2.8	4892	225
0305	6	7.3	8.3	3.9	4929	236
0405	5	8.3	9.6	4.2	4909	230
0505	8	8.1	9.3	4.4	5011	260
0605	5	9.8	10.9	4.8	4998	256
0705	3	10.4	13.1	4.9	5019	262
0805	2	11.0	13.0	5.0	5009	259
0905	2	11.6	14.0	5.8	4955	244
1005	2	10.1	12.0	5.2	4930	237
1105	1	10.0	11.0	-	5007	259
1205	1	10.8	13.4	-	5051	271
1305	1	10.3	11.2	-	5007	259
1405	0	-	-	-	-	-
1505	3	10.4	11.0	-	5049	270
1605	4	10.4	11.8	4.7	4962	246
1705	3	10.1	11.7	4.9	4927	236
1805	5	9.8	11.4	5.0	4913	232
1905	11	7.8	9.1	3.8	4938	239
2005	7	6.4	9.4	4.1	4899	227
2105	5	5.2	7.2	4.6	4891	225
2205	4	4.6	6.4	-	4987	253
2305	6	4.6	6.0	3.1	4922	234

TIME IN UT, FREQUENCIES IN MHZ, P' & EVH'F IN KM

APPENDIX E

PROGRAMS FOR OBTAINING N(H)
PROFILES FROM OBLIQUE IONOGRAMS

- (1.) Stepwise formulation of the Smith (1970) method.
- (2.) Listing of program NHSMITH (including subroutine DELTADIST).
- (3.) Stepwise formulation of the Rao (1973) method.
- (4.) Listing of program NHRAO (including subroutines DELTAPATH, etc.)
- (5.) Listing of program NHGEORGE for George (1970) method.

(1.) Smith Method (Program NHSMITH)

(a) For nth Segment

1. Input (P_n, f_n) point from oblique ionogram.
2. Square of plasma frequency (from (5.38))

$$f_{N_n}^2 = f_n^2 \left(1 - \frac{D^2}{P_n^2} \right)$$

3. Minimum and maximum elevation angles (from (5.43) and (5.44)) :

$$\Delta_{\min_n} = \cos^{-1} \left[\frac{r_{n-1}}{R} \sqrt{1 - \frac{f_{N_{n-1}}^2}{f_n^2}} \right]$$

$$\Delta_{\max_n} = \cos^{-1} \left[\frac{r_{n-1}}{R} \sqrt{1 - \frac{f_{N_n}^2}{f_n^2}} \right]$$

For each of a number of trial Δ_j 's, $\Delta_{\min_n} < \Delta_j < \Delta_{\max_n}$, perform

steps 4. - 10. below (subroutine DELTADIST) to determine ground ranges D_j covered at these elevation angles.

From experience, set

$$\Delta_1 = \frac{\Delta_{\min_n} + \Delta_{\max_n}}{2}$$

$$\Delta_2 = \Delta_{\max_n} - (\Delta_{\max_n} - \Delta_{\min_n}) \times 0.01$$

for first two trial Δ_j 's.

Subroutine DELTADIST (steps 4 - 10)

4. Radius of reflection (from (5.39)) :

$$r_n = \frac{P_n}{D} R \cos \Delta_j$$

5. Segment constants (from (5.40) and (5.41)) :

$$A_n = \frac{f_{N_n}^2 r_n - f_{N_{n-1}}^2 r_{n-1}}{r_n - r_{n-1}}$$

$$B_n = r_{n-1} (A_n - f_{N_{n-1}}^2)$$

6. Constant c (from (5.25)),

$$c = -R^2 \cos^2 \Delta_j$$

7. For each segment $i = 1, \dots, n$, constants a and b (from (5.25)) :

$$a = 1 - \frac{A_i}{f_n^2}$$

$$b = \frac{B_i}{f_n^2}$$

and ground range in segment i (from (5.26)) :

$$D_i = R \left[\sin^{-1} \left(\frac{br + 2c}{r \sqrt{b^2 - 4ac}} \right) \right]_{r_{i-1}}^{r_i}$$

8. Sum these to obtain $\sum_{i=1}^n D_i$

9. Ground range below ionosphere (from (5.21)) :

$$D_o = R \left[\cos^{-1} \left(\frac{R}{r_o} \cos \Delta_j \right) - \Delta_j \right]$$

10. Total ground range (from (5.28)) :

$$D_j = 2D_o + 2 \sum_{i=1}^n D_i$$

11. For $j > 2$, perform successive linear interpolations for next Δ_j using previous two trial values :

$$\Delta_j = \Delta_{j-2} + (\Delta_{j-1} - \Delta_{j-2}) \frac{(D - D_{j-2})}{(D_{j-1} - D_{j-2})}$$

where $D =$ true ground range.

Proceed until either

(i) $|D - D_j| < \delta$, in which case put $\Delta_n = \Delta_j$

- or (ii) $j = j_{\text{end}}$, in which case perform Lagrange interpolation on the set (D_j, Δ_j) to find Δ_n which yields D . With this "true" elevation angle Δ_n

12. Radius of reflection (from (5.39)) :

$$r_n = \frac{P_n}{D} R \cos \Delta_n$$

13. Segment constants (from (5.40) and (5.41)) :

$$A_n = \frac{f_{N_n}^2 r_n - f_{N_{n-1}}^2 r_{n-1}}{r_n - r_{n-1}}$$

$$B_n = r_{n-1} \left(A_n - f_{N_{n-1}}^2 \right)$$

14. Output electron density and true height :

$$N_n = 12404.45 f_{N_n}^2$$

$$h_n = r_n - R$$

and return to 1. for next point.

15. When terminator P = 9999 is read in, fit parabola for profile peak as follows :

$$\text{Define } x_1 = r_{n-2}, \quad x_2 = r_{n-1}, \quad x_3 = r_n$$

$$y_1 = N_{n-2}, \quad y_2 = N_{n-1}, \quad y_3 = N_n$$

Determinant

$$\det = x_1^2 (x_2 - x_3) - x_2^2 (x_1 - x_3) + x_3^2 (x_1 - x_2)$$

Parameters a, b, c (from (5.54)) :

$$a = \frac{y_1 (x_2 - x_3) - y_2 (x_1 - x_3) + y_3 (x_1 - x_2)}{\det}$$

$$b = \frac{x_1^2 (y_2 - y_3) - x_2^2 (y_1 - y_3) + x_3^2 (y_1 - y_2)}{\det}$$

$$c = \frac{x_1^2 (x_2 y_3 - x_3 y_2) - x_2^2 (x_1 y_3 - x_3 y_1) + x_3^2 (x_1 y_2 - x_2 y_1)}{\det}$$

16. Peak height and electron density (from (5.56) and (5.57)) :

$$h_{\max} = -\frac{b}{2a} - R$$

$$N_{\max} = ah_{\max}^2 + bh_{\max} + c$$

(b) For 1st Segment

1. Input minimum base height $h_{o \min}$ and first two points (P_1, f_1) , (P_2, f_2) from oblique ionogram.

2. Square of plasma frequency for first point (from (5.38)) :

$$f_{N_1}^2 = f_1^2 \left(1 - \frac{D^2}{P_1^2} \right)$$

3. Minimum and maximum values of base radius (from (5.46)) :

$$r_{o \min} = R + h_{o \min}$$

$$r_{o \max} = R \cos\left(\frac{D}{2R}\right) + R \sin\left(\frac{D}{2R}\right) \sqrt{\frac{P_1^2}{D^2} - 1}$$

For each of a number of trial r_{o_k} 's ($r_{o \min} \leq r_{o_k} < r_{o \max}$) perform steps 4 - 10 below.

4. Min. and max. elevation angles (from (5.45) & (5.43)) :

$$\Delta_{\min_1} = \tan^{-1} \left(\frac{r_{o_k} \cos\left(\frac{D}{2R}\right) - R}{r_{o_k} \sin\left(\frac{D}{2R}\right)} \right)$$

$$\Delta_{\max_1} = \cos^{-1} \left(\frac{r_{o_k}}{R} \sqrt{1 - \frac{f_{N_1}^2}{f_1^2}} \right)$$

For each of a number of trial Δ_j 's, $\Delta_{\min_1} < \Delta_j < \Delta_{\max_1}$, perform

steps 4 - 10 of (a) to determine ground ranges D_j covered at these elevation angles (subroutine DELTADIST) with $r_o = r_{o_k}$.

First interpolation : as in step 11. of (a), find Δ which yields true ground range D . With this Δ_1 , proceed with steps 5 - 10 below.

5. Radius of reflection (from (5.39)) :

$$r_1 = \frac{P_1}{D} R \cos \Delta_1$$

6. Segment constants (from (5.40) and (5.41)) :

$$A_1 = \frac{f_{N_1}^2 r_1}{r_1 - r_{o_k}} \quad (\text{since } f_{N_{n-1}}^2 = f_{N_o}^2 = 0)$$

$$B_1 = r_{o_k} A_1$$

7. Use these constants and (P_2, f_2) :
square of plasma frequency (from (5.38)) :

$$f_{N_2}^2 = f_2^2 \left(1 - \frac{D^2}{P_2^2} \right)$$

8. Radius of reflection (from (5.20)) :

$$r_2 = \frac{B_1}{A_1 - f_{N_2}^2}$$

9. Elevation angle (from (5.49)) :

$$\Delta_2 = \cos^{-1} \left(\frac{D}{P_2} \frac{r_2}{R} \right)$$

10. Perform steps 4 - 10 of (a) (subroutine DELTADIST) with $\Delta_j = \Delta_2$ to determine ground range D_k covered by ray at this elevation angle.

11. Second interpolation :

Use $r_{o_1} = r_{o_{\min}}$

and $r_{o_2} = r_{o_{\max}} - (r_{o_{\max}} - r_{o_{\min}}) \times 0.01$

and then for $k > 2$, successive linear interpolation for next r_{o_k} :

$$r_{o_k} = r_{o_{k-2}} + (r_{o_{k-1}} - r_{o_{k-2}}) \frac{(D - D_{k-2})}{(D_{k-1} - D_{k-2})}$$

where $D =$ true ground range.

Proceed with steps 4 - 10 above until either

(i) $|D - D_k| < \delta,$

in which case put $r_o = r_{o_k}$

or(ii) $k = k_{\text{end}},$

in which case perform Lagrange interpolation on the set

(D_k, r_{o_k}) to find r_o which yields true $D.$

12. With this "true" r_o (if (ii)) repeat steps 4 - 10.

(2.) Listing of program NHSMITH

```
C ***** NHSMITH
C
C   MASTER NHSMITH
C   =====
C THIS PROGRAM CALCULATES AN EFFECTIVE N(H) PROFILE FROM
C P,F DATA ON AN OBLIQUE IONOGRAM BY THE SEGMENT METHOD
C OF M.S.SMITH REF. J.A.T.P. 32, 1047 (1970).
C INPUT DATA COMPATIBLE WITH THAT FOR PROGRAM OVIO
    REAL DELTA(10),DJGUESS(10),DKGUESS(10),ROGUESS(10),
    +     EDENS(50),HEAD(4),HEIGHT(50),DENSITY(50)
    DOUBLE PRECISION X(3),Y(3),DET
    COMMON/DUNK/IPRINT,A(50),B(50),R(50),RN,RM,RO,RE,
    +     D,P,N,F,F2,FN2N,FN2M
    COMMON/AMGRAPH3/CHAR,NCROSS,ISUP,ISO,NOAXES,NONUMX,NONUMY

C CANNOT USE DATA STATEMENT FOR COMMON VARIABLES
    D = 4470.84
    RE = 6371.35
    DACCUR = 0.02

C INPUT IONOGRAM I.D. DATA AND PLOTTING DATA
    READ(5,5010) HEAD,OFFSET
    READ(5,5020) IPLOT,IPRINT,IC,NHD,J,K,N,NPL,NPX,NPY
    READ(5,5030) ESIZE,HSIZE
    READ(5,5040) NHOP,HOMIN,JEND,KEND,IFILE,KARRAY,KCOEFF

C DOUBLE INTERPOLATION FOR BASE HEIGHT HO
C INPUT FIRST TWO P,F PAIRS
    READ(5,5030) P1,FA
    READ(5,5030) P2,FB

    P1=(P1+OFFSET)/FLOAT(NHOP)
    P2=(P2+OFFSET)/FLOAT(NHOP)
    D=D/FLOAT(NHOP)

    N=1
    P=P1
    F=FA
    DELTAN=0.0

C LOWER AND UPPER BOUNDS ON RO
    ROMIN=RE+HOMIN
    PHI=D/(2.0*RE)
    ROMAX=RE*COS(PHI)+RE*SIN(PHI)*SQRT(P*P/(D*D)-1.0)
    IF(ROMIN.GE.ROMAX) ROMIN=ROMAX-10.0
    HO=ROMAX-RE

C PRINT IONOGRAM I.D. AND HO LIMITS
    IF(IPRINT.EQ.0) WRITE(6,6000)
    WRITE(6,6010) HEAD(2),HEAD(3),HEAD(4),NHOP
    WRITE(6,6020) HOMIN,HO,RE,D

C SET FLAG AND LOOP THRU FOR UP TO KEND GUESSES OF RO
    ROGUESS(1)=ROMIN
    ROGUESS(2)=ROMAX-(ROMAX-ROMIN)*0.01
    IFLAG=0
    K=1

10  RO=ROGUESS(K)
    HO=RO-RE
    IF(IPRINT.EQ.1) WRITE(6,7010) K,RO,HO
20  RM=RO
    FN2M=0.0
    GO TO 40

C MAIN LOOP : INPUT PATH,FREQUENCY PAIR
```

```

30  READ(5,5030) P,F
    IF(P.EQ.9999.) GO TO 160
    P=(P+OFFSET)/FLOAT(NHOP)
C PLASMA FREQUENCY SQUARED (ENSURE FN2N > LAST FN2N)
40  F2=F*F
    FN2N=F2*(1.-D*D/(P*P))
    IF(FN2N.GT.FN2M+0.01) GO TO 50
    P=P+1.0/FLOAT(NHOP)
    GO TO 40
50  CONTINUE
    IF(IPRINT.EQ.1,AND,IFLAG.GT.0) WRITE(6,6000)
    IF(IPRINT.EQ.1) WRITE(6,7020) N,F,F2,FN2N,RM,P,D
C MIN AND MAX ELEVATION ANGLES
    IF(N.EQ.1) DELMIN=ATAN((RO*COS(PHI)-RE)/(RO*SIN(PHI)))
    IF(N.GT.1) DELMIN=ACOS((RM/RE)*SQRT(1.0-FN2M/F2))
    DELMAX=ACOS(RM*D/(P*RE))
    DELMAX=DELMIN+ABS(DELMAX-DELMIN)
    IF(IPRINT.EQ.1) WRITE(6,7030) DELMIN,DELMAX
C GROUND DISTANCE FOR EACH OF UP TO JEND ANGLES
C LINEAR INTERPOLATION TO OBTAIN SUCCESSIVE GUESSES
    DELTA(1)=DELMIN+(DELMAX-DELMIN)*0.10
    DELTA(2)=DELMAX-(DELMAX-DELMIN)*0.01
    J=1
60  CONTINUE
    IF(DJGUESS(1).LT.D) DELTA(3)=(3.0*DELMIN+DELMAX)/4.0
    IF(IPRINT.EQ.1) WRITE(6,7040) J,DELTA(J)
    CALL DELTADIST(DELTA(J),DJGUESS(J))
    IF(ABS(DJGUESS(J)-D).LT.DACCUR) GO TO 80
    J=J+1
    IF(J.GT.JEND) GO TO 70
    IF(J.EQ.2) GO TO 60
    DELTA(J)=DELTA(J-2)+(DELTA(J-1)-DELTA(J-2))
    + *(D-DJGUESS(J-2))/(DJGUESS(J-1)-DJGUESS(J-2))
    GO TO 60
C INTERPOLATE FOR DELTA GIVING TRUE DISTANCE
70  DELTAN=ALAGRANGE(DJGUESS,DELTA,D,JEND)
    GO TO 90
C TRUE RADIUS R(N) AND SEGMENT CONSTANTS A(N),B(N)
80  DELTAN=DELTA(J)
90  R(N)=P*RE*COS(DELTAN)/D
    RN=R(N)
    A(N)=(FN2N*RN-FN2M*RM)/(RN-RM)
    B(N)=RM*(A(N)-FN2M)
    IF(IPRINT.EQ.1) WRITE(6,7050) N,DELTAN,RN,A(N),B(N)
    IF(IFLAG.EQ.0) GO TO 110
C ELECTRON DENSITY AND TRUE HEIGHT
100 RN=RN-RE
    EDENS(N)=FN2N*12404.45
    DELTAN=DELTAN*57.29577951
    FN2N=SQRT(FN2N)
    IF(IPRINT.EQ.1) WRITE(6,6040)
    WRITE(6,6050) RN,EDENS(N),A(N),B(N),N,FN2N,F,P,DELTAN
C RETURN TO READ NEXT P,F PAIR FOR NEXT SEGMENT
    DELTAN=DELTAN/57.29577951
    FA=F
    FN2M=FN2N*FN2N
    RM=R(N)
    N=N+1

```

```

        IF(IFLAG.EQ.1) GO TO 150
        GO TO 30
C END OF MAIN LOOP
C FOR EACH TRIAL RO, DISTANCE FOR ELEVATION ANGLE DELTA2
C AT FREQUENCY FB (IFLAG = 0)
110    P=P2
        F=FB
        F2=F*F
        FN2N=F2*(1.-D*D/(P*P))
        RN=B(1)/(A(1)-FN2N)
        DELTA2=ACOS(D*RN/(P*RE))
        IF(IPRINT.EQ.1) WRITE(6,7060) K,RO,RN,DELTA2,F,FN2N,P
        CALL DELTADIST(DELTA2,DKGUESS(K))
        P=P1
        F=FA
        IF(ABS(DKGUESS(K)-D).LT.DACCUR) GO TO 130
        K=K+1
        IF(K.EQ.2) GO TO 10
        IF(K.GT.KEND) GO TO 120
        ROGUESS(K)=ROGUESS(K-2)+(ROGUESS(K-1)-ROGUESS(K-2))
+      * (D-DKGUESS(K-2))/(DKGUESS(K-1)-DKGUESS(K-2))
        GO TO 10
C INTERPOLATE FOR RO GIVING TRUE DISTANCE
120    RO=ALAGRANGE(DKGUESS,ROGUESS,D,KEND)
        GO TO 140
130    RO=ROGUESS(K)
C IONOSPHERIC BASE HEIGHT HO
140    HO=RO-RE
        WRITE(6,6030) HO
        IF(IPRINT.EQ.0) WRITE(6,6040)
        IF(IPRINT.EQ.1) WRITE(6,6000)
C RESET FLAG AND REPEAT USING 'TRUE' RO FOR N=1
        IFLAG=1
        IF(K.GT.KEND) GO TO 20
        FN2N=F*F*(1.0-D*D/(P*P))
        GO TO 90
C RESET FLAG AND REPEAT FOR N=2
150    P=P2
        F=FB
        IFLAG=2
        GO TO 40
C IF P=9999 HAS BEEN READ IN, DETERMINE PARAMETERS
C FOR PROFILE PEAK (ASSUMED PARABOLIC : NE=AR2+BR+C)
160    N=N+1
        DO 170 I=1,3
        X(I)=R(N+I-5)
170    Y(I)=EDENS(N+I-5)
180    DET=X(1)*X(1)*(X(2)-X(3))-X(2)*X(2)*(X(1)-X(3))
+      +X(3)*X(3)*(X(1)-X(2))
        AAP=(Y(1)*(X(2)-X(3))-Y(2)*(X(1)-X(3))
+      +Y(3)*(X(1)-X(2)))/DET
        BRP=(X(1)*X(1)*(Y(2)-Y(3))-X(2)*X(2)*(Y(1)-Y(3))
+      +X(3)*X(3)*(Y(1)-Y(2)))/DET
        CCP=(X(1)*X(1)*(X(2)*Y(3)-X(3)*Y(2))
+      -X(2)*X(2)*(X(1)*Y(3)-X(3)*Y(1))
+      +X(3)*X(3)*(X(1)*Y(2)-X(2)*Y(1)))/DET
C PEAK RADIUS AND EDENS (ENSURE R > LAST R)
        R(N)=-BRP/(2.0*AAP)
        IF(R(N).GT.R(N-2)) GO TO 190

```

```
X(3)=X(3)+0.10
R(N-2)=X(3)
GO TO 180

190 CONTINUE
IF(IPRINT.EQ.0) GO TO 200
WRITE(6,6000)
WRITE(6,7120)(I,X(I),Y(I),I=1,3)
WRITE(6,7130) DET,R(N),N

200 EDENS(N)=AAP*R(N)*R(N)+BBP*R(N)+CCP
R(N)=R(N)-RE
FN2N=SQRT(EDENS(N)/12404.45)
WRITE(6,6060) R(N),EDENS(N),FN2N,AAP,BBP,CCP

IF(IPLOT.EQ.0.AND.IFILE.EQ.0) GO TO 250

C SHIFT R,EDENS ARRAYS UP ONE POSITION

DO 210 I=1,N-2
J=N-I
A(J)=A(J-1)
B(J)=B(J-1)
R(J)=R(J-1)-RE
210 EDENS(J)=EDENS(J-1)
A(1)=0.0
B(1)=0.0
R(1)=H0
EDENS(1)=0.0
A(N)=AAP
B(N)=BBP
B(N+1)=CCP

C IF IPLOT = 1 PLOT PROFILE

IF(IPLOT.NE.1) GO TO 220
ISUP=1

CALL AMGRAPH(6,0,0,0,4HARJR,R,ESIZE,HSIZE,HEAD,NHD)
+ CALL AMAXISLABEL(23HELECTRON DENSITY (CM-3),
+ 11HEIGHT (KM),NPX,NPY)
+ CALL AMGRAPH(6,0,N,IC,EDENS,R,ESIZE,HSIZE,
+ 21HN(H) PROFILE (SMITH),NPL)
CALL AMGRAPH(6,0,0,2,EDENS,R,ESIZE,HSIZE,HEAD,0)

220 CONTINUE

C IF IFILE = 1 WRITE HEIGHT & DENSITY ARRAYS TO DISC
C IF IFILE = 2 WRITE A & B ARRAYS AS WELL

IF(IFILE.EQ.0) GO TO 250
WRITE(6,7100)
WRITE(6,7110)(I,R(I),EDENS(I),A(I),B(I),I=1,50)

CALL USEFILE(2,2HED,12HARJRDATA01 ,1,0)

IELEM=KARRAY
WRITE(6,7070) IELEM,N
CALL PUTARRAY(2,IELEM,R)
WRITE(6,7075) IELEM,N
CALL PUTARRAY(2,IELEM,EDENS)

IF(IFILE.NE.2) GO TO 250
IELEM=KCOEFF
WRITE(6,7080) IELEM,N
CALL PUTARRAY(2,IELEM,A)
N=N+1
WRITE(6,7085) IELEM,N
CALL PUTARRAY(2,IELEM,B)
N=N-1

250 STOP OK

C FORMAT STATEMENTS

5010 FORMAT(4A8,E0.0)
5020 FORMAT(10I0)
5030 FORMAT(2E0.0)
5040 FORMAT(10,E0.0,5I0)
```

```

6000 FORMAT(1H1)
6010 FORMAT(1H ,21X,36HN(H) PROFILE FROM OBLIQUE IONOGRAM ,3A8,
+      I4,10H HOP TRACE,/,1H ,21X,74(1H-),/,1H )
6020 FORMAT(1H0,23HBASE HEIGHT HO : MIN =,F7.2,7H MAX =,
+      F7.2,3H KM,9X,17HEARTH RADIUS RE =,F8.2,3H KM,8X,
+      12HDISTANCE D =,F8.2,3H KM,/,1H )
6030 FORMAT(1H0,29HINTERPOLATED BASE HEIGHT HO =,F7.2,3H KM,
+      7X,38HSMITH METHOD WITH SEGMENTS OF THE FORM ,
+      32H FN2 = A - B/R WHERE R = RE + H ,/,1H )
6040 FORMAT(1H0,29H H (KM) NE (CM-3)
+      40HSEGMENT PARAMETERS A(N),B(N) N
+      46HFN (MHZ) F (MHZ) P (KM) DELTA (DEG))
6050 FORMAT(1H0,F8.2,3(1PE16.4),I8,OPF12.4,F11.2,F13.2,F13.4)
6060 FORMAT(1H0,F8.2,1PE16.4,6X,30HPARABOLIC FIT FOR PROFILE PEAK,
+      OPF16.4,/,25H PEAK PARAMETERS A,B,C,3(1PE16.4))

7010 FORMAT(4H1K =,I3,13H ROGUESS =,F9.2,13H HOGUESS =,F8.2)
7020 FORMAT(/,4H N =,I3,6H F =,F7.2,7H F2 =,F8.2,8H FN2 =,
+      F7.2,7H RM =,F10.2,6H P =,F10.2,6H D =,F10.2)
7030 FORMAT(/,22H ELEV ANGLE DELTA MIN,F10.6,6H MAX,F10.6)
7040 FORMAT(/,4H J =,I3,13H DELTA(J) =,F12.6)
7050 FORMAT(/,4H N =,I3,13H DELTA(N) =,F10.6,
+      9H R(N) =,F9.2,20H CONSTANTS A(N) =,1PE12.4,
+      9H B(N) =,1PE12.4,/,1H ,100(1H-))
7060 FORMAT(/,4H K =,I3,13H ROGUESS =,F9.2,9H R(2) =,F9.2,
+      13H DELTA(2) =,F10.6,6H F =,F6.2,8H FN2 =,
+      F6.2,6H P =,F9.2,/,1H )
7070 FORMAT(/,41H FIRST FILE ELEMENT NO FOR HEIGHT ARRAY,16,
+      13H ARRAY SIZE,I6)
7075 FORMAT(/,41H FIRST FILE ELEMENT NO FOR DENSITY ARRAY,16,
+      13H ARRAY SIZE,I6)
7080 FORMAT(/,41H FIRST FILE ELEMENT NO FOR A SEG COEFFS,16,
+      13H ARRAY SIZE,I6)
7085 FORMAT(/,41H FIRST FILE ELEMENT NO FOR B SEG COEFFS,16,
+      13H ARRAY SIZE,I6)
7100 FORMAT(23H1ARRAYS WRITTEN TO DISC,/,4H I,8X,4HR(I),
+      9X,8HEDENS(I),10X,4HA(I),12X,4HB(I),/,1H )
7110 FORMAT(1H ,I3,OPF14.4,1P3E17.6)
7120 FORMAT(1H ,I3,1P2D24.10)
7130 FORMAT(/,6H DET =,1PD22.10,11H RMAX =,E16.6,
+      8H N =,I4)
END

```

```

C ***** DELTADIST
C   SUBROUTINE DELTADIST(DEL,DIST)
C   =====
C THIS SUBROUTINE CALCULATES TOTAL GROUND DISTANCE DIST
C COVERED BY A RAY WITH ELEVATION ANGLE DEL
C   EXTERNAL DDFUN
C   DOUBLE PRECISION AA,BB,CC,XX,RRE
C   COMMON/FUNK/AA,BB,CC,XX,RRE
C   COMMON/DUNK/IPRINT,A(50),B(50),R(50),RN,RM,RO,RE,
+     D,P,N,F,F2,FN2N,FN2M
C CALCULATE RADIUS R(N)
C   R(N)=P*RE*COS(DEL)/D
C   RN=R(N)
C SEGMENT CONSTANTS A(N),B(N)
C   A(N)=(FN2N*RN-FN2M*RM)/(RN-RM)
C   B(N)=RM*(A(N)-FN2M)
C   IF(IPRINT.EQ.1) WRITE(6,7010) N,R(N),A(N),B(N)
C   IF(IPRINT.EQ.1) WRITE(6,7020)
C GROUND DISTANCE FOR ALL SEGMENTS I FROM 1 TO N
C DEFINE CONSTANTS AA,BB,CC
C   DISUM=0.
C   CC=-RE*RE*COS(DEL)*COS(DEL)
C   DO 10 I=1,N
C   AA=1.-A(I)/F2
C   BB=B(I)/F2
C DEFINE LIMITS AND CALCULATE INTEGRAL FOR SEGMENT I
C   IF(I.EQ.1) RLOWER=RO
C   IF(I.GT.1) RLOWER=R(I-1)
C   IF(IPRINT.EQ.1) WRITE(6,7030) I,AA,BB,CC,RLOWER,R(I)
C   DISEG=DDFUN(R(I))-DDFUN(RLOWER)
C GROUND DISTANCE OF RAY WHILE PASSING THRU SEGMENT I AND SUM
C   IF(IPRINT.EQ.1) WRITE(6,7040) DISEG
C   DISEG=RE*RE*COS(DEL)*DISEG
C   DISUM=DISUM+DISEG
10  IF(IPRINT.EQ.1) WRITE(6,7050) DISEG,DISUM
C   CONTINUE
C TOTAL GROUND DISTANCE (GUESS) AND RETURN
C   DFRSP=RE*(ACOS(RE*COS(DEL)/RO)-DEL)
C   DIST=2.0*DFRSP+2.0*DISUM
C   IF(IPRINT.EQ.1) WRITE(6,7060) DFRSP,DISUM,DIST
C   RETURN
C FORMAT STATEMENTS
7010 FORMAT(4H N =,I3,9H R(N) =,F10.2,9H A(N) =,1PE12.4,
+ 9H B(N) =,1PE12.4,25H SUBROUTINE DELTADIST)
7020 FORMAT(3H I,7X,2HAA,11X,2HBB,11X,2HCC,7X,10HRLOWER,
+ 17HRUPPER,11X,RINTEG,8X,15HDISEG,15H DISUM)
7030 FORMAT(1H I,2,3(1PD13.4),2(OPF10.2))
7040 FORMAT(1H+,61X,1PE13.4)
7050 FORMAT(1H+,74X,2F10.2)
7060 FORMAT(13H DFRSP =,F10.2,16H DIONOSPHERE =,F10.2,
+ 22H GROUND DIST GUESS =,F10.2)
C   END

```

```
C ***** DDFUN
C FUNCTION DDFUN(R)
C =====
C DOUBLE PRECISION AA, BB, CC, XX, RR, RRE
C COMMON/FUNK/AA, BB, CC, XX, RRE
C RR=R
C XX=(BB*RR+2.0D00*CC)/(DABS(RR)
+ *DSQRT(DABS(BB*BB-4.0D00*AA*CC)))
C DDFUN=DATAN2(XX, DSQRT(DABS(1.0D00-XX*XX)))/DSQRT(-CC)
C RETURN
C END
```

(3.) Rao method (Program NHRAO)

(a) FOR nth SEGMENT

1. Input (P_n, f_n) point from oblique ionogram.
2. Smith approximation for square of plasma frequency (from (5.38)) :

$$f_{N_n}^2 = f_n^2 \left(1 - \frac{D^2}{P_n^2} \right)$$

3. Smith approximation for max. and min. elevation angles (from (5.43) and (5.44)) :

$$\Delta_{\min_n} = \cos^{-1} \left[\frac{r_{n-1}}{R} \sqrt{1 - \frac{f_{N_{n-1}}^2}{f_n^2}} \right]$$

$$\Delta_{\max_n} = \cos^{-1} \left[\frac{r_{n-1}}{R} \sqrt{1 - \frac{f_{N_n}^2}{f_n^2}} \right]$$

For each of a number of trial Δ_j 's, $\Delta_{\min_n} < \Delta_j < \Delta_{\max_n}$, perform

steps 4 - 12 below to determine pathlength P_j for each of these elevation angles. (Subroutine DELTAPATH)

For the first two trial Δ_j 's use

$$\Delta_1 = \Delta_{\min} + (\Delta_{\max} - \Delta_{\min}) \times 0.01$$

$$\Delta_2 = \Delta_{\max} - (\Delta_{\max} - \Delta_{\min}) \times 0.01$$

and then obtain successive Δ_j 's by linear interpolation (see step 12).

Subroutine DELTAPATH (steps 4 - 11)

4. Ground range below ionosphere (from (5.21)) :

$$D_o = R \left[\cos^{-1} \left(\frac{R}{r_o} \cos \Delta_j \right) - \Delta_j \right]$$

5. For each segment $1 \leq i \leq n - 1$, constants and ground range in this segment (from (5.25) and (5.26)) :

$$a = f_n^2 - A_i$$

$$b = B_i$$

$$c = -f_n^2 R^2 \cos^2 \Delta_j$$

and then

$$D_i = R \left[\sin^{-1} \left(\frac{br + 2c}{r \sqrt{b^2 - 4ac}} \right) \right]_{r_{i-1}}^{r_i}$$

6. Ground range thru segment n is then (from (5.28)) $\frac{1}{2}$ true $D - D_0$ and sum of D_i 's, $i = 1, \dots, n-1$:

$$D_n = \frac{D}{2} - D_0 - \sum_{i=1}^{n-1} D_i$$

7. Segment constants (from (5.36) and (5.35)) :

$$B_n = 2f_n^2 R \cos \Delta_j \left[\frac{R \cos \Delta_j}{r_{n-1}} + \sqrt{1 - \frac{f_{N_{n-1}}^2}{f_n^2} - \frac{R^2 \cos^2 \Delta_j}{r_{n-1}^2} \cot \frac{D_n}{R}} \right]$$

$$A_n = \frac{f_{N_{n-1}}^2}{r_{n-1}} + \frac{B_n}{r_{n-1}}$$

8. Radius of reflection r_n (from (5.33)) :

$$a = f_n^2 - A_n, \quad b = B_n, \quad c \text{ as before}$$

$$r_n = \frac{2c}{-b + \sqrt{b^2 - 4ac}}$$

9. Group path below ionosphere (from Figure 5.2) :

$$P_0 = \frac{r_0 \sin\left(\frac{D_0}{R}\right)}{\cos \Delta_j}$$

10. Group path thru each segment $i = 1, \dots, n$ (from (5.27)) :

$$a = f_n^2 - A_i, \quad b = B_i, \quad c \text{ as before}$$

$$P_i = f_n \left[\frac{1}{a} \sqrt{ar^2 + br + c} + \frac{b}{2a} \frac{1}{\sqrt{-a}} \sin^{-1} \left(\frac{2ar + b}{\sqrt{b^2 - 4ac}} \right) \right]_{r_{i-1}}^{r_i}$$

11. Total group path P_j for elevation angle Δ_j (from (5.29)):

$$P_j = P_o + \sum_{i=1}^n P_i$$

Main program NHRAO

12. For $j > 2$, perform successive linear interpolations for next Δ_j using previous two trial values :

$$\Delta_j = \Delta_{j-2} + (\Delta_{j-1} - \Delta_{j-2}) \frac{P_n - P_{j-2}}{P_{j-1} - P_{j-2}}$$

where P_n = true group path for freq. f_n .

Proceed until either

(i) $|P_n - P_j| < \delta$ in which case put $\Delta_n = \Delta_j$

or (ii) $j = j_{\text{end}}$ in which case perform Lagrange interpolation on the set (P_j, Δ_j) to find Δ_n corresponding to P_n .

13. With this "true" elevation angle Δ_n determine A_n, B_n, r_n as in steps 4 to 8. Of course if (i) above is the case we have already determined these so just use the last values.

14. Square of plasma frequency (from (5.20)) :

$$f_{N_n}^2 = A_n - \frac{B_n}{r_n}$$

15. Output electron density and true height :

$$N_n = 12404.427 f_{N_n}^2$$

$$h_n = r_n - R$$

and return to step 1 for next point.

16. When terminator $P_n = 9999$ is read in, fit a parabola for the profile peak using the last three points on the profile :

$$\begin{aligned} \text{let } x_1 &= r_{n-2} & y_1 &= f_{N_{n-2}}^2 \\ x_2 &= r_{n-1} & y_2 &= f_{N_{n-1}}^2 \\ x_3 &= r_n & y_3 &= f_{N_n}^2 \end{aligned}$$

Then determinant

$$\det = x_1^2 (x_2 - x_3) - x_2^2 (x_1 - x_3) + x_3^2 (x_1 - x_2)$$

and parameters a, b, c (from (5.54)) :

$$a = \frac{y_1 (x_2 - x_3) - y_2 (x_1 - x_3) + y_3 (x_1 - x_2)}{\det}$$

$$b = \frac{x_1^2 (y_2 - y_3) - x_2^2 (y_1 - y_3) + x_3^2 (y_1 - y_2)}{\det}$$

$$c = \frac{x_1^2 (x_2 y_3 - x_3 y_2) - x_2^2 (x_1 y_3 - x_3 y_1) + x_3^2 (x_1 y_2 - x_2 y_1)}{\det}$$

17. Profile peak parameters (from (5.56) and (5.57)) :

$$h_{\max} = -\frac{b}{2a} - R$$

$$\text{and } f_{N_{\max}}^2 = a r_{\max}^2 + b r_{\max} + c$$

$$N_{\max} = 12404.427 f_{N_{\max}}^2$$

(b) FOR 1st SEGMENT

1. Input minimum base height $h_{o_{\min}}$ and first two points (P_1, f_1) , (P_2, f_2) from oblique ionogram.
2. Min. and max. values of base radius r_o (from (5.46)) :

$$r_{o_{\min}} = R + h_{o_{\min}}$$

$$r_{o_{\max}} = R \cos\left(\frac{D}{2R}\right) + R \sin\left(\frac{D}{2R}\right) \sqrt{\frac{P_1^2}{4R^2 \sin^2\left(\frac{D}{2R}\right)} - 1}$$

For each of a number of trial r_{o_k} 's, $r_{o_{\min}} \leq r_{o_k} < r_{o_{\max}}$,

perform steps 3 - 17 below. For the first two trial values use

$$r_{o_1} = r_{o_{\min}}, \quad r_{o_2} = r_{o_{\max}} - (r_{o_{\max}} - r_{o_{\min}}) \times 0.01$$

3. Min. and max. elevation angles (from (5.45) and (5.44)) :

$$\Delta_{\min} = \tan^{-1} \left(\frac{r_{o_k} \cos\left(\frac{D}{2R}\right) - R}{r_{o_k} \sin\left(\frac{D}{2R}\right)} \right)$$

$$\Delta_{\max} = \cos^{-1} \left(\frac{r_{o_k} D}{R P_1} \right)$$

For each of a number of trial Δ_j 's, $\Delta_{\min} < \Delta_j < \Delta_{\max}$, perform steps 4 - 12 below (analogous to, but considerably simplified compared with, steps 4 - 12 of (a) since $f_{N_{n-1}} = f_{N_o} = 0$) with

$$r_o = r_{o_k}$$

Subroutine DELTAPATH

4. Ground range below ionosphere again

$$D_o = R \left[\cos^{-1} \left(\frac{R}{r_o} \cos \Delta_j \right) - \Delta_j \right]$$

5. Ground range thru first segment is then simply $D_1 = \frac{D}{2} - D_o$

6. Segment constants (from (5.36) with $f_{N_{n-1}} = 0$ and (5.35) respectively) :

$$B_1 = 2 f_1^2 R \cos \Delta_j \left[\frac{R}{r_o} \cos \Delta_j + \sqrt{1 - \frac{R^2}{r_o^2} \cos^2 \Delta_j} \cot \frac{D_1}{R} \right]$$

$$A_1 = \frac{B_1}{r_o}$$

7. Let $a = f_1^2 - A_1$

$$b = B_1$$

$$c = -f_1^2 R^2 \cos^2 \Delta_j$$

8. Then radius of reflection r_1 (from (5.33)) :

$$r_1 = \frac{2c}{-b + \sqrt{b^2 - 4ac}}$$

9. Group path below ionosphere (from Figure 5.2) :

$$P_o = \frac{r_o \sin \left(\frac{D_o}{R} \right)}{\cos \Delta_j}$$

10. Group path thru 1st segment (from (5.27)) :

$$P_1 = f_1 \left[\frac{1}{a} \sqrt{ar^2 + br + c} + \frac{b}{2a \sqrt{-a}} \sin^{-1} \left(\frac{2ar + b}{\sqrt{b^2 - 4ac}} \right) \right]_{r_o}^{r_1}$$

11. Total group path for elevation angle Δ_j (from (5.29)) :

$$P_j = 2P_o + 2P_1$$

Main program NHRAO

12. As in step 12 of (a), for $j > 2$ perform successive linear interpolations for next Δ_j and proceed thru steps 4 - 11 until either

(i) $|P_1 - P_j| < \delta$ in which case put $\Delta_1 = \Delta_j$

or (ii) $j = j_{\text{end}}$ in which case perform Lagrange interpolation on the set (P_j, Δ_j) to find Δ_1

13. As in step 13 of (a), if (ii) is the case, repeat steps 4 - 11 with $\Delta_j = \Delta_1$ to redetermine A_1, B_1 and r_1 .

14. We now calculate elevation angle Δ_2 utilizing these constants A_1 and B_1 and the second path, freq. pair (P_2, f_2) . For an initial estimate, use the approximations of Smith (5.38) and (5.49) :

$$f_{N_2}^2 = f_2^2 \left(1 - \frac{D^2}{P_2^2} \right)$$

$$r_2 = \frac{B_1}{A_1 - f_{N_2}^2}$$

$$\Delta_2 = \cos^{-1} \left(\frac{r_2}{R} \frac{D}{P_2} \right)$$

15. Improve this by performing Newton-Raphson iteration procedure using the expression for the ground range in freespace + 1st segment ((5.21) and (5.26)) (subroutine DELTANEW)

Again we have $a = f_2^2 - A_1$

$$b = B_1$$

$$c = -f_2^2 R^2 \cos^2 \Delta_2$$

Now define the variables

$$u = br_o + 2c$$

$$v = r_o \sqrt{b^2 - 4ac}$$

$$g = \frac{R}{r_o} \cos \Delta_2$$

Then function $F(\Delta_2)$ is

$$F = \cos^{-1} \frac{u}{v} + \cos^{-1} g - \Delta - \frac{D}{2R}$$

and its derivative $F'(\Delta_2)$ is

$$F' = \frac{4c \tan \Delta \left(\frac{ar_o^2 u}{v^2} + 1 \right)}{\sqrt{v^2 - u^2}} + \frac{g \tan \Delta - 1}{\sqrt{1 - g^2}}$$

and new estimate of root is

$$\Delta_{\text{new}} = \Delta - \frac{F(\Delta)}{F'(\Delta)} \quad \text{by Newton-Raphson.}$$

Iterate until Δ converges to within a specified accuracy.

Main program NHRAO

16. With this elevation angle Δ_2 and f_2 perform steps 4 - 12 above (subroutine DELTAPATH) to determine group path estimate P_k corresponding to trial base radius r_{o_k} .

17. For $k > 2$ perform successive linear interpolations for next r_{o_k} :

$$r_{o_k} = r_{o_{k-2}} + \left(r_{o_{k-1}} - r_{o_{k-2}} \right) \frac{(P_2 - P_{k-2})}{(P_{k-1} - P_{k-2})}$$

Proceed thru steps 3 - 16 until either

(i) $|P_2 - P_k| < \delta$ in which case put $r_o = r_{o_k}$

or (ii) $k = k_{\text{end}}$ in which case perform Lagrange interpolation on the set (P_k, r_{o_k}) to find the true r_o .

18. Output base height

$$h_o = r_o - R$$

Reset flag and if (ii) is the case, repeat steps 3 - 13 above using true r_o ; if (i) is the case proceed immediately to step 19.

19. Square of plasma frequency (from (5.20)) :

$$f_{N_1}^2 = A_1 - \frac{B_1}{r_1}$$

and output electron density and real height

$$N_1 = 12404.427 f_{N_1}^2$$

$$h_1 = r_1 - R$$

20. Reset flag and proceed to step 2 of (a) for (P_2, f_2) which has already been read in.

(4.) Listing of program NHRAO

```
C ***** NHRAO
C
C   MASTER NHRAO
C   =====
C THIS PROGRAM CALCULATES AN EFFECTIVE N(H) PROFILE FROM
C P,F DATA ON AN OBLIQUE IONOGRAM BY THE SEGMENT METHOD
C OF M.S.SMITH REF. J.A.T.P. 32, 1047 (1970), MODIFIED
C BY N.N.RAO REF. J.A.T.P. 35, 1561 (1973).
C INPUT DATA COMPATIBLE WITH THAT FOR PROGRAM OVIO
C
C   REAL DELTA(10),PJGUESS(10),PKGUESS(10),ROGUESS(10),
+     EDENS(50),HEAD(4)
C
C   DOUBLE PRECISION X(3),Y(3),DET,AA,BB,CC,XX,RRE
C
C   COMMON/FUNK/AA,BB,CC,XX,RRE
C   COMMON/DUNK/IPRINT,A(50),B(50),R(50),RN,RM,RO,RE,
+     D,P,N,F,F2,FN2N,FN2M,JFLAG,DNSEG
C   COMMON/AMGRAPH3/CHAR,NCROSS,ISUP,ISO,NOAXES,NONUMX,NUMY
C
C CANNOT USE DATA STATEMENT FOR COMMON VARIABLES
C
C   D = 4470.84
C   RE = 6371.35
C   PACCUR = 0.02
C   NITER = 10
C   DACCUR = 1.0E-06
C
C INPUT IONOGRAM I.D. DATA AND PLOTTING DATA
C
C   READ(5,5010) HEAD,OFFSET
C   READ(5,5020) IPLOT,IPRINT,IC,NHD,J,K,N,NPL,NPX,NPY
C   READ(5,5030) ESIZE,HSIZE
C   READ(5,5040) NHOP,HOMIN,JEND,KEND,IFILE,KARRAY,KCOEFF
C
C DOUBLE INTERPOLATION FOR BASE HEIGHT HO
C
C INPUT FIRST TWO P,F PAIRS
C
C   READ(5,5030) P1,FA
C   READ(5,5030) P2,FB
C
C   P1=(P1+OFFSET)/FLOAT(NHOP)
C   P2=(P2+OFFSET)/FLOAT(NHOP)
C   IF(P1.EQ.P2) P1=P1-0.10
C   D=D/FLOAT(NHOP)
C
C   N=1
C   P=P1
C   F=FA
C   DELTAN=0.0
C
C LOWER AND UPPER BOUNDS ON RO
C
C   ROMIN=RE+HOMIN
C   PHI=D/(2.0*RE)
C   ROMAX=RE*COS(PHI)+SQRT(P*P/4.0-RE*RE*SIN(PHI)*SIN(PHI))
C   IF(ROMIN.GE.ROMAX) ROMIN=ROMAX-10.0
C   HO=ROMAX-RE
C
C PRINT IONOGRAM I.D. AND HO LIMITS
C
C   IF(IPRINT.EQ.0) WRITE(6,6000)
C   WRITE(6,6010) HEAD(2),HEAD(3),HEAD(4),NHOP
C   WRITE(6,6020) HOMIN,HO,RE,D
C
C SET FLAGS AND LOOP THRU FOR UP TO KEND GUESSES OF RO
C
C   ROGUESS(1)=ROMIN
C   ROGUESS(2)=ROMAX-(ROMAX-ROMIN)*0.01
C   IFLAG=0
C   JFLAG=0
C   K=1
C
C 10   RO=ROGUESS(K)
C     HO=RO-RE
C     IF(IPRINT.EQ.1) WRITE(6,7010) K,RO,HO
C 20   RM=RO
```

```

    FN2M=0.0
    GO TO 40

C MAIN LOOP : INPUT PATH,FREQUENCY PAIR
30  READ(5,5030) P,F
    IF(P.EQ.9999.) GO TO 170
    P=(P+OFFSET)/FLOAT(NHOP)

C PLASMA FREQUENCY SQUARED (APPROXIMATION)
40  F2=F*F
    FN2N=F2*(1.-D*D/(P*P))

C IF FULL PRINTING REQUIRED FOR PARTICULAR N INSERT HERE
    IF(IPRINT.EQ.1.AND.IFLAG.GT.0) WRITE(6,7000)
    IF(IPRINT.EQ.1) WRITE(6,7020) N,F,F2,FN2N,RM,D,P

C MIN AND MAX ELEVATION ANGLES
C MIN IS LARGEST FROM ALL SEGMENT JUNCTIONS UP TO N-1
    IF(N.EQ.1) DELMIN=ATAN((RO*COS(PHI)-RE)/(RO*SIN(PHI)))
    IF(N.GT.1) DELMIN=ACOS((RM/RE)*SQRT(1.0-FN2M/F2))
    IF(DELMIN.LT.DELTAN) DELMIN=DELTAN
    IF(N.LT.3) GO TO 55
    DO 50 I=1,N-2
    DELMAX=1.0-EDENS(I)/(12404.427*F2)
    IF(DELMAX.LE.0.0) GO TO 50
    DELMAX=(R(I)/RE)*SQRT(DELMAX)
    IF(DELMAX.GT.1.0) GO TO 50
    DELMAX=ACOS(DELMAX)
    IF(DELMAX.GT.DELMIN) DELMIN=DELMAX
50  CONTINUE
55  DELMAX=RM*D/(P*RE)
    IF(DELMAX.LT.1.0) GO TO 57
    IF(IFLAG.GT.0) GO TO 56
    ROGUESS(K)=ROGUESS(K)-(ROMAX-ROMIN)*0.1
    GO TO 10
56  P=P+1.0/FLOAT(NHOP)
    GO TO 40
57  DELMAX=ACOS(DELMAX)
    DELMAX=DELMIN+ABS(DELMAX-DELMIN)
    IF(IPRINT.EQ.1) WRITE(6,7030) DELMIN,DELMAX

C GROUP PATHLENGTH FOR EACH OF UP TO JEND ANGLES
C LINEAR INTERPOLATION TO OBTAIN SUCCESSIVE GUESSES
    DELTA(1)=DELMIN+(DELMAX-DELMIN)*0.01
    DELTA(2)=DELMAX-(DELMAX-DELMIN)*0.01
    J=1

60  IF(IPRINT.EQ.1) WRITE(6,7040) J,DELTA(J)
    CALL DELTAPATH(DELTA(J),PJGUESS(J))

C IF PATH ROUTINE BOMBED OUT, CORRECT DELTA OR P
    IF(JFLAG.NE.1) GO TO 65
    DELTA(J)=DELTA(J)+(1.0-DNSEG)/5090.91
    JFLAG=0
    GO TO 60

65  IF(JFLAG.NE.2) GO TO 70
    P=P+1.0/FLOAT(NHOP)
    JFLAG=0
    GO TO 40

C CHECK ACCURACY AND NUMBER OF ITERATIONS
70  IF(IPRINT.EQ.1) WRITE(6,7140) PJGUESS(J)
    IF(ABS(PJGUESS(J)-P).LT.PACCUR) GO TO 80
    J=J+1
    IF(J.EQ.2) GO TO 60
    IF(J.GT.JEND) GO TO 75
    DELTA(J)=DELTA(J-2)+(DELTA(J-1)-DELTA(J-2))
    + *(P-PJGUESS(J-2))/(PJGUESS(J-1)-PJGUESS(J-2))
    GO TO 60

C INTERPOLATE FOR DELTA GIVING TRUE PATHLENGTH

```

C THEN CALCULATE TRUE RADIUS AND SEGMENT CONSTANTS

```
75 DELTAN=ALAGRANGE(PJGUESS,DELTA,P,JEND)
   JFLAG=3
   CALL DELTAPATH(DELTAN,PJGUESS(JEND))
   JFLAG=0
   GO TO 90
80 DELTAN=DELTA(J)
90 RN=R(N)
   FN2N=A(N)-B(N)/RN
   IF(IPRINT.EQ.1) WRITE(6,7050) N,DELTAN,RN,A(N),B(N)
   IF(IFLAG.EQ.0) GO TO 100
```

C ELECTRON DENSITY AND TRUE HEIGHT

```
RN=RN-RE
EDENS(N)=FN2N*12404.427
DELTAN=DELTAN*57.29577951
FN2N=SQRT(FN2N)
IF(IPRINT.EQ.1) WRITE(6,6040)
WRITE(6,6050) RN,EDENS(N),A(N),B(N),N,FN2N,F,P,DELTAN
```

C RETURN TO READ NEXT P,F PAIR FOR NEXT SEGMENT

```
DELTAN=DELTAN/57.29577951
FA=F
P1=P
FN2M=FN2N*FN2N
RM=R(N)
N=N+1
```

```
IF(IFLAG.EQ.1) GO TO 160
GO TO 30
```

C END OF MAIN LOOP

C FOR EACH TRIAL RO, PATHLENGTH FOR ELEVATION ANGLE DELTA2
C AT FREQUENCY FB (IFLAG = 0). INITIAL APPROX TO DELTA2
C FROM SMITH, IMPROVED BY N-R ITERATION IN SUBR DELTANNEW

```
100 P=P2
    F=FB
    R1=RN
    F2=F*F
    FN2N=F2*(1.-D*D/(P*P))
    RN=B(1)/(A(1)-FN2N)
    DELTA2=ACOS(D*RN/(P*RE))
    IF(IPRINT.EQ.1) WRITE(6,7060) K,DELTA2,RN,F,FN2N,P
    IF(IPRINT.EQ.1) WRITE(6,7000)
```

```
CALL DELTANNEW(DELTA2,NITER,DACCUR)
```

```
110 IF(IPRINT.EQ.1) WRITE(6,7060) K,DELTA2,RN,F,FN2N,P
```

```
CALL DELTAPATH(DELTA2,PKGUESS(K))
```

```
IF(JFLAG.EQ.0) GO TO 120
DELTA2=DELTA2+2.0*DACCUR
JFLAG=0
GO TO 110
```

C CHECK ACCURACY AND NUMBER OF ITERATIONS

```
120 IF(IPRINT.EQ.1) WRITE(6,7150) K,ROGUESS(K),PKGUESS(K),P
    P=P1
    F=FA
    IF(ABS(PKGUESS(K)-P2).LT.PACCUR) GO TO 140
    K=K+1
    IF(K.EQ.2) GO TO 10
    IF(K.GT.KEND) GO TO 130
    ROGUESS(K)=ROGUESS(K-2)+(ROGUESS(K-1)-ROGUESS(K-2))
    +*(P2-PKGUESS(K-2))/(PKGUESS(K-1)-PKGUESS(K-2))
    GO TO 10
```

C INTERPOLATE FOR RO GIVING TRUE PATHLENGTH

130 RO=ALAGRANGE(PKGUESS,ROGUESS,P2,KEND)
GO TO 150

140 RO=ROGUESS(K)

C IONOSPHERIC BASE HEIGHT HO

150 HO=RO-RE
WRITE(6,6030) HO
IF(IPRINT.EQ.0) WRITE(6,6040)

C RESET FLAG AND REPEAT USING 'TRUE' RO FOR N=1

R(N)=R1
IFLAG=1
IF(K.GT.KEND) GO TO 20
GO TO 90

C RESET FLAG AND REPEAT FOR N=2

160 P=P2
F=FR
IFLAG=2
GO TO 40

C IF P=9999 HAS BEEN READ IN, DETERMINE PARAMETERS
C FOR PROFILE PEAK (ASSUMED PARABOLIC : $FN2 = A*R^2 + B*R + C$)

170 N=N+1
DO 180 I=1,3
X(I)=R(N+I-5)
180 Y(I)=EDENS(N+I-5)/12404.427
190 DET=X(1)*X(1)*(X(2)-X(3))-X(2)*X(2)*(X(1)-X(3))
+ X(3)*X(3)*(X(1)-X(2))
+ Y(1)*(X(2)-X(3))-Y(2)*(X(1)-X(3))
+ Y(3)*(X(1)-X(2))/DET
BBP=(X(1)*X(1)*(Y(2)-Y(3))-X(2)*X(2)*(Y(1)-Y(3))
+ X(3)*X(3)*(Y(1)-Y(2)))/DET
CCP=(X(1)*X(1)*X(2)*Y(3)-X(3)*Y(2))
+ -X(2)*X(2)*X(1)*Y(3)-X(3)*Y(1))
+ +X(3)*X(3)*(X(1)*Y(2)-X(2)*Y(1))/DET

C PEAK RADIUS AND EDENS (ENSURE R > LAST R)

R(N)=-BBP/(2.0*AAP)
IF(R(N).GT.R(N-2)) GO TO 200
X(3)=X(3)+0.10
R(N-2)=X(3)
GO TO 190

200 IF(IPRINT.EQ.0) GO TO 210
WRITE(6,6000)
WRITE(6,7120)(I,X(I),Y(I),I=1,3)
WRITE(6,7130) DET,R(N),N

210 FN2N=AAP*R(N)*R(N)+BBP*R(N)+CCP
EDENS(N)=FN2N*12404.427
R(N)=R(N)-RE
FN2N=SQRT(FN2N)
WRITE(6,6060) R(N),EDENS(N),FN2N,AAP,BBP,CCP
IF(IPLOT.EQ.0.AND.IFILE.EQ.0) GO TO 250

C SHIFT R,EDENS ARRAYS UP ONE POSITION

DO 220 I=1,N-2
J=N-I
A(J)=A(J-1)
B(J)=B(J-1)
R(J)=R(J-1)-RE
220 EDENS(J)=EDENS(J-1)
A(1)=0.0
B(1)=0.0
R(1)=HO
EDENS(1)=0.0
A(N)=AAP

B(N)=BBP
B(N+1)=CCP

C IF IPLOT = 1 PLOT PROFILE

IF(IPLOT.NE.1) GO TO 230
ISUP=1

CALL AMGRAPH(6,0,0,0,4HARJR,R,ESIZE,HSIZE,HEAD,NHD)
CALL AMAXISLABEL(23HELECTRON DENSITY (CM-3),
+ 11HHEIGHT (KM),NPX,NPY)
CALL AMGRAPH(6,0,N,IC,EDENS,R,ESIZE,HSIZE,
+ 21HN(H) PROFILE (RAO) ,NPL)
CALL AMGRAPH(6,0,0,2,EDENS,R,ESIZE,HSIZE,HEAD,0)

C IF IFILE = 1 WRITE HEIGHT & DENSITY ARRAYS TO DISC
C IF IFILE = 2 WRITE A & B ARRAYS AS WELL

230 IF(IFILE.EQ.0) GO TO 250
WRITE(6,7100)
WRITE(6,7110)(I,R(I),EDENS(I),A(I),B(I),I=1,50)

CALL USEFILE(2,2HED,12HARJRDATA01 ,1,0)

IELEM=KARRAY
WRITE(6,7070) IELEM,N
CALL PUTARRAY(2,IELEM,R)
WRITE(6,7075) IELEM,N
CALL PUTARRAY(2,IELEM,EDENS)

IF(IFILE.NE.2) GO TO 250
IELEM=KCOEFF
WRITE(6,7080) IELEM,N
CALL PUTARRAY(2,IELEM,A)
N=N+1
WRITE(6,7085) IELEM,N
CALL PUTARRAY(2,IELEM,B)
N=N-1

250 STOP OK

C FORMAT STATEMENTS

5010 FORMAT(4A8,E0.0)
5020 FORMAT(10I0)
5030 FORMAT(2E0.0)
5040 FORMAT(10,E0.0,5I0)

6000 FORMAT(1H1)
6010 FORMAT(1H ,20X,36HN(H) PROFILE FROM OBLIQUE IONOGRAM ,3A8,
+ I4,10H HOP TRACE,/,1H ,20X,74(1H-))
6020 FORMAT(1HO,23HBASE HEIGHT HO : MIN =,F7.2,7H MAX =,
+ F7.2,3H KM,9X,17HEARTH RADIUS RE =,F8.2,3H KM,8X,
+ 12HDISTANCE D =,F8.2,3H KM)
6030 FORMAT(1HO,29HINTERPOLATED BASE HEIGHT HO =,F7.2,3H KM,
+ 7X,36HRAO METHOD WITH SEGMENTS OF THE FORM,
+ 3H FN2 = A - B/R WHERE R = RE + H)
6040 FORMAT(1HO,29H H (KM) NE (CM-3)
+ 40HSEGMENT PARAMETERS A(N),B(N) N
+ 46HFN (MHZ) F (MHZ) P (KM) DELTA (DEG))
6050 FORMAT(1HO,F8.2,3(1PE16.4),I8,OPF12.4,F11.2,F13.2,F13.4)
6060 FORMAT(1HO,F8.2,1PE16.4,8X,30HPARABOLIC FIT FOR PROFILE PEAK,
+ OPF14.4,/,25H PEAK PARAMETERS A,B,C ,1P3E16.4,
+ 6X,26HWHERE FN2 = A*R2 + B*R + C)

7000 FORMAT(1H)
7010 FORMAT(4H1K =,I3,15H ROGUESS(K) =,F11.4,
+ 14H HOGUESS =,F10.4)
7020 FORMAT(4HON =,I3,6H F =,F6.2,7H F2 =,F9.4,8H FN2 =,
+ F8.4,7H RM =,F11.4,6H D =,F11.4,6H P =,F11.4)
7030 FORMAT(/,22H ELEV ANGLE DELTA MIN,F10.6,6H MAX,F10.6)
7040 FORMAT(/,4H J =,I3,13H DELTA(J) =,F10.6)
7050 FORMAT(/,4H N =,I3,13H DELTA(N) =,F10.6,
+ 9H R(N) =,F11.4,20H CONSTANTS A(N) =,1PE12.4,
+ 9H B(N) =,1PE12.4)
7060 FORMAT(/,4H K =,I3,13H DELTA(2) =,F10.6,9H R(2) =,F11.4,
+ 6H F =,F6.2,8H FN2 =,F6.2,6H P =,F11.4)
7070 FORMAT(/,41H FIRST FILE ELEMENT NO FOR HEIGHT ARRAY,I6,
+ 13H ARRAY SIZE,I6)
7075 FORMAT(/,41H FIRST FILE ELEMENT NO FOR DENSITY ARRAY,I6,

```
+      13H   ARRAY SIZE,I6)
7080 FORMAT(//,41H FIRST FILE ELEMENT NO FOR A SEG COEFFS,I6,
+      13H   ARRAY SIZE,I6)
7085 FORMAT(//,41H FIRST FILE ELEMENT NO FOR B SEG COEFFS,I6,
+      13H   ARRAY SIZE,I6)
7100 FORMAT(23H1ARRAYS WRITTEN TO DISC,/,4H I,
+      8X,4HH(I),11X,5HNE(I),12X,4HA(I),13X,4HB(I),/,1H )
7110 FORMAT(1H ,I3,OPF14.4,1P3E17.6)
7120 FORMAT(1H ,I3,1P2D24.10)
7130 FORMAT(/,6H DET =,1PD22.10,11H      RMAX =,E16.6,
+      8H      N =,I4)
7140 FORMAT(1H+,78X,12HPJGUESS(J) =,F11,4)
7150 FORMAT(/,4H K =,I3,15H  ROGUESS(K) =,F11.4,14H  PGUESS(K) =,
+      F11.4,11H  TRUE P =,F11.4)

END
```

```

C ***** DELTAPATH
C   SUBROUTINE DELTAPATH(DEL,PATH)
C   =====
C THIS SUBROUTINE CALCULATES TOTAL GROUP PATHLENGTH PATH
C COVERED BY A RAY WITH ELEVATION ANGLE DEL
C   EXTERNAL DFUN,PFUN
C   DOUBLE PRECISION AA,BB,CC,XX,RRE
C   COMMON/FUNK/AA,BB,CC,XX,RRE
C   COMMON/DUNK/IPRINT,A(50),B(50),R(50),RN,RM,RO,RE,
+   D,P,N,F,F2,FN2N,FN2M,JFLAG,DNSEG
C GROUND RANGE BELOW IONOSPHERE
C   DFRSP=RE*(ACOS((RE/RO)*COS(DEL))-DEL)
C   IF(IPRINT.EQ.1) WRITE(6,7000) N,DFRSP
C GROUND RANGE FOR ALL SEGMENTS I FROM 1 TO N-1
C   I=1
C   RRE=RE
C   DISUM=0.0
C   CC=-F2*RE*RE*COS(DEL)*COS(DEL)
C   IF(N.EQ.1) GO TO 20
C   AA=F2-A(1)
C   BB=B(1)
C   DISUM=DISUM+DFUN(R(1))-DFUN(RO)
C   IF(N.EQ.2) GO TO 20
C   DO 10 I=2,N-1
C   AA=F2-A(I)
C   BB=B(I)
C   DISUM=DISUM+DFUN(R(I))-DFUN(R(I-1))
10  CONTINUE
20  IF(IPRINT.EQ.1) WRITE(6,7040) DISUM
C GROUND RANGE FOR SEGMENT N
C (IF NEGATIVE RETURN AND INCREASE DEL)
C   DNSEG=(D-2.0*DFRSP-2.0*DISUM)/2.0
C   IF(DNSEG.GT.0.0) GO TO 30
C   JFLAG=1
C   IF(IPRINT.EQ.1) WRITE(6,7070) JFLAG,DNSEG
C   RETURN
C SEGMENT CONSTANTS A(N),B(N) AND RADIUS R(N)
30  BN=(RE/RM)*COS(DEL)
C   CN=1.0-FN2M/F2-BN*BN
C   IF(CN.GE.0.0) GO TO 40
C   JFLAG=2
C   IF(IPRINT.EQ.1) WRITE(6,7080) JFLAG,CN
C   RETURN
40  B(N)=2.0*F2*BN*RM*(BN+SQRT(CN)/TAN(DNSEG/RE))
C   A(N)=FN2M+B(N)/RM
C   AA=F2-A(N)
C   BB=B(N)
C   R(N)=(2.0*DNSEG*CC)/(-BB+DSQRT(BB*BB-4.0*DNSEG*AA*CC))
C   IF(IPRINT.EQ.1) WRITE(6,7050) DNSEG,A(N),B(N),R(N)
C   IF(JFLAG.EQ.3) RETURN
C PATHLENGTH BELOW IONOSPHERE
C   PFRSP=RO*SIN(DFRSP/RE)/COS(DEL)
C   IF(IPRINT.EQ.1) WRITE(6,7060) PFRSP
C PATHLENGTH FOR ALL SEGMENTS I FROM 1 TO N
C   I=1
C   AA=F2-A(1)
C   BB=B(1)
C   PISUM=F*(PFUN(R(1))-PFUN(RO))

```

```
IF(N.EQ.1) GO TO 60

DO 50 I=2,N
AA=F2-A(I)
BB=B(I)
PISUM=PISUM+F*(PFUN(R(I))-PFUN(R(I-1)))
50 CONTINUE
60 IF(IPRINT.EQ.1) WRITE(6,7030) PISUM

C TOTAL PATHLENGTH GUESS AND RETURN
PATH=2.0*PFRSP+2.0*PISUM

RETURN

C FORMAT STATEMENTS
7000 FORMAT(4H N =,I3,10H DFRSP =,F11.4,
+ 25H SUBROUTINE DELTAPATH,10X,7H DISUM = )
7030 FORMAT(8H PISUM =,F11.4)
7040 FORMAT(1H+,69X,OPF11.4)
7050 FORMAT(8H DNSEG =,F11.4,9H A(N) =,1PE12.4,9H B(N) =,
+ 1PE12.4,9H R(N) =,OPF11.4)
7060 FORMAT(1H+,83X,7HPFRSP =,F11.4)
7070 FORMAT(8H JFLAG =,I2,10H DNSEG =,F12.4)
7080 FORMAT(8H JFLAG =,I2,7H CN =,1PE16.6)

END

C ***** DFUN
C FUNCTION DFUN(R)
C =====
DOUBLE PRECISION AA,BB,CC,XX,RR,RRE
COMMON/FUNK/AA,BB,CC,XX,RRE
RR=R
XX=(BB*RR+2.0D00*CC)
+ /((DABS(RR)*DSQRT(DABS(BB*BB-4.0D00*AA*CC)))
DFUN=RRE*DATAN2(XX,DSQRT(DABS(1.0D00-XX*XX)))
RETURN
END

C ***** PFUN
C FUNCTION PFUN(R)
C =====
DOUBLE PRECISION AA,BB,CC,XX,RR,RRE
COMMON/FUNK/AA,BB,CC,XX,RRE
RR=R
XX=(2.0D00*AA*RR+BB)
+ /DSQRT(DABS(BB*BB-4.0D00*AA*CC))
PFUN=DSQRT(DABS(AA*RR*RR+BB*RR+CC))/AA
+ (BB/(2.0D00*AA*DSQRT(-AA)))
+ *DATAN2(XX,DSQRT(DABS(1.0D00-XX*XX)))
RETURN
END

C ***** DELTANEW
C SUBROUTINE DELTANEW(DEL,NITER,ACCUR)
C =====
C THIS SUBROUTINE PERFORMS NEWTON-RAPHSON ITERATION
C ON ANGLE DEL USING EXPRESSION FOR GROUND RANGE IN
C FREESPACE + FIRST SEGMENT
DOUBLE PRECISION AA,BB,CC,U,V,DDEL,RRO,FUN,FDASH,RRE
```

```
COMMON/FUNK/AA,BB,CC,U,RRE
COMMON/DUNK/IPRINT,A(50),B(50),R(50),RN,RM,RO,RE,
+ D,P,N,F,F2,FN2N,FN2M

RRO=RO
I=1

C ITERATION LOOP FOR NEWTON RAPHSON PROCEDURE
10 DELAST=DEL
DDEL=DEL

C INTERMEDIATE VARIABLES
AA=F2-A(1)
BB=B(1)
CC=-F2*RE*RE*COS(DEL)*COS(DEL)
U=BB*RRO+2.0000*CC
V=RRO*DSQRT(BB*RB-4.0000*AA*CC)
G=(RE/RO)*COS(DEL)
IF(IPRINT.EQ.1) WRITE(6,7010) AA,BB,CC,U,V,G

C FUNCTION FUN(DEL) = 0 AND DERIVATIVE FDASH
FUN=ACOS(G)-DEL-D/(2.0*RE)
FUN=FUN+DATAN(DSQRT(V*V/(U*U)-1.0000))

FDASH=G*TAN(DEL)/SQRT(1.0-G*G)-1.0
FDASH=FDASH+4.0000*CC*(DSIN(DDEL)/DCOS(DDEL))
+ *(AA*RRO*RRO*U/(V*V)+1.0000)/DSQRT(V*V-U*U)

C NEW ESTIMATE OF ROOT DEL
DEL=DDEL-FUN/FDASH
IF(IPRINT.EQ.1) WRITE(6,7020) FUN,FDASH,DEL,I

C CHECK NO OF ITERATIONS AND ACCURACY
I=I+1
IF(I.GT.NITER) GO TO 20
IF(ABS(DEL-DELAST).GT.ACCUR) GO TO 10

20 RETURN

C FORMAT STATEMENTS (FOR IPRINT = 1)
7010 FORMAT(1H ,1P5D13.4,E13.4)
7020 FORMAT(1H+,78X,1P2D13.4,0PF11.6,I4)

END
```

(5.) Listing of program NHGEORGE

C ***** NHGEORGE

MASTER NHGEORGE

C THIS PROGRAM CALCULATES AN APPROXIMATE N(H) PROFILE FROM
C AN OBLIQUE IONOGRAM BY THE SEGMENT METHOD OF P.L.GEORGE
C REF. J.A.T.P. 32 , 905 (1970)

REAL NE(50),R(50),A(50),HEAD(4),ELIM(3),HLIM(3)
DOUBLE PRECISION X(3),Y(3),DET
COMMON /AMGRAPH1/ HGT,PAGE,DASHLN,TICK,SET,SPACE,SHIFT,SYMB
COMMON /AMGRAPH3/ CHAR,NCROSS,ISUP
DATA D/4470.84/,RE/6371.35/

C INPUT I.D. AND PLOTTING DATA

READ (5,5010) HEAD,OFFSET
READ (5,5020) IPLOT,IPRINT,IC,NHD,I,J,N,NPL,NPX,NPY
READ (5,5030) ESIZE,HSIZE,ESIZE,HSIZE,ELIM(1),ELIM(2),
+ HLIM(3),HLIM(2),ELIM(1),ELIM(2),HLIM(3),HLIM(2)
READ (5,5040) NHOP
ISUP = 1
HGT = 0.4
SYMB = 0.2
CALL COPY8(CHAR,1HC)
D = D/FLOAT(NHOP)

C INPUT FIRST 2 POINTS AND DETERMINE BASE HEIGHT

READ (5,5100) PMIN,FI
READ (5,5100) P,F
PMIN = (PMIN+OFFSET)/FLOAT(NHOP)
P = (P+OFFSET)/FLOAT(NHOP)
AI = RE*SIN(D/(2.*RE))
RO = SQRT(PMIN*PMIN/4.-AI*AI)-RE*(1.-COS(D/(2.*RE)))
WRITE (6,6010) HEAD(2),HEAD(3),HEAD(4),NHOP
WRITE (6,6020) RO,RE,D
WRITE (6,6030)
RO = RO+RE

C PARAMETERS OF FIRST SEGMENT

N = 1
DELTA = ACOS(2.*RE*SIN(D/(2.*RE))/(P+0.21*(P-PMIN)))-D/(2.*RE)
FUN = RE*RE*COS(DELTA)*COS(DELTA)
FI = SQRT(1.-FUN/(RO*RO))
R(1) = (P-PMIN)*FI/4.+RO
H = R(1)-RE
FN = F*FI
NE(1) = 12404.427*FN*FN
A(1) = NE(1)/(R(1)-RO)
DELTA = DELTA*57.29578
WRITE (6,6100) H,NE(1),A(1),N,FN,F,P,DELTA
N = 2

C MAIN LOOP : INPUT P,F PAIR

100 READ (5,5100) P,F
IF (P.EQ.9999.) GO TO 300
P = (P+OFFSET)/FLOAT(NHOP)

C ELEVATION ANGLE AND PATH BELOW IONOSPHERE

150 DELTA = ACOS(2.*RE*SIN(D/(2.*RE))/(P+0.21*(P-PMIN)))-D/(2.*RE)
FUN = RE*RE*COS(DELTA)*COS(DELTA)
PO = SQRT(RO*RO-FUN)-RE*SIN(DELTA)

C PATH THRU FIRST SEGMENT

AI = 1.-FUN/(R(1)*R(1))
XI = NE(1)/(12404.427*F*F)
FI = 2.*(SQRT(AI)-SQRT(AI-XI))/XI
PISUM = FI*(R(1)-RO)
IF (N.EQ.2) GO TO 250

C PATH THRU SEGMENTS BELOW REFLECTION SEGMENT

DO 200 I = 2,N-1
AI = 1.-FUN/(R(I)*R(I))
XI = NE(I)/(12404.427*F*F)

```
XIM = NE(I-1)/(12404.427*F*F)
IF (XI.GT.AI.OR.XIM.GT.AI) P=P+0.1/FLOAT(NHOP)
IF (XI.GT.AI.OR.XIM.GT.AI) GO TO 150
FI = 2.*(SQRT(AI-XIM)-SQRT(AI-XI))/(XI-XIM)
200 PISUM = PISUM+FI*(R(I)-R(I-1))

C PARAMETERS FOR SEGMENT N
250 AI = 1.-FUN/(R(N-1)*R(N-1))
    XI = 1.-FUN/(RO*RO)
    XIM = NE(N-1)/(12404.427*F*F)
    IF (XI.GT.AI.OR.XIM.GT.AI) P=P+0.1/FLOAT(NHOP)
    IF (XI.GT.AI.OR.XIM.GT.AI) GO TO 150
    FI = 2.*(SQRT(AI-XIM)-SQRT(AI-XI))/(XI-XIM)
    R(N) = (P-2.*PO-2.*PISUM)/(2.*FI)+R(N-1)
    IF (R(N).LT.R(N-1)) P=P+0.1/FLOAT(NHOP)
    IF (R(N).LT.R(N-1)) GO TO 150
    H = R(N)-RE
    FN = F*SQRT(1.-FUN/(R(N)*R(N)))
    NE(N) = 12404.427*FN*FN
    A(N) = (NE(N)-NE(N-1))/(R(N)-R(N-1))
    DELTA = DELTA*57.29578
    WRITE (6,6100) H,NE(N),A(N),N,FN,F,P,DELTA
    N = N+1
    GO TO 100

C IF P=9999 HAS BEEN READ IN, DETERMINE PARAMETERS
C FOR PROFILE PEAK (ASSUMED PARABOLIC : NE = A*H2 + B*H + C)
300 N = N+1
    DO 310 I = 1,3
    X(I) = R(N+I-5)-RE
310 Y(I) = NE(N+I-5)
320 DET = X(1)*X(1)*(X(2)-X(3))-X(2)*X(2)*(X(1)-X(3))
    + X(3)*X(3)*(X(1)-X(2))
    AAP = (Y(1)*(X(2)-X(3))-Y(2)*(X(1)-X(3))
    + Y(3)*(X(1)-X(2)))/DET
    BBP = (X(1)*X(1)*(Y(2)-Y(3))-X(2)*X(2)*(Y(1)-Y(3))
    + X(3)*X(3)*(Y(1)-Y(2)))/DET
    CCP = (X(1)*X(1)*(X(2)*Y(3)-X(3)*Y(2))
    + -X(2)*X(2)*(X(1)*Y(3)-X(3)*Y(1))
    + X(3)*X(3)*(X(1)*Y(2)-X(2)*Y(1)))/DET

C PEAK HEIGHT AND NE (ENSURE H > LAST H)
H = -BBP/(2.0*AAP)
IF(H.GT.X(3)) GO TO 330
X(3) = X(3)+0.10/FLOAT(NHOP)
R(N-2) = X(3)+RE
GO TO 320
330 NE(N) = AAP*H*H+BBP*H+CCP
    R(N) = H
    FN = SQRT(NE(N)/12404.427)
    WRITE(6,6040) H,NE(N),FN,AAP,BBP,CCP

C IF IPLOT = 1 PLOT PROFILE
IF (IPLOT.NE.1) GO TO 500
DO 350 I = 1,N-2
J = N-I
350 R(J) = R(J-1)-RE
    NE(J) = NE(J-1)
    R(1) = RO-RE
    NE(1) = 0

    ELIM(3) = ELIM(2)
    HLIM(1) = HLIM(2)
    CALL AMGRAPH(6,0,0,0,4HARJR,R,ESIZE,HSIZE,HEAD,NHD)
    CALL AMAXISLABEL(23HELECTRON DENSITY (CM-3),
    + 11HEIGHT (KM),NPX,NPY)
    CALL AMGRAPH(6,0,3,IC,ELIM,HLIM,ESIZE,HSIZE,
    + 21HN(H) PROFILE (GEORGE),NPL)
    CALL AMGRAPH(6,22,N,1,NE,R,ESIZE,HSIZE,HEAD,0)
    CALL AMGRAPH(6,0,0,2,NE,R,ESIZE,HSIZE,HEAD,0)
500 STOP OK

5010 FORMAT (4A8,E0.0)
5020 FORMAT (10I0)
5030 FORMAT (12E0.0)
5040 FORMAT (I0)
```

```
5100 FORMAT (2E0.0)
6010 FORMAT (1H1,12X,36HN(H) PROFILE FROM OBLIQUE IONOGRAM ,3A8,
+ I4,10H HOP TRACE,/,1H,12X,74(1H-))
6020 FORMAT (1H0,16HBASE HEIGHT HO =,F7.2,3H KM,11X,
+ 17HEARTH RADIUS RE =,F8.2,3H KM,11X,12HDISTANCE D =,F8.2,
+ 3H KM/47HGEORGE METHOD WITH LINEAR SEGMENTS OF THE FORM,
+ 53H NE = A(N) * (H-H(N-1)) + NE(N-1) , H(N-1) < H < H(N))
6030 FORMAT (1H0,29H H (KM) NE (CM-3)
+ 32HGRADIENT A(N) N FN (MHZ),
+ 38H F (MHZ) P' (KM) DELTA (DEG))
6040 FORMAT(1H0,F8.2,1PE16.4,9X,12HPROFILE PEAK,
+ 0PF15.4,/,26H PEAK PARAMETERS A,B,C ,1P3E15.4,
+ 3X,25HWHERE NE = A*H2 + B*H + C)
6100 FORMAT (1H0,F8.2,1P2E16.4,I8,0PF12.4,F11.2,F13.2,F13.4)
END
```

APPENDIX F

ADDITIONAL COMPUTER PROGRAMS

1. Listing of program OVIP, including subroutines NHPF (a version of NHPR) and NMODE, to compute N(h) profiles from oblique (via the equivalent vertical ionogram) and vertical ionograms.
2. Listing of program PROFILES to read profiles from disc and plot.
3. Listing of version of subroutine NEDNE for ray tracing through "oblique profiles".
4. Listing of version of subroutine NHPR to read profiles from disc for ray tracing.
5. Listing of subroutine CORR for correlation analysis.

1. Listing of Program OVIP

```

C ***** OVIP
      MASTER OVIP
C THIS PROGRAM READS DATA FROM AN OBLIQUE IONOGRAM AND
C PRODUCES THE EQUIVALENT VERTICAL ONE, READS DATA FROM
C A VERTICAL IONOGRAM AND PLOTS BOTH ON THE SAME AXES.
C IT THEN CALLS NHPP TO PRODUCE N(H) PROFILES FROM BOTH
C IONOGRAMS AND PLOTS THESE (IF NPLOT IS SET EQUAL TO 1).
C TO PLOT ONLY EQUIV VERT IOGM AND/OR PROFILE SET JPLOT = 0
C TO PLOT ONLY IONOGRAM(S) SET IPLOT = 1 AND NPLOT = 0
C TO PLOT ONLY PROFILE(S) SET IPLOT = 0 AND NPLOT = 1
C IF IFILE = 1, HEIGHT & DENSITY ARRAYS WRITTEN TO DISC
C FILE STARTING AT FILE ELEMENT NUMBER KARRAY;
C IF IFILE = 2, A & B SEGMENT COEFFS WRITTEN AS WELL
C STARTING AT FILE ELEMENT NUMBER KCOEFF.
C OBLIQUE DATA INPUT FORMAT COMPATIBLE WITH THAT OF NHOR.
C VERTICAL DATA INPUT FORMAT COMPATIBLE WITH THAT OF NHPR
      REAL FDASH(50),HDASH(50),FVERO(50),HVERO(50),HEADO(4),
+       HEAD(4),FBORD(3),HBORD(3),EBORD(3),ZBORD(3),
+       OBNE(50),OBHT(50),VENE(50),VEHT(50),ZA(50)
      REAL KN,NEO,NEA(50)
      COMMON/PRFL/FH,DIP,A(50),B(50),AAP,BBP,CCP,SLAT,SLON
      COMMON/AMGRAPH1/HGT,PAGE,DASHLN,TICK,SET,SPACE,SHIFT,SYMB
      COMMON/AMGRAPH3/CHAR,NCROSS,ISUP,ISO,NOAXES,NONUMX,NONUMY
      COMMON/ARGRAPH1/IQX,IQY
      EQUIVALENCE (FDASH(1),OBNE(1)),(HDASH(1),OBHT(1))
      EQUIVALENCE (FVERO(1),VENE(1)),(HVERO(1),VEHT(1))
C CANNOT USE DATA STATEMENT FOR COMMON VARIABLES
      D=4470.84
      RE=6371.35
      KFLAG=1
      ISUP=1
      IQX=0
      IQY=0
      SET=3.0
      HGT=0.8
      HGT1=0.2
      SYMB=0.15
      CALL COPY8(CHAR,1H0)
C INPUT OBLIQUE IONOGRAM I.D. DATA AND PLOTTING DATA
      READ(5,5001) HEADO,OFFSET
      READ(5,5002) IPLOT,NPLOT,IC,NHD,NIL,NIX,NIY,NPL,NPX,NPY
      READ(5,5003) FSIZE,HSIZE,ESIZE,ZSIZE,FBORD(1),FBORD(2),
+       HBORD(3),HBORD(2),EBORD(1),EBORD(2),ZBORD(3),ZBORD(2)
+       READ(5,5004) NHOP,HOMIN,JEND,KEND,IFILE,KARRAY,KCOEFF,
+       IFLAG,JPLOT
C DISTANCE, CHORD LENGTH, ARC HEIGHT AND CORRECTION FACTOR
      D=D/FLOAT(NHOP)
      SN=2.*RE*SIN(D/(2.*RE))
      BN=RE*(1.-COS(D/(2.*RE)))
      KN=0.00004745*D+0.97095
      I=1
C INPUT OBLIQUE P,F DATA
10  READ(5,5010) P,F
      IF(P.GE.9999.) GO TO 30
      IF(I.EQ.1) PO=P+OFFSET
      P=(P+OFFSET)/FLOAT(NHOP)
C EQUIVALENT VERTICAL FREQUENCY AND VIRTUAL HEIGHT
      FDASH(I)=(F/KN)*SQRT(1.-SN*SN/(P*P))
      HDASH(I)=SQRT(P*P-SN*SN)/2.-BN
      IF(I.EQ.1) GO TO 20
      IF(FDASH(I).LT.FDASH(I-1)) FDASH(I)=FDASH(I-1)
20  I=I+1
      GO TO 10

```

```

30  IEND=I-1
    FOF2=F
    IF(FOF2.LT.FDASH(IEND)) FOF2=FDASH(IEND)
    WRITE(6,6001) HEADO,NHOP
    WRITE(6,6005)
    WRITE(6,6003)
    WRITE(6,6010)(I,HDASH(I),FDASH(I),I=1,IEND)
    WRITE(6,6020) FOF2
    SLAT=-33.29
    SLON=26.5267
    FH=0.82
    DIP=-60.0

    IF(IPLOT.NE.1.AND.NPLOT.NE.1) GO TO 40
C PLOTTING CALLS : INITIALISE PLOTTER
    CALL AMGRAPH(6,0,0,0,4HARJR,HDASH,FSIZE,HSIZE,HEADO,0)
    HGT=HGT1
C SET PLOTTING LIMITS FOR IONOGRAM AND DRAW AXES
    IF(IPLOT.NE.1) GO TO 40
    FBORD(3)=FBORD(2)
    HBORD(1)=HBORD(2)
    CALL COPY(11,HEAD(1),1,11HIONOGRAMS ,1)
    CALL COPY(16,HEAD(1),12,HEADO(1),15)
    CALL COPY(5,HEAD(1),28,5H ,1)
    CALL AMAXISLABEL(15HFREQUENCY (MHZ),
+ 19HVIRTUAL HEIGHT (KM),NIX,NIY)
    CALL AMGRAPH(6,0,3,IC,FBORD,HBORD,FSIZE,HSIZE,HEAD,NHD)
C DRAW EQUIVALENT VERTICAL IONOGRAM
    CALL COPY(1,CHAR,1,1H0,1)
    CALL AMGRAPH(6,22,IEND,1,FDASH,HDASH,FSIZE,HSIZE,HEAD,0)
    XLAB=FBORD(1)+0.5
    YLAB=HBORD(1)-100.
    HGT=SYMB
    CALL AMLABEL(XLAB,YLAB,27HOBlique EQUIVALENT VERTICAL,
+ 27,0.0,0)
    HGT=HGT1
C N(H) PROFILE FROM EQUIVALENT VERTICAL IONOGRAM
40  WRITE(6,6030) HEADO
    CALL NHPF(FDASH,HDASH,IEND,FOF2,NEA,ZA,HNO,NEO,HMAX)
    IPTS=IEND+2
    DO 50 I=1,IPTS-2
    J=IPTS-I
    OBNE(J)=NEA(J-1)
    OBHT(J)=ZA(J-1)
    A(J)=A(J-1)
50  B(J)=B(J-1)
    OBNE(1)=0.0
    OBHT(1)=HNO
    A(1)=0.0
    B(1)=0.0
    OBNE(IPTS)=NEO
    OBHT(IPTS)=HMAX
C IF IFILE > 0 WRITE H & NE ARRAYS TO DISC
    IF(IFILE.EQ.0) GO TO 60
    CALL USEFILE(2,2HED,12HARJRDATA01 ,1,0)
    IELEM=KARRAY
    WRITE (6,6050) IELEM,IPTS
    CALL PUTARRAY(2,IELEM,OBHT)
    WRITE (6,6055) IELEM,IPTS
    CALL PUTARRAY(2,IELEM,OBNE)
    KARRAY=IELEM
C IF IFILE = 2 WRITE A & B ARRAYS TO DISC
    IF(IFILE.NE.2) GO TO 60
    IELEM=KCOEFF
    A(IPTS)=AAP
    WRITE(6,6060) IELEM,IPTS
    CALL PUTARRAY(2,IELEM,A)
    B(IPTS)=BBP

```

```
B(IPTS+1)=CCP
IPTS=IPTS+1
WRITE(6,6065) IELEM,IPTS
CALL PUTARRAY(2,IELEM,B)
IPTS=IPTS-1
KCOEFF=IELEM

C INPUT VERTICAL IONOGRAM I.D. DATA AND H',F FOR O-RAY
60 READ(5,5001) HEAD
   I=4
   CALL COMP(I,HEAD(1),1,4H####,1)
   IF (I.EQ.4) GO TO 140
   READ(5,5005) FH,DIP,SLAT,SLON,IHOP
   DO 70 I=1,50
   VENE(I)=0.0
   VEHT(I)=0.0
   A(I)=0.0
70 B(I)=0.0
   J=1
80 READ(5,5010) H,F
   IF(H.GE.9999.) GO TO 90
   FVERO(J)=F
   HVERO(J)=H
   J=J+1
   GO TO 80
90 JEND=J-1
   FOF2=F
   WRITE(6,6002) HEAD
   WRITE(6,6004) SLAT,SLON
   WRITE(6,6005)
   WRITE(6,6003)
   WRITE(6,6010) (J,HVERO(J),FVERO(J),J=1,JEND)
   WRITE(6,6020) FOF2

C DRAW VERTICAL INCIDENCE IONOGRAM O - RAY
IF (IPL0T.NE.1.OR.JPLOT.NE.1) GO TO 95
CALL COPY(1,CHAR,1,HEAD(1),1)
CALL AMGRAPH(6,22,JEND,1,FVERO,HVERO,FSIZE,HSIZE,HEAD,0)
YLAB=YLAB-2.*(HBORD(2)-HBORD(3))*HGT/HSIZE
HGT=SYMR
CALL AMLABEL(XLAB,YLAB,HEAD,11,0.0,0)
HGT=HGT1

C N(H) PROFILE FROM VERTICAL INCIDENCE IONOGRAM
95 WRITE(6,6040) HEAD
   CALL NHPF(FVERO,HVERO,JEND,FOF2,NEA,ZA,HNO,NEO,HMAX)
   JPPTS=JEND+2
   DO 100 J=1,JPPTS-2
   I=JPPTS-J
   VENE(I)=NEA(I-1)
   VEHT(I)=ZA(I-1)
   A(I)=A(I-1)
100 B(I)=B(I-1)
   VENE(1)=0.0
   VEHT(1)=HNO
   A(1)=0.0
   B(1)=0.0
   VENE(JPPTS)=NEO
   VEHT(JPPTS)=HMAX

C IF IFILE > 0 WRITE H & NE ARRAYS TO DISC
IF (IFILE.EQ.0) GO TO 110
IELEM=KARRAY
WRITE (6,6050) IELEM,JPPTS
CALL PUTARRAY(2,IELEM,VEHT)
WRITE (6,6055) IELEM,JPPTS
CALL PUTARRAY(2,IELEM,VENE)
KARRAY=IELEM

C IF IFILE = 2 WRITE A & B ARRAYS TO DISC
IF(IFILE.NE.2) GO TO 110
IELEM=KCOEFF
A(JPPTS)=AAP
WRITE(6,6060) IELEM,JPPTS
CALL PUTARRAY(2,IELEM,A)
```

```
B(JPTS)=BBP
B(JPTS+1)=CCP
JPTS=JPTS+1
WRITE(6,6065) IELEM,JPTS
CALL PUTARRAY(2,IELEM,B)
JPTS=JPTS-1
KCOEFF=IELEM

C SET PLOTTING LIMITS AND DRAW AXES FOR PROFILES
110 IF(NPLOT.NE.1) GO TO 130
    IF (KFLAG.EQ.0) GO TO 120
    EBORD(3)=EBORD(2)
    ZBORD(1)=ZBORD(2)
    CALL AMAXISLABEL(23HELECTRON DENSITY (CM-3),
+                   11HEIGHT (KM),NPX,NPY)
    CALL AMGRAPH(6,0,3,IC,EBORD,ZBORD,ESIZE,ZSIZE,
+              17H N(H) PROFILES,NPL)

C DRAW PROFILE FROM EQUIVALENT VERTICAL IONOGRAM
    CALL COPY (1,CHAR,1,1H0,1)
    CALL AMGRAPH(6,22,IPTS,1,OBNE,OBHT,ESIZE,ZSIZE,HEAD,0)

C DRAW PROFILE FROM VERTICAL INCIDENCE IONOGRAM
    CALL COPY(1,CHAR,1,HEAD(1),1)
120 IF (JPLOT.EQ.1)
+   CALL AMGRAPH(6,22,JPTS,1,VEVE,VEHT,ESIZE,ZSIZE,HEAD,0)
130 KFLAG=0
    GO TO 60

C TERMINATION CALL TO PLOTTER
140 IF (IPLOT.EQ.1.OR.NPLOT.EQ.1)
+   CALL AMGRAPH(6,0,0,2,FDASH,HDASH,FSIZE,HSIZE,HEAD,0)
    STOP OK

C FORMAT STATEMENTS
5001 FORMAT(4A8,E0.0)
5002 FORMAT(10I0)
5003 FORMAT(12E0.0)
5004 FORMAT(10,E0.0,7I0)
5005 FORMAT(4E0.0,I0)
5010 FORMAT(2E0.0)

6000 FORMAT(/)
6001 FORMAT(1H1,33HEQUIVALENT VERTICAL IONOGRAM FROM,/,/,
+          1H,4A8,/,1H,13,9H HOP MODE)
6002 FORMAT(1H1,32HVERTICAL INCIDENCE IONOGRAM FROM,/,/,
+          1H,4A8)
6003 FORMAT(/,30H PT VIRT HT FREQ,/,1H )
6004 FORMAT(/,1H,3HLAT,F10.4,3X,3HLON,F9.4)
6005 FORMAT(/,18H ORDINARY RAY)
6010 FORMAT(1H,13,2X,2F12.2)
6020 FORMAT(/,1H,18X,6HFOF2 =,F5.2)
6030 FORMAT(1H1,40HELECTRON DENSITY PROFILE FROM EQUIVALENT,
+          24H VERTICAL IONOGRAM,4A8)
6040 FORMAT(1H1,38HELECTRON DENSITY PROFILE FROM VERTICAL,
+          26H INCIDENCE IONOGRAM,4A8)
6050 FORMAT(/,41H FIRST FILE ELEMENT NO FOR HEIGHT ARRAY,I6,
+          13H ARRAY SIZE,I6)
6055 FORMAT(/,41H FIRST FILE ELEMENT NO FOR DENSITY ARRAY,I6,
+          13H ARRAY SIZE,I6)
6060 FORMAT(/,41H FIRST FILE ELEMENT NO FOR A SEG COEFFS,I6,
+          13H ARRAY SIZE,I6)
6065 FORMAT(/,41H FIRST FILE ELEMENT NO FOR B SEG COEFFS,I6,
+          13H ARRAY SIZE,I6)

END
```

C ***** NHPF

SUBROUTINE NHPF(F,H,NPT,FP,NEA,ZA,HNO,NEO,HMAX)

C COMPUTES N(H) (ELECTRON DENSITY VS REAL HEIGHT) PROFILE FROM THE ORDINARY RAY TRACE OF AN IONOGRAM.

C C PARAMETERS AS FOLLOWS :

C F,H : INPUT ARRAYS OF FREQUENCY AND VIRTUAL HEIGHT
C NPT : NUMBER OF F,H POINTS FROM IONOGRAM (UP TO 50)
C FP : CRITICAL FREQUENCY FOF2
C NEA,ZA : OUTPUT ARRAYS OF ELECTRON DENSITY AND REAL HEIGHT
C HNO : OUTPUT BASE HEIGHT OF IONOSPHERE
C NEO : MAXIMUM ELECTRON DENSITY
C HMAX : HEIGHT OF MAXIMUM ELECTRON DENSITY

REAL F(NPT),H(NPT),NEA(NPT),ZA(NPT),F2(50)
REAL YA(7),WA(7),XA(2),NEO

COMMON/PRFL/FH,DIP,A(50),B(50),AAP,BBP,CCP,SLAT,SLON

C ABSCISSAE AND WEIGHTS FOR 6 POINT GAUSSIAN INTEGRATION

YA(1) = 0.0
YA(2) = -.93246951420
YA(3) = -.66120938647
YA(4) = -.23861918608
YA(5) = .23861918608
YA(6) = .66120938647
YA(7) = .93246951420
WA(1) = 0.0
WA(2) = .17132449238
WA(3) = .36076157305
WA(4) = .46791393457
WA(5) = .46791393457
WA(6) = .36076157305
WA(7) = .17132449238

C SQUARES OF PLASMA FREQUENCIES

F2(1)=F(1)*F(1)
DO 10 N=2,NPT
IF(F(N).LE.F(N-1)) F(N)=F(N-1)+0.01
10 F2(N) = F(N)*F(N)
IF(FP.LE.F(NPT)) FP=F(NPT)+0.01
ZA(1) = H(1)
ANGLE = 90.0 + DIP

C CONVERT TO RADIANS

ANGLE = 0.017453293*ANGLE
CA = COS(ANGLE)
SA = SIN(ANGLE)
SA2 = SA*SA

C CALCULATE COEFFICIENTS OF PARABOLIC SEGMENTS

DO 90 N = 2,NPT
Y = FH/F(N)
J = N - 1
IF (J.GT.1) GO TO 40
A(2) = 0.0
XA(1) = SQRT(1. - F2(1)/F2(2))
Z = 0.0
DO 30 I = 2,7
XD = XA(1)*(YA(I) + 1.)/2.
X = 1. - XD*XD
30 Z = Z + WA(I)*XD*GMU(X,Y,CA,SA2)
Z = F2(2)*XA(1)*Z
B(2) = (H(2) - H(1))/Z
ZA(2) = H(1) + B(2)*(F2(2) - F2(1))
GO TO 90
40 ZD = 0.0
DO 60 L = 2,J
XA(1) = F2(L-1)
XA(2) = F2(L)
Z = 0.0
DO 50 I = 2,7

```

XD = XA(1) + (XA(2) - XA(1))*(YA(I) + 1.)/2.
X = XD/F2(N)
50 Z = Z + WA(I)*GMU(X,Y,CA,SA2)*(2.*A(L)*XD + B(L))
Z = (XA(2) - XA(1))*Z/2.
60 ZD = ZD + Z
XA(1) = SQRT(1. - F2(N-1)/F2(N))
Z = 0.0
DO 70 I = 2,7
XD = XA(1)*(YA(I) + 1.)/2.
X = 1. - XD*XD
70 Z = Z + WA(I)*X*XD*GMU(X,Y,CA,SA2)
Z = XA(1)*(F(N)**4)*(2.*A(N-1)*F2(N-1) + B(N-1))*Z/F2(N-1)
ZD = H(N) - H(1) - ZD - Z
XA(1) = SQRT(1. - F2(N-1)/F2(N))
Z = 0.0
DO 80 I = 2,7
XD = XA(1)*(YA(I) + 1.)/2.
X = 1. - XD*XD
80 Z = Z + WA(I)*XD*GMU(X,Y,CA,SA2)*(1. - F2(N)*X/F2(N-1))
Z = XA(1)*F2(N)*Z
B(N) = ZD/Z
A(N) = (2.*A(N-1)*F2(N-1) + B(N-1) - B(N))
1 / (2.*F2(N-1))
1 ZA(N) = ZA(N-1) + A(N)*(F(N)**4 - F(N-1)**4)
+ B(N)*(F2(N) - F2(N-1))
90 CONTINUE

WRITE (6,6000) FH,DIP,SLAT,SLON
WRITE (6,6001)
DO 100 I = 1,NPT
NEA(I) = 12404.427*F2(I)
100 WRITE (6,6002) H(I),F(I),NEA(I),ZA(I),A(I),B(I),I

```

C CALCULATE PARAMETERS OF F2 LAYER MAXIMUM

```

NEO = 12404.427*FP*FP
S = NEA(NPT-1) - NEA(NPT)
T = NEA(NPT-1) - NEO
U = NEA(NPT) - NEO
V = ZA(NPT-1) - ZA(NPT)
P = (V**4)/4.0
Q = V*V*(ZA(NPT-1)*U + ZA(NPT)*T)
R = S*(T*ZA(NPT)**2 - U*ZA(NPT-1)**2)
BBP = ((-Q) - SQRT(Q*Q - 4.*P*R))/(2.*P)
W = (ZA(NPT-1))**2 - (ZA(NPT))**2
Z = ZA(NPT-1) + ZA(NPT)
AAP = (NEA(NPT-1) - NEA(NPT))/W
1 - BRP/Z
CCP = NEO + BBP*BBP/(4.*AAP)
HNO = ZA(1) - B(2)*NEA(1)/12404.427
HMAX = (-BBP)/(2.*AAP)
WRITE (6,6003) AAP,BRP,CCP
WRITE (6,6004) HNO,HMAX,NEO
RETURN

6000 FORMAT(/1H ,24HELECTRON GYROFREQUENCY =,F9.4,
+ 4H MHZ/,1H ,19X,5HDIP =,F9.4,4H DEG/,1H ,14X,
+ 10HLATITUDE =,F9.4,4H DEG/,1H ,13X,11HLONGITUDE =,
+ F9.4,4H DEG,17X,8HSEGMENTS,
+ 34H OF THE FORM H = A*FN4 + B*FN2 + C )
6001 FORMAT(1H0,24H VIRT HT (KM) ,6X,
+ 25HNE (CM-3) ,6X,
+ 26HA(N) SEGMENT COEFFS B(N),8X,1HN/,1H )
6002 FORMAT(1H ,0PF11.4,F12.4,1PE17.6,0PF13.4,1P2E18.6,17)
6003 FORMAT(1H //15H F2 PEAK: A =,1PE14.6,6H B =,1PE14.6,
+ 6H C =,1PE14.6,28H WHERE NE = A*H2 + B*H + C )
6004 FORMAT(1H //16H BASE HT HNO =,F10.4,3H KM //
+ 16H PEAK HT HMAX =,F10.4,3H KM //
+ 16H PEAK NE NEO =,1PE13.6)

```

END

C ***** GMU

REAL FUNCTION GMU(X,Y,CA,SA2)

C THIS FUNCTION CALCULATES GROUP REFRACTIVE INDEX

E = 2.*(1. - X)*CA/(SA2*Y)

```

G = SQRT(1. + E*E)
R = E/(1. + G)
S = Y*CA
C = 1. + R*S
W = 1. - X/C
V = SQRT(W)
+ GMU = V + X*(1. + C + S*E*(1. + X)/(G*(G + 1.)*(1. - X)))
  / (2.*V*C*C)
RETURN
END

```

C ***** NMODE

 SUBROUTINE NMODE(P,HE,PHIE,HF)

C THIS SUBROUTINE INPUTS A PATHLENGTH P AND GIVEN HEIGHT HE
C OF ONE HOP. IT OUTPUTS THE VALUES OF PHIE=DE/2*A, WHERE
C DE = DISTANCE COVERED IN THE "E HOP" AND A = RADIUS OF EARTH,
C AND HF, THE VIRTUAL HEIGHT OF THE OTHER HOP.
C THE NEWTON-RAPHSON ALGORITHM IS USED TO IMPROVE THE ROOT PHIE.
C AN INITIAL ESTIMATE OF PHIE IS INPUT.

 COMMON/MODI/A,D,PHI,NITER,DELTA

 N=1

C ITERATION LOOP FOR NEWTON-RAPHSON PROCEDURE ON PHIE

 10 PHIEK=PHIE

C INTERMEDIATE VARIABLES

 S=A*SIN(PHIE)
 H=HE+A*(1.-COS(PHIE))
 T=ATAN(H/S)+PHI-2.*PHIE

C FORM FUNCTION F(PHIF) SUCH THAT F(PHIE)=0

 TERM1=SQRT(H*H+S*S)
 TERM2=A*SIN(PHI-PHIE)/COS(T)
 F=TERM1+TERM2-P/2.

C FORM FUNCTION FDASH(PHIE)=DF/DPHIE

 TERM1=(A+HE)*S/SQRT(H*H+S*S)
 TERM2=A*COS(PHI-PHIE)/COS(T)
 GUNK1=A*SIN(PHI-PHIE)*TAN(T)/COS(T)
 GUNK2=(S*S-H*A*COS(PHIE))/(H*H+S*S)
 TERM3=GUNK1*(GUNK2-2.)
 FDASH=TERM1-TERM2+TERM3

C NEW ESTIMATE OF ROOT PHIE

 PHIE=PHIE-F/FDASH

C CHECK NUMBER OF ITERATIONS

 N=N+1
 IF(N.GT.NITER) GO TO 20

C CHECK ACCURACY OF PHIE AND LOOP BACK IF NECESSARY

 DPHIE=ABS(PHIE-PHIEK)
 IF(DPHIE.GT.DELTA) GO TO 10

C NEW ESTIMATE OF H'F

 S=A*SIN(PHIE)
 H=HE+A*(1.-COS(PHIE))
 T=ATAN(H/S)+PHI-2.*PHIE
 TERM1=A*SIN(PHI-PHIE)*TAN(T)
 TFRM2=A*(1.-COS(PHI-PHIE))
 HF=TERM1-TERM2

C RETURN FINAL VALUES OF H'F, PHIE

 20 RETURN
 END

2. Listing of Program PROFILES

```

C ***** PROFILES
C MASTER PROFILES
C THIS PROGRAM READS A NUMBER OF SETS OF REAL HEIGHT AND ELECTRON
C DENSITY ARRAYS FOR N(H) PROFILES, EACH 'SET' CONSISTING OF UP TO
C 6 PROFILES. EACH ARRAY HAS DIMENSION 50.
C THE ARRAYS ARE READ FROM DISC STARTING AT FILE ELEMENT NO IELEM(J),
C J = 1-6. IF IPLOT(J) = 1 IT PLOTS THE PROFILE. THE ARRAYS HAVE
C BEEN WRITTEN TO DISC BY PROGRAMS NHOR, NHOS AND OVIO.
C J = 1 : PROFILE DIRECT FROM OBLIQUE IONOGRAM BY RAO METHOD
C J = 2 : PROFILE DIRECT FROM OBLIQUE IONOGRAM BY SMITH METHOD
C J = 3 : PROFILE FROM OBLIQUE VIA EQUIVALENT VERTICAL IONOGRAM
C J = 4 : PROFILE FROM R.S.A. VERTICAL INCIDENCE IONOGRAM
C J = 5 : PROFILE FROM SANAÉ VERTICAL INCIDENCE IONOGRAM
C J = 6 : PROFILE FROM GRAHAMSTOWN VERTICAL INCIDENCE IONOGRAM

REAL H(50),NE(50),HEAD(4),XLIM(3),YLIM(3),CHAX(6),LABEL1(4),
+ LABEL2(4),LABEL3(4),LABEL4(4),LABEL5(4),LABEL6(4)
INTEGER IPLOT(6),IELEM(6),MODE(6)

COMMON/AMGRAPH1/HGT,PAGE,DASHLN,TICK,SET,SPACE,SHIFT,SYMB
COMMON/AMGRAPH3/CHAR,NCROSS,ISUP,ISO,NOAXES,NONUMX,NONUMY
COMMON/ARGRAPH1/IQX,IQY

DATA CHAX/1HA,1HB,1HE,1HR,1HS,1HG/,MODE/22,22,22,22,22,22/
DATA LABEL1(1)/32H FROM OBLIQUE IONOGRAM (RAO) /
DATA LABEL2(1)/32H FROM OBLIQUE IONOGRAM (SMITH) /
DATA LABEL3(1)/32H FROM EQUIV. VERTICAL IONOGRAM /
DATA LABEL4(1)/32H FROM R.S.A. VERTICAL IONOGRAM /
DATA LABEL5(1)/32H FROM SANAÉ VERTICAL IONOGRAM /
DATA LABEL6(1)/32H FROM GRAHAMSTOWN IONOGRAM /

HGT1=0.35
HGT=HGT1
SYMB1=0.20
SYMB2=0.20
SYMB=SYMB1
SET=5.0
SPACE=10.0
ISUP=1
IQX=1
IQY=0

CALL AMGRAPH(6,0,0,0,4HARJR,H,XSIZE,YSIZE,HEAD,U)
CALL USEFILE(2,2HED,12HARJRDATA01 ,1,0)

10 READ (5,5000) HEAD
   READ (5,5010) IPLOT,IELEM
   IF(IPLOT(1).GE.9) GO TO 50
   READ (5,5020) IC,NHD,NXL,NYL,XSIZE,YSIZE,XLIM(1),XLIM(2),
+ YLIM(3),YLIM(2),XLBL,YLBL,NLBL

   IPLOTS=IPLOT(1)+IPLOT(2)+IPLOT(3)+IPLOT(4)+IPLOT(5)+IPLOT(6)
   IF(IPLOTS.EQ.0) GO TO 20
   XLIM(3)=XLIM(2)
   YLIM(1)=YLIM(2)
   YSCALE=(YLIM(2)-YLIM(3))/YSIZE
   SHIFT=XSIZE+SPACE+5.0*HGT
   CALL AMAXISLABEL(23HELECTRON DENSITY (CM-3),
+ 16HREAL HEIGHT (KM),NXL,NYL)
   CALL AMGRAPH(6,0,3,IC,XLIM,YLIM,XSIZE,YSIZE,HEAD,NHD)
20 HGT=SYMB2

DO 40 J=1,6
  IF(IELEM(J).EQ.0) GO TO 40
  WRITE(6,6000) HEAD
  K=IELEM(J)
  WRITE(6,6200) K
  CALL GETARRAY(2,K,H)
  WRITE(6,6200) K
  CALL GETARRAY(2,K,NE)
  M=MODE(J)
  DO 30 I=1,50
30 IF (H(I).EQ.0.0) GO TO 35
35 N=I-1
   IF (H(N).GT.H(N-1)+20.) H(N)=H(N-1)+20.
   IF (NE(N).GT.NE(N-1)*1.05) NE(N)=NE(N-1)*1.05

```

```
CALL COPY8(CHAR,CHAX(J))
IF(J.EQ.1) WRITE(6,6001)
IF(J.EQ.2) WRITE(6,6002)
IF(J.EQ.3) WRITE(6,6003)
IF(J.EQ.4) WRITE(6,6004)
IF(J.EQ.5) WRITE(6,6005)
IF(J.EQ.6) WRITE(6,6006)
WRITE(6,6010)
WRITE(6,6100)(I,H(I),NE(I),I=1,N)

IF(IPLOT(J).NE.1) GO TO 40
CALL AMGRAPH(6,M,N,1,NE,H,XSIZE,YSIZE,HEAD,0)

SYMB=SYMB2
IF(J.GT.1) YLBL=YLBL-2.0*HGT*YSCALE
IF(J.EQ.1) CALL AMLABEL(XLBL,YLBL,LABEL1,NLBL,0.0,0)
IF(J.EQ.2) CALL AMLABEL(XLBL,YLBL,LABEL2,NLBL,0.0,0)
IF(J.EQ.3) CALL AMLABEL(XLBL,YLBL,LABEL3,NLBL,0.0,0)
IF(J.EQ.4) CALL AMLABEL(XLBL,YLBL,LABEL4,NLBL,0.0,0)
IF(J.EQ.5) CALL AMLABEL(XLBL,YLBL,LABEL5,NLBL,0.0,0)
IF(J.EQ.6) CALL AMLABEL(XLBL,YLBL,LABEL6,NLBL,0.0,0)
40 SYMB=SYMB1

HGT=HGT1
GO TO 10

50 IF(IPLOTS.GT.0)
+ CALL AMGRAPH(6,0,0,2,NE,H,XSIZE,YSIZE,HEAD,0)
STOP OK

5000 FORMAT(4A8)
5010 FORMAT(12I0)
5020 FORMAT(4I0,8E0.0,I0)

6000 FORMAT(1H1,4A8,/,1H )
6006 FORMAT(/,40H N(H) PROFILE FROM GRAHAMSTOWN VERTICAL ,
+ 19HINCIDENCE IONOGRAM )
6005 FORMAT(/,43H N(H) PROFILE FROM SANAE VERTICAL INCIDENCE ,
+ 9H IONOGRAM )
6004 FORMAT(/,44H N(H) PROFILE FROM R.S.A. VERTICAL INCIDENCE ,
+ 9H IONOGRAM )
6003 FORMAT(/,41H N(H) PROFILE FROM OBLIQUE VIA EQUIVALENT ,
+ 18H VERTICAL IONOGRAM )
6002 FORMAT(/,42H N(H) PROFILE DIRECT FROM OBLIQUE IONOGRAM,
+ 16H (SMITH METHOD))
6001 FORMAT(/,42H N(H) PROFILE DIRECT FROM OBLIQUE IONOGRAM,
+ 14H (RAO METHOD))
6010 FORMAT(/,6H I,10X,4HH(I),13X,5HNE(I),/,1H )
6100 FORMAT(1H,15,OPF15.2,1PE20.4)
6200 FORMAT(/,16H FILE ELEMENT NO,I6)

END
```

3. Listing of Subroutine NEDNE

```
C *****NEDNE
SUBROUTINE NEDNE (DNE,H)
REAL NE,NEO,NEA
COMMON /CONT/ HGT,THETA,PHI,ALPHA,BETA,NCR,NP,NPR,NAME
COMMON /CPRF/ NE,NEO(2),HNO(2),HMAX(2),HD1,HD2,HCR,RNO,RMAX,RERTH
COMMON /CARY/ NEA(2,50),ZA(2,50),A(2,50),B(2,50),NPT(2),
1 AAP(2),BBP(2),CCP(2),RLAT(2),DELLAT
COMMON /CSEG/ N
COMMON /CHOP/ NHOP,NHOPS,NNH,INH(4)
DATA NNAME /4HNEDN/
NAME=NNAME

C THIS VERSION OF NEDNE IS USED WHEN THE PROFILE IS
C COMPUTED FROM AN OBLIQUE IONOGRAM BY PROGRAM NHOBLIQUE
C CALCULATE NE AND DNE/DH AT HEIGHT H

R=RERTH+H
10 IF (H - HNO(NNH)) 70,70,20
20 IF (H - ZA(NNH,NPT(NNH))) 30,30,100

C FIND WHICH SEGMENT N WE ARE IN, I.E. FIND N,
C 1 <= N <= NPT, SUCH THAT H(N-1) <= H <= H(N)
30 IF (N.GT.NPT(NNH)) N=NPT(NNH)
DEL = H - ZA(NNH,N)
IF (DEL) 40,90,60
40 IF (N.EQ.1) GO TO 90
N = N-1
DEL = H - ZA(NNH,N)
IF (DEL) 40,90,80
50 N = N+1
60 DEL = H - ZA(NNH,N+1)
IF (DEL) 80,80,50

C IF H <= HO, I.E. BELOW IONOSPHERE, VALUES ARE ZERO
70 NE = 0.0
DNE= 0.0
GO TO 110
80 N = N + 1

C IN SEGMENT N WE HAVE FN2 = A(N) - B(N)/R
90 NE = 12404.427*(A(NNH,N)-B(NNH,N)/R)
DNE= 12404.427*B(NNH,N)/(R*R)
IF (NE.LT.0.0) NE=0.0
GO TO 110

C IF H > H(NPT) I.E. NEAR PEAK USE PARABOLIC FIT FN2=A*R2+B*R+C
100 NE = 12404.427*(AAP(NNH)*R*R + BBP(NNH)*R + CCP(NNH))
DNE= 12404.427*(2.*AAP(NNH)*R + BBP(NNH))
110 RETURN
END
```

4. Listing of Subroutine NHPR

```
C ***** NHPR
      SUBROUTINE NHPR
C THIS VERSION OF NHPR READS REAL HEIGHT AND ELECTRON DENSITY
C ARRAYS AS WELL AS ARRAYS OF SEGMENT COEFFICIENTS FROM A DISC FILE
      REAL NE,NEO,NEA,FILENAME(2),HEAD(4),ARRAY(50)
      COMMON /CONT/ HGT,THETA,PHI,ALPHA,BETA,NCR,NP,NPR,NAME
      COMMON /CPRF/ NE,NEO(2),HNO(2),HMAX(2),HD1,HD2,HCR,RNO,RMAX,RERTH
      COMMON /CARY/ NEA(2,50),ZA(2,50),A(2,50),B(2,50),NPT(2),
      + AAP(2),BBP(2),CCP(2),RLAT(2),DELLAT
      COMMON /CSEG/ N
      COMMON /CHOP/ NHOP,NHOPS,NNH,INH(4)
      DATA NNAME/4HNNHPR/
      NAME=NNAME
C READ IN 4A8 ALPHAMERIC TITLE OF IONOGRAM ETC
C IF PROFILE IS FROM AN OBLIQUE IONOGRAM PUT FH = 0
      READ(5,5010) HEAD
      READ(5,5020) FH,DIP,RLAT(NNH),RLON
C READ IN NAME OF DISC FILE, GENERATION NO AND FIRST FILE
C ELEMENT NOS FOR HEIGHT ARRAY (IT IS ASSUMED THAT THE DENSITY
C ARRAY FOLLOWS IMMEDIATELY) AND FOR ARRAY OF COEFFICIENTS A
C (IT IS ASSUMED THAT THE ARRAY OF COEFFS B FOLLOWS IMMEDIATELY)
      READ(5,5030) FILENAME,IGEN,KARRAY,KCOEFF
      CALL USEFILE(2,2HED,FILENAME(1),IGEN,0)
C READ HEIGHT ARRAY FROM DISC
      K=KARRAY
      CALL GETARRAY(2,K,ARRAY)
      HNO(NNH)=ARRAY(1)
      DO 10 N=1,50
      ZA(NNH,N)=ARRAY(N+1)
      IF(ZA(NNH,N).EQ.0.0) GO TO 20
10  CONTINUE
20  NPT(NNH)=N-2
      HMAX(NNH)=ARRAY(N)
C READ DENSITY ARRAY FROM DISC
      CALL GETARRAY(2,K,ARRAY)
      DO 30 N=1,NPT(NNH)
30  NEA(NNH,N)=ARRAY(N+1)
      NEO(NNH)=ARRAY(N+1)
C READ A COEFFS AND PEAK COEFF AAP FROM DISC
      K=KCOEFF
      CALL GETARRAY(2,K,ARRAY)
      DO 40 N=1,NPT(NNH)
40  A(NNH,N)=ARRAY(N+1)
      AAP(NNH)=ARRAY(N+1)
C READ B COEFFS AND PEAK COEFFS BBP,CCP FROM DISC
      CALL GETARRAY(2,K,ARRAY)
      DO 50 N=1,NPT(NNH)
50  B(NNH,N)=ARRAY(N+1)
      BBP(NNH)=ARRAY(N+1)
      CCP(NNH)=ARRAY(N+2)
C PRINT VALUES
      WRITE (6,6000) FILENAME
      IF (FH.EQ.0.0) WRITE(6,6005) HEAD
      IF (FH.NE.0.0) WRITE(6,6010) HEAD
      IF(FH.EQ.0.0) WRITE(6,6020) RERTH
      IF(FH.NE.0.0) WRITE(6,6030) FH,DIP,RLAT(NNH),RLON
      WRITE(6,6040)
      DO 60 N=1,NPT(NNH)
      FN=SQRT(NEA(NNH,N)/12404.427)
60  WRITE(6,6050) FN,NEA(NNH,N),ZA(NNH,N),A(NNH,N),B(NNH,N),N
      WRITE(6,6060) AAP(NNH),BBP(NNH),CCP(NNH)
```

```
IF(FH.EQ.0.0) WRITE(6,6070)
IF(FH.NE.0.0) WRITE(6,6080)
WRITE(6,6090) HNO(NNH),HMAX(NNH),NEO(NNH)
CALL FREEFILE(2)
RLAT(NNH)=0.017453293*RLAT(NNH)
RETURN

5010 FORMAT(4A8)
5020 FORMAT(4E0.0)
5030 FORMAT(2A8,3I0)
6000 FORMAT(1H+,17X,11HREAD FROM ,2A8)
6005 FORMAT(//,32H ELECTRON DENSITY PROFILE FROM ,A8,
+ 11H IONOGRAM ,3A8)
6010 FORMAT(//,39H ELECTRON DENSITY PROFILE FROM VERTICAL,
+ 11H IONOGRAM ,4A8)
6020 FORMAT(//1H ,13X,35HSEGMENTS OF THE FORM  $FN2 = A - B/R$  ,
+ 27H WHERE  $R = RE + H$  AND  $RE =$  ,F8.2,3H KM )
6030 FORMAT(//,25H ELECTRON GYROFREQUENCY = ,F9.4,4H MHZ,
+ /,1H ,19X,5HDIP = ,F9.4,4H DEG,/,1H ,14X,10HLATITUDE = ,
+ F9.4,4H DEG,/,1H ,13X,11HLONGITUDE = ,F9.4,4H DEG ,
+ 17X,42HSEGMENTS OF THE FORM  $H = A*FN4 + B*FN2 + C$  )
6040 FORMAT(//1H0,16X,8HFN (MHZ),6X,25HNE (CM-3) REAL HT (KM) ,
+ 6X,26HA(N) SEGMENT COEFFS B(N),8X,1HN,/,1H )
6050 FORMAT(1H ,11X,F12.4,1PE17.6,0PF13.4,1P2E18.6,17)
6060 FORMAT(//,15H F2 PEAK: A = ,1PE14.6,6H B = ,1PE14.6,
+ 6H C = ,1PE14.6)
6070 FORMAT(1H+,70X,26HWHERE  $FN2 = A*R2 + B*R + C$  )
6080 FORMAT(1H+,71X,25HWHERE  $NE = A*H2 + B*H + C$  )
6090 FORMAT(1H //16H BASE HT HNO = ,F10.4,3H KM //
+ 16H PEAK HT HMAX = ,F10.4,3H KM //
+ 16H PEAK NE NEO = ,1PE13.6 )
END
```

5. Listing of Subroutine CORR

```
C ***** CORR
C SUBROUTINE CORR(X,Y,XNAME,YNAME,N,IPRINT,IORDER,R,SIGMA)
C THIS SUBROUTINE PERFORMS ANALYSIS OF CORRELATION BETWEEN
C TWO VARIABLES X AND Y. IT CALCULATES
C (1) THE CORRELATION COEFFICIENT R
C (2) THE SIGNIFICANCE LEVEL SIGMA OF THIS R
C (3) THE CRITICAL R AT THIS SIGNIFICANCE LEVEL, I.E. THE
C LOWEST R FOR THE NUMBER OF VALUES USED WHICH WOULD
C BE SIGNIFICANT AT SIGNIFICANCE LEVEL SIGMA
C (4) THE 95% AND 99% CONFIDENCE INTERVALS FOR R, I.E. THE
C LIMITS WITHIN WHICH WE ARE 95% AND 99% CERTAIN THE
C TRUE POPULATION COEFFICIENT RHO MUST LIE
C
C PARAMETERS ARE AS FOLLOWS :
C
C X,Y : REAL ARRAYS (DIMENSION N) OF VALUES TO BE CORRELATED
C XNAME, : REAL A8 ALPHA VARIABLES OR 8 CHARACTER TEXT CONSTANTS
C YNAME : NAMES OF X AND Y
C N : NUMBER OF PAIRS OF X,Y VALUES (MAXIMUM 100)
C IPRINT : =0 NO PRINTING =1 PRINT RESULTS =2 VALUES & RESULTS
C IORDER : =0 NO ORDERING =1 PRINT VALUES ORDERED WRT X
C R : CORRELATION COEFFICIENT
C SIGMA : SIGNIFICANCE LEVEL
C
C DIMENSION X(N),Y(N),SI(5),TC(5,11),XX(100),YY(100),II(100)
C
C DATA LEND,SI/11, 2,.1, .05, .01, .001/
C DATA TC/1.372,1.812,2.228,3.169,4.587,1.325,1.725,2.086,2.845,
C + 3.850, 1.310,1.697,2.042,2.750,3.646,1.303,1.684,2.021,2.704,
C + 3.551, 1.299,1.676,2.009,2.678,3.496,1.296,1.671,2.000,2.660,
C + 3.460, 1.293,1.667,1.994,2.648,3.435,1.292,1.664,1.990,2.639,
C + 3.416, 1.291,1.662,1.987,2.632,3.402,1.290,1.660,1.984,2.626,
C + 3.390, 1.284,1.650,1.967,2.591,3.318/
C
C PRINT HEADINGS ETC
C
C IF(IPRINT.EQ.0) GO TO 50
C CALL COPY8(XNAM,XNAME)
C CALL COPY8(YNAM,YNAME)
C WRITE(6,6001)XNAM,YNAM
C IF(IPRINT.EQ.2.AND.IORDER.NE.1)
C + WRITE(6,6002)(I,I,X(I),Y(I),I=1,N)
C
C IF IORDER = 1 ORDER WRT X
C
C IF(IPRINT.LT.2.OR.IORDER.NE.1) GO TO 50
C DO 10 I=1,N
C XX(I)=X(I)
C YY(I)=Y(I)
10 II(I)=I
C DO 30 I=1,N-1
C J=I+1
C XM=XX(I)
C DO 20 K=I+1,N
C IF(XM.GT.XX(K)) J=K
20 XM=XX(J)
C YM=YY(J)
C IM=II(J)
C XX(J)=XX(I)
C XX(I)=XM
C YY(J)=YY(I)
C YY(I)=YM
C II(J)=II(I)
C II(I)=IM
30 WRITE(6,6002) I,II(I),XX(I),YY(I)
C WRITE(6,6002) N,II(N),XX(N),YY(N)
C
C CALCULATE MEANS AND VARIANCES
C
50 RN=N
C SUMX=0.0
C SUMY=0.0
C DO 60 I=1,N
C SUMX=SUMX+X(I)
60 SUMY=SUMY+Y(I)
C SUMX=SUMX/RN
C SUMY=SUMY/RN
```

```
SUMX2=0.0
SUMY2=0.0
SUMXY=0.0
DO 70 I=1,N
SUMX2=SUMX2+(X(I)-SUMX)*(X(I)-SUMX)
SUMY2=SUMY2+(Y(I)-SUMY)*(Y(I)-SUMY)
70 SUMXY=SUMXY+(X(I)-SUMX)*(Y(I)-SUMY)
SUMX2=SUMX2/(RN-1.0)
SUMY2=SUMY2/(RN-1.0)
SUMXY=SUMXY/(RN-1.0)
```

C CORRELATION COEFFICIENT R

```
R=SUMXY/SQRT(SUMX2*SUMY2)
```

C CRITICAL R FROM T DISTRIBUTION OF FUNCTION TA
C AT SIGNIFICANCE LEVEL SIGMA

```
TA=ABS(R)/SQRT((1.0-R*R)/(RN-2.0))
L=N/10
IF(FLOAT(N)/10.0-FLOAT(L).GE.0.5) L=L+1
IF(L.GT.10) L=LEND
SIGMA=0.5
I=1
TC(I,L)=0.695
```

```
DO 90 K=1,5
IF(TA.GT.TC(K,L)) I=K
IF(TA.GT.TC(K,L)) SIGMA=SI(K)
90 CONTINUE
RC=TC(I,L)/SQRT(TC(I,L)*TC(I,L)+RN-2.0)
IF(R.LT.0.0) RC=-RC
```

C 95% AND 99% CONFIDENCE INTERVALS FOR R

```
Z=0.5*ALOG((1.0+R)/(1.0-R))
SZ=1.0/SQRT(RN-3.0)
CI5L=EXP(2.0*(Z-1.960*SZ))
CI5U=EXP(2.0*(Z+1.960*SZ))
CI9L=EXP(2.0*(Z-2.576*SZ))
CI9U=EXP(2.0*(Z+2.576*SZ))
CI5L=(CI5L-1.0)/(CI5L+1.0)
CI5U=(CI5U-1.0)/(CI5U+1.0)
CI9L=(CI9L-1.0)/(CI9L+1.0)
CI9U=(CI9U-1.0)/(CI9U+1.0)
```

C PRINT RESULTS OF CORRELATION ANALYSIS

```
IF(IPRINT.LT.1) GO TO 100
WRITE(6,6003) R
WRITE(6,6004) N,SIGMA,RC
WRITE(6,6005) CI5L,CI5U,CI9L,CI9U
100 CONTINUE
```

C FORMAT STATEMENTS

```
6000 FORMAT(1H1)
6001 FORMAT(1HD,/,11X,22H CORRELATION ANALYSIS : ,/,/,
+ 6X,14HNO I X = ,A8,5H Y = ,A8,/,1H )
6002 FORMAT(1H,2X,2I5,F12.4,F14.4)
6003 FORMAT(/,4X,28H CORRELATION COEFFICIENT R = ,F6.3)
6004 FORMAT(/,16,28H VALUES. SIGNIFICANCE LEVEL ,F4.3,/,/,
+ 19X,13H CRITICAL R = ,F6.3)
6005 FORMAT(/,24H 95% CONFIDENCE INTERVAL ,F7.3,3H TO ,F7.3,
+ /,24H 99% CONFIDENCE INTERVAL ,F7.3,3H TO ,F7.3)
```

```
RETURN
```

```
END
```

REFERENCES

- Agy, V., K. Davies and R. Salaman (1959) : An atlas of oblique incidence ionograms. NBS Tech. Note no. 31, Office of Technical Services, U.S. Dept. of Commerce, Washington D.C.
- Appleton, E.V. and W.J.G. Beynon (1940) : The application of ionospheric data to radio communication problems, Part I. Proc. Phys. Soc. 52, 518-533.
- Backus, G.E. and J.F. Gilbert (1967) : Numerical application of a formalism for geophysical inverse problems. Geophys. J.R. Astron. Soc. 13, 247-276.
- Barish, F.D. and J.G. Roederer (1969) : Conjugate intersects to selected geophysical stations. STP Notes no. 4, 91-109.
- Barry, G.H. and R.B. Fenwick (1965) : Extra-terrestrial and ionospheric sounding with synthesised frequency sweeps. Hewlett-Packard J. 16, no. 11, 8-12.
- Barry, G.H. and R.B. Fenwick (1969) : Oblique chirp sounding, oblique ionospheric radio wave propagation at frequencies near the lowest usable high frequency. AGARD Conf. Proc. 13, 487-501 (Ed. T.B. Jones, Slough).
- Barry, G.H. (1971) : A low-power vertical incidence ionosonde. IEEE Trans. Geosci. Electron. GE-9, 86-89.
- Bartning, B. (1978) : Group delay variations at oblique incidence resulting from medium-scale travelling ionospheric disturbances. Radio Sci. 13, 147-157.
- Bates, H.F. and A.E. Goddard (1964) : On the precise determination of high-frequency propagation times. J. Geophys. Res. 69, 4722-4724.
- Berger, M.J., S.M. Seltzer and K. Maeda (1970) : Energy deposition by auroral electrons in the atmosphere. J. Atmos. & Terr. Phys. 32, 1015-1045.
- Bond, F.R. and I.L. Thomas (1971) : The southern auroral oval. Aust. J. Phys. 24, 97-102.
- Bowman, G.G. (1969) : Ionization trough below the F2 layer maximum. Planet. & Space Sci. 17, 777-796.
- Brace, L.H., E.H. Maier, J.H. Hoffman, J. Whitteker and G.G. Shephard (1976) : Deformation of the night side plasmasphere and ionosphere during the August 1972 geomagnetic storm. J. Geophys. Res. 79, 5211-5218.
- Bradley, P.A. (1970) : Focusing of radio waves reflected from the ionosphere at low angles of elevation. Electron. Lett. 6, 457-458.
- Bradley, P.A. and J.R. Dudeney (1973) : A simple model of the vertical distribution of electron concentration in the ionosphere. J. Atmos. & Terr. Phys. 35, 2131-2146.
- Breit, G. and M.A. Tuve (1926) : A test for the existence of the conducting layer. Phys. Rev. 28, 554-575.
- Bulmer, A.R. (1977) : Disc handling package. Unpublished report, Dept. of Computer Science, Rhodes University.

- Chernov, Yu. A. (1968) : Some theorems on the equivalent hop in ionospheric radio propagation. *Telecommun. & Radio Eng. Part 2.* 23, 73-75.
- Chiu, Y.T. (1976) : Planetary scale wave response to auroral heating of the neutral atmosphere. *J. Geophys. Res.* 81, 1231-1240.
- Chuang, S.L. and K.C. Yeh (1977) : A method for inverting oblique sounding data in the ionosphere. *Radio Sci.* 12, 135-140.
- Coffey, H.E. and J.A. McKinnon (1977) (eds.) : Collected data reports for STIP interval II 20 March - 5 May 1976. Report UAG-61, NGSDC, Boulder.
- Croft, T.A. and R.B. Fenwick (1963) : Chart for determining the effects of ionospheric tilts using an idealized model. *J. Res. Nat. Bur. Stand. (USA) : Section D (Radio Science)* 67D, 735-745.
- Croft, T.A. (1967) : HF radio focusing caused by the electron distribution between ionospheric layers. *J. Geophys. Res.* 72, 2343-2355.
- Croft, T.A. and H. Hoogasian (1968) : Extract ray calculations in a quasi-parabolic ionosphere with no magnetic field. *Radio Sci.* 3, 69-74.
- Dahlquist, G. and A. Björck (1974) : Numerical Methods (transl. N. Anderson). Prentice-Hall, Englewood Cliffs, N.J.
- Dalgarno, A., W.B. Hanson, N.W. Spencer and E.R. Schmerling (1973) : The Atmosphere Explorer mission. *Radio Sci.* 8, 263-266.
- Davies, K. (1965) : Ionospheric Radio Propagation. NBS Monograph 80, U.S. Dept. of Commerce, Washington D.C.
- Davies, K. (1967) : A nomenclature for oblique ionospheric soundings and ray tracing. *Radio Sci.* 2, 1395-1396.
- De Kock, E.J. (1977) : Computer assisted ionogram scaling. B.Sc. (Hons) Project, Dept. of Physics, Rhodes University.
- De Voogt, A.H. (1953) : The calculation of the path of a radio ray in a given ionosphere. *Proc. Inst. Radio Engrs.* 41, 1183-1186.
- De Voogt, A.H. (1960) : Ionospheric models as an aid for the calculation of ionospheric propagation quantities. *Proc. Inst. Radio Engrs.* 48, 341-346.
- Dickinson, L.G., S.E. Boselly and W.S. Burgmann (1974) : Defense Meteorological Satellite Program (DMSP) user's guide. Rept. AWS-TR-74-250, Scott AFB, Illinois.
- Dieminger, W. (1963) : Recommendations of the Lindau meeting on oblique incidence soundings of the ionosphere. *IQSY Notes no. 4*, 25-33.
- Dixon, W.J. and F.J. Massey (1969) : Introduction to Statistical Analysis (3rd edition). McGraw-Hill, New York.
- Dudeney, J.R. (1974) : A simple empirical method for estimating the height and semithickness of the F2-layer at the Argentine Islands, Graham Land. British Antarctic Survey Rept. no. 88, NERC, London.
- Dudeney, J.R. (1978) : An improved model of the variation of electron concentration with height in the ionosphere. *J. Atmos. & Terr. Phys.* 40, 195-203.

- Evans, S. (1968) : Comment on 'The reflection properties of radio waves on the ice cap'. (Yoshino, 1967). IEEE Trans. Antennas & Propag. (USA) AP-16, 363-364.
- Folkestad, K. (1968) : Exact ray computations in a tilted ionosphere with no magnetic field. Radio Sci. 3, 81-84.
- Francis, S.H. (1974) : Theory of medium-scale traveling ionospheric disturbances. J. Geophys. Res. 79, 5245-5260.
- Francis, S.H. (1975) : Global propagation of atmospheric gravity waves : a review. J. Atmos. & Terr. Phys. 37, 1011-1054.
- George, P.L. (1970) : True height analysis of oblique incidence HF radio wave data. J. Atmos. & Terr. Phys. 32, 905-916.
- Georges, T.M. (1968) : HF Doppler studies of travelling ionospheric disturbances. J. Atmos. & Terr. Phys. 30, 735-746.
- Georges, T.M. and J.J. Stephenson (1969) : HF radar signatures of travelling ionospheric irregularities, 3D ray tracing simulation. Radio Sci. 4, 679-696.
- Gething, P.J.D. (1962) : Relation between oblique and ground path-lengths in ionospheric propagation over a curved earth. Nature 193, 260-261.
- Gething, P.J.D. (1965) : Relationship between phase path and effective path for oblique ionospheric propagation. J. Atmos. & Terr. Phys. 27, 57-66.
- Gething, P.J.D. and R.G. Maliphant (1967) : Unz's application of Schlomilch's integral equation to oblique incidence observations. J. Atmos. & Terr. Phys. 29, 599-600.
- Gething, P.J.D. (1969) : The calculation of electron density profiles from oblique ionograms. J. Atmos. & Terr. Phys. 31, 347-354.
- Gething, P.J.D. (1974) : Phase path characteristics for oblique ray paths. J. Atmos. & Terr. Phys. 36, 1-8.
- Gething, P.J.D. (1978) : Radio Direction Finding. Peter Peregrinus/Institution of Electrical Engineers, London.
- Ginzburg, V.L., L.V. Kurnosova, V.I. Logachev, A.A. Razorenov, I.A. Sirotkin and M.I. Fradkin (1962) : Investigation of charged particle intensity during the flights of the second and third space ships. Planet. & Space Sci. 9, 845-854.
- Gledhill, J.A., D.G. Torr and M.R. Torr (1967) : Ionospheric disturbance and electron precipitation from the outer radiation belt. J. Geophys. Res. 72, 209-214.
- Gledhill, J.A. (1971) : Scientific results of the South African Antarctic Ionosphere Program 1962-1970. S. Afr. J. Antarct. Res. 1, 3-10.
- Gledhill, J.A. and M.H. Williams (1971) : Harmonic analysis of the F2 critical frequencies at several Antarctic stations. J. Atmos. & Terr. Phys. 33, 1055-1066.
- Gledhill, J.A. (1975) : The International Magnetospheric Study (IMS) and the Antarctic and Southern Hemisphere Aeronomy Year (ASHAY). S. Afr. J. Antarct. Res. 5, 53-56.

- Gledhill, J.A. (1976) : Aeronomic effects of the South Atlantic Anomaly. Rev. Geophys & Space Phys. 14, 173-187.
- Gledhill, J.A. and C.Y. Huang (1977) : Expected effects of electron precipitation in ionization of the ionosphere in the South Atlantic Anomaly. S.A. Inst. Phys. 22nd Annual Conf., Grahamstown. (unpublished)
- Gledhill, J.A. and J.P.S. Rash (1978) : The event of March 26, 1976 at SANAE. S.A. Inst. Phys. 23rd Annual Conf., Pretoria. (unpublished)
- Gledhill, J.A., R. Haggard and J.P.S. Rash (1978) : Ionospheric behaviour at SANAE, Antarctica; Grahamstown, South Africa and intermediate points. To be published in UAG Rept.
- Greenspan, J.A. and C.A. Stone (1964) : The longitudinal variation of night airglow intensity in the region of the South Atlantic magnetic anomaly. J. Geophys. Res. 69, 465-469.
- Haggard, R. and J.A. Gledhill (1976) : Observations of the ionosphere over the South Atlantic Ocean. S. Afr. J. Antarct. Res. 6, 14-18.
- Haggard, R. (1977) : Preliminary observations of the ionosphere over the Southern Ocean. S.A. Inst. Phys. 22nd Annual Conf., Grahamstown. (unpublished)
- Haggard, R. (1978) : Observations of the ionosphere over the Southern Ocean. S.A. Inst. Phys. 23rd Annual Conf., Pretoria. (unpublished)
- Haselgrove, J. (1955) : Ray theory and a new method for ray tracing. In : The Physics of the Ionosphere. The Physical Society, London.
- Haydon, G.W. and D.L. Lucas (1968) : Predicting ionospheric electron density profiles. Radio Sci. 3, 111-119.
- Hill, G.E. (1963) : Sudden enhancements of F-layer ionization in polar regions. J. Atmos. Sci. 20, 492-497.
- Howe, H.H. and D.E. McKinnis (1967) : Ionospheric electron-density profiles with continuous gradients and underlying ionization corrections, II : Formulation for a digital computer. Radio Sci. 2, 1135-1158.
- Huang, C.Y. (1977) : Precipitation effects on atmospheric electron densities. M.Sc. Thesis, Dept. of Physics, Rhodes Univ.
- Hunsucker, R.D. and L.H. Tveten (1967) : Large travelling ionospheric disturbances observed at mid-latitudes utilizing the high resolution backscatter technique. J. Atmos. & Terr. Phys. 29, 909-916.
- Hunsucker, R.D. and H.F. Bates (1969) : Survey of polar and auroral region effects on HF propagation. Radio Sci. 4, 347-365.
- IAGA Commission 2 (1976) : International Geomagnetic Reference Field 1975. J. Geophys. Res. 81, 5163-5164.
- ICL (1969) : Find-2 Multiple Enquiry System. Manual, International Computers Limited, London.
- ICL (1975) : Direct Access Sorting. Manual, International Computers Limited, London.

- Jackson, J.E. (1956) : A new method for obtaining electron-density profiles from P'-f records. J. Geophys. Res. 61, 107-127.
- Jones, R.M. and J.J. Stephenson (1975) : A versatile three dimensional ray tracing computer program for radio waves in the ionosphere. OT Rept. 75-76, Office of Telecommunications, U.S. Dept. of Commerce, Washington D.C.
- Kamide, Y. and J.D. Winningham (1977) : A statistical study of the 'instantaneous' nightside auroral oval : the equatorward boundary of electron precipitation as observed by the Isis 1 and 2 satellites. J. Geophys. Res. 82, 5573-5588.
- Kerblay, T.S. and Ye. M. Kovalevskaya (1967) : Computation of MUF in the presence of a horizontal ionospheric inhomogeneity. Geomagn. & Aeron. (USA) 7, 92-95.
- Kift, F (1960) : Propagation of high-frequency radio waves to long distances. Proc. Instn. Electr. Eng. (GB) 107B, 127-140.
- Köhnlein, W. and W.J. Raitt (1977) : Position of the mid-latitude trough in the topside ionosphere as deduced from ESRO 4 observations. Planet. & Space Sci. 25, 600-602.
- Kopka, H. and H.G. Möller (1968) : Interpretation of anomalous oblique incidence sweep-frequency records using ray tracing. Radio Sci. 3, 43-51.
- Kroehl, H.W. and M.A. Henning (1977) : Equatorward boundary of the northern hemisphere auroral oval for 20 March through 5 May 1976. In : Rept. UAG-61 (Coffey and McKinnon, 1977).
- Kroehl, H.W., M.A. Henning and C-I. Meng (1977) : Low energy precipitating electrons over the polar caps recorded by instruments on DMSP satellites. In : Rept. UAG-61 (Coffey and McKinnon, 1977).
- Kuriki, I., I. Kasuya, H. Hojo and K. Tanohata (1974) : Analysis of the maximum observed frequencies on oblique ionograms by ray tracing technique. J. Radio Res. Lab. (Japan) 21, 161-190.
- Lambert, S. and J.P.S. Rash (1975) : A ray tracing approach to vertical and oblique incidence ionograms. S.A. Inst. Phys. 20th Annual Conf., Durban. (unpublished)
- Lambert, S. (1977) : Studies in ionospheric ray tracing. M.Sc. Thesis, Dept. of Physics, Rhodes Univ.
- Lee, M.K. and J.S. Nisbet (1975) : Propagation predictions and studies using a ray tracing program combined with a theoretical ionospheric model. IEEE Trans. Antennas & Propag. (USA) AP-23, 132-136.
- Maliphant, R.G. and D.B. Muldrew (1963) : Accurate transmission curves for vertical incidence ionograms and the production of a general transmission slider. Meeting on oblique sounding of the ionosphere, Lindau. (unpublished)
- Martyn, D.F. (1935) : The propagation of medium radio waves in the ionosphere. Proc. Phys. Soc. 47, 323-339.
- Mather, R.A., F.C. Wilson and R. Schneible (1965) : Determining ionospheric parameters over regions of denied access. IEEE Trans. Aerosp. & Electron. Syst. (USA) AES-1, 104-107.
- McIlwain, C.E. (1961) : Coordinates for mapping the distribution of magnetically trapped particles. J. Geophys. Res. 66, 3681-3691.

- Milsom, J.D. (1977) : Extract ray-tracing through the Bradley-Dudeney model ionosphere. *Marconi Rev.*, Third quarter 1977, 172-196.
- Möller, H.G. (1964) : Variable frequency pulse transmission tests at oblique incidence over distances between 1000 and 2000 km. Translation published by Stanford Res. Inst., Menlo Park, California.
- Möller, H.G. (1967) : Oblique sweep-frequency experiments over a 2000 km north-south subauroral path. *Radio Sci.* 2, 77-86.
- Muldrew, D.B. (1959) : An ionospheric ray-tracing technique and its application to a problem in long distance radio propagation. *I.R.E. Trans. Antennas & Propagation* AP-7, 393-396.
- Muldrew, D.B. and R.G. Maliphant (1962) : Long-distance one-hop ionospheric radio wave propagation. *J. Geophys. Res.* 67, 1805-1815.
- Muldrew, D.B. (1965) : F-layer ionization troughs deduced from Alouette data. *J. Geophys. Res.* 70, 2635-2650.
- Naiman, A., R. Rosenfeld and G. Zirkel (1972) : Understanding Statistics. McGraw-Hill, New York.
- NGSDC (1975) : DMSP (DAPP) precipitating electron data. User Information Sheet E-3 1975, NGSDC, U.S. Dept. of Commerce, Boulder, Colorado.
- Nielson, D.L. (1968) : Ray path equations for an ionized layer with a horizontal gradient. *Radio Sci.* 3, 101-109.
- Paul, A.K. (1967) : Ionospheric electron-density profiles with continuous gradients and underlying ionization corrections : I. The mathematical-physical problem of real-height determination from ionograms. *Radio Sci.* 2, 1127-1133.
- Piggott, W.R. and K. Rawer (1972) : URSI Handbook of ionogram interpretation and reduction (2nd edition). Rept. UAG-23, NGSDC, U.S. Dept. of Commerce, Boulder, Colorado.
- Piggott, W.R. and E. Hurst (1976) : Solar proton and electron precipitation effects detected by ionosondes. *J. Atmos. & Terr. Phys.* 38, 619-622.
- Piggott, W.R. and K. Rawer (1978) : Revision of chapters 1-4 of URSI Handbook of ionogram interpretation and reduction. Rept. UAG-23A, NGSDC, U.S. Dept. of Commerce, Boulder, Colorado.
- Poole, A.W.V. (1974) : N(h) profiles from vertical ionograms - program NHPR. Dept. of Physics, Rhodes Univ. (unpublished)
- Rao, N. Narayana (1973) : A note on the analysis of oblique ionograms. *J. Atmos. & Terr. Phys.* 35, 1561-1563.
- Rash, J.P.S. and Poole, A.W.V. (1975) : SANAE - Grahamstown oblique soundings - a preliminary study. S.A. Inst. Phys. 20th Annual Conf. Durban. (unpublished)
- Rash, J.P.S. (1976) : Transmission times of radio waves between SANAE and Grahamstown. S.A. Inst. Phys. 21st Annual Conf., Johannesburg. (unpublished)

- Rash, J.P.S. (1977) : Correlations between electron fluxes and oblique incidence ionospheric parameters between SANAE and Grahamstown. S.A. Inst. Phys. 22nd Annual Conf., Grahamstown. (unpublished)
- Rash J.P.S. and R. Haggard (1977) : Investigation of the ionosphere between SANAE and Grahamstown at vertical and oblique incidence. S.A. Inst. Phys. 22nd Annual Conf., Grahamstown. (unpublished)
- Rawer, K., S. Ramakrishnan and D. Bilitza (1975) : Preliminary reference profiles for electron and ion densities and temperatures proposed for the international reference ionosphere. IPW Sci. Rept. W.B.2, Inst. für Physikalische Wettraumforschung, Freiburg, F.R.G.
- Rees, M.H. (1963) : Auroral ionization and excitation by incident energetic electrons. Planet & Space Sci. 11, 1209-1218.
- Roederer, J.G., W.N. Hess and E.G. Stassinopoulos (1965) : Conjugate intersects to selected geophysical stations. GSFC Rept. X-642-65-182, Goddard Space Flight Centre, Greenbelt, Maryland.
- R.U.C.C. (1978) : MAXIMOP User Manual (revised edition). Computer Centre, Rhodes Univ.
- Rush, C.M., D. Miller and J. Gibbs (1974) : The relative daily variability of foF2 and hmF2 and their implications for HF radio propagation. Radio Sci. 9, 749-756.
- Rush, C.M. and W.R. Edwards (1975) : Sensitivity of HF circuit simulations to electron density models. Radio Sci. 10, 867-874.
- Rush, C.M. and T.J. Elkins (1975) : An assessment of the magnitude of the F-region absorption on HF radio waves using realistic electron density and collision frequency models. Telecommun. J. (Engl. Ed.) (Switzerland) 42, 476-488.
- Rycroft, M.J. and S.J. Burnell (1970) : Statistical analysis of the ionospheric trough and the plasmopause. J. Geophys. Res. 75, 5600-5604.
- Rycroft, M.J. and J.O. Thomas (1970) : The magnetospheric plasmopause and the electron density trough at the Alouette I orbit. Planet. & Space Sci. 18, 65-80.
- Sharp, G.W. (1966) : A mid-latitude trough in the nighttime ionosphere. J. Geophys. Res. 71, 1345-1356.
- Smith, M.S. (1970) : The calculation of ionospheric profiles from data given on oblique incidence ionograms. J. Atmos. & Terr. Phys. 32, 1047-1056.
- Smith, Newbern (1939) : The relation of radio sky-wave transmission to ionospheric measurements. Proc. Inst. Radio Engrs. 27, 332-347.
- Sulzer, P.G. (1955) : Sweep-frequency pulse transmission measurements over a 2400 km path. J. Geophys. Res. 60, 411-420.
- Terry, P.D. (1974) : Ray tracing in three dimensional geophysical polar co-ordinates. Dept. of Applied Mathematics, Rhodes Univ. (unpublished)
- Terry, P.D. (1975) : Graph plotting facilities on the 1901T. Manual, Dept. of Applied Mathematics, Rhodes Univ.

- Terry, P.D. and A. Gagliardini (1977) : Magnetic field models in the South Atlantic region. Private communication.
- Torr, D.G. (1966) : Ionospheric effects in the Southern Radiation Anomaly. Ph.D. Thesis, Dept. of Physics, Rhodes Univ.
- Torr, D.G., M.R. Torr, R.A. Hoffman and J.C.G. Walker (1976) : Global characteristics of 0.2 to 26 keV charged particles at F region altitudes. *Geophys. Res. Lett.* 3, 305-308.
- Tulunay, Y.K. and A.R.W. Hughes (1973) : A satellite study of the mid-latitude trough in electron density and VLF radio emissions during the magnetic storm of 25-27 May 1967. *J. Atmos. & Terr. Phys.* 35, 153-163.
- Unz, H. (1963) : Schlomilch's integral equation. *J. Atmos. & Terr. Phys.* 25, 101-102.
- Unz, H. (1966) : Schlomilch's integral equation for oblique incidence. *J. Atmos. & Terr. Phys.* 28, 315-316.
- Wieder, B. (1955) : Some results of a sweep-frequency propagation experiment over an 1150 km E-W path. *J. Geophys. Res.* 60, 395-409.
- Wrenn, G.L. and W.J. Raitt (1975) : *In situ* observations of mid-latitude ionospheric phenomena associated with the plasmopause. *Ann. Geophys.* 31, 17-28.
- Wright, J.W. and T.N. Gautier (1960) : Note on a test of the equivalence theorem for sporadic E propagation. *J. Res. Nat. Bur. Stand. (USA) : Section D (Radio Science)* 64D, 347-348.
- Wright, J.W. and G.H. Smith (1967) : Review of current methods for obtaining electron density profiles from ionograms. *Radio Sci.* 2, 1119-1125.
- Yoshino, T. (1962) : The reflection properties of radio waves on the ice cap. *IEEE Trans. Antennas & Propag. (USA)* AP-15, 542-552.